Dynamical backaction effects between localised spins and electronic conductors

Stephanie Matern

A thesis submitted for the degree of PhD
at the
University of St Andrews

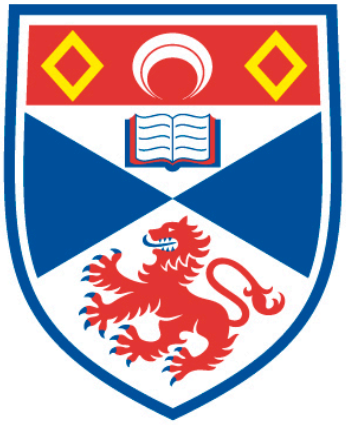

2020

Identifier to use to cite or link to this thesis:
DOI: https://doi.org/10.17630/sta/52

Dynamical backaction effects between localised spins and electronic conductors

Stephanie Matern

In this thesis we present an investigation of the influence of quantum correlations on a quantum system's dynamical behaviour. Our focus is specifically on the time dependence of quantum spins in an environment of itinerant electrons. This is an archetype for strong correlation physics, whose dynamical onset is the central correlation effect investigated in this work.

We derive an analytic result for the time evolution of a single localised quantum spin in weak contact with conduction electrons. This result is obtained from a detailed analysis of the pole structure of the Nakajima-Zwanzig equation for the reduced density matrix in Laplace space. We provide a description of the full time range, from very short times in which a novel result for non-Markovian behaviour is obtained, to long times in which we recover the well-known exponential decay expressions. For the short times we show how the non-Markovian memory effects of the spin's dynamics arise from the backaction of coherent electronic particle-hole fluctuations.

As an application of the fast dynamics we propose a cooling protocol going beyond the paradigm of thermodynamic cycles. The protocol relies on a rapid pump scheme with a repeated reinitialisation of the fast quantum coherent dynamics, with each repetition carrying away a small amount of heat from the electronic environment. This protocol is temperature independent and designed to circumvent a natural bottleneck in standard demagnetisation cooling due to long relaxation times at low temperatures.

Finally we extend the dynamics to a pair of localised spins coupled through the same electronic environment, using a self-consistent projection operator framework. In contrast to the conventional RKKY coupling we derive a set of coupled equations including the temporal and spatial correlations. This set becomes finite through a meticulous identification of the electronic fluctuations responsible for the coupled dynamics, allowing for a numerical solution.

Declarations

Candidate's declaration

I, Stephanie Matern, do hereby certify that this thesis, submitted for the degree of PhD, which is approximately 45,000 words in length, has been written by me, and that it is the record of work carried out by me, or principally by myself in collaboration with others as acknowledged, and that it has not been submitted in any previous application for any degree. I was admitted as a research student at the University of St Andrews in August 2016. I received funding from an organisation or institution and have acknowledged the funder(s) in the full text of my thesis.

Date, Signature of candidate

Supervisor's declaration

I hereby certify that the candidate has fulfilled the conditions of the Resolution and Regulations appropriate for the degree of PhD in the University of St Andrews and that the candidate is qualified to submit this thesis in application for that degree.

Date, Signature of supervisor

Permission for publication

In submitting this thesis to the University of St Andrews we understand that we are giving permission for it to be made available for use in accordance with the regulations of the University Library for the time being in force, subject to any copyright vested in the work not being affected thereby. We also understand, unless exempt by an award of an embargo as requested below, that the title and the abstract will be published, and that a copy of the work may be made and supplied to any bona fide library or research worker, that this thesis will be electronically accessible for personal or research use and that the library has the right to migrate this thesis into new electronic forms as required to ensure continued access to the thesis. I, Stephanie Matern, confirm that my thesis does not contain any third-party material that requires copyright clearance. The following is an agreed request by candidate and supervisor regarding the publication of this thesis:

- Printed copy
  Embargo on all of print copy for a period of 1 year on the following ground(s):
  Publication would preclude future publication
  Supporting statement for printed embargo request
  Parts of my PhD work is not published yet and the paper including this work is in preparation.

- Electronic copy
  Embargo on all of electronic copy for a period of 1 year on the following ground(s):
  Publication would preclude future publication
  Supporting statement for electronic embargo request
  A scientific paper including the unpublished work from my thesis is pending.

- Title and Abstract
  I agree to the title and abstract being published.

Date, Signature of candidate

Date, Signature of supervisor

Underpinning Research Data or Digital Outputs

Candidate's declaration

I, Stephanie Matern, hereby certify that no requirements to deposit original research data or digital outputs apply to this thesis and that, where appropriate, secondary data used have been referenced in the full text of my thesis.

Date, Signature of candidate

Acknowledgements

First and foremost, I would like to thank my PhD supervisor Bernd Braunecker for countless meetings and emails, all the scientific advice, and deeply relaxed responses to urgent and seemingly close-to-life-threatening physics problems. I would also like to thank him for not writing emails during holidays and his reminders to actually take some days off over Christmas.

Second, I am grateful for the support from everyone in the physics theory department and the managing team of the CM-CDT, who helped to overcome many of the scientific and administrative hurdles.

Asides from the scientific side, I would like to say thank you! to the individuals who made my time in Scotland enjoyable and often took the edge off the occasionally stressful PhD- and research-life. So thanks to: FM for supplying an unfathomable amount of coffee (sometimes I even paid for it!) and explanations about ARPES data on some compound I have never heard of and immediately forgot; LK, JJP and TO for listening to all the rants and all the (mainly) remote advice in all situations; IM for surprise dinners, hiking and climbing trips; SRT, VN and KBA, who were ready pretty much whenever for coffee, food, and long walks with conversations about everything, sometimes even including some physics; EM for all the running and climbing and chocolate; MC for rejuvenating more or less weekly dips into the North Sea which stopped me questioning my sanity, the excellent pancakes helped as well; CHJ for being there and keeping me sane throughout the writing process during a pandemic by organising little outdoor adventures; CM, who never came to visit me in Scotland; $(KM)^2$ for all the encouragement and support over many many years although I don't think I ever managed to explain my research properly; and my highly efficient typo-hunting squad CHJ, IS, KBA, MC, and VN.

Funding

This work was supported by the Engineering and Physical Sciences Research Council under grant number EP/L015110/1.

Contents

List of figures

1 Introduction

A realistic quantum system is never truly isolated but part of a bigger structure. Interactions between the system and the environment are unavoidable. In a strict sense, an isolated quantum system as often considered in textbook descriptions does not exist. On the one hand, this can be seen as a nuisance, for instance with regard to decoherence of well prepared quantum states. On the other, it is an opportunity to investigate and eventually exploit the dynamics and correlations between system and environment. Experimental advances across many fields open the door to investigate quantum correlations on the nanoscale and at low temperatures. For example ultracold atom experiments present a platform for simulating small scale quantum systems and studying their dynamics [1–4]. Magnetic resonance techniques allow for probing local fields of small spin ensembles [5–8]. Looking into the field of quantum computation, nanostructures such as quantum dots [9, 10], superconducting setups [11, 12] or single atoms [13] can be used to realise qubits. Closely related is the field of quantum information where the correlations between different parts of the quantum system serve as a valuable resource [14, 15]. The common theme of these examples is the consequences of the system-bath interaction on the behaviour within the system, understood through the correlations due to that interaction.

In this work we address the influence of the system's surroundings on its dynamics, with a particular focus on the short time dynamics and the quantum correlations built up between system and environment. The example systems treated consist of localised spins embedded in a electronic conductor. Such a model is a building block to describe the experimental setups across the different fields mentioned above, ranging from capturing the relaxation of a magnetic moment in a resonance experiment, to describing the decay of a coherent state or spin qubit.

The dynamical response of certain systems provides a noninvasive way to probe it. A well known and widely used example is magnetic resonance imaging with its application in medicine. Here, the excitation of an ensemble of spins (the hydrogen nuclei in the human body) and their decay back into the equilibrium states provide us with a diagnostic tool to, e.g., distinguish different tissues in the human body. The relevant observable is the relaxation time [16, 17], which is the average time it takes for a system to return to its

equilibrium state. Magnetic resonance experiments such as nuclear magnetic resonance (NMR) and electron spin resonance techniques (ESR) help us to learn about the current state of the system by analysing the resonance peaks present. In many scenarios the relaxation time itself is a fit parameter based on the classical model of a magnetic moment and its reaction to an outer magnetic field [18]. The typical decay rate allows us to extract information about the effects on the system's dynamics due to the interaction between system and bath. A prominent example in condensed matter systems is the so-called Korringa law [19, 20] which indicates Fermi liquid behaviour. It connects the shift of the resonance peak due to local magnetic fields to the relaxation time and the temperature. Its failure is often connected to strongly correlated phases and interacting systems [21–23].

With the advances of magnetic resonance experiments pushing into the nanometre regime [5–8], as well as using nuclear spins for computational tasks [24], the question arises if one would need to take into account quantum correlations to describe the relaxation dynamics correctly. In strongly correlated systems the spatial correlations such as magnetic ordering are often taken into account [23]. But, when considering Lorentz invariant systems, time and space should be treated on the same footing. Investigating quench dynamics and the importance of temporal correlations for the dynamical behaviour in correlated many-body systems is an active field of research [25–27]. In our contribution we go beyond the phenomenological description to address the influence of temporal correlations in the dynamical behaviour of a spin system coupled to a bath of itinerant electrons.

Short lived quantum correlations driven by the environment are important for the dynamics of the system. A prominent example is quantum dots which are a promising platform to realise spin qubits [9, 10, 28]. Here, the microscopic knowledge of the quantum dynamics is essential to understand the relaxation processes and mechanisms that set the decoherence time. How long a quantum state remains coherent is especially important for any process where the state is used for computational purposes [24, 28–30]. With the work presented here we hope to make steps towards increasing our understanding in how environments may be engineered to achieve desired effects on a quantum system [31–34].

The environment does not necessarily only lead to decoherence and decay but can also mediate an effective interaction between the parts of quantum systems. One example is the Ruderman–Kittel–Kasuya–Yosida (RKKY) interaction between localised spins through the conduction electrons [35–37]. Parts of the work presented here develop an approach based on [38] which enables us to study a collection of quantum systems that are effectively coupled by the shared environment. In a quantum information setting a coupling to the bath and the mediated effective interaction has been shown to influence

the entanglement [39]. Entanglement between quantum states is used as a resource for quantum informational tasks and protocols [14, 15]. In a condensed matter setting it has been suggested that the entanglement between magnetic impurities can be tuned by an external magnetic field [40]. Using the platform of localised spins we investigate what role temporal correlations play in the dynamical behaviour of quantum systems containing more than one spin. Furthermore the environment can be utilised to transport heat from one reservoir to the next. This is the case for any thermodynamic process where work is done by the system, such as in an Otto motor or a refrigerator. The condensed matter setup of the latter uses the demagnetisation of nuclear spins to cool down the surrounding electrons [41–47]. As experiments push for lower and lower temperatures down into the microkelvin regime for nanostructures [45] and even into the nanokelvin regime on cold atom platforms [48], the idea to utilise quantum coherent effects to support or speed up the relaxation processes is easily at hand [49–52]. In the quantum counterpart to the classical Otto motor, single molecule quantum heat engines are experimental accessible platforms to study such effects [53–55].

The methods developed in the field of open quantum systems provide a framework to investigate the underlying nature of the dynamics. An open quantum system describes a setup where the system of interest is coupled to a large environment [56–60]. The full dynamics are intractable due the extensive number of degrees of freedom making the exact description challenging. However, the aim is to still capture the effects of the environment on the quantum system's dynamics. The object of interest here is the reduced density matrix, where the degrees of freedom of the environment are traced out. Then, its equation of motion is given by a master equation.

Quantum master equations are widely used to obtain information about time-dependent properties [56–60]. The starting point to derive a master equation for the reduced density of the system on the microscopic level is the von Neumann equation and in many physical setups the equation of motion is given by a master equation of Lindblad form [61, 62]. At the heart of the Lindblad master equations sits the Born-Markov approximation. Within this approximation the bath is treated as a large memoryless reservoir, i.e., it is always in equilibrium and the interaction with the system cannot change the state of the reservoir [56, 63]. The state of a system in contact with such a reservoir thermalises and decays exponentially fast, such as the magnetisation of a paramagnet after turning off the external magnetic field.

However, at sufficiently short times, the memory time of the system-bath correlations are finite. On this short time scale the dynamics are dominated by quantum correlations, leading to a memory effects which in turn can result in non-Markovian dynamics [59, 60]. In this work we will focus on a coherent backaction of the electronic environment onto the

spin system [33, 34, 64] and the resulting dynamics including the non-Markovian evolution due to a finite memory time of the system. To capture memory effects a generalised quantum master equation approach beyond the Lindblad description is necessary. There are different paths to derive such generalised quantum master equations beyond the Markovian approximation [56, 65]. One example is a field-theoretic approach within a path integral formulation which relies on the Feynman-Vernon influence functional [66]. Another route, which is the one followed in this work, is the projection operator method [56, 65, 67–69]. The technique relies on finding a closed equation of motion for the system's dynamics by a projection onto the relevant part of the system-bath setup. Formally, the projection corresponds to tracing out the degrees of freedom of the environment. This leads to a generalised quantum master equation known as the Nakajima-Zwanzig equation [67–69] which is used throughout the work presented here. Incorporating the Born-Markov approximation would directly lead to a Born-Markov master equation or even Lindblad equation [56]. The full Nakajima-Zwanzig equation is time-nonlocal and the memory kernel, which is the operator encoding the convolution of different times, makes it generally difficult to solve. In some cases, this difficulty can be sidestepped by analysing the equation of motion in Laplace space [64, 70, 71]. In our approach we make use of the Laplace transformation to gain access to the full quantum dynamics of a localised spin embedded in electron conductor. From the projection operator technique one can also derive a time-convolutionless master equation which is local in time in contrast to the Nakajima-Zwanzig equation. The complication of keeping track of the system's history in this case is hidden in the inversion of a superoperator and an unique solution cannot be found in all cases [56]. Any generalised master equation has the potential to capture non-Markovian dynamics. The non-Markovian contributions are encoded in the influence functional [66, 72, 73], time-dependent coefficients [71, 74, 75] or the memory kernel [64, 76], depending on the chosen approach. Much work has been dedicated to explain the dynamics of a two-level system coupled to a bosonic environment [77–80] or spin bath [64, 81–83], while the dynamics of systems coupled to a fermionic bath are much less understood [33, 34, 84–86].

In this work we step also away from bosonic environment and we assume an itinerant electronic environment as found in a metal or semiconductor. Since the bath is fermionic the underlying dynamical response is determined by the Pauli principle and we are able to probe strongly correlated systems. The coherence and relaxation mechanisms play a fundamental role to understand the full quantum dynamical response of such systems. Using a projection operator method to formulate a generalised quantum master equation, the main question concerns the resulting dynamics for the spin system while taking into account the full quantum coherent backaction from the bath. In Chapter 2 the methods

and the theoretical groundwork are presented. This includes a general discussion about dynamics in open quantum systems before the Nakajima-Zwanzig equation is derived. This generalised master equation is the starting point for the systems discussed in this thesis. Furthermore, we derive an extension to the Nakajima-Zwanzig equation based on a self-consistent projection operator method [38]. Chapter 3 presents the results for an explicit example system of a single spin coupled to an electronic conductor. After presenting the phenomenological approach to the decay of a magnetic moment we use the open quantum system framework to derive the full coherent quantum dynamics of the example system. The full dynamics show a fast initial decay that we are utilising to propose a cooling protocol in Chapter 4. In this setup, the surrounding bath is cooled by driving an ensemble of quantum systems. The scientific findings of Chapters 3 and 4 are published in [87]. In Chapter 5 we adapt a generalised master equation approach that allows for a time-dependent bath state. Within this framework we are able to address multiple spins in the same electronic environment. Lastly, we conclude our findings in Chapter 6.

2

Non-Markovian dynamics in open quantum systems

Studying dynamics in systems out of equilibrium gained a lot of attention in recent years due to the ability to simulate small quantum systems experimentally [2, 3, 26]. Experimental platforms such as cold atoms system [1, 2] or trapped ions [88, 89] enable us to address questions ranging from quench dynamics in closed system to open quantum system dynamics in solid state physics as well as quantum optics.

Within the open quantum system perspective, there has been an increasing interest in the joint quantum dynamics of system and environment mediated by the system-bath interaction [26, 60]. The environment, formed by surrounding matter or radiation, is often treated as a bath that destroys the system's quantum coherence. In many cases, it is assumed that the interaction with the bath is instantaneous and only the current state of the environment is important. This is the Markovian approximation where correlations within the bath in time are disregarded. In many cases the Markovian description captures the system's dynamics. Only at short times as well as in systems with strong system-bath coupling or finite baths, treating the bath as a memoryless reservoir is not sufficient. During the memory time, time-dependent bath correlations build up. They lead to so-called memory effects and a generalised master equation is needed to describe the resulting dynamics where the full history of the system-bath correlations are taken into account. In the work presented in this thesis we will include a coherent backaction from the bath back onto the system which is the result of such memory effects. In this chapter we give a short overview about dynamics in open quantum systems on a more general footing. We will cover the Born-Markov approximation, followed by an overview of different techniques to capture non-Markovian dynamics and how non-Markovianity can be utilised. Furthermore we will derive a generalised quantum master equation within the projection operator approach known as the Nakajima-Zwanzig equation [67, 68] as well as an extension [38] which treats the bath state self-consistently in contrast to the usual equilibrium. Those equations are our starting point to investigate coherent backaction effects in the spin systems discussed in later chapters.

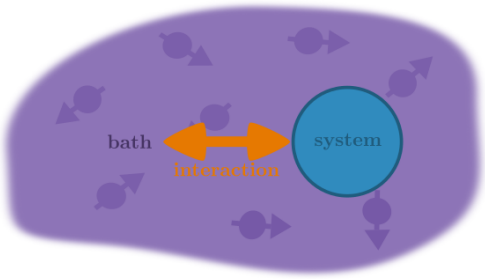

Figure 2.1: Sketch of an open quantum system. The system is embedded in a large bath or environment. The Hamiltonian of the full setup splits into the system contribution H_S, the environment H_B and the interaction H_{int} between them.

2.1 Dynamics in an open quantum system

In most realistic settings, a quantum system is not closed but in contact with an environment, as it is otherwise impossible to interact with or probe the system. The framework of open systems takes into account the influence by the environment or bath on the quantum system's dynamics due to an interaction between the two which is sketched in Fig. 2.1. In the subsequent discussion about the standard approach to open quantum system we adopt the derivations of the references [56, 65] to lay the groundwork for further developments. The Hamiltonian $H(t)$ of the full system, including the quantum system and its environment, can be written as

$$H(t) = H_0 + H_{\text{int}}(t), \tag{2.1}$$

with explicit time dependence of the interaction term H_{int}. The Hamiltonian $H_0 = H_S + H_B$ is the free Hamiltonian describing the system and the bath evolution, respectively. The terms bath and environment are used throughout this thesis to describe the surrounding of the open quantum system. The term bath is used for large reservoir in a thermal state and a less specific surrounding is described as environment. In particular we will study the effects of an electronic environment where the coupling between the quantum system and the electrons is a spin-spin interaction. To discuss the dynamics of such systems the density matrix $\rho(t)$ is used. Knowing the full time dependence of the density matrix allows for the computation of any physical observable including their time evolution. The full dynamics of a given Hamiltonian and the equation of motion for the

density matrix $\rho(t)$ are determined by the von Neumann equation

$$\dot{\rho}(t) = -i\left[H(t), \rho(t)\right]. \tag{2.2}$$

The square brackets $[\cdot,\cdot]$ denote the commutator and H is the system's Hamiltonian as in Eq. (2.1). Here and henceforth we set $\hbar = 1$. Introducing the Liouvillian superoperator L the equation can be written as

$$\dot{\rho}(t) = L(t)\rho(t), \tag{2.3}$$

with $L(\cdot) = -i[H, \cdot]$. Assuming the perturbation is the main cause of complications it is advantageous to transform into a frame rotating with the free evolution. In this interaction picture the time evolution of the unperturbed Hamiltonian is H_0 and the perturbation is H_{int} from Eq. (2.1), the time evolution of the density matrix $\hat{\rho}$ is given by

$$\hat{\rho}(t) = \hat{U}(t, t_0)\rho(t_0)\hat{U}^\dagger(t, t_0), \tag{2.4}$$

where $\hat{\cdot}$ is used to denote an operator in the interaction picture. The interaction picture time evolution operator $\hat{U}$ is defined as

$$\hat{U}(t, t_0) = U_0^\dagger(t, t_0)U(t, t_0), \tag{2.5}$$

with the evolution U_0 of the non-interacting system

$$U_0(t, t_0) = e^{-iH_0(t-t_0)}, \tag{2.6}$$

and $U(t, t_0)$ the time evolution operator for the full system. Then the von Neumann equation in the interaction picture can be written as

$$\frac{d}{dt}\hat{\rho}(t) = -i\left[\hat{H}_{\text{int}}(t), \hat{\rho}(t)\right] = \hat{L}_{\text{int}}(t)\hat{\rho}(t). \tag{2.7}$$

Here, the interaction Hamiltonian $\hat{H}_{\text{int}}$ is evolved under the evolution of the free system

$$\hat{H}_{\text{int}}(t) = U_0^\dagger(t, t_0)H_{\text{int}}(t)U_0(t, t_0). \tag{2.8}$$

Integrating Eq. (2.7) leads to the formal solution

$$\hat{\rho}(t) = \hat{\rho}(t_0) - i \int_{t_0}^{t} dt' \left[\hat{H}_{\text{int}}(t'), \hat{\rho}(t')\right]. \tag{2.9}$$

To extract any physical meaning from the general solution one has to make one or more assumptions for most cases. Widely used is the approximation of a weak system-environment coupling. In this weak coupling limit where the interaction between system and bath is small, we can treat the equation of motion for the density matrix Eq. (2.7) perturbatively. A generic system-bath setup is sketched on the left in Fig. 2.2. To capture second order processes in the interaction, the formal solution Eq. (2.9) is inserted back into the von Neumann equation in Eq. (2.2) which leads to

$$\frac{d}{dt}\hat{\rho}(t) = -\int_{t_0}^{t} dt' \left[\hat{H}_{\text{int}}(t), \left[\hat{H}_{\text{int}}(t'), \hat{\rho}(t')\right]\right], \tag{2.10}$$

under the condition that

$$\left[\hat{H}_{\text{int}}, \hat{\rho}(t_0)\right] = 0. \tag{2.11}$$

To go beyond second order in the interaction, one can iterate this procedure which leads to more nested commutators of the interaction Hamiltonian at different times.

Generally we are only interested in the reduced density matrix of the the system ρ_S where we trace out the degrees of freedom of the environment

$$\rho_S(t) = \text{Tr}_B \left\{\hat{\rho}(t)\right\}. \tag{2.12}$$

To find a closed equation of motion for ρ_S we assume that

$$\hat{\rho}(t_0) = \rho_S(t_0) \tag{2.13}$$

from which the condition Eq. (2.11) directly follows. In many situations, such as setups with a weak coupling between system and a large environment, it is justified to further assume that the full density matrix $\hat{\rho}(t)$ can be approximated by a product state between system $\rho_S(t)$ and environment ρ_B

$$\hat{\rho}(t) = \rho_S(t) \otimes \rho_B. \tag{2.14}$$

The underlying reasoning for this assumption is given by the Born approximation from scattering theory. In this case it is assumed that the wave function is not significantly

changed by a weak scattering potential and only a first order correction in the potential is taken into account [90]. In the open quantum system setting we assume that the state of the environment with a macroscopic number of degrees of freedom is not significantly changed by the interaction with the much smaller quantum system which justifies Eq. (2.14). Additionally, the state of the bath itself is often assumed to be in thermal equilibrium at some temperature $T = 1/\beta$ and is written as a Gibbs state

$$\rho_B = \frac{e^{-\beta H_B}}{\mathrm{Tr}\left\{e^{-\beta H_B}\right\}}. \tag{2.15}$$

Therefore, tracing over the environment in Eq. (2.10) leads to a master equation for the reduced density state of the system under the approximation in Eq. (2.14)

$$\frac{d}{dt}\rho_S(t) = -\int_{t_0}^{t} dt' \,\mathrm{Tr}_B\left\{\left[\hat{H}_{\mathrm{int}}(t), \left[\hat{H}_{\mathrm{int}}(t'), \rho_S(t') \otimes \rho_B\right]\right]\right\}. \tag{2.16}$$

The structure of Eq. (2.16) is still complicated if $H_{\mathrm{int}}(t)$ has some non-trivial time-dependence due to the convolution. Later on, we will see that this equation is basically the Nakajima-Zwanzig equation. This is a generalised master equation able to take into account memory effects due to time-dependent bath correlations. For now, Eq. (2.16) is simplified further by employing the Markov approximation. Combining the assumption Eq. (2.14) with the Markov approximation is referred to as Born-Markov approximation [56] and its effects is sketched in Fig. 2.2. It assumes that the current state of the system does not depend on any previous state and therefore neglects any dependence on the history of the system-bath interaction. This means that the integral Eq. (2.16) is nonzero only over a short time interval in which ρ_S remains unchanged. In practice, this allows us to replace $\rho_S(t')$ by $\rho_S(t)$ in the integrand of Eq. (2.16). We now make the substitution $t' \to t - t'$ and send the upper limit of the integral to infinity while choosing $t_0 = 0$. The last step is justified under the assumption that the bath correlations, which are build up in the nested commutator structure, decay sufficiently fast. This is visualised in the sketch on the right of Fig. 2.2. With these assumptions and substitutions in place, we arrive at the Born-Markov master equation

$$\frac{d}{dt}\rho_S(t) = -\int_{0}^{\infty} dt' \,\mathrm{Tr}_B\left\{\left[\hat{H}_{\mathrm{int}}(t), \left[\hat{H}_{\mathrm{int}}(t-t'), \rho_S(t) \otimes \rho_B\right]\right]\right\}. \tag{2.17}$$

The Born-Markov master equation is local in time and the complication of the time-convoluted structure of Eq. (2.16) is eliminated. To get to the widely used Lindblad equation [61, 62] the interaction H_{int} is split into products of system and bath operators,

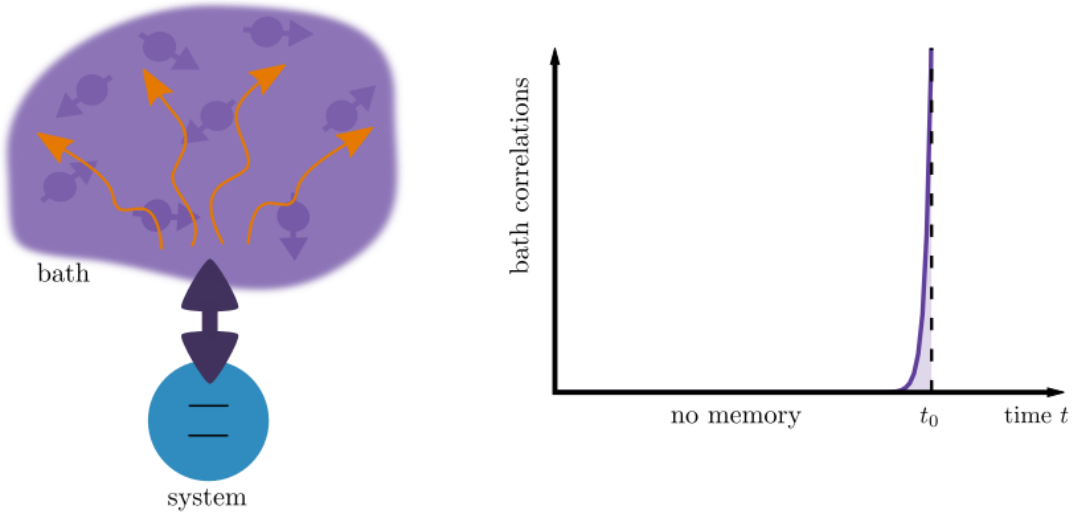

Figure 2.2: On the left-hand side we show a sketch of a small, two-level quantum system coupled to a large environment with many degrees of freedom. The interaction between system and bath is weak and the full density matrix can be written as Eq. (2.14). Induced excitations in the environment indicated by the orange arrows dissipate into the bath without changing the state of the reservoir. The corresponding time evolution of correlations within the bath is sketched on the right. For the system's evolution at time t_0 only the current bath state is significant for the system's dynamics according to the Markov approximation. The bath correlations decay exponentially fast and the history of the system-bath evolution is irrelevant on the system time scale.

A_j and B_j

$$H_{\text{int}} = \sum_j A_j \otimes B_j. \tag{2.18}$$

The operators A_j can be decomposed into the eigenoperatos $A_j(\omega)$ of the system Hamiltonian H_S. The frequency ω is the difference in energy between system eigenstates and within the secular or rotating wave approximation all contributions of different frequencies are neglected. Finding the system and bath operators in the interaction picture and inserting them for the interaction Hamiltonian $\hat{H}_{\text{int}}$ in Eq. (2.17) leads to an equation of motion of the Lindblad form

$$\dot{\rho}_S(t) = -i\left[H', \rho_S(t)\right] + \mathcal{D}(\rho_S(t)) \tag{2.19}$$

with the dissipator $\mathcal{D}$

$$\mathcal{D} = \sum_{\omega} \sum_{\alpha,\beta} \gamma_k \left(A_\beta(\omega)\rho_S(t)A_\alpha^\dagger(\omega) - \frac{1}{2}\left[A_\alpha^\dagger(\omega)A_\beta(\omega), \rho_S(t)\right]\right). \tag{2.20}$$

The first term in Eq. (2.19) corresponds to the contribution of the system Hamiltonian H_S via the eigenoperators or Lindblad operators $A_j(\omega)$ to the dynamics and is known as the Lamb shift

$$H' = \sum_{\omega} \sum_{\alpha,\beta} S_{\alpha\beta} A_{\alpha}^{\dagger}(\omega) A_{\beta}(\omega). \tag{2.21}$$

It captures the fact that due to the system-bath interaction the eigenenergies of the system alone are renormalised. The prefactors $S_{\alpha\beta}$ are defined via the one-sided Fourier transformations of the bath correlation functions

$$\Gamma_{\alpha\beta} = \int_0^{\infty} dt \, \mathrm{Tr}_B \left\{ B_{\alpha}^{\dagger}(t) B_{\beta}(0) \right\} \tag{2.22}$$

originating from the integrand in Eq. (2.17) and

$$S_{\alpha\beta}(\omega) = \frac{1}{2i} \left(\Gamma_{\alpha\beta}(\omega) - \Gamma_{\beta\alpha}^{*}(\omega) \right). \tag{2.23}$$

The dissipator $\mathcal{D}$ in Eq. (2.19) encodes the information of how much the evolution of the reduced system is altered by surrounding environment by the rates $\gamma_{\alpha\beta}$. More concretely, the dissipation rates $\gamma_{\alpha\beta}$ are given by the real part of the bath correlation functions

$$\gamma_{\alpha\beta}(\omega) = \Gamma_{\alpha\beta}(\omega) + \Gamma_{\beta\alpha}^{*}(\omega) \tag{2.24}$$

They are the characteristic decay rates of a system in contact with a bath. Some of the components correspond to, e.g., the relaxation and decoherence times T_1 and T_2 of the decay of a magnetic moments coupled to an environment.
Eq. (2.19) is the most general equation which describes the quantum dynamics of a system which ensures a completely positive and trace preserving (CPTP) map. This was first shown independently by Lindblad [61] as well as by Gorini, Kossakowski and Sudarshan [62]. Positivity means that the eigenvalues of a matrix are real and positive. The density matrix is a statistical operator and its eigenvalues correspond to the probability of a certain state. It is therefore crucial to preserve positivity during the time evolution. Due to the statistical nature of the density matrix one has to find the system it describes in some state. Consequently, the trace of the density matrix must be normalised to a constant. This physical property must also be preserved during the time evolution. When deriving a quantum master equation, no matter which approach is chosen, we need to make sure that the master equation is a CPTP map, at least for the time within the regime of validity.

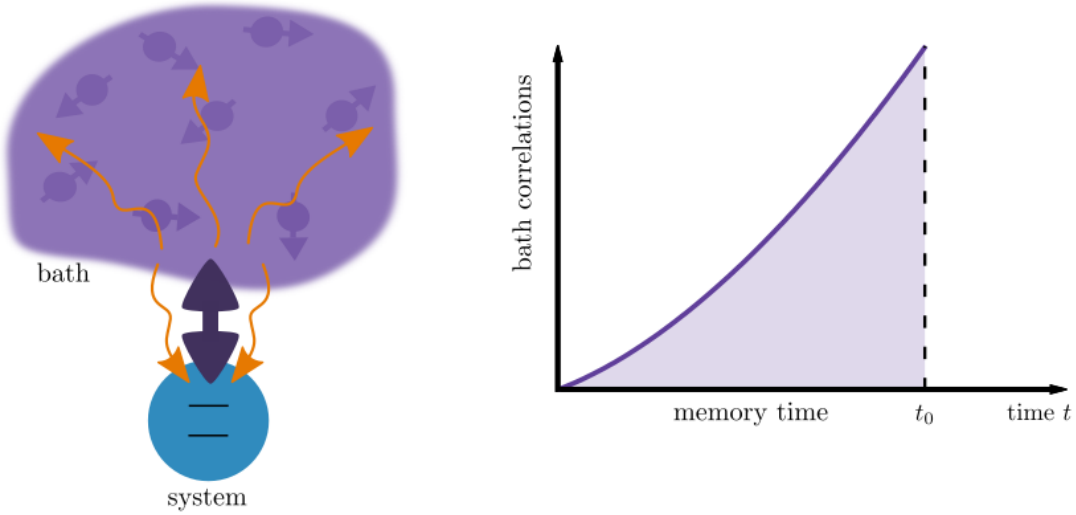

Figure 2.3: On the left we again sketch a small quantum system coupled to large reservoir, similar to Fig. 2.2. Stepping away from the Markov approximation the induced excitations in bath indicated by the orange wavy lines can impact the system dynamics through memory effects, specifically a coherent backaction. The correlations within the bath decay on a finite time scale set by the memory time, which is not much smaller than the characteristic time scale of the system evolution, as shown on the right. Therefore the system's evolution is affected by the whole history of bath correlations up to the time t_0.

2.1.1 Beyond Lindblad and Born-Markov master equations

Dynamics described by a master equation that goes beyond the Born-Markov approximation are generally termed as non-Markovian dynamics [59, 60]. A master equation that describes the dynamics of the quantum system beyond the Lindblad description Eq. (2.19) is easily obtained from Eq. (2.16). Replacing the reduced density system $\rho(t')$ by $\rho(t)$ we arrive at the Redfield equation [91]

$$\frac{d}{dt}\rho_S(t) = -\int_{t_0}^{t} dt' \, \mathrm{Tr}_B \left\{ \left[\hat{H}_{\mathrm{int}}(t), \left[\hat{H}_{\mathrm{int}}(t'), \rho_S(t) \otimes \rho_B \right] \right] \right\}. \tag{2.25}$$

The Redfield equation is local in time, nonetheless it sill captures some of the bath correlations that build up over time. Unlike the Born-Markov approximation, it takes into account the current time in the integration limit and therefore the bath correlation maintain a time-dependence. Not only the current state of the bath is relevant but also the history of the bath correlation building up over a memory time τ_M affect the system's dynamics which is sketched in Fig. 2.3. Other time-local approaches lead to Lindblad-like equations of motion, where the rates are allowed to be time-dependent and therefore they are able to capture more complicated dynamics [71, 74, 76]. If one takes into account the

full history of the system, i.e., the state of the density matrix at the current time does depend on all past times, as in Eq. (2.16), one arrives at generalised quantum master equations such as the Nakajima-Zwanzig equation [67, 68]. We will derive the Nakajima-Zwanzig equation using the projection operator technique in detail in Section 2.2, which is the starting point for the investigations presented in this thesis. In the Nakajima-Zwanzig equation the effects of the whole history of the system-bath coupling enter intuitively through a memory kernel which connects different times. Solving the dynamics in a time-nonlocal description is generally difficult. We will be able to sidestep this difficulty by analysing the equation of motion in Laplace space [64, 71]. Within the projection operator approach it is also possible to derive a time-convolutioness master equation local in time [56, 75, 76, 92]. To find a solution the inverse of an operator is required which does not always have a unique solution [56].

Other perturbative approaches include reaction coordinate and collision models [93]. Here, one (or a few) modes from the environment are incorporated into the quantum system itself. Within this enlarged system, the system-bath dynamics are treated more carefully. Closely related is the idea to map the bath degrees of freedom onto an semi-infinite chain [94]. Apart from the projection operator technique, master equations can be formulated within a field-theoretical approach. Historically, this was done for quantum systems with harmonic environments. They rely on a path integral formalism [72], utilising the Feynman-Vernon influence functional [66], to capture dynamics beyond the Markovian regime [73]. Combining these ideas with an efficient setup of tensor networks [95, 96] led to powerful computational approaches to simulate the dynamics in open quantum systems [97–99], even for fermionic environments [86].

For any type of generalised master equations based on a perturbative approach there is no unambiguous procedure to ensure that the evolution of system under a master equation beyond a Lindblad description maintains the positivity of the density matrix [100] and one has to rely on case to case studies [74, 101, 102]. In the past few years, an enormous theoretical effort was made to classify non-Markovian dynamics and find suitable measure which determine the degree of non-Markovianity as well as make the definition of non-Markovian dynamics more rigorous [59, 101, 103] in order to understand the conditions for a CPTP evolution.

With the growing understanding of non-Markovian dynamics the idea to exploit memory effect is plausible. For example, non-Markovian dynamics have been shown to lead to noise cancellation [34] as well as playing a role in quantum information error correction protocols [104] or modifying the Stark shift [105]. On the experimental side, non-Markovian effects are measurable [49, 106], which hopefully enables us to employ non-Markovianty in quantum thermal machines [50, 52, 107–110]. These are only a few

examples and we will come back to them and expand further throughout this work.

2.1.2 Initial slip

Non-Markovian dynamics can only occur on short time scales or when the environment is small, when quantum fluctuations dominate over temperature induced fluctuations as they destroy any coherence. However, after this short time which is the memory time τ_M of the system, the evolution becomes Markovian. The memory time τ_M is set by an energy scale within the system, e.g., the temperature T. Instead of finding a general quantum master equation that would correctly describe the short time behaviour during the memory time of the system, one can try to formulate a modified, effective Markovian master equation. This master equation then is only valid for times $t > \tau_M$. It takes into account non-Markovian or short-time effects by an initial slip of the time evolution of the density matrix. Originally, the slippage scheme was introduced as a procedure to maintain the positivity of the density matrix evolution [111–113]. The initial slip is defined by the offset between the real initial value of the density matrix and the initial value of the effective evolution

$$\rho_S(0) - \rho_{\text{eff}}(0). \tag{2.26}$$

To determine the initial slip one compares the full dynamics of the reduced density matrix

$$\rho_S(t) = e^{L_{\text{full}}t}\rho_S(0) \tag{2.27}$$

and the effective dynamics under the evolution of the Liouvillian L_{eff}

$$\rho_S^{\text{eff}}(t) = e^{L_{\text{eff}}t}\rho_S^{\text{eff}}(0). \tag{2.28}$$

The idea of the initial slip is sketched in Fig. 2.4. The orange line marks the correct evolution of $\rho_s(t)$ under the full Liouvillian L_{full} according to Eq. (2.27). The effective, Markovian evolution defined in Eq. (2.28) is shown in purple. For times beyond the memory time, $t > \tau_M$, both density matrices Eqs. (2.27) and (2.28) have the same time evolution. They only differ at short times for $t < \tau_M$ and the offset in Eq. (2.26) at $t = 0$ defines the initial slip. The initial conditions for both density matrices fulfil the relation

$$\rho_{\text{eff}}(0) = \mathcal{S}\rho_S(0). \tag{2.29}$$

where the slippage operator $\mathcal{S}$ was introduced [114, 115]. The slippage modifies the initial condition of the evolution. Since the evolution is the same for long times the dynamics for

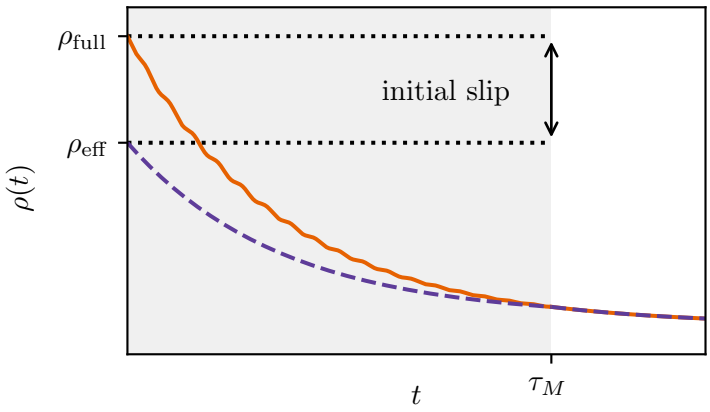

Figure 2.4: The time evolution of the density matrix is sketched. Evolution under L_{full} is shown by the orange line, and the effective evolution is represented by the dashed, purple curve. Adjusting the initial condition for the effective evolution by an initial slip leads to the recovery of correct evolution for times $t > \tau_T$. For $t < \tau_M$ the effective evolution does not bear any physical meaning.

the reduced density matrix can be approximated with the evolution under the effective Liouvillian

$$\rho_S(t) \approx e^{L_{\text{eff}}t}\mathcal{S}\rho_S(0). \tag{2.30}$$

The form of the slippage operator S depends on the actual physical system. It encodes the difference of the bath correlation functions at short and long times. The non-Markovian effects are thus hidden in the slippage. Taking them into account effectively leads to a modified initial condition Eq. (2.29). The evolution under the effective dynamics with the modified initial condition makes sure that the evolution is physical and the correct one, but only for times $t > \tau_M$. As a simple example for an initial slip, we assume the effective evolution to be Markovian, and the dynamics of a single component of the density matrix is an exponential decay, similar to [74],

$$\rho_{\text{eff}}(t) = e^{-\gamma t}\rho_S^{\text{eff}}(0) \tag{2.31}$$

where the rates γ are given by the bath correlation functions as in Eq. (2.24) for a specific system. For the full quantum dynamics, that are also valid for times shorter than the memory time τ_T, in a time-local form of the time evolution might be given by

$$\dot{\rho}_S(t) = -\gamma'(t)\rho_S(t), \tag{2.32}$$

with the solution

$$\rho_S(t) = e^{-\int_0^t dt' \gamma'(t')} \rho_S(0) \tag{2.33}$$

where the rates γ' are time-dependent and capture non-Markovian effects. Equating Eqs. (2.32) and (2.33) at long times allows us to read off the appropriate initial slip

$$\rho_S^{\text{eff}}(0) = \exp\left[\left(-\int_0^t dt' \gamma'(t') + \gamma\right) t\right] \rho_S(0). \tag{2.34}$$

Initial slips are discussed in the literature as a mechanism to avoid a non-positive map when deriving a master equation from a microscopic Hamiltonian, e.g. via projection operator techniques [111–114, 116]. However, one needs to keep in mind that the initial slip does not have any quantitative information about the short time dynamics in the system [74]. The effective evolution is only physical for times larger than the memory time. Later on, we will use the initial slip to describe the offset between the Markovian dynamics and the full quantum dynamics in the spirit of Eq. (2.26), although we will have access to the full dynamics.

2.2 Nakajima-Zwanzig equation

In this section we introduce the generalised quantum master equation known as the Nakajima-Zwanzig equation [67, 68]. It is a time-nonlocal equation of motion for the reduced density matrix and explicitly takes into account the quantum correlations building up due to the system-bath interaction in time. Therefore, this master equation captures coherent backaction effects between the system and the bath which will lead to non-Markovian dynamics on short time scales. The Nakajima-Zwanzig equation forms the starting point to calculate the dynamics of an example system in Chapter 3. The following derivation is based on a projection operator method and it follows the references [56, 65]. First, we consider the full density matrix $\rho(t)$ of a system-environment structure and assume it can be split into a relevant and an irrelevant part [65, 68]

$$\rho(t) = \rho_{\text{rel}}(t) + \rho_{\text{irr}}(t). \tag{2.35}$$

The relevant part of the density matrix ρ_{rel} captures slow fluctuations while the rapidly fluctuating contribution is described by the irrelevant part ρ_{irr}. Later on, in the open quantum system setting, ρ_{rel} will correspond to the system part and ρ_{irr} is associated with the environment degrees of freedom. The aim is to be able to write the expectation

value of any observable A only in terms of the relevant part ρ_{rel} such that

$$\langle A \rangle = \mathrm{Tr}\left\{A\rho(t)\right\} = \mathrm{Tr}\left\{A\rho_{\mathrm{rel}}(t)\right\}, \tag{2.36}$$

with the trace over all degrees of freedom and consequently

$$\mathrm{Tr}\left\{A\rho_{\mathrm{irr}}(t)\right\} = 0. \tag{2.37}$$

It can formally be achieved by introducing a projection operator P. The linear map P is required to project onto the relevant subspace of the Hilbert space such that Eq. (2.36) is true and

$$\langle A \rangle = \mathrm{Tr}\left\{A\rho(t)\right\} = \mathrm{Tr}\left\{AP\rho(t)\right\}. \tag{2.38}$$

is satisfied. To be able to address all remaining states in the given Hilbert space, the complement Q of the projection P is defined with

$$P + Q = \mathbb{1}. \tag{2.39}$$

Furthermore, the projections P and Q satisfy

$$P^2 = P \tag{2.40}$$

$$Q^2 = Q, \tag{2.41}$$

and combing this with Eq. (2.39) it follows directly that

$$PQ = QP = 0. \tag{2.42}$$

The action of the operators P and Q projection onto different part of the density matrix is sketched in Fig. 2.5. The aim is, to derive an equation for the reduced density matrix related to $P\rho(t)$. The equation of motion for $P\rho$ as well as $Q\rho$ follow from the von Neumann Eq. (2.2) and we obtain

$$\frac{d}{dt}P\rho = PL\rho(t) = PLP\rho(t) + PLQ\rho(t), \tag{2.43}$$

$$\frac{d}{dt}Q\rho = QL\rho(t) = QLP\rho(t) + QLQ\rho(t), \tag{2.44}$$

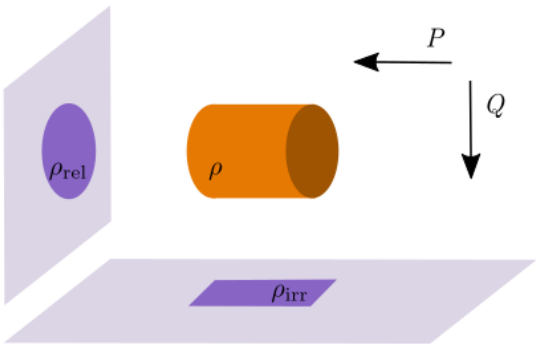

Figure 2.5: Sketch of the action of the operators P and Q which project onto the relevant and irrelevant part of the density matrix ρ.

where we used the identity Eq. (2.39) in the second step. The Liouvillian $L = -i[H, \cdot]$ is defined via the time-independent Hamiltonian H

$$H = H_0 + H_{\text{int}} \tag{2.45}$$

with the free system-bath Hamiltonian $H_0 = H_S + H_B$ and the interaction term H_{int} as before. Now we find a formal solution of Eq. (2.44) which is then inserted into Eq. (2.43). A formal solution of Eq. (2.44) can be found by introducing an integrating factor $h(t, t_0)$ such that

$$h(t, t_0)\frac{d}{dt}Q\rho(t) - h(t, t_0)QLQ\rho(t) = h(t, t_0)QLP\rho(t). \tag{2.46}$$

The function $h(t, t_0)$ itself is defined via the differential equation [68]

$$\frac{d}{dt}h(t, t_0) = -h(t, t_0)QL. \tag{2.47}$$

The inverse $h^{-1}(t, t_0)$ of its general solution is often identified as a time propagator [56]

$$h^{-1}(t, t_0) = G(t, t_0) = \hat{T} \exp\left[\int_{t_0}^{t} dt' QL\right], \tag{2.48}$$

where we introduced the time-ordering operator $\hat{T}$, which orders its arguments chronologically. Since here the Liouvillian L is time-independent the time propagator reduces to

$$G(t, t_0) = e^{QL(t-t_0)} \quad \text{and} \quad G(t_0, t_0) = 1. \tag{2.49}$$

Thus, the differential equation Eq. (2.46) can be written as

$$\frac{d}{dt}\left(h(t,t_0)Q\rho(t)\right) = h(t,t_0)QLP\rho(t). \tag{2.50}$$

Using the definition of the time propagator above the solution is given by [65, 68]

$$\begin{aligned} Q\rho(t) &= G(t,t_0)Q\rho(t_0) + \int_{t_0}^{t} dt'\, G(t,t')QLP\rho(t') \\ &= Qe^{LQ(t-t_0)}\rho(t_0) - \int_{t_0}^{t} dt'\, Qe^{LQ(t-t')}LP\rho(t'). \end{aligned} \tag{2.51}$$

Thus, we find an explicit expression for the term $Q\rho(t)$. Replacing the corresponding term in Eq. (2.43) we immediately arrive at the Nakajima-Zwanzig equation [67, 68]

$$\frac{d}{dt}P\rho(t) = PLP\rho(t) + PLQe^{LQ(t-t_0)}\rho(t_0) + \int_{t_0}^{t} dt'\, PLQe^{iLQ(t-t')}LP\rho(t'). \tag{2.52}$$

This equation is a closed equation of motion for the relevant part of the system $\rho_{\mathrm{rel}}(t)$ closely related to projection of the full density matrix $P\rho(t)$. The notion of relevant and irrelevant parts provides the formal background and is generally applicable [65]. For open systems, as considered here, the splitting comes quite naturally between system and bath. In addition this will allow us to do a few more useful transformations. We are interested in the system dynamics for which the reduced density matrix

$$\rho_S(t) = \mathrm{Tr}_B\left\{\rho(t)\right\}, \tag{2.53}$$

is sufficient. A good choice for the projector P is then

$$P(\cdot) = \mathrm{Tr}_B\left\{\cdot\right\} \otimes \rho_B, \tag{2.54}$$

where ρ_B is the reduced density of the environment and the trace is taken over the bath degrees of freedom. In a physical setup the initial state is often prepared and brought in contact with the environment at t_0. Therefore, there are no correlations between the system and bath at t_0. The initial state for the full density matrix can be chosen as product state between system and bath

$$\rho(t_0) = \rho_S(t_0) \otimes \rho_B(t_0). \tag{2.55}$$

Consequently, $P\rho(t_0) = \rho(t_0)$ and the second term in Eq. (2.52) is zero. Just as the Hamiltonian can be split into its constituent parts, the Liouvillian superoperator L can

be written as

$$L = L_0 + L_{\text{int}}, \tag{2.56}$$

with $L_0 = L_S + L_B$. Inserting this into Eq. (2.52) the first term reduces to $P(L_S + L_{\text{int}})P\rho_S(t)$ as $PL_BP = 0$. The initial bath state is often taken to be thermal Gibbs state in equilibrium. As the interaction H_{int} usually induces an excitation in the bath we require odd moments of the interaction Liouvillian to vanish

$$PL_{\text{int}}P = 0, \tag{2.57}$$

and the first term of Eq. (2.52) reduces to $PL_SP\rho(t)$. Otherwise it would violate conservation laws like energy or particle conservation within the system. Furthermore, the combination PLQ is only non-zero for the interaction part, $PLQ = PL_{\text{int}}Q$ and correspondingly $QLP = QL_{\text{int}}P$ according to Eq. (2.42). In the integral of the last term in Eq. (2.52), the time evolution involving the Q projection can be written as [65]

$$Qe^{LQt} = Q^2e^{LQt} = Qe^{QLt}Q. \tag{2.58}$$

Using these relations and tracing over the bath degrees of freedom, the Nakajima-Zwanzig equation for the reduced density matrix ρ_S of an open quantum system reads

$$\dot{\rho_S}(t) = L_S\rho_S(t) + \int_{t_0}^{t} dt' \,\text{Tr}_B \left\{ L_{\text{int}} Q e^{iQL(t-t')} L_{\text{int}} \rho_S(t') \otimes \rho_B \right\}. \tag{2.59}$$

The Nakajima-Zwanzig equation is an exact quantum master equation to all orders in the interaction which takes into account temporal correlations and their history. Unfortunately, at this point it only presents a formal solution and cannot provide any detailed insight into the system dynamics. The integro-differential equation is hard to solve with the difficulty hidden in the time-convolution of the integrand. The evolution operator $\exp[iQL(t-t')]$ encodes the build up of the bath correlation functions over time. Defining the memory kernel

$$\Sigma(t-t')(\cdot) = \text{Tr}_B \left\{ L_{\text{int}} Q e^{iQL(t-t')} L_{\text{int}} \rho_B \otimes (\cdot) \right\} \tag{2.60}$$

Eq. (2.59) becomes

$$\dot{\rho_S}(t) = L_S\rho_S(t) + \int_{t_0}^{t} dt' \,\Sigma(t-t')\rho_S(t'). \tag{2.61}$$

This last equation will be the starting point in the following to employ further approximations to the Nakajima-Zwanzig equation.

2.2.1 Born approximation of Nakajima-Zwanzig equation

In the weak coupling limit Eq. (2.61) can be expanded in the interaction strength. The time evolution operator $\exp[QL(t-t')]$ obeys the Schwinger-Dyson equation [65]

$$e^{Q(L_0+L_{\rm int})t} = e^{QL_0t} + \int_0^t dt'\, e^{QL_0(t-t')} Q L_{\rm int} e^{QLt'}, \tag{2.62}$$

where $L_0 = L_S + L_B$ is the unperturbed Liouvillian. The identity provides a controlled way to expand the memory kernel Eq. (2.60) to arbitrary orders in the interaction strength. The expansion is perturbative in the interaction Hamiltonian $H_{\rm int}$ but we stress that there is no assumption on the time evolution and all memory effects are taken into account. Up to second order in the interaction the memory kernel is then given by

$$\Sigma^{(2)}(t-t')(\cdot) = \mathrm{Tr}_B \left\{ L_{\rm int} Q e^{QL_0(t-t')} L_{\rm int} \rho_B \otimes (\cdot) \right\}. \tag{2.63}$$

Using the identity $\mathbb{1} - P = Q$ and the fact, the projection P has no effect inside the trace the Born approximation of the memory kernel reduces to

$$\Sigma^{(2)}(t-t')(\cdot) = \mathrm{Tr}_B \left\{ L_{\rm int} e^{L_0(t-t')} L_{\rm int} \rho_B \otimes (\cdot) \right\}. \tag{2.64}$$

Inserting this expression back into the full Nakajima-Zwanzig equation (2.61)

$$\dot\rho_S(t) = L_0\rho_S(t) + \int_{t_0}^t dt'\, \mathrm{Tr}_B \left\{ L_{\rm int} e^{L_0(t-t')} L_{\rm int} \rho_B \otimes \rho_S(t') \right\}, \tag{2.65}$$

or

$$\dot\rho_S(t) = L_0\rho_S(t) + \int_{t_0}^t dt'\, \Sigma^{(2)}(t-t')\rho_S(t'). \tag{2.66}$$

In Chapter 3 we will use this last equation as the starting point to employ further approximations to the Nakajima-Zwanzig equation and study the dynamics of a single spin embedded in an electronic environment. Taking into account all memory effects we determine the full quantum coherent dynamics in detail.

We can now connect the Nakajima-Zwanzig equation to the Markovian formulation in Section 2.1. Assuming that the correlations in the bath decay sufficiently fast and therefore faster then any correlations in the system, the interaction between bath and system is instantaneous and does not depend on the history of the joint evolution. This

is the Markov approximation and the reduced density matrix of the system ρ_S within the integral is again taken to be

$$\rho_S(t') \to \rho_S(t). \tag{2.67}$$

Adjusting the integration limits in the same way as in Section 2.1, the equation of motion within the Born-Markov approximation reads

$$\dot{\rho}_S(t) = L_0\rho_S(t) + \int_0^\infty dt' \,\mathrm{Tr}_B \left\{ L_{\mathrm{int}} e^{L_0(t-t')} L_{\mathrm{int}} \rho_B \right\} \rho_S(t). \tag{2.68}$$

This equation corresponds to Eq. (2.17) after transforming into the interaction picture. Similarly, the Redfield master equation in Eq. (2.25) is recovered by only changing the time index of the reduced density matrix according to Eq. (2.67).

2.3 Self-consistent projection operator method

In this section a generalised master equation based on the projection operator method is derived. However, in contrast to the derivation of the Nakajima-Zwanzig equation (2.59), the projection operator itself is time-dependent. The result will be a self-consistent master equation similar to the Nakajima-Zwanzig equation which was proposed by Degenfeld-Schonburg and Hartmann [38]. In contrast to the Nakajima-Zwanzig equation, the bath reference state has a time dependence. It is constantly updated and takes into account the changes in the environment. The derivation presented here follows the derivation in the appendix of the original paper [38].

The starting point is the setup that a quantum system, possibly in its own environment, is coupled to (many) other quantum systems, which are essentially copies of the first one. One can think of a lattice with some coordination number and a single quantum system at each lattice point, sketched in Fig. 2.6 for a single impurity spin in an electron spin bath. Then we are interested in the dynamics of one of the systems, e.g. system S_0, in contact with all the other ones. All other systems act as bath to the system of interest labelled S_0. The time-dependent projections will lead to a reference bath state which is self-consistently determined by all local dynamics in each subsystem S_n. The starting point for the equation of motion for the full density matrix is once again given by the von Neumann equation

$$\dot{\rho}(t) = L\rho(t), \tag{2.69}$$

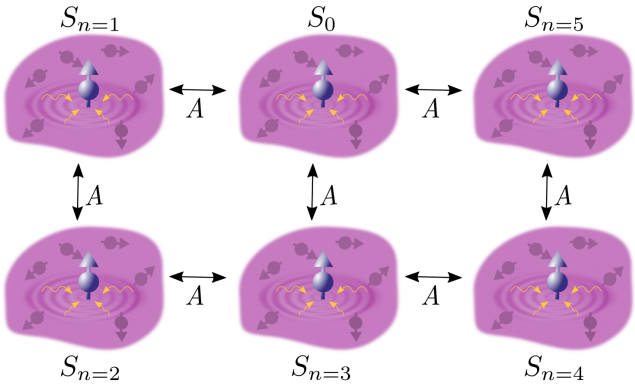

Figure 2.6: Sketch of an array of coupled quantum system, for example an impurity spin in an electronic spin bath. Each localised spin is incorporated in its own environment and each of the subsystems has some local dynamics, possibly including memory effects which are indicated by the ripples and wavy lines. One subsystem is chosen as system of interest, here S_0, and all other systems S_n act as a bath for S_0. They interact with each other by some coupling A.

where the Liouvillian superoperator is by

$$L = L_0 + L_{\text{int}} = \sum_{n=0}^{N} L_{S_n} + L_{\text{int}}. \tag{2.70}$$

The Liouvillian L_0 is given by the sum of all Liouvillians L_{S_n} containing the eigendynamics for each subsystem S_n. The interaction between the subsystems of coupling strength A can be split into the interaction terms that are directly in contact with the system of interest S_0 and all other interactions between the subsystems deep within the bath

$$L_{\text{int}} = \sum_{n=1}^{Z} L_{\text{int}}^{S_0,S_n} + L_{\text{int}}^{\not S_0}. \tag{2.71}$$

Throughout we use the notation $\not S_j$ to denote all subsystems excluding the system S_j. Instead of having a generic bath made of fermionic or bosonic modes, here the environment formed by the neighbouring quantum systems is allowed to have more structure. Each system can have its own local dynamics, indicated by the ripples and wavy arrows in Fig. 2.6. As in the case for the time-independent projection operators we want to find an equation of motion for the relevant part of the density matrix, i.e., the reduced density matrix of the system in which we are interested. The projection operator P is now defined as

$$P_t^{S_0}(\cdot) = \text{Tr}_{\not S_0}\{\cdot\} \otimes \rho_{\not S_0}, \tag{2.72}$$

where the projection P carries a time index. All subsystems $\not{S}_0$ act as bath to the system of interest S_0. The density matrix for all systems acting as the environment is assumed to be a product state of all individual systems

$$\rho_{\not{S}_0}(t) = \bigotimes_{S_n \neq S_0} \rho_{S_n}(t). \tag{2.73}$$

Each reduced density matrix is self-consistently defined as

$$\rho_{S_n} = \mathrm{Tr}_{\not{S}_n} \{\rho(t)\} \tag{2.74}$$

at all times t. The complement $Q_t^{S_0}$ to the projection $P_t^{S_0}$ is

$$Q_t^{S_0} = \mathbb{1} - P_t^{S_0}. \tag{2.75}$$

Both projections obey the relations

$$\left(P_t^{S_0}\right)^2 = P_t^{S_0}, \tag{2.76}$$

$$\left(Q_t^{S_0}\right)^2 = Q_t^{S_0}, \tag{2.77}$$

$$P_t^{S_0} Q_t^{S_0} = Q_t^{S_0} P_t^{S_0} = 0, \tag{2.78}$$

similar to the relations in Section 2.2. Additionally,

$$\dot{P}_t^{S_0} = -\dot{Q}_t^{S_0}, \tag{2.79}$$

$$\dot{P}_t^{S_0} Q_t^{S_0} = -\dot{Q}_t^{S_0} P_t^{S_0} = 0. \tag{2.80}$$

The first identity follow directly from the definition Eq. (2.75), the second can be proven by utilising the first one, a full proof can be found in Appendix A. Each projector concerns only a single subsystem such that there is no need for a special relation between the projectors for different subsystems. To find an equation of motion for the reduced density matrix ρ_{S_0} defined via the projection $P_t^{S_0}$

$$\begin{aligned} P_t^{S_0}\rho(t) &= \mathrm{Tr}_{\not{S}_0} \{\rho(t)\} \otimes \rho_{\not{S}_0}(t) \\ &= \rho_{S_0}(t) \otimes \bigotimes_{S_n \neq S_0} \rho_{S_n}(t), \end{aligned} \tag{2.81}$$

we start with the von Neumann equation Eq. (2.69) for the relevant part and the irrelevant

part of the density matrix

$$\frac{d}{dt}\left(P_t^{S_0}\rho(t)\right) = \left(\dot{P}_t^{S_0} + P_t^{S_0}L\right)P_t^{S_0}\rho(t) + P_t^{S_0}LQ_t^{S_0}\rho(t) \tag{2.82}$$

$$\frac{d}{dt}\left(Q_t^{S_0}\rho(t)\right) = \left(-\dot{P}_t^{S_0} + Q_t^{S_0}L\right)P_t^{S_0}\rho(t) + Q_t^{S_0}LQ_t^{S_0}\rho(t). \tag{2.83}$$

As before, the aim is to find a solution to Eq. (2.83). However, in contrast to the derivation of the Nakajima-Zwanzig equation, we need an expression for $\dot{P}_t^{S_0}P_t^{S_0}\rho(t)$, where

$$\begin{aligned}\dot{P}_t^{S_0}(\cdot) &= \frac{d}{dt}\left[\mathrm{Tr}_{\not S_0}\{\cdot\}\otimes\rho_{\not S_0}(t)\right] \\ &= \mathrm{Tr}_{\not S_0}\{\cdot\}\otimes\left(\frac{d}{dt}\rho_{\not S_0}(t)\right),\end{aligned} \tag{2.84}$$

to proceed. This term can be written as

$$\begin{aligned}\dot{P}_t^{S_0}P_t^{S_0}\rho(t) &= \mathrm{Tr}_{\not S_0}\{\rho(t)\}\otimes\left(\frac{d}{dt}\mathrm{Tr}_{\not S_n}\{\rho(t)\}\right) \\ &= \rho_{S_0}(t)\otimes\dot{\rho}_{\not S_0}(t).\end{aligned} \tag{2.85}$$

The last part is a short hand for the time derivative for the all reduced density matrices that act as a bath to the system S_0

$$\dot{\rho}_{\not S_0}(t) = \sum_{S_j\neq S_0}\dot{\rho}_{S_j}(t)\otimes\bigotimes_{S_n\neq S_j}\rho_{S_n}(t). \tag{2.86}$$

Including the reduced density matrix $\rho_{S_0}(t)$ for the system of interest we arrive at

$$\dot{P}_t^{S_0}P_t^{S_0}\rho(t) = \sum_{S_j\neq S_0}\mathrm{Tr}_{\not S_j}\{\dot{\rho}(t)\}\otimes\bigotimes_{S_n\neq S_j}\rho_{S_n}(t). \tag{2.87}$$

The equation of motion for the full density matrix $\rho(t)$ is determined by the von Neumann equation and we can substitute in the full Liouvillian L in the derivative

$$\begin{aligned}\mathrm{Tr}_{\not S_j}\{\dot{\rho}(t)\} &= \mathrm{Tr}_{\not S_j}\left\{\left(\sum_{k=1}^{N}L_{S_k} + L_{\mathrm{int}}\right)\rho(t)\right\} \\ &= \mathrm{Tr}_{\not S_j}\left\{\sum_{k=1}^{N}L_{S_k}\rho(t)\right\} + \mathrm{Tr}_{\not S_j}\left\{L_{\mathrm{int}}\rho(t)\right\}.\end{aligned} \tag{2.88}$$

Splitting the traces of the first term leads to

$$\mathrm{Tr}_{\not S_j}\left\{\sum_{k=1}^{N} L_{S_k}\rho(t)\right\} = \mathrm{Tr}_{\not S_j}\left\{\sum_{k=1,k\neq j}^{N} L_{S_k}\rho(t)\right\} + \mathrm{Tr}_{\not S_j}\left\{L_{S_j}\rho(t)\right\}, \tag{2.89}$$

where

$$\mathrm{Tr}_{\not S_j}\left\{\sum_{k=1,k\neq j}^{N} L_{S_k}\rho(t)\right\} = 0. \tag{2.90}$$

To show that this identity holds, we consider a single trace for simplicity

$$\mathrm{Tr}_{S_k}\left\{L_{S_k}\rho(t)\right\} = -i\mathrm{Tr}_{S_k}\left\{[H_k,\rho]\right\}. \tag{2.91}$$

Expanding in the eigenstates e_k, e_k' of the system S_k the trace can be expressed as

$$\mathrm{Tr}_{S_k}\left\{L_{S_k}\rho(t)\right\} = -i\sum_{e_k,e_k'}\left(\langle e_k|H_k|\ e_k'\rangle\langle e_k'|\rho(t)|e_k\rangle - \langle e_k|\rho(t)|\ e_k'\rangle\langle e_k'|H_k|e_k\rangle\right). \tag{2.92}$$

In the eigenbasis the factor $\langle e_k|H_k|\ e_k'\rangle$ commutes with the density matrix term such

$$\begin{aligned}\mathrm{Tr}_{S_k}\left\{L_{S_k}\rho(t)\right\} &= -i\sum_{e_k,e_k'}\left(\langle e_k|H_k|\ e_k'\rangle\langle e_k'|\rho(t)|e_k\rangle - \langle e_k'|H_k|e_k\rangle\langle e_k|\rho(t)|\ e_k'\rangle\right)\\ &= -i\sum_{e_k,e_k'}\langle e_k|H_k|e_k'\rangle\left(\langle e_k'|\rho(t)|e_k\rangle - \langle e_k'|\rho(t)|e_k\rangle\right)\\ &= 0.\end{aligned} \tag{2.93}$$

Then, Eq. (2.90) holds as the above relation is valid for all individual subsystems S_k. Returning to Eq. (2.88), we obtain

$$\begin{aligned}\mathrm{Tr}_{\not S_j}\left\{\dot\rho(t)\right\} &= \mathrm{Tr}_{\not S_j}\left\{L_{S_j}\rho(t)\right\} + \mathrm{Tr}_{\not S_j}\left\{L_{\mathrm{int}}\rho(t)\right\}\\ &= L_{S_j}\rho_{S_j}(t) + \mathrm{Tr}_{\not S_j}\left\{L_{\mathrm{int}}\rho(t)\right\},\end{aligned} \tag{2.94}$$

where we used that in the first term the operator L_{S_j} only acts on the subsystem S_j and is therefore unaffected by trace over all degrees of freedom in all other subsystems. Finally, we find an expression for $\dot P_t^{S_0}P_t^{S_0}\rho(t)$ by substituting Eq. (2.94) into Eq. (2.87)

$$\dot P_t^{S_0}P_t^{S_0}\rho(t) = \sum_{S_j\neq S_0}\left(L_{S_j}\rho_{S_j}(t) + \mathrm{Tr}_{\not S_j}\left\{L_{\mathrm{int}}\rho(t)\right\}\right)\otimes\bigotimes_{S_n\neq S_j}\rho_{S_n}(t). \tag{2.95}$$

To ease the notation we define a new projection operator

$$\begin{aligned} P_t^{\not S_0}(\cdot) &= \sum_{S_j \neq S_0} P_t^{S_j}(\cdot) \\ &= \sum_{S_j \neq S_0} \bigotimes_{S_j \neq S_n} \rho_{S_j}(t) \otimes \mathrm{Tr}_{\not S_j}\{\cdot\}, \end{aligned} \tag{2.96}$$

and the final expression for $\dot{P}_t^{S_0} P_t^{S_0}$ can be written as

$$\begin{aligned} \dot{P}_t^{S_0} P_t^{S_0} \rho(t) &= L_{\not S_0} P_t^{S_0} \rho(t) + P_t^{\not S_0} L_{\mathrm{int}} \rho(t) \\ &= L_{\not S_0} P_t^{S_0} \rho(t) + P_t^{\not S_0} L_{\mathrm{int}} \left(P_t^{S_0} + Q_t^{S_0} \right) \rho(t). \end{aligned} \tag{2.97}$$

Substituting Eq. (2.97) into the equation of motion for the irrelevant part in of the density matrix $Q_t^{S_0}\rho(t)$ in Eq. (2.83) leads to

$$\frac{d}{dt}\left(Q_t^{S_0}\rho(t)\right) = \left(-L_{\not S_0} - P_t^{\not S_0} L_{\mathrm{int}} + Q_t^{S_0} L\right) P_t^{S_0}\rho(t) + \left(-P_t^{\not S_0} L_{\mathrm{int}} + Q^{S_0} L\right) Q_t^{S_0}\rho(t). \tag{2.98}$$

To simplify this further we make use of the fact that $\mathrm{Tr}_{S_n}\{L_{S_n}\cdot\} = 0$, as seen in Eq. (2.93), and that $P_t^{S_0} L_{S_0} = L_{S_0} P_t^{S_0}$ which follows directly from the definition of the projection as L_{S_0} only acts on subsystem S_0. The equation of motion of $Q_t^{S_0}\rho(t)$ is therefore

$$\frac{d}{dt}\left(Q_t^{S_0}\rho(t)\right) = \mathcal{C}_t L_{\mathrm{int}} P_t^{S_0}\rho(t) + \left(\mathcal{C}_t L_{\mathrm{int}} + L_0\right) Q_t^{S_0}\rho(t), \tag{2.99}$$

with $L_0 = \sum_{S_n} L_{S_n}$ and where we defined the superoperator

$$\mathcal{C}_t = -P_t^{\not S_0} + Q_t^{S_0} = \mathbb{1} - \sum_{S_n} P_t^{S_n}. \tag{2.100}$$

We can formally solve the differential equation by introducing an integrating factor as previously in Eq. (2.46). Here, the function $h(t, t_0)$ has to satisfy

$$\frac{d}{dt} h(t, t_0) Q_t^{S_0}\rho(t) = -h(t, t_0)\left(\mathcal{C}_t L_{\mathrm{int}} + L_0\right) Q_t^{S_0}\rho(t). \tag{2.101}$$

The function $h(t, t_0)$ again takes the form of a time propagator given by

$$h^{-1}(t, t_0) = G(t, t_0) = T_{\leftarrow} \exp\left[\int_{t_0}^{t} dt' \left(\mathcal{C}_{t'} L_{\mathrm{int}} + L_0\right)\right], \tag{2.102}$$

with the chronological time-ordering operator $T_{\leftarrow}$ and the solution of Eq. (2.99) then

reads

$$Q_t^{S_0}\rho(t) = G(t,t_0)Q_t^{S_0}\rho(t_0) + \int_{t_0}^{t} dt'\, G(t,t')\mathcal{C}_{t'}L_{\mathrm{int}}P_t^{S_0}\rho(t'). \tag{2.103}$$

In the last step we insert the solution Eq. (2.103) into the equation of motion of the relevant part of the system Eq. (2.82) and trace out all subsystems that act as a bath to the system S_0

$$\begin{aligned}\dot{\rho}_{S_0}(t) = \mathrm{Tr}_{\not S_0}\left\{\dot{P}_t^{S_0}P_t^{S_0}\rho(t)\right\} + \mathrm{Tr}_{\not S_0}\left\{P_t^{S_0}LP_t^{S_0}\rho(t)\right\} \\ + \int_{t_0}^{t} dt' \mathrm{Tr}_{\not S_0}\left\{P_t^{S_0}LG(t,t')\mathcal{C}_{t'}L_{\mathrm{int}}P_t^{S_0}\rho(t')\right\}.\end{aligned} \tag{2.104}$$

The first term vanishes as

$$\mathrm{Tr}_{\not S_0}\left\{\dot{P}_t^{S_0}P_t^{S_0}\rho(t)\right\} = \mathrm{Tr}_{\not S_0}\left\{L_{\not S_0}P_t^{S^0}\rho(t) + P_t^{\not S_0}L_{\mathrm{int}}\rho(t)\right\} = 0, \tag{2.105}$$

and the second one reduces to

$$\begin{aligned}\mathrm{Tr}_{\not S_0}\left\{P_t^{S_0}LP_t^{S_0}\rho(t)\right\} &= \mathrm{Tr}_{\not S_0}\left\{P_t^{S_0}\left(L_{S_0} + L_{\not S_0} + L_{\mathrm{int}}\right)P_t^{S_0}\rho(t)\right\} \\ &= L_{S_0}\rho_{S_0}(t) + \mathrm{Tr}_{\not S_0}\left\{L_{\mathrm{int}}P_t^{S_0}\rho(t)\right\}.\end{aligned} \tag{2.106}$$

Finally, we arrive at a Nakajima-Zwanzig-like closed equation of motion for the reduced density matrix of the subsystem S_0 [38]

$$\dot{\rho}_{S_0}(t) = L_{S_0}\rho_{S_0}(t) + \mathrm{Tr}_{\not S_0}\left\{L_{\mathrm{int}}P_t^{S_0}\rho(t)\right\} + \int_{t_0}^{t} dt' \mathrm{Tr}_{\not S_0}\left\{L_{\mathrm{int}}G(t,t')\mathcal{C}_{t'}L_{\mathrm{int}}P_t^{S_0}\rho(t')\right\}. \tag{2.107}$$

It grants access to the dynamics of a particular subsystem in a many-body quantum system. In addition to the Nakajima-Zwanzig approach Eq. (2.107) correlations within *all* subsystems are captured by the superoperator $\mathcal{C}_t$. The bath reference state formed by the subsystems acting as a bath to the system of interest maintains a time dependence and is determined self-consistently. However, Eq. (2.107) is generally difficult to solve due to the complexity of a time-nonlocal description known from the Nakajima-Zwanzig approach. Additionally, the time propagator or dynamical map $G(t,t')$ in Eq. (2.102) takes a more complicated form as its explicitly depends on the projection C_t. In order to simplify the structure of Eq. (2.107) we expand the time propagator as a Dyson series [38, 65] in powers of the interaction Liouvillian L_{int} which we used before in Eq. (2.62).

This leads to the expression

$$\begin{aligned} G(t,t') &= T\exp\left[\int_{t'}^{t} dt''\,(L_0 + \mathcal{C}_{t''}L_{\mathrm{int}})\right] \\ &= e^{L_0(t-t')} + \int_{t'}^{t} dt''\, e^{L_0(t-t'')}\mathcal{C}_{t''}L_{\mathrm{int}}G(t,t''). \end{aligned} \tag{2.108}$$

Going up to the second order in the interaction corresponds to the Born approximation. Furthermore, we note that L_{int} according to Eq. (2.71) can be split into the terms that directly couple to the system of interest and all other ones. Since we defined the bath reference state as a product state in Eq. (2.73) all terms containing the interaction within the bath $L_{\mathrm{int}}^{\not{S}_0}$ drop out. Only interactions between the system S_0 and its nearest neighbours are relevant, consequently the full interaction Liouvillian L_{int} can be replaced by the relevant terms $L_{\mathrm{int}}^{S_0,S_n}$. Inserting these considerations into Eq. (2.107) we arrive at the master equation

$$\begin{aligned} \dot{\rho}_{S_0}(t) = L_{S_0}\rho_{S_0}(t) &+ \sum_{n=1}^{Z} \mathrm{Tr}_{\not{S}_0}\left\{L_{\mathrm{int}}^{S_0,S_n}P_t^{S_0}\rho(t)\right\} \\ &+ \sum_{n=1}^{Z}\int_{t_0}^{t} dt' \mathrm{Tr}_{\not{S}_0}\left\{L_{\mathrm{int}}^{S_0,S_n}e^{L_0(t-t')}\mathcal{C}_{t'}^{S_0,S_n}L_{\mathrm{int}}^{S_0,S_n}P_t^{S_0}\rho(t')\right\}, \end{aligned} \tag{2.109}$$

where Z is the number of neighbours the system of interest S_0 is directly coupled to. Not only the interaction Liouvillian reduces to the terms of directly coupled subsystems but also the projector $\mathcal{C}_t^{S_0,S_n} = \mathbb{1} - \sum_{\langle S_0 S_n\rangle} P_t^{S_n}$ where the sum only runs over the neighbours. We will use this master equation as a starting point to study two localised spins in a common environment with indirect coupling via the shared bath. The time-dependent projection in this approach enables us to use a self-consistently determined bath state at every time step. In contrast to the standard Nakajima-Zwanzig equation, introducing more system degrees of freedom, e.g., more impurity spins, the equation itself does not become more complicated as the influence of neighbouring spins is purely covered by summing over all relevant subsystems. However, a time-dependent projection introduces a time-dependent bath state of which we need to take care. In Chapter 5 we will derive the equation of motion for the impurity spins, considering the itinerant electrons as the bath and then reversing the setup. Treating the impurity spins as a bath will lead to an equation of motion for the electronic environment, more precisely we find equations of motions for the relevant bath correlation functions which need to be solved as well.

3

Coherent backaction in single spin systems

In many physical setups, the understanding of the system's dynamical behaviour is crucial to interpret their performance. At low temperatures one might need to take into account quantum correlations to correctly describe the relaxation process in an NMR experiment [5–8] or predict the coherence time for a qubit which can be realised on many experimental platforms [9–13]. Most realistic and indeed interesting physics occurs when the system is coupled to a larger environment. The framework of open quantum systems provides a recipe to tackle these questions [56–58].

In this chapter we investigate the dynamics of a single spin coupled to an electronic environment in detail. This type of system is the fundamental building block to model an NMR system or qubit state. Starting from the Nakajima-Zwanzig equation (2.66) we derive an equation of motion up to second order in the system-bath interaction. The generalised master equation gives access to the full time evolution while taking into account the full history of the system's dynamics. We analyse the equation of motion for the localised spin density in Laplace space and our analytic solution covers the full quantum coherent time evolution. At long times the decay is purely exponential in agreement with Markovian dynamics. The decay is characterised by the relaxation and decoherence time, T_1 and T_2, and recovers the expected results from the literature. At short times, the system's dynamics is dominated by coherent quantum fluctuations which in turn lead to non-Markovian dynamics.

Investigating the implication of the memory effects, we find that even in the simple non-interacting example system the coherent backaction of the electronic bath has a notable effect on the localised spin dynamics. Although a Fermi gas has an innocent description, its physical properties are dominated by the Pauli principle. Similar to a quantum critical strongly correlated system they are largely independent of further microscopic details and dependent only on a few universal parameters such as the Fermi energy E_F, the temperature T and possibly a driving voltage or the magnetic field [23, 117]. These characteristics make the simple, free Fermi gas an appealing candidate to study corre-

lated, coherent dynamics. The critical behaviour is indeed evident in the fact that the Fermi gas exhibits a strong correlation response such as the Kondo effect [118, 119] or the Fermi-edge singularity [120–123]. With our focus on the short time dynamics we are exploring the onset of exactly these correlated many-body responses.

3.1 Decay mechanism in spin systems

We start by outlining the phenomenological description of the time evolution of the magnetisation of a nuclear spin ensemble in contact with conduction electrons. The intuitive approach leads to the macroscopic Bloch equations [18] which describe the decay of the magnetisation of a spin ensemble. Treating the localised or nuclear spins and the surrounding electrons as statistical ensembles we can characterise the decay by a single parameter which is the temperature T. The decay is governed by the bath's thermal fluctuations which are the primary channel for dissipation. Therefore, it is expected that the relaxation time T_1 is set by the temperature of the bath. Indeed, the relaxation time increases for lower temperature. This behaviour is captured by the Korringa relation [19, 20] which predicts the proportionality $T_1 \sim 1/T$. We then link to the the density matrix approach where we highlight which assumptions will no longer be valid in our further investigation.

3.1.1 Bloch equations

Before turning to a specific interaction between nuclear and electron spins, we present a phenomenological argument following the references [16, 17] which results in an equation of motion for the magnetisation of a spin ensemble interacting with its surrounding, known as the Bloch equations [18]. The first observation is that in a homogeneous magnetic field the magnetisation of an ensemble of free spins can be described by

$$\dot{\mathbf{M}} = \gamma \mathbf{M} \times \mathbf{B}. \tag{3.1}$$

This is a fully classical equation of motion for a magnetic moment $\mathbf{M}$ with a gyromagnetic ratio γ in a static field $\mathbf{B}$. Furthermore, in a static field chosen to point along the z direction, the magnetisation saturates at its equilibrium value $M_0 = M_z = B_z$. The equilibrium is reached according to

$$\frac{d}{dt} M_z = -\frac{1}{T_1}(M_z - M_0) \tag{3.2}$$

with the longitudinal relaxation time T_1. The relaxation time T_1 is the average time, a spin ensemble needs to get back to equilibrium after excitation by an externally applied field. At this point T_1 is an experimental observable. Later on, we find an expression for the relaxation time beyond the classical description based on the probability of transition rates for the spin flips induced by the interaction between spin system and surrounding electrons. If the spin ensemble acquires a transverse field component by, e.g., a short magnetic pulse, we can observe that the transverse magnetisation decays with

$$\frac{d}{dt}M_x = -\frac{M_x}{T_2}, \tag{3.3}$$

$$\frac{d}{dt}M_y = -\frac{M_y}{T_2}, \tag{3.4}$$

with the transverse relaxation time T_2. The transverse component decays because of the interaction with its surrounding. The last assumption states that we can combine the free motion Eq. (3.1) of the spins with the observed relaxation of Eqs. (3.2) to (3.4). Thus, we arrive at the Bloch equations [18]

$$\frac{d}{dt}M_x = \gamma M_y B_z - \frac{M_x}{T_2}, \tag{3.5}$$

$$\frac{d}{dt}M_y = \gamma M_x B_z - \frac{M_y}{T_2}, \tag{3.6}$$

$$\frac{d}{dt}M_z = -\frac{1}{T_1}(M_z - M_0), \tag{3.7}$$

for the choice of the homogeneous field along z. This set of macroscopic equations are purely classical and it describes the magnetisation of an ensemble of spin. The longitudinal and transverse relaxation times T_1, T_2 are the accessible observables in magnetic resonance and spin echo experiments. The Bloch equation (3.7) leads to an exponential decay of the magnetisation. In the next section we step away from the phenomenological description. We will see that the decay of the magnetic moment remains exponential in a high temperature expansion which corresponds to a Markovian description of the time evolution.

3.1.2 Spin-lattice relaxation

To characterise the relaxation mechanism of spin ensemble in contact with an environment it proves useful to assign the temperatures T_I and T_{el} to the statistical ensemble of nuclear spins and the electronic environment, respectively. Then the relaxation process, e.g., in metal, can be interpreted as an equilibration between the nuclear spin system and the

conduction electrons. If we describe each part as a statistical ensemble, which itself is in equilibrium, the only free parameter is indeed given by the temperature of the corresponding system. In the following we derive an expression for the relaxation time T_1 based on the concept of a spin and lattice temperature, T_I and T_{el}, where we adapt the approach of [16, 17].

The ensemble of nuclear spins with inverse temperature $\beta = 1/T_I$ can be described by a density matrix

$$\rho_I \sim e^{-\beta H}, \tag{3.8}$$

with H the Hamiltonian of the spin system. The average energy E_{avg} for the spin system can be obtained in two different ways, namely from the statistical point of view and from the microscopic transitions. Their comparison leads to an expression for the T_1 time over which the spin temperature reaches equilibrium with the lattice or electron temperature. One the one hand, by postulating a spin temperature the average energy E_{avg} is given by

$$E_{\mathrm{avg}} = \mathrm{Tr}\left\{\rho H\right\} = \frac{1}{Z}\mathrm{Tr}\left\{He^{-\beta H}\right\} \tag{3.9}$$

with the partition sum Z and H the Hamiltonian describing the system. Within a high temperature expansion this leads to

$$E_{\mathrm{avg}} = -\frac{1}{Z_{T\to\infty}}\beta\mathrm{Tr}\left\{H^2\right\} = -\frac{1}{Z_{T\to\infty}}\beta\sum_n E_n^2, \tag{3.10}$$

where n labels the eigenenergies E_n of the Hamiltonian. A high temperature expansion is justified because the energy difference between two neighbouring states is small. We are looking at the Zeeman levels of nuclear spins and compared to the level splitting any other energy scale is large. In our investigation of the decay dynamics of single spin we explicitly do not use a high temperature expansion and therefore keep the quantum fluctuations which lead to a non-Markovian contribution. The change in the average energy E_{avg} is then given by

$$\frac{d}{dt}E_{\mathrm{avg}} = -\frac{d}{dt}\beta\frac{1}{Z_{T\to\infty}}\sum_n E_n^2. \tag{3.11}$$

On the other hand, the average energy is given by all the energies of every available state

$$E_{\mathrm{avg}} = \sum_n p_n E_n \tag{3.12}$$

with the probability p_n of finding the state $|n\rangle$ occupied. The probabilities follow a Boltzmann distribution

$$p_n = \frac{1}{Z} e^{-\beta E_n}, \tag{3.13}$$

and $\sum_n p_n = 1$. The rate of change for occupancy is governed by transition probabilities $W_{i\to f}$ from an initial state $|i\rangle$ to a finial state $|f\rangle$ and we find

$$\frac{d}{dt} p_n = \sum_m p_m W_{m\to n} - p_n W_{n\to m}. \tag{3.14}$$

Here, only the diagonal part of the density matrix is used for the rate equation. Omitting the off-diagonal terms, which contain the quantum coherences, corresponds to a classical description which is fully justified by the high temperature expansion. If the nuclear spin system and the lattice are in thermal equilibrium, the transition in one direction is as likely the inverse process

$$p_m^{\mathrm{eq}} W_{m\to n} = p_n^{\mathrm{eq}} W_{n\to m}, \tag{3.15}$$

and they obey the detailed balance. The equilibrium temperature can be approximated as the lattice temperature since the reservoir is large compared to the nuclear spin system. Using the equilibrium temperature in Eq. (3.13) and inserting it into the rate equation (3.14) we find the detailed balance relation between the transition probabilities $W_{n\to m}$ and the inverse process

$$W_{n\to m} = W_{m\to n} e^{\beta_{\mathrm{el}}(E_m - E_n)}. \tag{3.16}$$

Inserting this result into Eq. (3.12) and taking the time derivative leads to a second expression for the change in the average energy

$$\begin{aligned} \frac{d}{dt} E_{\mathrm{avg}} &= \frac{1}{2} \sum_{n,m} p_m W_{m\to n} \left(1 - e^{\beta(E_m - E_n)} e^{-\beta_L (E_m - E_n)}\right) (E_n - E_m) \\ &\approx \frac{1}{2 Z_{T\to\infty}} \sum_{n,m} W_{m\to n} (\beta - \beta_L) (E_n - E_m)^2 . \end{aligned} \tag{3.17}$$

To get to the last line we can use the high-temperature expansion and approximate $p_m \approx Z_{T\to\infty}^{-1}$. Comparing Eq. (3.17) to Eq. (3.11) the change in the nuclear spin system's

temperature throughout the equilibration process is given by [16, 17]

$$\frac{d}{dt}\beta = \frac{\beta_{\mathrm{el}} - \beta}{T_1}, \tag{3.18}$$

with the inverse relaxation time T_1

$$T_1^{-1} = \frac{1}{2}\frac{\sum_{n,m} W_{m\to n}\,(E_m - E_n)^2}{\sum_n E_n^2.}. \tag{3.19}$$

We can relate Eq. (3.18) to the Bloch equation of z-component Eq. (3.7) via Curie's law $M \sim \beta$ where the relaxation time T_1 indeed corresponds to the characteristic time scale for the decay of a magnetic moment. Nonetheless, the rate equation (3.18) for the spin temperature is not limited to nuclear spins and conduction electrons but is valid for any type of localised spin in an electronic environment.

For an explicit expression for the relaxation time T_1 we can compute the transition probabilities W in Eq. (3.19) with Fermi's golden rule [124, 125]

$$W_{i\to f} = \frac{2\pi}{\hbar}|\langle f|V|i\rangle|^2\delta(E_i - E_f - \Delta E). \tag{3.20}$$

The states $|i\rangle$ and $|f\rangle$ are the initial and final spin states of the transition with the corresponding energies E_i and E_f, ΔE is the energy difference of adjacent states and V is the scattering potential. In a metal this potential corresponds to the hyperfine contact interaction between nuclear and s-electron spins

$$H_{\mathrm{int}} = -A\delta(x_I)\mathbf{I}\cdot\mathbf{S}, \tag{3.21}$$

with the nuclear spin $\mathbf{I}$ at position x_I and the itinerant electronic spin $\mathbf{S}$. The hyperfine coupling is given by [16, 17]

$$A = \frac{8\pi}{3}\gamma_e\gamma_n\hbar^2, \tag{3.22}$$

where γ_n and γ_e are the gyromagnetic ratios for the nuclei and electrons, respectively. Using Eq. (3.20) to compute the transition probabilities leads finally to an expression for the relaxation time [16, 17, 19]

$$\frac{1}{T_1} \sim A^2\,(\nu(E_F))^2\,k_B T \tag{3.23}$$

with the density of states $\nu(E_F)$ at the Fermi energy. The proportionality of $1/T_1 \sim T$ is the Korringa relation [19] which we comment on further in Section 3.1.4.

3.1.3 Connection to open quantum systems

To obtain an estimate for T_1 in Eq. (3.19) one needs to calculate the weights of the transition probability $W_{i\to f}$ for a specific interaction between nuclear spins and the lattice. They are, one the one hand, given by Fermi's golden rule in Eq. (3.20) as discussed above. On the other hand they can be determined in the density matrix description. The eigenvalues of the density matrix determine the probability amplitudes of each eigenstate. A state then consists of a linear combination of those eigenstates. The transition rates $W_{i\to f}$ directly correspond to the rate of change for the corresponding entry in the density matrix for the spin system $\rho_S(t)$

$$\left(\dot{\rho}_S(t)\right)_{mn} = W_{m\to n}. \tag{3.24}$$

The calculation of the transition probabilities using a density matrix approach [126], which in a more general formulation leads to the Redfield equation (2.25) [63, 91], builds on the phenomenological description introduced in Section 3.1.1. Within the Born-Markov equation or the Lindblad description, the transition probabilities, and consequently the characteristic decay times T_1 and T_2, are determined by the bath correlation functions such as Eq. (2.24). The exact form of the bath correlations is set by the interaction term of the Hamiltonian describing the system-bath structure. For the description of a localised spin in contact with an electronic reservoir we assume again the contact interaction in Eq. (3.21). With this interaction we can write the interaction Hamiltonian of Eq. (2.18) as

$$H_{\text{int}} = -A \sum_{\alpha=x,y,z} I^{\alpha} \otimes S^{\alpha}_{j=0}, \tag{3.25}$$

where the sum is taken over all spin components of the localised spin $\mathbf{I}$ and the electron spin $\mathbf{S}$. The Hamiltonian for the impurity spin is given by the Zeeman term

$$H_S = b_z^I I^z \tag{3.26}$$

in an external field in z-direction. The prefactor is defined by $b_z^I = g_I \mu_I B_z$ with the g-factor of the impurity spin g_I and its magnetic moment μ_I. Within the Lindblad description the equation of motion in Eq. (2.19) can be derived as follows. The eigenoperators $A_\alpha(\omega)$ are defined via the projection onto the eigenspaces belonging to the eigenvalues $\pm b_z^I$ of the system Hamiltonian H_S. Their difference can take the values $\omega = 0, \pm 2b_Z^I$.

The corresponding Fourier transformed bath correlation functions are

$$\Gamma_{\alpha\beta}(\omega) = A^2 \int_0^\infty dt\, e^{-i\omega t}\ \mathrm{Tr}_{\mathrm{el}} \left\{ S^\alpha(t) S^\beta(0) \right\} \tag{3.27}$$

with the trace over the electronic bath. The renormalisation of the energy states of the localised spin due to the bath coupling corresponds to the Lamb shift in Eq. (2.21). Here, any contribution of $S_{\alpha\beta} \sim \Gamma_{\alpha\beta} - \Gamma^*_{\beta\alpha}$ for $A_\alpha(\omega)A_\beta(\omega) \sim I_z$ will shift the energy states. For the dissipating part, the decay rates $\gamma_{\alpha\beta}(\omega)$ are given by the electron spin correlation functions

$$\gamma_{\alpha\beta}(\omega) = A^2 \int_{-\infty}^\infty e^{-i\omega t} \mathrm{Tr}_{\mathrm{el}} \left\{ S^\alpha(t) S^\beta(0) \right\}. \tag{3.28}$$

Their components determine the decay rates T_1 and T_2 for the longitudinal and transverse decay of the localised spin. The exact form of the bath correlation functions will be calculated later when the generalised approach beyond the Born-Markov description is presented. The underlying question is how these correlations alter the system's decay dynamics when the entire history of the system-bath interaction is taken into account and if the dynamical behaviour deviates from a pure exponential decay.

3.1.4 Knight shift and Korringa relation

In standard magnetic resonance experiments, the location of the resonance peak determines the energy of the magnetic moment and the linewidth carries information about the lifetime. In an external magnetic field B each nuclear spin I is not only subject to the applied field. The conduction electrons in a metal are paramagnetic. Their response modifies the local field which then influences the nuclear spin on top of the external field [16, 17, 23]. A schematic of a localised spin in a paramagnetic environment is shown in Fig. 3.1(a). In a resonance experiment therefore the nuclear resonance frequency is shifted by is the Knight shift K [127], according to this local field. It is proportional to the magnetic susceptibility χ of the conduction electrons in the magnetic field

$$K \sim \langle I_{\mathrm{local}} \rangle \sim \chi B. \tag{3.29}$$

Fig. 3.1(b) displays a typical resonance signal. Its width is associated with the life time of the state, here we chose the relaxation time T_1 as an example. Due to the locally enhanced field the nuclear Larmor frequency ω_0 is shifted $\tilde{\omega}_0 = \omega_0 + K$ where $K \sim \Delta H$. In the density matrix picture parts of the renormalisation of the energies of the system Hamiltonian in Eq. (3.26) due to the Lamb shift would further contribute to the shift of

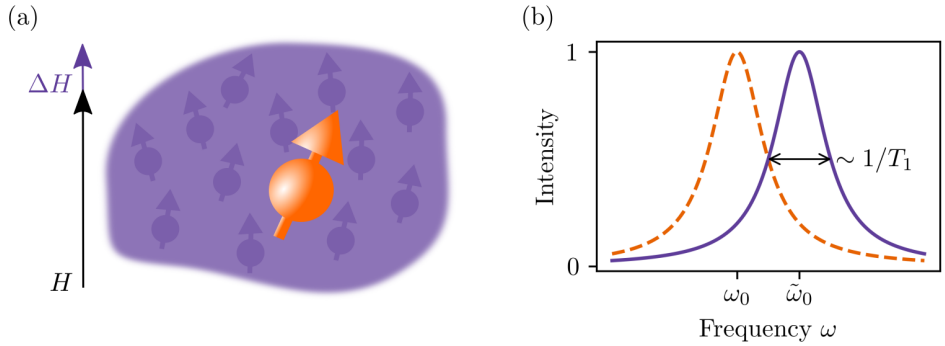

Figure 3.1: (a) Schematic of a nuclear spin in a metal. The external magnetic field is locally enhanced by ΔH due to the magnetic polarisation of the conduction electrons. (b) The Knight shift corresponds to the shift of the NMR signal at ω_0 for a field H (orange dashed line) due to the locally enhanced field $H + \Delta H$ to new resonance frequency $\tilde{\omega}_0 = \omega_0 + K$ (solid purple line).

the resonance peak. For simple metals, the Knight shift can be related to the relaxation time T_1 [16, 17, 20]

$$T_1 K^2 = \frac{\hbar}{4\pi k_B T} \frac{\gamma_e^2}{\gamma_I^2} \tag{3.30}$$

which is know as the Korringa relation [19]. The Korringa relaxation connects the temperature T and the relaxation time T_1. They obey

$$T_1 T = \kappa, \tag{3.31}$$

where κ is a material dependent constant. The relation in Eq. (3.31) is used to identify the state of the conduction electrons. Electrons which can be described as a non-interacting Fermi gas are expected to recover $T_1 \sim 1/T$. In such a simple metal the restriction by the Pauli principle allows only a small number of electrons around the Fermi energy to interact and therefore relax the nuclear spin. Experimentally, the violation of the Korringa behaviour hints at strong correlations in the electron system which is used as an indicator of the breakdown of the Fermi liquid description [21, 22]. The interactions renormalising the Fermi liquid then modify the Korringa constant κ. The change in κ gives an indication about the presence of interactions. Descriptions including strong correlation effects usually take into account spatial correlations, for example anti-ferromagnetic fluctuations [23]. The Korringa relation is a direct consequence of the high temperature expansion and the Markov approximation. How the Korringa behaviour is affected by temporal correlations remains unclear in many correlated systems which is the motivation for our study in the following.

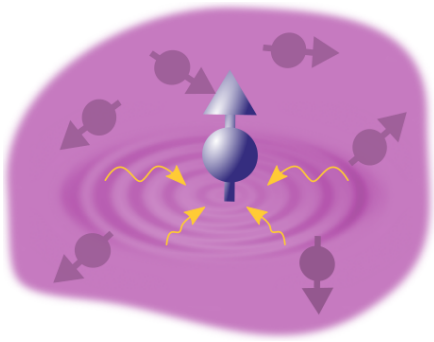

Figure 3.2: Schematics of the considered system: An impurity spin is coupled to itinerant electrons. The ripples indicate the contact interaction between localised spin and the surrounding bath and the creation of an excitation in the bath. The coherent backaction due to the short lived electron correlations are represented by the wavy lines.

3.2 Short and long time dynamics of a localised spin in an electronic conductor

The full time evolution of a localised spin, e.g., a nuclear spin, coupled to itinerant electrons through a contact interaction is now derived. We focus in particular on memory effects leading to non-Markovian behaviour. A sketch of the considered system is shown in Fig. 3.2. Taking into account the full history of the system-bath interaction, we investigate how the decay is altered by the short lived quantum correlations. Even for the environment of the non-interacting electrons a memory effect due to the restriction of fluctuations by the Fermi surface becomes apparent. Our approach is based on an expansion of the exact Nakajima-Zwanzig equation in the coupling constant, set up in such a way that the analytical structure of the memory kernel that causes the non-Markovian behaviour is preserved. The analytical result describes the full time range from the short time non-Markovian contributions to the well-known exponential decay expressions. The short time dynamics of the localised spin is dominated by a logarithmic temperature independent decay before crossing over to the standard thermally induced exponential decay. The considered model can be described by the Kondo-type Hamiltonian

$$H = \sum_{k\sigma} \epsilon_k c^\dagger_{k\sigma} c_{k\sigma} + b^{\mathrm{el}}_z \sum_j S_{z,j} + b^I_z I_z + A\mathbf{I}\cdot\mathbf{S}_{j=0}. \tag{3.32}$$

The spin operators $\mathbf{I}$ and $\mathbf{S}$ for the localised spin and the electrons are normalised to $|\mathbf{I}| = |\mathbf{S}| = 1$. The first term in the Hamiltonian models the free Fermi gas with the energy dispersion ϵ_k and fermionic creation and annihilation operators $c^\dagger_{k\sigma}$ and $c_{k\sigma}$. The momenta k label all possible electronic states with spin index σ. The second is the Zeeman

term for the electronic spin operators

$$\mathbf{S}_j = \sum_{\sigma\sigma'} c^\dagger_{j\sigma} \boldsymbol{\tau}_{\sigma\sigma'} c_{j\sigma'} \tag{3.33}$$

written in terms of the real-space creation and annihilation operators for the electrons, $c^\dagger_{j\sigma}$ and $c_{j\sigma'}$ at position j with the vector $\boldsymbol{\tau}$ of Pauli matrices. For the ease of notation we assume an underlying lattice to describe the electron system and we discuss the continuum limit later on. The prefactor $b_z^{\mathrm{el}} = g\mu_B B_z$ includes the electronic g-factor, the Bohr magneton μ_B and the external, uniform magnetic field B_z applied along the z-axis. These two terms correspond to the bath Hamiltonian H_B. The third term corresponds to the Zeeman term of the localised spin with $b_z^I = g_I \mu_I B_z$, where g_I is the appropriate g-factor for the impurity spin and its magnetic moment μ_I in the external field. Additionally, we neglect the paramagnetic magnetisation of the electrons because it is proportional to b_z^{el} which is usually small. This allows us to set

$$\langle S(t) \rangle = 0, \tag{3.34}$$

which corresponds to disregarding the Knight shift [127]. To include the Knight shift we could add it into the rotating frame picture or subtract $\langle S \rangle$ from the spin operators and only treat spin fluctuations. As our focus will be on the decay and not the deterministic precession, neglecting the Knight shift makes the formalism for the decay more accessible. The interaction term couples the impurity spin to its electronic environment through the contact spin-spin interaction of strength A. The Zeeman term of the localised spin causes principally a spin precession. To avoid that the physics is obscured by the latter it is helpful to switch to the rotating frame where the precession is removed by the transformation

$$H \to H - b_z^I J_z \tag{3.35}$$

with the total angular momentum for the z-component

$$J_z = I_z + \sum_j S_{z,j}. \tag{3.36}$$

Then, the Hamiltonian Eq. (3.32) takes a simplified form in the rotating frame

$$H = \sum_{k\sigma} \epsilon_k c^\dagger_{k\sigma} c_{k\sigma} + b_z \sum_j S_{z,j} + A\mathbf{I} \cdot \mathbf{S}_{j=0}, \tag{3.37}$$

where we defined $b_z = b_z^{\mathrm{el}} - b_z^I$. In the rotating frame the spin operators transform as

$$\begin{aligned} I_\pm &\to I_\pm e^{\pm i b_z^I t}, & S_{\pm,j} &\to S_\pm e^{\pm b_z^I t}, \\ I_z &\to I_z, & S_{z,j} &\to S_{z,j}, \end{aligned} \tag{3.38}$$

under the assumption in Eq. (3.34) and where

$$I_\pm = \frac{1}{2}\left(I_x \pm i I_y\right), \tag{3.39}$$

$$S_{\pm,j} = \frac{1}{2}\left(S_{x,j} \pm S_{y,j}\right). \tag{3.40}$$

We assume the localised spin operator $\mathbf{I}$ to be a spin-1/2 operator. The advantage of considering spin-1/2 is the most accessible algebra while maintaining all the general physics. For any other choice of a quantum spin we expect similar dynamical behaviour as a larger spin does not introduce any other correlations. The spin system is a two-level system and all its states can be expressed with the four operators $I_\uparrow, I_\downarrow, I_\pm$ where we define

$$I_\uparrow = \frac{1}{2}\left(\mathbb{1} + I_z\right), \tag{3.41}$$

$$I_\downarrow = \frac{1}{2}\left(\mathbb{1} - I_z\right). \tag{3.42}$$

They will form the basis to address the system dynamics using the density matrix description.

3.2.1 Memory effects in a simple metal

To capture the dynamics of the impurity spin driven by the interaction with the electron spins we adopt a Nakajima-Zwanzig approach similar to [64]. The Nakajima-Zwanzig master equation (2.59) provides then an equation of motion for the reduced density matrix ρ_I describing the impurity spin

$$\rho_I = \mathrm{Tr}_{\mathrm{el}}\left\{\rho\right\}, \tag{3.43}$$

where ρ is the full density matrix of the whole system, including the impurity spin and the electronic environment. Since the model is formulated in a rotating frame, the first term of the Nakajima-Zwanzig equation is zero and we have

$$\frac{d}{dt}\rho_I(t) = \int_0^t dt' \Sigma_I^{\mathrm{Born}}(t-t')\rho_I(t'), \tag{3.44}$$

which is valid within the Born approximation Eq. (2.66) and therefore up to second order in the interaction A. The memory kernel is given by

$$\Sigma_I^{\text{Born}}(t-t')(\cdot) = \text{Tr}_{\text{el}}\left\{L_{\text{int}} e^{L_0(t-t')} L_{\text{int}} \rho_{\text{el}} \otimes (\cdot)\right\}. \tag{3.45}$$

The non-interacting part of the Liouvillian is, due to the rotating frame, defined solely by the free electronic Hamiltonian

$$L_0(\cdot) = -i\,[H_0, \cdot] \tag{3.46}$$

with

$$H_0 = \sum_{k\sigma} \epsilon_k c_{k\sigma}^\dagger c_{k\sigma} + b_z \sum_j S_{z,j}. \tag{3.47}$$

The interaction Liouvillian contains the spin-spin coupling term with

$$L_{\text{int}}(\cdot) = -i\,[H_{\text{int}}, (\cdot)] = -i\,[A\mathbf{I}\cdot\mathbf{S}, (\cdot)]\,. \tag{3.48}$$

To solve the integro-differential Eq. (3.44) we study it in the Laplace space. The Laplace transformation removes the convolution within the time integral of Eq. (3.44). Full details for the Laplace transformation of Eq. (3.44) can be found in Appendix B. In Chapter 5 we will address the dynamics of two localised spins in contact with a common electronic environment. In this setup the Laplace transform is no longer helpful because the time convolution within the equation of motion cannot be removed. However, in the current setup of a single spin the analysis of the reduced density matrix in Laplace space leads to a closed analytical expression for the full time evolution.

In general, the Laplace transform $\tilde{f}(s)$ of some function $f(t)$ is defined as

$$\tilde{f}(s) = \int_0^\infty dt\, e^{-ts} f(t) \tag{3.49}$$

where the Laplace variable s has to fulfil $\text{Re}(s) > 0$. Later on the result will be analytically continued to the full complex plane to pick up the pole structure. The latter fully determines the system's dynamics which in turn is found by the inverse Laplace transformation. As mentioned above, the Laplace transform of Eq. (3.44) removes the convolution in the time integral and we arrive at

$$\tilde{\rho}_I(s) = \left(s\mathbb{1} - \widetilde{\Sigma}_I(s)\right)^{-1} \rho_I(t=0), \tag{3.50}$$

with the initial condition $\rho_I(t=0)$. The Laplace transform of the memory kernel is given by

$$\widetilde{\Sigma}_I = \mathrm{Tr}_{\mathrm{el}}\left\{L_{\mathrm{int}}\left(s\mathbb{1} + L_0\right) L_{\mathrm{int}}\rho_{\mathrm{el}}\right\}, \tag{3.51}$$

and the details for the Laplace transform starting from Eq. (3.44) can be found in Appendix B. We first solve for the localised spin dynamics in Laplace space and then return to the real time domain.

3.2.1.1 Matrix representation of the memory kernel

It is advantageous to move into a basis spanned by the localised spin operators $\{I_\uparrow, I_\downarrow, I_-, I_+\}$ for the analysis. It will allow us to use a vector representation of the reduced density matrix in the superoperator space where the superoperators are represented by 4×4 matrices. The spin operator form a complete basis as they fulfil the commutation relations

$$[I_z, I_\pm] = \pm I_\pm, \tag{3.52}$$

$$[I_+, I_-] = I_z, \tag{3.53}$$

where $I_z = I_\uparrow - I_\downarrow$ according to Eqs. (3.41) and (3.42), $I_\pm$ is defined in Eq. (3.39). In this basis the localised spin density matrix decomposes into

$$\rho_I = \rho_\uparrow I_\uparrow + \rho_\downarrow I_\downarrow + \rho_- I_+ + \rho_+ I_-. \tag{3.54}$$

Due to the decomposition the density matrix components are determined by the coefficients ρ_β with $\beta = \uparrow, \downarrow, -, +$ which are just complex numbers. For the expectation values for the different impurity spin components we have

$$\langle I_\beta \rangle = \mathrm{Tr}_I\left\{I_\beta \rho_I\right\} = I\rho_\beta \tag{3.55}$$

after tracing over the system's degrees of freedom. Choosing this specific basis, every operator O can be written as a product of operators, with one part acting only on the system's degrees of freedom and the other part only acting on the electronic ones, i.e.,

$$O = o_\uparrow I_\uparrow + o_\downarrow I_\downarrow + o_+ I_- + o_- I_+. \tag{3.56}$$

In the following, lower case operators are used when they only act on the electronic degrees of freedom, upper case operators are reserved for the localised spin operators. Within this basis all superoperators are represented by 4×4 matrices and will be denoted by a

double hat $\hat{\hat{(\cdot)}}$ throughout the discussion. The non-interacting part of the Hamiltonian can be written as

$$H_0 = h_0 \otimes \mathbb{1}_I. \tag{3.57}$$

Therefore, the matrix representation for the Liouvillian superoperator $\hat{\hat{L}}_0$ is given by

$$\hat{\hat{L}}_0 = L^-_{h_0} \mathbb{1}_I. \tag{3.58}$$

The superscript $-$ denotes the commutator, i.e., $L^-_{h_0} o = -i[h_0, o]$. To find matrix representation for the interaction Liouvillian we decompose the interaction Hamiltonian into system and bath operators

$$H_{\text{int}} = h_\uparrow I_\uparrow + h_\downarrow I_\downarrow + h_+ I_- + h_- I_+, \tag{3.59}$$

with $h_\uparrow = -h_\downarrow = h_z = S_{z,0}/2$ and $h_\pm = 2AS_{\pm,0}$. To find the matrix representation of the interaction Liouvillian $\hat{\hat{L}}_{\text{int}}$ we need to determine its action on the general operator O defined by Eq. (3.56) in the localised spin basis. All components of $\hat{\hat{L}}_{\text{int}}$ are given by the commutator $[H_{\text{int}}, O]$ where all entries are labelled by the all combinations of $o_\alpha I_\beta$ with $\alpha, \beta = \uparrow, \downarrow, -, +$. The explicit calculation can be found in Appendix C.1. The matrix representation of the interaction Liouvillian is then given by

$$\hat{\hat{L}}_{\text{int}} = \begin{pmatrix} L^-_{h_z} & 0 & h^L_- & -h^R_+ \\ 0 & -L^-_{h_z} & -h^R_- & h^L_+ \\ h^L_+ & -h^R_+ & -L^+_{h_z} & 0 \\ -h^R_- & h^L_- & 0 & L^+_{h_z} \end{pmatrix}. \tag{3.60}$$

Again the superscript $-$ refers to the commutator and the superscript $+$ refers to the anti-commutator with the bath operator in the subscript. The superscripts R, L indicate if the electron operator acts from the right- or left-hand side, e.g., $h^R_- O = O h_-$ and $h^L_- O = h_- O$. Using the matrix representations for the Liouvillian superoperators in the definition of the memory kernel in Eq. (3.51) leads to an explicit expression for the memory kernel

$$\hat{\hat{\Sigma}}_I(s) = \begin{pmatrix} F_1(s) & -F_2(s) & 0 & 0 \\ -F_1(s) & F_2(s) & 0 & 0 \\ 0 & 0 & F_-(s) + F_z(s) & 0 \\ 0 & 0 & 0 & F_+(s) + F_z(s) \end{pmatrix}. \tag{3.61}$$

The Laplace transformation of the electron spin-spin correlation functions $F_{1,2,\pm,z}(s)$ are defined as

$$F_1(s) = 2A^2 \int_0^\infty dt\, e^{-st} \mathrm{Re}\left[e^{ib_z^I t} \langle S_{-,0}(t) S_{+,0}(0)\rangle\right], \tag{3.62}$$

$$F_2(s) = 2A^2 \int_0^\infty dt\, e^{-st} \mathrm{Re}\left[e^{ib_z^I t} \langle S_{+,0}(t) S_{-,0}(0)\rangle\right], \tag{3.63}$$

$$F_-(s) = A^2 \int_0^\infty dt\, e^{-\left(s+ib_z^I\right)t} \langle\{S_{+,0}(t), S_{-,0}(0)\}\rangle, \tag{3.64}$$

$$F_+(s) = A^2 \int_0^\infty dt\, e^{-\left(s-ib_z^I\right)t} \langle\{S_{-,0}(t), S_{+,0}(0)\}\rangle, \tag{3.65}$$

$$F_z(s) = \frac{A^2}{2} \int_0^\infty dt\, e^{-st} \langle\{S_{z,0}(t), S_{z,0}(0)\}\rangle, \tag{3.66}$$

where the shorthand $\langle\cdot\rangle$ replaces the trace $\mathrm{Tr}_{\mathrm{el}}\{\cdot\rho_{\mathrm{el}}\}$ over the electronic degrees of freedom and ρ_{el} is the equilibrium state of the bath. Notice that ρ_{el} is at the end of each trace. The Hamiltonian of the electrons is quadratic so that later on, the spin-spin correlators simply decouple to fermionic expectations values of particles and holes according to Wick's theorem [128]. Additional details regarding the derivation of the matrix representation of the memory kernel can be found in Appendix C.2.

Each superoperator acts on the system vector

$$\vec{\rho}_I = (\rho_\uparrow, \rho_\downarrow, \rho_-, \rho_+)^T, \tag{3.67}$$

such that we can solve the equation of motion for the density matrix for each component. From the structure of the memory kernel in Eq. (3.61) we see that the evolution of the components $\rho_{\uparrow,\downarrow}$ fully decouple from the components $\rho_\pm$ in a similar manner to the classical description with the Bloch Eqs. (3.5) to (3.7). This corresponds to the decay along different directions. The evolution of the longitudinal component along the z-direction is given by $\rho_z = \rho_\uparrow - \rho_\downarrow$. The components $\rho_\pm$ describe the decay in the transverse direction.

3.2.2 Pole structure and inverse Laplace transformation

The impurity spin dynamics are driven by the coupling to conduction electrons and the exact nature of the effects are captured by the bath correlation functions. With the explicit expression for the memory kernel $\hat{\tilde{\Sigma}}(s)$, the equation of motion in Eq. (3.50) for the density matrix coefficients takes the form

$$\vec{\tilde{\rho}}(s) = \left(s\mathbb{1} - \hat{\tilde{\Sigma}}(s)\right)^{-1} \vec{\rho}_I(t=0). \tag{3.68}$$

To proceed, we determine the inverse of the superoperator

$$\left(s\mathbb{1}-\hat{\hat{\Sigma}}(s)\right)^{-1}=\begin{pmatrix} s-F_1(s) & F_2(s) & 0 & 0 \\ F_1(s) & s-F_2(s) & 0 & 0 \\ 0 & 0 & s-F_-(s)-F_z(s) & 0 \\ 0 & 0 & 0 & s-F_+(s)-F_z(s) \end{pmatrix}^{-1}. \tag{3.69}$$

Its inverse is given by the inverse of each 2×2 block on the diagonal and we obtain

$$\left(s\mathbb{1}-\hat{\hat{\Sigma}}(s)\right)^{-1}=\begin{pmatrix} M_1^{-1} & 0 \\ 0 & M_2^{-1} \end{pmatrix}, \tag{3.70}$$

with

$$M_1^{-1}=\begin{pmatrix} \frac{s-F_2(s)}{s(s-F_1(s)-F_2(s))} & \frac{-F_2(s)}{s(s-F_1(s)-F_2(s))} \\ \frac{-F_1(s)}{s(s-F_1(s)-F_2(s))} & \frac{s-F_1(s)}{s(s-F_1(s)-F_2(s))} \end{pmatrix}, \tag{3.71}$$

$$M_2^{-1}=\begin{pmatrix} \frac{1}{s-F_-(s)-F_z(s)} & 0 \\ 0 & \frac{1}{s-F_-(s)-F_z(s)} \end{pmatrix}. \tag{3.72}$$

Consequently, the impurity spin longitudinal and transverse components, $\tilde{\rho}_z(s) = \tilde{\rho}_\uparrow(s) - \tilde{\rho}_\downarrow(s)$ and $\tilde{\rho}_\pm(s)$, in the Laplace domain are given by

$$\tilde{\rho}_z(s)=\frac{s\rho_z(t=0)-F_2(s)+F_1(s)}{s\left[s-F_1(s)-F_2(s)\right]}, \tag{3.73}$$

$$\tilde{\rho}_\pm(s)=\frac{\rho_\pm(t=0)}{s-F_\pm(s)-F_z(s)}, \tag{3.74}$$

with the initial values for the reduced density matrix $\rho_{z,\pm}(t=0)$. Returning to the real time domain involves the inverse Laplace transform $s\to t$ which is defined as

$$k(t)=\frac{1}{2\pi i}\lim_{R\to\infty}\int_{\lambda-iR}^{\lambda+iR} ds\, e^{ts}\tilde{k}(s), \tag{3.75}$$

for some function $k(t)$ and its Laplace transformation $\tilde{k}(s)$. The complex number λ is chosen such that all singularities of $\tilde{k}(s)$ are located to the left of the integration contour. The complex line integral is known as the Bromwich contour and it is sketched in Fig. 3.3.

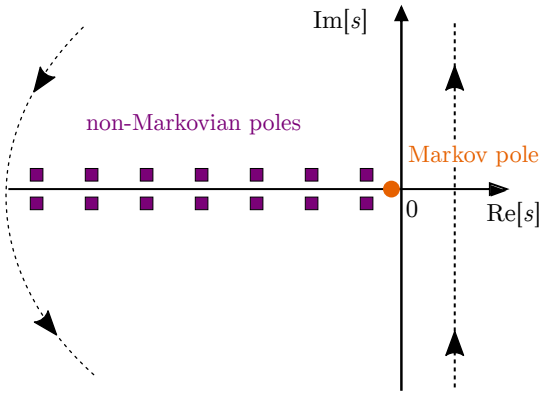

Figure 3.3: Sketch of the pole structure in Laplace space. The Bromwich contour for the inverse Laplace transformation is marked by the black dashed line, it is closed at $R \to \infty$. It encloses all possible poles, Markovian and non-Markovian, of the different density matrix components in Laplace space in Eq. (3.73).

The density matrix coefficients in the time domain are then given by

$$\rho_z(t) = \lim_{R\to\infty} \int_{\lambda-iR}^{\lambda+iR} \frac{ds}{2\pi i} e^{st} \frac{s\rho_z(t=0) - F_2(s) + F_1(s)}{s\left[s - F_1(s) - F_2(s)\right]}, \tag{3.76}$$

$$\rho_\pm(t) = \lim_{R\to\infty} \int_{\lambda-iR}^{\lambda+iR} \frac{ds}{2\pi i} e^{st} \frac{\rho_\pm(t=0)}{s - F_\pm(s) - F_z(s)}. \tag{3.77}$$

We will solve the inverse Laplace transform later on, but we already comment on some the general features in the following.

The system's dynamics is fully encoded in the pole structure of the integrands in Eqs. (3.76) and (3.77). Within a Markovian treatment the s dependence of the memory kernel $\widetilde{\Sigma}$ is neglected and the spin-spin correlation functions F_α (Eq. (3.62) to Eq. (3.66)) in the memory kernel would reduce to $F_\alpha(s = 0)$. They then indeed correspond to the bath correlation functions that appear in the Lindblad description Eq. (3.27). The smallest pole that enters in this case is located at $s = \widetilde{\Sigma}(s = 0)$.

Beyond the Born-Markov approximation the Markovian behaviour is still captured by the singularity closest to $s = 0$. This is because $t \sim 1/s$ and consequently $s = 0$ corresponds to long times in the real time domain. In Fig. 3.3 the Markovian poles is marked in orange. However, keeping the s dependence of $\widetilde{\Sigma}$ provides a small but crucial difference. The small correction due to the full s dependence is the source of the initial slip discussed in Section 2.1.2 of the full time evolution. The reduced amplitude of the Markovian evolution is compensated for by the non-Markovian contribution. Taking into account the full s dependence of the electron response functions leads to a sequence of additional poles, which are sketched in Fig. 3.3. We will be able to identify them as the

non-Markovian part of the dynamics and calculate their contribution.

Up to this point, the discussion is general and not limited to the specific example of itinerant electrons. The information of the dynamical behaviour is encoded in the bath correlation functions $F_\alpha(s)$. If they are known, the analysis of the pole structure in Laplace space can be transferred to different physical setups with different types of environments. After locating the singularities and identifying the Markov and non-Markovian poles, one performs the inverse Laplace transform and arrives at the full time evolution up to the second order in the interaction. The exact details of the dynamical behaviour for the explicit example of the impurity spin are the focus of Sections 3.2.4 and 3.2.5.

3.2.3 Bath correlations in Laplace space

The electron spin-spin correlation functions $F_\alpha(s)$ (Eqs. (3.62) to (3.66)) carry the information about the impurity spin's dynamics in contact with the electronic environment. These time-nonlocal correlation functions capture the short-lived coherent quantum fluctuations that will lead to non-Markovian dynamics. To analyse them further, we model the itinerant electron bath as a free Fermi gas. Since the interaction is restricted to a contact interaction at $j = 0$ we can write the electron spin $\mathbf{S}_j$ in momentum space as

$$\mathbf{S}_{j=0} = \sum_{kk',\sigma\sigma'} c^\dagger_{k\sigma} \boldsymbol{\tau}_{\sigma\sigma'} c_{k'\sigma'}. \tag{3.78}$$

For simplicity, we first consider the zero field limit, $b^I_z = 0$. In this case, the spin-spin correlation functions are all identical due to the $SU(2)$ symmetry of the Fermi gas, $F_1 = F_2 = F_\pm = F_z$. In particular, the correlator $F_z(s)$ is given by

$$F_z(s) = -\frac{A^2}{2}\frac{a^{2d}}{(2\pi)^d}\int_0^t dt\, e^{-ts} \sum_{kk',\sigma} \left[e^{i(\epsilon_k - \epsilon_{k'})t} \left\langle c^\dagger_{k_\sigma} c_{k\sigma} \right\rangle \left\langle c_{k'\sigma} c^\dagger_{k'\sigma} \right\rangle + \text{c.c} \right], \tag{3.79}$$

where c.c. denotes the complex conjugate. We choose here a discrete k summation, assuming an underlying lattice with the lattice constant a with the volume a^{2d} of the first Brillouin zone in d spatial dimensions. However, a continuum description would yield the same result. The Hamiltonian H_0 is diagonal in the electronic creation and annihilation operators $c^\dagger_{k\sigma}$ and $c_{k\sigma}$ such that the time evolution of the spin operators is simply given by the phase factor $\exp(\pm i\epsilon_k t)$. To perform the summation over momenta k, k' the density of states

$$\nu(\epsilon) = \frac{a^d}{(2\pi)^d}\frac{d^d k}{d\epsilon} \tag{3.80}$$

is introduced in a contiuum limit such that the summation can be replaced by an integral over the energy ϵ. Since the relevant excitations influencing the dynamics of the system are the particle-hole fluctuations close to the Fermi surface we shall consider a sufficiently wide band such that $\nu(\epsilon)$ can be set constant to $\nu_0 = \nu(E_F)$ in the energy integration. As such ν_0 does not overshadow the universal physics near the Fermi energy E_F. However, it also gives rise to ultra-violet divergences since a constant density of states is extended to high energies. To resolve this problem we introduce a cutoff ξ_0 and replace the density of states by

$$\nu(\epsilon) = \nu_0 e^{-|\epsilon|/\xi_0}. \tag{3.81}$$

The energy ϵ is chosen such that $\epsilon = 0$ corresponds to the Fermi energy E_F. The replacement in Eq. (3.81) for the true density of states has the advantage of incorporating all non-universal high energy physics in a single parameter ξ_0. Through the expansions in ξ_0 it is then possible to precisely separate universal low energy from non-universal high energy physics. To simplify the discussion of the spin-spin correlators we define the functions

$$F(s) = -\frac{1}{\nu_0}\int_0^\infty dt\, e^{-ts}\int d\epsilon\, \nu(\epsilon)e^{i\epsilon t}f(\epsilon)\int d\epsilon'\nu(\epsilon')e^{-i\epsilon' t}\left(1-f(\epsilon')\right), \tag{3.82}$$

and

$$G(s) = -\frac{1}{\nu_0}\int_0^\infty dt\, e^{-ts}\int d\epsilon\, \nu(\epsilon)e^{-i\epsilon t}f(\epsilon)\int d\epsilon'\nu(\epsilon')e^{i\epsilon' t}\left(1-f(\epsilon')\right), \tag{3.83}$$

with the Fermi-Dirac distribution

$$f(\epsilon) = \frac{1}{1+\exp\left[\frac{\epsilon}{k_B T}\right]}, \tag{3.84}$$

where k_B is the Boltzmann constant. Note that $s \in \mathbb{C}$ such that $G(s)$ is not simply the complex conjugate of $F(s)$. Eq. (3.82) corresponds to the first term of Eq. (3.79), apart from a modified prefactor, after replacing the sum over all momenta with the integral over the energy ϵ, ϵ'. Similarly, Eq. (3.83) corresponds to complex conjugate term in Eq. (3.79) and the difference in comparison to the function $F(s)$ is the reverse time evolution of the expectation values. To solve the integral over the energy, we assume a symmetric form of the density of states, $\nu(\epsilon) = \nu(-\epsilon)$, and for the distribution of the holes we use that

$1 - f(\epsilon) = f(-\epsilon)$. With these assumptions we arrive at

$$F(s) = -\int_0^\infty dt\, e^{-ts} \left[\int d\epsilon\, e^{-|\epsilon|/\xi_0} e^{i\epsilon t} f(\epsilon) \right]^2 . \tag{3.85}$$

Using the residue theorem a closed form of the energy integral is found, see Appendix D.1 for details,

$$F(s) = -\int_0^\infty dt\, e^{-ts} \frac{(\pi k_B T)^2}{\sin^2\left(\pi k_B T \left(it + \xi_0^{-1}\right)\right)}. \tag{3.86}$$

The high energy cutoff manages the divergence of the integrand at short times. The ξ_0-independent contribution captures the universal behaviour around the Fermi surface in the low energy sector. Finally, the time integral of the Laplace transform Eq. (3.86) leads to a hypergeometric function, see Appendix D.2. After an expansion in the inverse cutoff ξ_0^{-1} we obtain

$$F(s) = i\xi_0 - \pi k_B T + s \left[\ln\left(\frac{2\pi k_B T}{i\xi}\right) + \psi\left(1 + \frac{s}{2\pi k_B T}\right) \right] \tag{3.87}$$

where we neglect all terms with negative power of ξ_0. In this expression, $\psi(z)$ is the digamma function

$$\psi(z) = \frac{\Gamma'(z)}{\Gamma(z)}, \tag{3.88}$$

where $\Gamma(z)$ is Euler's Gamma function and the prime indicates the derivative with respect to z. Expressions with the digamma function can often be found in the literature for integrals involving the Fermi function [129, 130]. Additionally, the constant $\psi(1)/2 = -\gamma/2$ is absorbed in the logarithm such that $\xi_0 \to \xi$ with

$$\xi = \xi_0 e^{\gamma/2}, \tag{3.89}$$

where γ is the Euler-Mascheroni constant. The redefinition is justified as the cutoff ξ is due to the non-universal behaviour at the band edges. An exact determination can only be done for an explicit model or through an experiment. Any other constant playing a similar role can therefore be absorbed into a renormalisation of the cutoff and does not change the universal behaviour. The result for the function $G(s)$ is found similarly, the

only difference is a conjugation in the cutoff $i\xi_0 \to -i\xi_0$ such that

$$\begin{aligned} G(s) &= F(s)|_{i\xi_0 \to -i\xi_0} \\ &= -i\xi_0 - \pi k_B T + s\left[\ln\left(\frac{2\pi k_B T}{-i\xi}\right) + \psi\left(1 + \frac{s}{2\pi k_B T}\right)\right]. \end{aligned} \tag{3.90}$$

The functions $F(s)$ and $G(s)$ can be used to write the response function in Eq. (3.79) as

$$F_z(s) = \alpha\left[F(s) + G(s)\right], \tag{3.91}$$

where the dimensionless coupling parameter

$$\alpha = (A\nu_0)^2 \tag{3.92}$$

was introduced. In the following discussion α will appear as the small expansion parameter. This is justified because we assumed the coupling strength A to be small and we are working within the Born approximation.

3.2.3.1 Low and high temperature limits

The only relevant parameter that dictates the behaviour of the bath at the Fermi level is the temperature T. Therefore, there are two distinct regimes for the response function $F_z(s)$. For high temperatures, where $\mathrm{Re}(s) < k_B T/\hbar$, thermal fluctuations dominate the dynamics. In the opposite limit, $\mathrm{Re}(s) > k_B T/\hbar$, quantum fluctuations prevail and the dominant contributions to the dynamics are driven by those quantum fluctuations. This leads to memory effects from the particle-hole fluctuations around the Fermi energy. The particle-hole fluctuations are a universal feature which only depends on the existence of the Fermi level. The introduction of the high energy cutoff ξ_0 earlier ensures that the bath correlator only captures the important physics around the Fermi energy. In the following, we study the low and high temperature limits of the correlator

$$F_z(s) = -2\alpha\pi k_B T + 2\alpha s\left[\ln\left(\frac{2\pi k_B T}{\xi}\right) + \psi\left(1 + \frac{s}{2\pi k_B T}\right)\right], \tag{3.93}$$

as it was defined in Eq. (3.91). First, we consider the limit $T \to 0$ where the quantum critical correlations in the bath are visible. In the low temperature limit of Eq. (3.93) the digamma function's asymptote is a logarithm [131], $\psi(z) \sim \ln(z)$, which cancels the

temperature dependence of the logarithm in the second term. This leads to

$$F_z(s) \sim 2\alpha s \ln\left(\frac{s}{\xi}\right). \tag{3.94}$$

The logarithmic behaviour of the response function hints at the underlying Kondo effect driven by quantum correlations. Calculating the spin-spin correlator at finite temperature and taking the limit $T \to 0$ bypasses a direct calculation at $T = 0$. The immediate evaluation for $T = 0$ leads to a branch cut along the negative real axis due to the logarithmic response and treating the branch cut analytically is much more involved. Second, in the limit of $\mathrm{Re}(s) \ll k_B T/\hbar$ the digamma function $\psi(z)$ tends to the Euler-Mascheroni constant $-\gamma$ [131], which again is absorbed in the cutoff $\xi \to \xi'$ similar to Eq. (3.89) and we obtain

$$F_z(s) \sim -2\alpha\pi k_B T + 2\alpha s \ln\left(\frac{2\pi k_B T}{\xi'}\right). \tag{3.95}$$

The first term, independent of the Laplace variable s, will later be identified as the Markovian contribution and it defines the relaxation time of the localised spin. The second term linear in s reduces the Markovian decay amplitude due to the renormalisation of the electron fluctuations. Already in these crude limits of the temperature we can infer that Markovian dynamics are relevant on timescales $t \gg \hbar/k_B T$. On the other hand we expect the non-Markovian effects of quantum correlations to cause a deviation from the standard Markovian dynamics at short times scale, $t < \hbar/k_B T$.

3.2.3.2 Bath correlation functions in a finite field

In a finite magnetic field, the full expressions for the spin-spin correlations functions are given by Eq. (3.62) to Eq. (3.66). They can also be expressed as combinations of the functions $F(s)$ and $G(s)$, which are defined in Eqs. (3.87) and (3.90), by shifting the argument in the Laplace transform such that

$$s \to s \pm i b_z^I. \tag{3.96}$$

The sign is determined by the corresponding phase factor in Eq. (3.62) to Eq. (3.66). The full expression for the bath correlation functions are therefore given by

$$F_1(s) = \alpha \left[F(s - ib_z^I) + G(s + ib_z^I) \right], \tag{3.97}$$

$$F_2(s) = \alpha \left[F(s + ib_z^I) + G(s - ib_z^I) \right], \tag{3.98}$$

$$F_-(s) = \alpha \left[F(s + ib_z^I) + G(s + ib_z^I) \right] = F_z(s + ib_z^I), \tag{3.99}$$

$$F_+(s) = \alpha \left[F(s - ib_z^I) + G(s - ib_z^I) \right] = F_z(s - ib_z^I), \tag{3.100}$$

$$F_z(s) = \alpha \left[F(s) + G(s) \right]. \tag{3.101}$$

3.2.4 Markovian dynamics

Using the explicit expressions for the spin-spin correlation functions, we analyse the corresponding singularities of the denominator in Eqs. (3.76) and (3.77). The Markovian behaviour is captured by the poles $s \sim \alpha$ and neglects the s dependence of the electronic response functions (Eq. (3.97) to Eq. (3.101)) which was discussed in Section 3.2.2.

For the longitudinal component we find a trivial pole at $1/s$ for $s = 0$. Splitting of the simple pole we rewrite $\tilde{\rho}_z(s)$ in Eq. (3.73) as

$$\tilde{\rho}_z(s) = \frac{1}{s} \frac{F_2(0) - F_1(0)}{F_1(0) + F_2(0)} + \frac{\rho_z(t=0) - \frac{F_2(0) - F_1(0)}{F_1(0) + F_2(0)}}{s - F_1(s) - F_2(s)}. \tag{3.102}$$

Here, the first term is time-independent and corresponds to the equilibrium value ρ_z^{eq} which is reached in the long time limit $t \to \infty$. Using the definitions for $F_1(s)$ and $F_2(s)$ in Eqs. (3.97) and (3.98) at $s = 0$ the equilibrium value evaluates to

$$\rho_z^{\mathrm{eq}} = \frac{F_2(0) - F_1(0)}{F_1(0) + F_2(0)} = -\tanh\left(\frac{b_z^I}{2k_B T} \right). \tag{3.103}$$

As expected the long time limit corresponds to the paramagnetic polarisation of the spin in a magnetic field. Eq. (3.103) is indeed the result obtained from standard thermodynamics when considering the polarisation of a two level system in a Zeeman field.

Further singularities can be found by requiring

$$s - F_1(s) - F_2(s) = 0, \tag{3.104}$$

and

$$s - F_\pm(s) - F_z(s) = 0, \tag{3.105}$$

for the decay of $\rho_z(t)$ and $\rho_\pm(t)$. Keeping in mind that the Markovian contribution neglects the short time dynamics and therefore contributions for finite values for s we want to solve the above two equations such that $s \approx 0$. All details on the derivation of the Markov poles and their residues can be found in Appendix E.1. The Markov pole of Eq. (3.104) to $O(\alpha)$ is given by

$$s_z^{\mathrm{M}} = -2\alpha \frac{b_z^I}{\tanh\left(\frac{b_z^I}{2k_bT}\right)}. \tag{3.106}$$

Note that this already includes an expansion in α as $s \sim \alpha$ and any further s dependence is neglected. For the transverse components of Eq. (3.105) we find

$$s_\pm^{\mathrm{M}} = -4\alpha\pi k_BT \mp i2\alpha b_z^I \left[2\ln\left(\frac{2\pi k_BT}{\xi'}\right) + \psi\left(1 \mp \frac{ib_z^I}{2\pi k_BT}\right)\right]. \tag{3.107}$$

The residues for the Markovian poles are

$$\mathrm{Res}\left(s_z^{\mathrm{M}}\right) = \frac{e^{s_z^{\mathrm{M}}t}}{1 - 4\alpha\left\{\ln\left(\frac{2\pi k_BT}{\xi}\right) + \mathrm{Re}\left[\psi\left(1 + \frac{ib_z^I}{2\pi k_BT}\right)\right]\right\}}, \tag{3.108}$$

$$\mathrm{Res}\left(s_\pm^{\mathrm{M}}\right) = \frac{e^{s^{\mathrm{M}}t}}{1 - 2\alpha\left[2\ln\left(\frac{2\pi k_BT}{\xi'}\right) + \psi\left(1 + \frac{ib_z^I}{2\pi k_BT}\right)\right]}. \tag{3.109}$$

The correction of $O(\alpha)$ in the denominator shows a reduction of the residue's weight and indicates that there is a missing part of the full dynamics which will be captured by the non-Markovian contribution. The Markov approximation assumes a time-local evolution of the reduced density matrix for the impurity spin which is characterised by an exponential decay. The time for the decay is set by the relaxation time T_1 and decoherence time T_2 for the two different components of the density matrix. The two characteristic times can be read off from the negative real part of the Markov poles in Eqs. (3.106) and (3.107) which enter the residues Eq. (3.108), i.e.,

$$\mathrm{Re}\left[s_{z,\pm}^{\mathrm{M}}\right] = -\frac{1}{T_{1,2}}. \tag{3.110}$$

Reintroducing $\hbar \neq 1$ such that the dimensions are fully correct, this leads to

$$T_1 = \frac{\hbar}{2\alpha} \tanh\left(\frac{b_z^I}{2k_B T}\right), \tag{3.111}$$

$$T_2 = \frac{\hbar \tanh\left(\frac{b_z^I}{2k_B T}\right)}{2\alpha\pi k_B T \tanh\left(\frac{b_z^I}{2k_B T}\right) + \alpha\pi b_z^I}. \tag{3.112}$$

For the T_1 time we recover the known results for the magnetic field dependence of the relaxation time [16, 17, 47]. In the case of a vanishing magnetic field $b_z^I = 0$, the two characteristic times coincide and

$$T_1 = T_2 = \frac{\hbar}{4\alpha\pi k_B T}. \tag{3.113}$$

Here, we find directly the proportionality between the relaxation time and the inverse temperature which is the Korringa relation of Eq. (3.31) [16, 17, 19, 20]. The Korringa constant $\kappa = T_1 T$ is identified as

$$\kappa = \frac{\hbar}{4\alpha\pi k_B T}, \tag{3.114}$$

as in the literature [16, 17, 47]. Since we recover the Korringa relation, we can conclude that the temporal correlations of the of the conduction electrons would not be able to explain the violation of the Korringa law in a Fermi liquid system at low temperatures as reported in [21]. In panel (a) of Fig. 3.4 we show the magnetic field dependence of the relaxation and decoherence time. Due to the $SU(2)$ symmetry, $T_1 = T_2$ in the zero field limit. Breaking this symmetry by applying a magnetic field leads to

$$T_1 = \frac{\hbar}{2\alpha\pi b_z^I}, \tag{3.115}$$

$$T_2 = \frac{\hbar}{\alpha\pi b_z^I}. \tag{3.116}$$

In the limit of large fields $b_z^I \gg k_B T$

$$T_2 = 2T_1, \tag{3.117}$$

which again agrees with the literature for systems with broken $SU(2)$ symmetry [16, 17, 132, 133]. In Fig. 3.4(b) the evolution of the ratio T_2/T_1 as a function of the external field is shown. For all fields, $T_1 < T_2 < 2T_1$ and the limit in Eq. (3.117) is reached rather slowly.

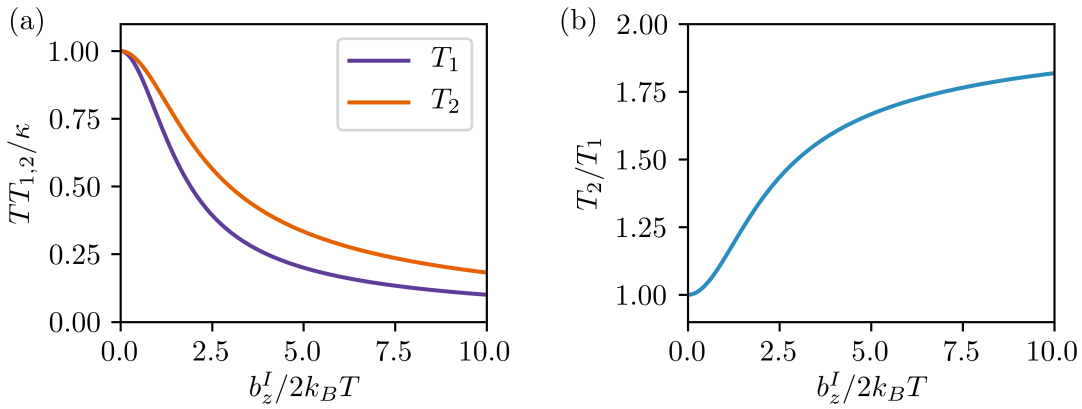

Figure 3.4: (a) Plot of $TT_{1,2}/\kappa$, with the Korringa constant $\kappa = \hbar/4\alpha\pi k_B$ as a function of the ratio of magnetic field and temperature $b_z^I/2k_BT$ to visualise the scaling behaviour of the T_1 and T_2 time as given in Eqs. (3.111) and (3.112). (b) The ratio T_2/T_1 is plotted across the same range as in (a), for large fields we achieve $T_2 = 2T_1$.

Knowing the residues for the Markov poles enables us to derive the Markovian contribution to the full time dynamics by performing the complex contour integration. For the two different components, the Markov decay is then given by

$$\rho_z^{\mathrm{M}}(t) = \rho_z^{\mathrm{eq}} + \frac{\left(\rho_z(t=0) - \rho_z^{\mathrm{eq}}\right) e^{-t/T_1}}{1 - 4\alpha\left\{\ln\left(\frac{2\pi k_B T}{\xi}\right) + \mathrm{Re}\left[\psi\left(1 + \frac{ib_z^I}{2\pi k_B T}\right)\right]\right\}}, \tag{3.118}$$

$$\rho_{\pm}^{\mathrm{M}}(t) = \frac{\rho_{\pm}(t=0) e^{-t/T_2} e^{i\omega\pm}}{1 - 2\alpha\left[2\ln\left(\frac{2\pi k_B T}{\xi'}\right) + \psi\left(1 + \frac{ib_z^I}{2\pi k_B T}\right)\right]}, \tag{3.119}$$

which simplifies in the zero field limit to

$$\rho_{z,\pm}^{\mathrm{M}}(t) = \frac{\rho_{z,\pm}(t=0) e^{-t/T_{1,2}}}{1 - 4\alpha\ln\left(\frac{2\pi k_B T}{\xi''}\right)}. \tag{3.120}$$

Here, in the constant ξ'' we absorbed the constant contribution of $\psi(1)/2$ and redefined the cutoff $\xi' \to \xi''$ in the spirit of Eq. (3.89). As indicated by the residues for the Markov poles, the amplitude of the Markovian decay is reduced from 1 to $[1 - O(\alpha)]$. Since our results are formulated for the rotating frame of reference we do not pick up the precession of a spin in an external field. For finite field the bath coupling renormalises the precession

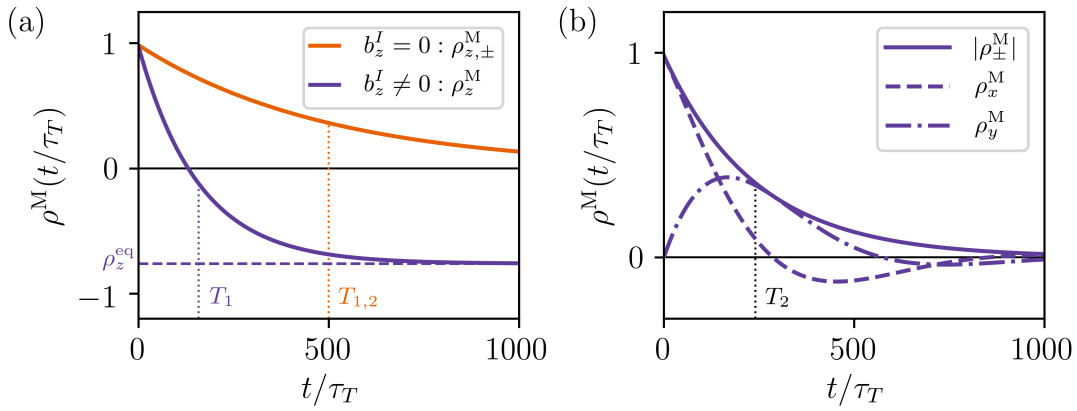

Figure 3.5: The Markovian decay of the reduced density matrix for the impurity spin is plotted as function of t/τ_T with $\tau_T = \hbar/2\pi k_B T$ for the parameters, $\alpha = 0.001$ and $k_B T = \xi/200$. The dotted line mark the $T_{1,2}$ times. In panel (a) the evolution of $\rho_{z,\pm}^{\mathrm{M}}$ in the zero-field limit is plotted (orange curve). For finite magnetic field, with $b = 2\pi k_B T$, ρ_z tends to the equilibrium value $\rho_z^{\mathrm{eq}} = -\tanh(1)$ indicated by the dashed purple line. For $b_z^I > 0$ the spin $\rho_z^{\mathrm{M}}(t=0) = 1$ is initialised against the magnetic field, hence, $\rho_z^{\mathrm{eq}} < 0$ in this case. Panel (b) shows the transverse components $\rho_\pm^{\mathrm{M}}$ in a finite field. The solid line corresponds to the absolute value $|\rho_\pm^{\mathrm{M}}|$ and the dashed lines to the real and imaginary parts, $\rho_x^{\mathrm{M}} = \mathrm{Re}[\rho_\pm^{\mathrm{M}}]$ and $\rho_y = \pm\mathrm{Im}[\rho_\pm^{\mathrm{M}}]$.

frequency of the transverse spin components to

$$\omega_\pm = \mp \frac{2\alpha b_z^I}{\hbar} \left\{ \ln\left(\frac{2\pi k_B T}{\xi'}\right) + \mathrm{Re}\left[\psi\left(1 \mp \frac{i b_z^I}{2\pi k_B T}\right)\right] \right\}. \tag{3.121}$$

Unlike the Knight shift discussed in Section 3.1.4, the frequencies $\omega_\pm$ have a strong magnetic field dependence which becomes non-linear for fields $b_z^I > 2\pi k_B T$ and for large enough fields even change sign. At low fields, the frequencies are linear in the field. In Fig. 3.5 we show the Markovian contribution to the full time evolution of the reduced density matrix. Panel (a) depicts the decay of the longitudinal component. In the zero-field limit (orange curve), $\rho_z(t)$ and $\rho_\pm(t)$ have the same evolution according to Eq. (3.120). The decay is characterised by single exponential with the characteristic relaxation or decoherence time marked with the dashed lines. For a finite field b_z^I, the z-components reaches the equilibrium state given by Eq. (3.103) marked ρ_z^{eq} in the plot. In panel (b) of Fig. 3.5 the Markovian decay of the transverse components is shown. The solid purple line represents the absolute value $|\rho_\pm(t)|$, the dashed lines show the real and imaginary parts $\rho_x(t) = \mathrm{Re}\,[\rho_\pm(t)]$ and $\rho_y(t) = \pm\mathrm{Im}\,[\rho_\pm(t)]$. A magnetic field of $b_z^I = 2\pi k_B T$ was chosen such that the precession of the spin with the frequency $\omega_\pm$ in Eq. (3.121) is of order $\omega \sim 1/T_2$ and therefore are clearly visible in the decay.

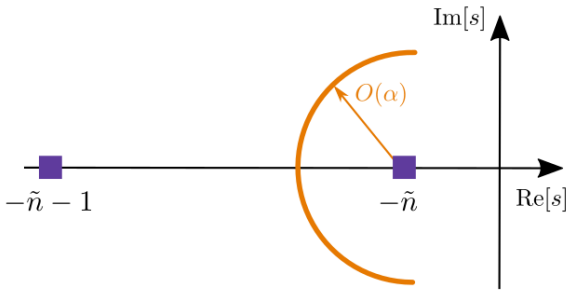

Figure 3.6: In the complex plane the $\psi(z)$ diverges at $z = -n$. Close to the singularity we expect to find a pole exactly where the small parameter α cancels the divergence and $\alpha\psi(z) = O(1)$. This is possible around a small region around the singularity $\tilde{n}$ marked by the orange semi-circle. The correction p of $O(\alpha)$ we want to determine pins down the exact point where $\alpha\psi(z) = O(1)$. In comparison to α the next singularity at $z = -\tilde{n} - 1$ is far away.

3.2.5 Non-Markovian dynamics

The spin-spin correlations functions for finite values of the Laplace variable s are dominated by the behaviour of the digamma function $\psi(z)$. The digamma function itself has a sequence of singularities at negative integers $z = -n$. This can easily be seen from its series expansion

$$\psi(1+z) = -\gamma + \sum_{n\geq 1} \frac{z}{n(z+n)}, \tag{3.122}$$

with γ the Euler–Mascheroni constant. In the expression of the spin-spin correlators F_α the digamma function appears always with the small prefactor α. Close to the singularities of $\psi(z)$, the small factor α cancels the divergence such that $\alpha\psi(z) \sim O(1)$. In Fig. 3.6 a single pole $z = -\tilde{n}$ is sketched. In the region marked by the orange semi-circle $\alpha\psi(z) \sim O(1)$ is fulfilled. Consequently, we expect to find the zeros of the denominator in Eqs. (3.76) and (3.77) near each singularity at $z = -n$. To determine the poles of Eqs. (3.76) and (3.77) we rely on the expansion in Eq. (3.122) and notice that the entire sum can be approximated by just the diverging term. This will lead to a rather straightforward equation to determine a correction p of $O(\alpha)$. The correction p is then the distance to the singularity at $z = -n$ and will correspond to the radius of the semi-circle in Fig. 3.6. Going through these steps we find a sequence of non-Markovian poles at $z_0 \approx -n + p$.

As in the Markovian case, we need to again solve

$$s - F_1(s) - F_2(s) = 0, \tag{3.123}$$

for the longitudinal component. In the zero field limit, the relevant digamma function is given by $\psi\left(1 + s/(2\pi k_B T)\right)$ and inserting the definitions of $F_1(s)$ and $F_2(s)$ into Eq. (3.123) leads to

$$0 = s + 4\alpha\pi k_B T - 4\alpha s \ln\left(\frac{2\pi k_B T}{\xi'}\right) - 4\alpha s\psi\left(1 + \frac{s}{2\pi k_B T}\right). \tag{3.124}$$

The second and third term are already $O(\alpha)$ and we neglect them as we are looking for a solution $s_0 \sim O(1)$. The location of s_0 is close to the divergence of $\psi(1 + s/2\pi k_B T)$ such that have

$$s_0 = -2\pi k_B T\tilde{n} + p, \tag{3.125}$$

with the small correction p of $O(\alpha)$ which is visualised in Fig. 3.6. Using the expansion in Eq. (3.122), we only need to keep the diverging term with $n = \tilde{n}$ and we obtain

$$0 = \left(s - 4\alpha \frac{\frac{s^2}{2\pi k_B T}}{\tilde{n}\left(\frac{s}{2\pi k_B T} + \tilde{n}\right)}\right)\Bigg|_{s\to s_0}. \tag{3.126}$$

Evaluating this last expression and only keeping the terms $O(1)$ leads to the correction p

$$\begin{aligned} 0 &= -2\pi k_B T\tilde{n} - 4\alpha\frac{(2\pi k_B T)^2\tilde{n}}{p} \\ \implies p &= -8\alpha\pi k_B T. \end{aligned} \tag{3.127}$$

Note that there is no dependence on the integer $\tilde{n}$ in the correction such that we are able to discuss the non-Markovian poles at each $\tilde{n}$ separately. Thus, the non-Markovian poles for $\rho_z(t)$ are located at

$$s_n = -2\pi k_B T n + p, \tag{3.128}$$

with integer number n. These poles indeed correspond to values near the Matsubara frequencies indicating the connection to the quantum fluctuations of the system. In fact, these are bosonic frequencies which means they arise from particle-hole fluctuations around the Fermi surface.

Again, we see the direct influence of the temperature on the dynamics. The distance

between two neighbouring non-Markovian poles is proportional to T. At large temperatures the first non-Markovian pole is 'far away' from the Markovian one close to $s \approx 0$ which hints at small non-Markovian contribution. This matches the expectation that the thermal fluctuations dominate over the quantum coherent correlations.

Each non-Markovian pole contributes with an exponential decay with a weight given by its residue. The corresponding residues, see Appendix E.2, for each of the poles s_n are given by

$$\mathrm{Res}(s_n) = \frac{4\alpha}{n} e^{s_n t}. \tag{3.129}$$

For large n, corresponding to short times, the weight $4\alpha/n$ is suppressed which we can understand if we recall that the non-Markovian contribution is driven by particle-hole fluctuations. Large n correspond to the creation of more particle-hole pairs where the probability decreases for increasing n at a given temperature T. The non-Markovian contribution to the full time evolution of the reduced density matrix can be found by summing up all residues belonging to the infinite sequence of non-Markovian poles. For $b_z^I = 0$ the evolution of $\rho_z(t)$ and $\rho_\pm(t)$ is identical and we obtain

$$\begin{aligned} \rho_{z,\pm}^{\mathrm{nM}}(t) &= \sum_{n\geq 1} \frac{4\alpha}{n} e^{-2\pi k_B T(n+4\alpha)t/\hbar} \rho_{z,\pm}(t=0), \\ &= -4\alpha e^{-4\alpha t/\tau_T} \ln\left(1 - e^{-t/\tau_T}\right) \rho_{z,\pm}(t=0), \end{aligned} \tag{3.130}$$

with the thermal time $\tau_T = \hbar/2\pi k_B T$. The collective sum of all particle-hole fluctuations leads to an exponential decay which is a modified logarithm. The characteristic decay is not set by the relaxation time T_1 but by the thermal time τ_T since

$$\ln\left(1 - e^{-t/\tau_T}\right) \sim e^{-t/\tau_T} \tag{3.131}$$

for times $t > \tau_T$ and is therefore shorter than the Markovian decay by $1/\alpha$. In the limit of small times $t \ll \tau_T$ the non-Markovian dynamics tend to a logarithmic decay

$$\rho_{z,\pm}^{\mathrm{nM}} \sim \ln(t/\tau_T), \tag{3.132}$$

which we will also discuss later in combination with the Markovian decay in Section 3.2.6.

To locate the non-Markovian poles at finite field we follow the same procedure as before, and here the relevant digamma function $\psi\left(1 + \left(s \pm i b_z^I/2\pi k_B T\right)\right)$ is shifted. For finite fields, the magnetic field dependence of the reduced density matrix differs for the components $\rho_z(t)$, $\rho_\pm$ and we have to treat them separately. Starting with the z-component, we

need to solve Eq. (3.123) for the finite field correlators $F_1(s)$ and $F_2(s)$ which are defined in Eqs. (3.97) and (3.98) and we obtain

$$0 = s - 2\alpha(s + ib_z^I)\psi\left(1 + \frac{s + ib_z^I}{2\pi k_B T}\right) - 2\alpha(s - ib_z^I)\psi\left(1 + \frac{s - ib_z^I}{2\pi k_B T}\right), \tag{3.133}$$

where we already dropped all $O(\alpha)$ terms. Again using the expansion Eq. (3.122) and keeping only the diverging term for a particular $\tilde{n}$ leads to

$$0 = s - 2\alpha\frac{\frac{(s+ib_z^I)^2}{2\pi k_B T}}{\tilde{n}\left(\frac{s+ib_z^I}{2\pi k_B T} + \tilde{n}\right)} - 2\alpha\frac{\frac{(s-ib_z^I)^2}{2\pi k_B T}}{\tilde{n}\left(\frac{s-ib_z^I}{2\pi k_B T} + \tilde{n}\right)}. \tag{3.134}$$

As before the pole will be close to the divergence such that inserting Eq. (3.125) into the last expression yields

$$0 = -2\pi k_B T\tilde{n} - 2\alpha\frac{(2\pi k_B T)^2\tilde{n}}{p + ib_z^I} - 2\alpha\frac{(2\pi k_B T)^2\tilde{n}}{p - ib_z^I}, \tag{3.135}$$

where we only keep $O(\alpha)$. The $\tilde{n}$ dependence drops out and we can solve for the correction p_r^z

$$p_r^z = -4\alpha\pi k_B T + r\sqrt{(4\alpha\pi k_B T)^2 - (b_z^I)^2}, \tag{3.136}$$

with $r = \pm$. For finite field we find two poles in close vicinity of the singularity of the digamma function given by

$$s_{n,r}^z = -2\pi k_B T n + p_r^z, \tag{3.137}$$

for every integer n.

For the residues of $r = \pm$ we obtain

$$\mathrm{Res}\left(s_{n,r}^z\right) = \frac{2\alpha}{n}e^{s_{n,r}^z t}\left[1 - r\frac{4\alpha\pi k_B T}{\sqrt{(4\alpha\pi k_B T)^2 - (b_z^I)^2}}\right], \tag{3.138}$$

details of the calculation can again be found in Appendix E.2.

In Fig. 3.7 the positions of the non-Markovian poles in Laplace space and the weight of the residue depending on the magnetic field are shown. To visualise the movement, with respect to the magnetic field, their location in the complex plane is sketched in panel (a). At zero field, there is only one non-Markovian pole for each n according to Eq. (3.128). Applying a finite field leads to a second pole appearing close the divergence

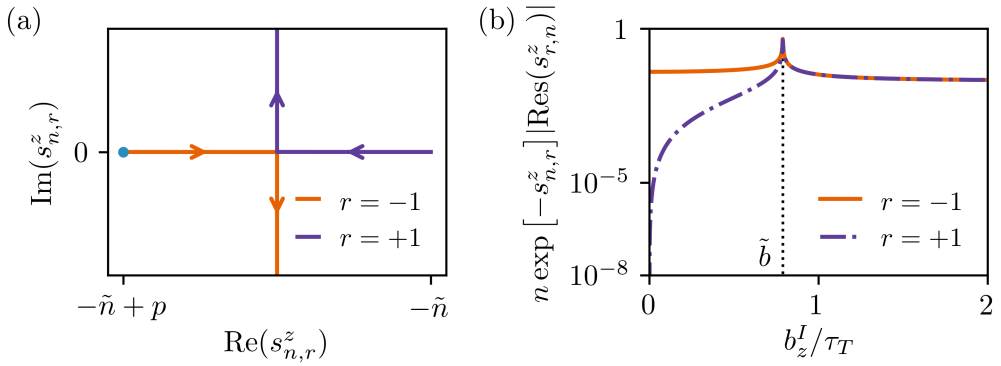

Figure 3.7: (a) Sketch of the position of the non-Markovian poles of Eq. (3.137) in Laplace space for a given $\tilde{n} = -2\pi k_B T n$ depending on the magnetic field. For $b^I_z = 0$, we find a single pole $\tilde{n} + p$ according to Eq. (3.128) marked in blue. For $b^I_z > 0$ a second pole appears close to $\tilde{n}$ on the real axis. With increasing field, the two poles, corresponding to $r = \pm 1$, approach each other on the real axis. At a critical field $\tilde{b} = 4\alpha\pi k_B T$ they meet. For even higher fields, they gain an increasing imaginary part. (b) Plot of the residue's weight as a function of the applied field b^I_z for both poles labelled by $r = \pm 1$. The residue of the pole appearing at $\tilde{n}$ in (a) has zero weight for $b^I_z = 0$ (purple line). It grows continuously until the weights for both residues diverge at $b^I_z = \tilde{b}$. They carry the same contributions to the overall dynamics for higher fields.

of the digamma function at $\tilde{n} = -2\pi k_B T$. This pole is invisible at $b^I_z = 0$ as its residue is proportional to b^I_z at low field. The positions of both poles are given by $s^z_{n,r}$ in Eq. (3.137). The pole for $r = -1$ follows the orange trajectory, and the pole corresponding to $r = +1$ the purple one. For magnetic fields $b^I_z < 4\alpha\pi k_B T$ both poles move towards each other with increasing field. This will lead to a modified decay rate in the time evolution. At a critical field $\tilde{b} = 4\alpha\pi k_B T$ they meet and for this field, only one non-Markovian pole for each n exists. For fields $b^I_z > 4\alpha\pi k_B T$ they split and they are leaving the real axis gaining a positive or negative imaginary part as indicated on the trajectories. Their distance to the real axis is symmetric and increases linearly with the magnetic field. The symmetry around the real axis can be understood in the following way. The component $\rho_z(t)$ in the chosen basis of the impurity spin represents the expectation values for the z-component $\langle I_z \rangle$. As I_z is a hermitian operator, it has real eigenvalues. Therefore the dynamics cannot become imaginary and only real valued oscillations are allowed. In Fig. 3.7(b) the weight of the residue, which corresponds to the last factor in Eq. (3.138) is plotted as a function of the magnetic field, again for both poles $s^z_{n,r}$ for $r = \pm 1$. We are able to recover the zero-field limit from Eq. (3.137) as the residue for $b^I_z = 0$ vanishes, therefore only the pole at $s^z_{n,r}$ for $r = -1$ contributes to the dynamics. For finite fields, the weight of the $r = +1$ branch increases until the residues at the critical field $\tilde{b} = 4\alpha\pi k_B T$ diverge. To determine the full dynamics, however, we sum over both $r = \pm 1$ and the divergences cancel. In

fields $b_z^I > 4\alpha\pi k_B T$ the residues' weights are evenly distributed, which corresponds to the situation of two non-Markovian poles at equal distance to the real axis.

For the transverse components $\rho_\pm^{\mathrm{nM}}(t)$ we find a similar situation. The only difference are the arguments of the digamma function, $\psi(1+s/2\pi k_B T)$ and $\psi(1+(s\mp ib_z^I/2\pi k_B T)$. We can make use of the calculation for ρ_z by shifting $s \to s \pm ib_z^I/2$ and $b_z^I \to b_z^I/2$. Including these changes, we find the location of the poles $s_{n,r}^\pm$

$$s_{n,r}^\pm = -2\pi k_B T n \mp \frac{i}{2} b_z^I + p_r^\pm, \tag{3.139}$$

with

$$p_r^\pm = p_r^z|_{b_z^I \to b_z^I/2} = -4\alpha\pi k_B T + r\sqrt{(4\alpha\pi k_B T)^2 - (b_z^I/2)^2}. \tag{3.140}$$

The corresponding residues are

$$\begin{aligned} \mathrm{Res}\left(s_{n,r}^\pm\right) &= \mathrm{Res}\left(s_{n,r}^z \mp ib_z^I\right)|_{b_z^I \to b_z^I/2} \\ &= \frac{2\alpha}{n} e^{s_{n,r}^\pm t}\left[1 - r\frac{4\alpha\pi k_B T}{\sqrt{(4\alpha\pi k_B T)^2 - (b_z^I/2)^2}}\right]. \end{aligned} \tag{3.141}$$

The poles $s_{n,r}^\pm$ follow the same pattern as $s_{n,r}^z$ discussed in Fig. 3.7 and the constant shift of $\mp ib_z^I$ in Eq. (3.139) modifies this only slightly.

The summation over all $2n$ residues in Eqs. (3.138) and (3.141), for each pair of poles $s_{n,r}^z, s_{n,r}^\pm$, leads to the non-Markovian part of the evolution for $\rho_z(t)$

$$\begin{aligned} \rho_z^{\mathrm{nM}}(t) &= \sum_{n\geq 1}\sum_{r=\pm} \mathrm{Res}\left(s_{n,r}^z\right)\left[\rho_z(t=0) - \rho_z^{\mathrm{eq}}\right] \\ &= -4\alpha e^{-4\alpha t/\tau_T} \ln\left(1 - e^{-t/\tau_T}\right) h(t, b_z^I)\left[\rho_z(t=0) - \rho_z^{\mathrm{eq}}\right], \end{aligned} \tag{3.142}$$

and

$$\begin{aligned} \rho_\pm^{\mathrm{nM}}(t) &= \sum_{n\geq 1}\sum_{r=\pm} \mathrm{Res}\left(s_{n,r}^\pm\right)\rho_\pm(t=0) \\ &= -4\alpha e^{\pm ib_z^I t/2\hbar} e^{-4\alpha t/\tau_T} \ln\left(1 - e^{-t/\tau_T}\right) h(t, b_z^I)\rho_\pm(t=0), \end{aligned} \tag{3.143}$$

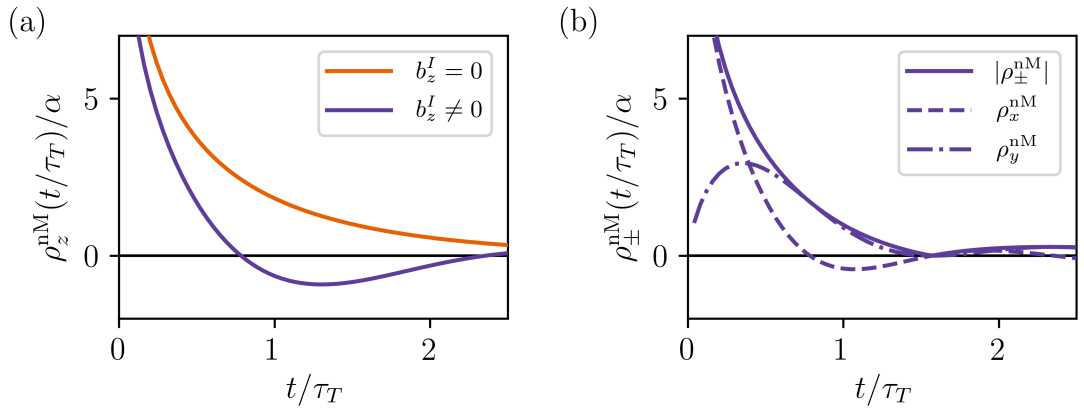

Figure 3.8: Non-Markovian decay of the components of the reduced density matrix is plotted as function of t/τ_T with $\tau_T = \hbar/2\pi k_B T$ for $\alpha = 0.001$. The solid orange curve in panel (a) shows the evolution $\rho_z^{\mathrm{nM}} = \rho_\pm^{nM}$ at zero magnetic field. The purple line corresponds to ρ_z at finite field. In panel (b) the evolution of $\rho_\pm^{\mathrm{nM}}$ for finite field is shown. The dashed lines correspond to ρ_x^{nM} and ρ_y^{nM} The finite field value is $b_z^I = 4\pi k_B T = 2\hbar/\tau_T$.

with the function

$$h(t, b_z^I) = \cosh\left(\frac{t}{\hbar}\sqrt{(4\alpha\pi k_B T) - (b_z^I)^2}\right) - \frac{4\alpha\pi k_B T}{\sqrt{(4\alpha\pi k_B T)^2 - (b_z^I)^2}} \sinh\left(\frac{t}{\hbar}\sqrt{(4\alpha\pi k_B T)^2 - (b_z^I)^2}\right). \tag{3.144}$$

The characteristic decay time of the non-Markovian part of the reduced density matrix differs from the Markovian part set by the relaxation and decoherence time T_1 and T_2. For times $t > \tau_T$ the logarithmic factor in the non-Markovian decay reduces to $\ln(1 - \exp[-t/\tau_T]) \sim \exp[-t/\tau_T]$ and therefore is $1/\alpha$ shorter than the characteristic times for the Markovian decay. Again, we see that the regime in which the non-Markovian behaviour is dominant is set by the temperature and high temperatures erase the memory effects. In the absence of a magnetic field or only small fields, the temperature remains the only scaling parameter able to influence the dynamics which is a manifestation of the scale-free nature of the Fermi gas. The effects of an external magnetic field are captured by the function $h(t, b_z^I)$. For low fields, it renormalises the decay as seen in the analysis of the poles in Fig. 3.7. For higher fields, $b > 4\alpha\pi k_B T$, $h(t, b_z^I)$ oscillates with the frequency $\sqrt{(b_z^I)^2 - (4\alpha\pi k_b T)^2}$. The frequency saturates at the nuclear cyclotron frequency $b_z^I/\hbar$ in the limit of large fields or low temperature T.

In Fig. 3.8 the non-Markovian part of the decay according to Eqs. (3.142) and (3.143)

is plotted. In the zero-field limit, the evolution of ρ_z^{nM} and $\rho_\pm^{\mathrm{nM}}$ coincides and is shown in panel (a) by the orange curve. The purple curves show the evolution for the different components at a finite field $b = 4\pi k_B T$. In panel (a) the decay of ρ_z^{nM} is plotted and panel (b) shows the absolute value $|\rho_\pm^{\mathrm{nM}}|$. The dashed lines correspond to the real and imaginary parts, $\rho_x^{\mathrm{nM}} = \mathrm{Re}(\rho_\pm^{\mathrm{nM}})$ and $\rho_y^{\mathrm{nM}} = \mp\mathrm{Im}(\rho_\pm^{\mathrm{nM}})$. The field is chosen to be large enough such that the oscillations it induces are of frequencies relevant to the non-Markovian time scale τ_T. In contrast to the oscillations of the Markovian part, here they appear for both components, ρ_z^{nM} and $\rho_\pm^{\mathrm{nM}}$. The onset field and frequencies vary for the different components due to their dependence on the function $h(t, b_z^I)$ for the longitudinal and $h(t, b_z^I/2)$ for transverse components. The dynamics for the impurity spin were derived under the assumption that an applied field does not magnetise the environment such that $\langle S_z \rangle \approx 0$. Therefore even high fields should not exceed $b_z^I \sim 2\pi k_B T$. Nonetheless, including the sample's magnetisation would lead to a constant shift of the magnetic field which can be absorbed in the field b_z^I itself. This would renormalise the positions of the non-Markovian poles. Therefore, we expect that the influence of the magnetic field captured by the function $h(t, b_z^I)$ in Eq. (3.144) remains a good approximation for higher fields $b_z^I \gg 2\pi k_B T$.

3.2.6 Full time evolution and initial slip

The full time evolution of the impurity spin's density matrix is given by the combination of Markovian contribution, Eqs. (3.106) and (3.107), and the non-Markovian part as derived in Eqs. (3.142) and (3.143). Adding the contributions leads to

$$\begin{aligned}\rho_z(t) = \rho_z^{\mathrm{eq}} + \frac{(\rho_z(t=0) - \rho_z^{\mathrm{eq}})\, e^{-t/T_1}}{1 - 4\alpha \left\{ \ln\left(\frac{2\pi k_B T}{\xi}\right) + \mathrm{Re}\left[\psi\left(1 + \frac{i b_z^I}{2\pi k_B T}\right)\right]\right\}} \\ - 4\alpha e^{-4\alpha t/\tau_T} \ln\left(1 - e^{-t/\tau_T}\right) h(t, b_z^I)\, [\rho_z(t=0) - \rho_z^{\mathrm{eq}}]\,, \end{aligned} \tag{3.145}$$

and

$$\begin{aligned}\rho_\pm(t) = \frac{\rho_\pm(t=0) e^{-t/T_2} e^{i\omega\pm}}{1 - 2\alpha \left[2\ln\left(\frac{2\pi k_B T}{\xi'}\right) + \psi\left(1 + \frac{i b_z^I}{2\pi k_B T}\right)\right]} \\ - 4\alpha e^{\pm i b_z^I t/2\hbar} e^{-4\alpha t/\tau_T} \ln\left(1 - e^{-t/\tau_T}\right) h(t, b_z^I/2) \rho_\pm(t=0). \end{aligned} \tag{3.146}$$

The universal dynamics for all times $t > \hbar/\xi$ are dominated by the non-Markovian part for times $t < \tau_T$. Then, they crossover to the exponential decay of the Markovian contribution for times $t > \tau_T$ where thermal fluctuations suppress the memory effects.

For very short times $t < \hbar/\xi$, the systems evolution is not universal and determined by

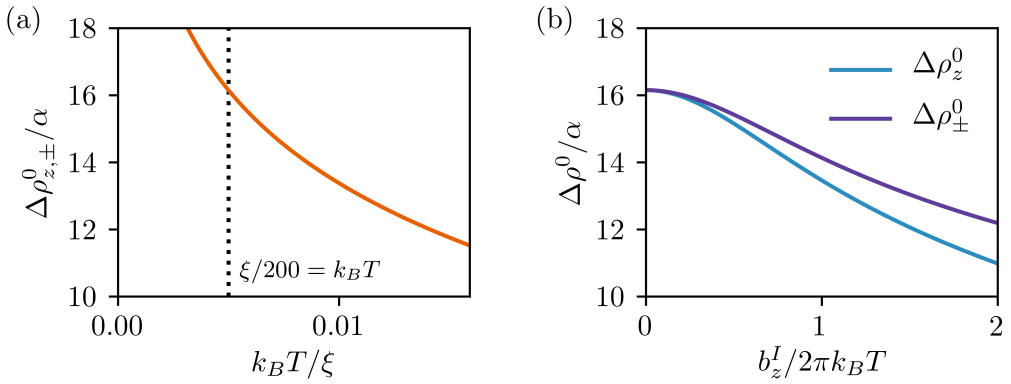

Figure 3.9: (a) The temperature dependence of the initial slip $\Delta\rho^0_{z,\pm}$ for $b^I_z = 0$ is plotted and $\xi \sim E_F$. The dashed line marks the initial slip amplitude for the parameters in Fig. 3.10. (b) The magnetic field dependence for $\Delta\rho^0_z$ (light blue) and $\Delta\rho^0_\pm$ (purple) is plotted for $k_BT = \xi/200$.

the band structure of the electronic bath. However, the evolution is quadratic in t which can be seen from a Taylor expansion around $t = 0$ of the equation of motion. In the limit $t \to 0$ Eq. (3.44) can be written as

$$\begin{aligned}\frac{d}{dt}\rho_I(t) &\approx \int_0^t dt' \Sigma_I(0)\rho_I(0) \\ &\approx t\Sigma_I(0)\rho_I(0).\end{aligned} \tag{3.147}$$

Integrating the last line leads to

$$\rho_I(t) \approx \left(1 + t^2\Sigma(t=0)\right)\rho_I(t=0). \tag{3.148}$$

After the initial, non-universal decay, the universal non-Markovian behaviour sets in. Its onset is logarithmic for both, longitudinal and transverse, components

$$\rho_{z,\pm}(t) \sim \ln\left(\frac{\xi t}{\hbar}\right) \tag{3.149}$$

and independent of the temperature. This logarithmic signature can be identified as the leading term of a Fermi edge singularity response in a many-body system [120–123]. Triggered by the local spin-spin interaction between impurity spin and itinerant electrons, this behaviour would lead to Kondo correlations when considering an interaction with an arbitrary number of induced spin flips [118, 119].

As discussed in Section 2.1.2 the amplitude of the non-Markovian contribution can be identified as an initial slip of the evolution [34, 111, 113, 114, 116]. The Markovian decay

in Eqs. (3.118) and (3.119) can be written as

$$\rho^{\mathrm{M}}_{z\pm}(t) \sim \frac{e^{-t/T_{1,2}}}{1+\Delta\rho^0_{z,\pm}}, \tag{3.150}$$

which defines the initial slip $\Delta\rho^0_{z,\pm}$ of $O(\alpha)$

$$\Delta\rho^0_z = \left| -4\alpha \left\{ \ln\left(\frac{2\pi k_B T}{\xi}\right) + \mathrm{Re}\left[\psi\left(1+\frac{ib^I_z}{2\pi k_B T}\right)\right]\right\}\right|, \tag{3.151}$$

$$\Delta\rho^0_\pm = \left| -2\alpha \left[2\ln\left(\frac{2\pi k_B T}{\xi'}\right) + \psi\left(1+\frac{ib^I_z}{2\pi k_B T}\right)\right]\right|. \tag{3.152}$$

In Fig. 3.9 we plot its temperature dependence in panel (a). The initial slip amplitude decays with increasing temperature T. This agrees with our expectation that for higher temperatures the non-Markovian contribution is washed out by the thermal fluctuations. Note, however, that $\xi \sim E_F$ and therefore $T \ll \xi$. In this limit the temperature dependence of the initial slip is negligible. The magnetic field dependence is displayed in Fig. 3.9(b). It shows that b^I_z only has a small effect on the slippage amplitude. The initial slip due the non-Markovian decay always leads to a systematic offset of the decay amplitude at all times $t > \tau_T$ for any T, b^I_z.

The full decay according to Eqs. (3.145) and (3.146) is plotted in Fig. 3.10. The initial slip is again indicated in panel (a). The solid orange line represents the full decay of $\rho_z(t)$ and $\rho_\pm(t)$ in the absence of a magnetic field. The orange dashed line indicates the Markovian contribution $\rho^{\mathrm{M}}_{z,\pm}$ and the dotted black lines corresponds to a purely Markovian evolution without taking into account the coherent backaction effects. The difference between the Markovian contributions in- and excluding memory effects marks the initial slip $\Delta\rho^0_{z,\pm}$ in the zero-field limit.

Similarly, in panel (b) the full evolution for a finite field $b^I_z \sim k_B T$ is plotted (solid lines) in comparison to a purely Markovian decay (black dotted line). In panel (c) again the full evolution for finite magnetic fields is shown, but on a logarithmic scale to focus on the non-Markovian features of the decay. The solid lines correspond to the same field as in (b) and the dashed lines to a higher field for which the oscillation of the function $h(t, b^I_z)$ become visible.

3.3 Summary and outlook

Starting from an open quantum system approach the full quantum coherent dynamics of an impurity spin coupled to an electronic bath has been derived. Following a generalised

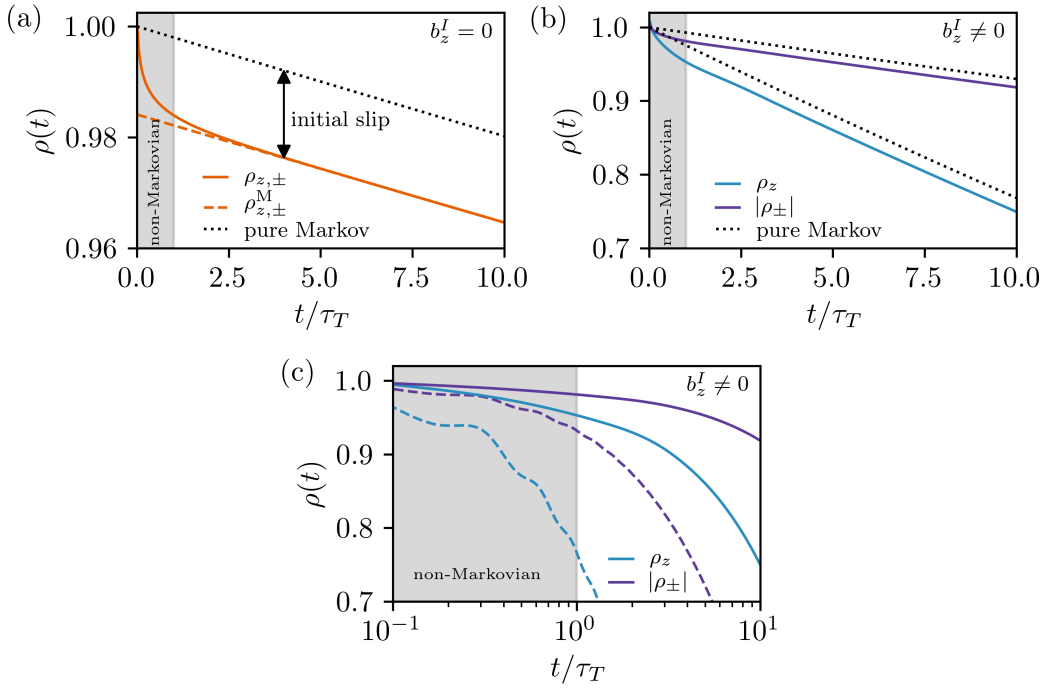

Figure 3.10: The full time evolution of the different components is plotted including Markovian and non-Markovian dynamics for $\alpha = 0.001$ and $k_BT = \xi/200$. The non-Markovian time regime for which $t < \tau_T$ is shaded in grey. In (a), the zero-field limit is shown. The solid orange line corresponds to the full evolution $\rho_{z,\pm}$ while the dashed line corresponds to only the Markovian decay from the calculation. The offset to a purely Markovian decay in a Born-Markov treatment (dotted black line) marks the initial slip. For finite field, the evolutions for ρ_z (blue) and $\rho_\pm$ (purple) differ, as shown in panel (b) with $b_z^I = 4\pi k_BT = 2\hbar/\tau_T$. For comparison, a purely Markovian decay $\exp(-t/T_{1,2})$ is marked by the dotted black lines. Panel (c) shows the decay for the same parameter choice as in (b) for the solid lines. The dashed lines show the decay for the corresponding component for a very large field, $b = 40\pi k_BT = 20\hbar/\tau_T$, such that the oscillations of the function $h(t, b_z^I)$ become noticeable.

master equation approach, we gained detailed insight in the system's dynamical behaviour through the analysis of the poles in Laplace space. The final result yields an analytic expression for the system dynamics in Eqs. (3.145) and (3.146), covering the short time dynamics which are driven by quantum correlations and then crossing into an exponential decay driven by thermal fluctuations. The conventional approach for the description of the decay of a magnetic moment interacting with an electronic reservoir leads to a strictly exponential decay characterised by the spin-lattice T_1 or spin-spin relaxation time T_2. It is based on the Bloch equations for the magnetisation and the relaxation times are introduced phenomenologically and a purely time-local Markovian time evolution is

assumed. The resulting decay is purely exponential and its characterised by the relaxation and decoherence time T_1 and T_2.

We recover this dynamical behaviour in the Markovian part of the decay. Furthermore, we find the Korringa relation, i.e. $TT_1 = \kappa$ with the Korringa constant $\kappa = 4\alpha\pi k_B$ and expressions for the relaxation times which are known in the literature. In contrast to the standard approach the amplitude of the Markovian decay is reduced from 1 to $[1 - O(\alpha)]$ which hints at the non-Markovian dynamics. This systematic offset corresponds to an initial slip of the starting conditions for the decay. If one would alter the initial condition according to this slippage, the purely Markovian evolution would not capture the correct dynamics for short times. In contrast to a mere slippage of the initial condition we have full access to the dynamics beyond the Markovian regime and therefore during the memory time of the system.

Beyond the Markovian regime, coherent backaction effects alter the localised spin dynamics. The characteristic time of the non-Markovian decay is set by the thermal time $\tau_T \sim 1/T$. The dependence on the temperature is not surprising as it is the only parameter describing the bath. The quantum correlations in the electronic environment are restricted by the temperature and the corresponding availability of free states above the Fermi level. Higher temperatures therefore wash out the small quantum coherent fluctuations of particle-hole excitations around the Fermi energy. At short times, the non-Markovian decay becomes temperature independent and purely logarithmic and therefore deviates from an exponential decay. The amplitude of the non-Markovian decay is set by the small parameter $\alpha = A^2/E_F^2$. For a typical metal such as copper with $\kappa = 1.27\,\mathrm{Ks}$ [47] and $E_F \sim$ eV, the value for α is tiny, $\alpha \sim 10^{-10}$. In semiconductors such as GaAs the coupling strength is $A = 90\,\mu\mathrm{eV}$ which leads to a slightly larger $\alpha \sim 10^{-7}$ with the Fermi energy in the meV regime [134–136]. However, a direct measurement of the non-Markovian decay remains challenging, though it might be possible to measure the offset $[1 - O(\alpha)]$ of the Markovian decay in a pump-probe experiment. A prepared state evolves for some time before it is brought back to its initial condition. The decay curve would be fitted to an purely exponential decay with its characteristic decay constant. Then the offset or initial slip at $t = 0$ and its temperature dependence is measurable.

Motivated by the long spin decoherence times in carbon nanotube quantum dots [137] we can make a connection to one dimensional systems. Our chosen approach to analyse the dynamics through the pole structure in Laplace state is not restricted to the bath chosen here. It could provide a way to investigate coherent backaction effects in stronger correlated systems, such as coupling a localised spin to a Luttinger liquid. The decay of correlations in a Luttinger liquid are already algebraic [138] and the coherent backaction effects will alter this further.

4

Electron cooling at low temperatures

The microscopic understanding of decay and relaxation mechanisms in quantum systems paves the way to employ dynamical effects, including those rooted in memory effects, to manipulate a quantum state in a desired manner.

At the intersection of the field of quantum information and quantum thermodynamics, the effect of quantum correlations is a vastly growing area of interest [139]. These quantum effects can be detected using thermodynamic measurements [53, 106]. With the realisation of single atom heat engines [54] it is possible to probe memory effects experimentally which allows us to engineer decoherence and control the information flow between a quantum system and its environment [140]. The intricate control of the quantum state of the system itself opens up the possibility to manipulate the environment, such as cooling the environment efficiently based on the system's behaviour on small scales [51]. There are many proposals and investigations which suggest that quantum correlations lead to a modified performance of the quantum heat engines [55, 141, 142]. Specifically, non-Markovianity alters and might improve the performance of quantum thermal machines [50, 52, 107–110, 143].

In the spirit of utilising the non-Markovian dynamics triggered by the system-bath interaction on short times scales, in this chapter we propose a protocol to effectively cool the environment. The cooling mechanism relies on the fast initial decay due to coherent backaction of the electrons onto the isolated spin which was investigated in Chapter 3. The idea is based on rapidly repeating the non-Markovian decay of an ensemble of localised spins. This driven system is out of equilibrium and we are not able to rely on a thermodynamic description for the system as a temperature cannot be defined. Therefore, instead of using the heat currents induced by temperature differences, we rely on the energy transfer between the localised spin system and the electrons. Since the electronic environment is treated as a macroscopic reservoir we can still assign a temperature to the electrons but not to the spin system with the exception of the initial and final state. With the proposed cooling protocol we bypass the natural bottleneck of cooling nanostructures

via nuclear demagnetisation. Nuclear demagnetisation cooling is slow at low temperatures due to the long relaxation time $T_1 \sim 1/T$. We show that our cooling protocol can be more efficient than the standard approach on a specific example of a semiconducting structure. A significant part of the work presented here are published results [87].

4.1 Cooling by nuclear magnetisation

To introduce cooling by demagnetisation we summarise the key principles and follow the discussion of [47]. In the 1920s demagnetisation cooling was proposed by Debye and Giauque [41, 42]. First experiments used paramagnetic salt and could reach temperatures between 2 mK and 1 K [47]. Since the 1960s this has been entirely replaced by nuclear spin cooling which reach temperatures well below 1 mK [144–146] and has become the standard for cooling down to ultra-low temperatures [21, 43, 45, 46, 147, 148].

In Fig. 4.1 the cycle for demagnetisation cooling is shown. Its cooling power relies on the magnetic disorder entropy of magnetic moments in a solid. At the initial temperature the spin system is subjected to an external magnetic field, leading to the magnetic order of spins. In the experimental setup the temperature is kept constant by an evaporating helium bath which absorbs the magnetisation heat. Then the magnetic field is adiabatically reduced. The adiabatic process keeps the entropy constant and therefore the nuclear spin temperature decreases which leads to a temperature bias between the spins and their environment. In turn the difference in temperature results in a cooling effect for the surrounding electrons as the spin and the electrons system establish the equilibrium state. Once the nuclear spin system is fully demagnetised the cooling power is used up, i.e., cooling by demagnetisation is an one-shot method and a cycle takes typically around ten hours [44]. In the following we describe the steps of the cooling cycle in more detail.

Starting with a pre-cooled nuclear spin system with temperature T_i, the spins are magnetised by an external magnetic field B_i while the spin temperature is kept constant. In Fig. 4.1 this corresponds to the path $A \to B$. For a typical cooling agent like copper, the initial temperature is $T \sim 10\,\mathrm{mK}$ in a magnetic field $B_i \sim 8\,\mathrm{T}$. The heat, which is released during the magnetisation for n moles, is given by

$$Q(T_i) = nT_i \int_0^{B_i} \left(\frac{\partial S}{\partial B}\right)_{T_i} dB. \tag{4.1}$$

During this process the entropy S of the nuclear spins is reduced from its maximum value

$$S_{\max} = R \ln (2I + 1) \tag{4.2}$$

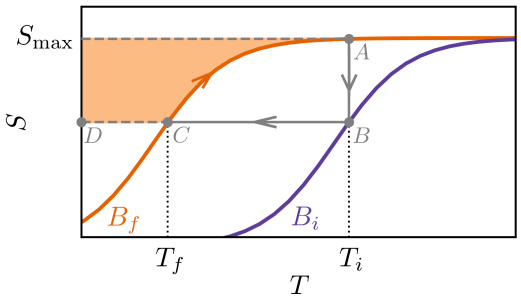

Figure 4.1: Sketch of cooling by demagnetisation where the entropy S is shown as a function of the spin temperature T. The spin system acting as the cooling agent is pre-cooled down to the initial temperature T_i and magnetised in an external field B_i. The generated heat by the magnetisation in Eq. (4.1) corresponds to the rectangle spanned by the points A, B, D and the maximum entropy $S_{\max}$ During this process along $A \to B$ then entropy is reduced. Adiabatically reducing the magnetic field to B_f ($B \to C$) leads to a decreasing temperature until T_f is reached. The spin system heats up along the orange curve $C \to A$ while cooling the surrounding electrons. The cooling power of the demagnetisation process is given by the shaded orange area.

with R the universal gas constant and I is the total spin.

In the next step, along $B \to C$, the external magnetic field is adiabatically reduced to a final magnetic field B_f. In this process the entropy remains constant, $\Delta S = 0$, and therefore

$$S\left(\frac{B_i}{T_i}\right) = S\left(\frac{B_f}{T_f}\right). \tag{4.3}$$

The final cooling power after the demagnetisation is then

$$Q(B_f) = n \int_{T_f}^{\infty} T \left(\frac{\partial S}{\partial T}\right)_{B_f} dT \tag{4.4}$$

and corresponds to the shaded area in Fig. 4.1. The heat Q is absorbed, therefore cooling the environment. The timescale for this cooling process is set by the spin-lattice relaxation time T_1. The Korringa relation [19] as discussed in Section 3.1.4 connects the relaxation time with the temperature

$$T_1 T = \kappa \tag{4.5}$$

with the Korringa constant κ. Typical values for the Korringa constants are $\sim 1\,\mathrm{Ks}$ for copper, $\sim 10\,\mathrm{Ks}$ for silver and $0.03\,\mathrm{Ks}$ for platinum [47]. Taking copper as a specific example, the relaxation time becomes very long, $T_1 \sim 10^3\,\mathrm{s}$, for an electron temperature

of $T \sim 1\,\mathrm{mK}$.

Because of these long relaxation times the thermalisation between the spin system and the electrons is very slow. Therefore, reaching a very low temperature for the nuclear spin system does not guarantee an equally low temperature for the reservoir electrons. The discrepancy between the temperatures are highly dependent on the material. For example, in rhodium the nuclear spin temperature is $\sim 100\,\mathrm{pK}$ while the electron temperature is $T \sim 0.1\,\mathrm{mK}$ [144, 145]. In other bulk metals, such as platinum, the difference in temperature are of the order of one magnitude, with a nuclear spin temperature of $T \sim 0.3\,\mu\mathrm{K}$ and the electron temperature at $T = 1.5\,\mu\mathrm{K}$ [146]. These discrepancies are usually the result of unavoidable heat leaks that mainly affect the electrons such that the cooling process becomes ineffective with the long T_1 times and cannot compensate for the heating. The situation to cool nanoelectronics is even more difficult because of the reduced thermal conductivity of semiconductors in comparison to a metal. Here the lowest temperatures achieved are in the millikelvin regime, while the nuclear spin temperature is $T \sim 100\,\mu\mathrm{K}$ [21, 43, 45, 46, 147, 148].

The reduced cooling efficiency due to the diverging relaxation times are a bottleneck to reach lower electron temperatures. Since the Korringa relation is mainly a result of the Fermi statistics, we can ask the question if there is a radically different way of bypassing this bottleneck and in the next section we offer a concrete proposal to do this.

4.2 Manipulating the bath: Low temperature electron cooling

As discussed above, the long relaxation times at low temperatures with $T_1 \sim 1/T$ present a natural bottleneck for cooling by demagnetisation. This motivates us to address the question of whether it is possible to cool the electronic system more efficiently when using the short time dynamics, opposed to the conventional method using the slower thermal relaxation in the Markovian regime. In the following we will study a macroscopic ensemble of localised spins which we assume to interact with the metal but not between themselves. This can be an ensemble of nuclear spins or any other type of localised spins, such as in the paramagnetic salts. Additionally, we assume that these spins are spin-1/2 for keeping the formalism as lean as possible and a similar result holds for any other spin. The cooling protocol will result in a pump scheme for the spin ensemble which repeatedly transfers a small amount of heat from the electronic system into the spin system.

In an external magnetic field the system Hamiltonian H_I corresponds to the Zeeman

energy

$$H_I = \sum_{j=1}^{N_I} \mu_I g_I B_z I_z^j, \tag{4.6}$$

with μ_I the magnetic moment of the localised spin and its g-factor g_I in an external magnetic field B_z along the z-direction. The space index j runs over all spins. Since we exclude direct or indirect spin-spin interactions we can treat each spin individually such that the reduced density matrix of the whole spin system is given by the product

$$\rho_I = \rho_{I,1} \otimes \cdots \otimes \rho_{I,N_I}, \tag{4.7}$$

with $\rho_{I,j}$ the density matrix of spin j. Under the assumption of identical initial states for every spin, the evolution of the full spin ensemble ρ_I is described by N_I copies of the evolution of a single spin. The energy current J_I of the ensemble can then be defined by

$$J_I = \frac{d}{dt} \mathrm{Tr}_{\mathrm{el}}\{H_I \rho(t)\} \tag{4.8}$$

where a current $J_I > 0$ corresponds to an energy flow from the electronic reservoir into the spin system. An estimate for the associated heat ΔQ which is transferred between electron and spin system over some time t is

$$\Delta Q(t) = \int_0^t dt' J_I(t'). \tag{4.9}$$

It should be emphasised that the transfer of energy and thus of heat always remains well defined even if the spin system is out of equilibrium and thermodynamics quantities such as the temperature cannot be defined. The energy transfer between spin system and electronic environment associated with each nuclear spin flip is fully determined by the longitudinal component $\rho_z(t)$ of the reduced density matrix. Therefore, we have

$$\Delta Q = N_I \mu_I g_I B_z I \left[\rho_z(t) - \rho_z(0)\right], \tag{4.10}$$

with the nuclear spin. The evolution of the reduced density matrix $\rho_z(t)$ is given by the full time evolution in Eq. (3.145). To utilise the quick, short time dynamics in the non-Markovian regime we focus on the decay for times shorter than the thermal time, $t \ll \tau_T$, before the slow Markovian decay sets in. In this regime, the decay of longitudinal

component $\rho_z(t)$ becomes temperature independent and is given by

$$\rho_z(t) = \rho_0 \left(1 - 4\alpha \ln\left(\frac{\xi t}{\hbar}\right)\right). \tag{4.11}$$

with $\alpha = (A/E_F)^2$ the small expansion parameter and the high energy cutoff ξ corresponding to the bandwidth. The parameter ρ_0 defines the difference between the initial and the equilibrium state

$$\rho_0 = \rho_z(0) - \rho_z^{\mathrm{eq}}. \tag{4.12}$$

Using the evolution for the reduced density matrix in Eq. (4.10) leads to

$$\Delta Q(t) = -4\alpha Q_z \rho_0 \ln\left(\frac{\xi t}{\hbar}\right), \tag{4.13}$$

with constant $Q_z = N_I \mu_I g_I B_z I = N_I b_z^I$, where as previously $b_z^I = \mu_I g_I B_z$. For the spin system to absorb energy we require $\Delta Q < 0$ and the initial state of the spins should minimise the Zeeman energy. Considering a magnetic field $B_z > 0$, the ground state of ultra cold spins corresponds to $\rho_z(0) \approx -1$ and therefore $\Delta Q < 0$ as $B_z(\rho_z(0) - \rho_z^{\mathrm{eq}}) < 0$. Explicitly, the constant ρ_0 is given by

$$\rho_0 = -\left(1 - \tanh\left(\frac{b_z^I}{2\pi k_B T}\right)\right) = -|\rho_0| \tag{4.14}$$

where we used the equilibrium value for the reduced density matrix as in Eq. (3.103). For most efficient cooling, the amplitude $B_z|\rho_0|$ should be maximised. However, a large magnetic field leads to small ρ_0 because of its dependence on the equilibrium value. Therefore, the parameter b_z^I should be of order of $2\pi k_B T$ to optimise the cooling efficiency. With these considerations the amplitude $B_z|\rho_0|$ should consequently scale with the temperature T, $B_z|\rho_0| \sim T$.

The analysis of the energy current in Eq. (4.8) shows that the transferred heat ΔQ is proportional to the small parameter α. Therefore, the cooling protocol needs to include many repetitions to utilise the fast initial slip of the system's decay. In Fig. 4.2 the idea of the cooling protocol is sketched. The solid purple line shows the full decay of $\rho_z(t)$ with a long relaxation time T_1. The conventional cooling method using nuclear demagnetisation would follow this curve. At low temperatures, the relaxation is slow as $T_1 \sim 1/T$, and it presents a natural bottleneck for the efficiency. The orange line depicts the decay within a pump scheme. After a short time, the spin ensemble is re-initialised and therefore goes through the fast initial decay repeatedly. The repeated initialisation could possibly be

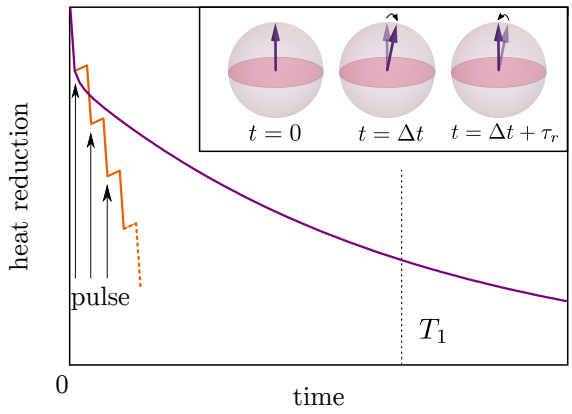

Figure 4.2: The sketch shows a visualisation of the cooling protocol: The protocol aims at transporting heat out of the electron system faster than conventional cooling methods (solid purple curve) by pumping the spins back into their initial state. The fast initial decay can repeatedly be used for the heat transfer (solid orange line). The inset show the corresponding state of the spin ensemble on the Bloch's sphere. The duration of one pump cycle is given by $t = \Delta t + \tau_r$, with $\Delta t \ll T_1$ and the time τ_r it takes for re-initialisation of the spin system.

done through resolved optical pumping of electron spins [149] or nuclear spins [150, 151], by optical pumping of hole spins [152], or by partial measurements [153]. With each pump cycle, a small amount of heat ΔQ according to Eq. (4.13) is transferred into the spin system. By pumping the spin system, some additional heat might be deposited back into the whole system, which is indicated by the small rise after each pulse along the orange curve in Fig. 4.2. The duration of each cycle is given by $\Delta t + \tau_r$. The time Δt is the time during which the system undergoes its fast evolution, $\Delta t \ll T_1$. The system is re-initialised over the time τ_r, which also needs to be of a similarly short times scale. In the inset of Fig. 4.2 the corresponding spin position is shown in the Bloch's sphere during one pump cycle to stress that for the system to be re-initialised we only need to correct a small amplitude of order α.

4.2.1 Thermodynamic requirements for the pumping scheme

In the following we will investigate in which parameter region the proposed cooling protocol could be more efficient than conventional cooling by exploring several conditions that we need to impose. The heat flow into the nuclear spin system and out of the electron spin system can be estimated as

$$Q_I = N_P \left(\Delta Q(\Delta t) + Q_I^P \right), \tag{4.15}$$

$$Q_{\text{el}} = N_P \left(-\Delta Q(\Delta t) + Q_r \right) + t J_{\text{ext}}^Q, \tag{4.16}$$

where $\Delta Q(\Delta t)$ is given by Eq. (4.13). The constants Q_I^P and Q_r are introduced to account for a possible heating due to the pulsing. For the heat balance of the electronic system we also include a constant energy current J_{ext}^Q over the duration t of the cooling protocol to model external heat leaks. Using the explicit expression in Eq. (4.13) and $t = N_P(\Delta t + \tau_r)$ the heat for the electron system can be written as

$$Q_{\text{el}}(t) = \frac{t}{\Delta t + \tau_r} \left(4\alpha Q_z \rho_0 \ln(\xi \Delta t) + Q_r\right) + t J_{\text{ext}}^Q. \tag{4.17}$$

The crucial condition such that cooling by the proposed mechanism is possible is

$$Q_{\text{el}} < 0. \tag{4.18}$$

From this constraint we can derive further conditions on the system parameters, such as the optimised time Δt between two pulses. The aim is to optimise the time Δt in order to maximise $|Q_{\text{el}}|$ over the duration t while ensuring that the process is faster than the relaxation time T_1. By dividing Eq. (4.17) by $|4\alpha Q_z \rho_0|$ and absorbing the constant into the logarithm, the cooling condition can be cast as

$$q_{\text{ext}} < q_{\text{cp}}. \tag{4.19}$$

The dimensionless parameter q_{cp} measures the efficiency of the cooling protocol and is defined as

$$q_{\text{cp}} = \frac{\tau_0}{\Delta t + \tau_r} \ln\left(\frac{\Delta t}{\tau_0}\right). \tag{4.20}$$

The influence of external heat leaks is measured by q_{ext} with

$$q_{\text{ext}} = \frac{\tau_0 J_{\text{ext}}^Q}{|4\alpha Q_z \rho_0|} \tag{4.21}$$

In the expression for q_{ext} and q_{cp}, the characteristic time τ_0, was introduced

$$\tau_0 = \frac{\hbar}{\xi} \exp\left[\frac{Q_r}{|4\alpha Q_z \rho_0|}\right]. \tag{4.22}$$

For the non-Markovian decay to be the dominant contribution to the dynamics, $\tau_0 < \tau_T$, with the thermal time $\tau_T \sim 1/T$. This last condition further provides a bound for the

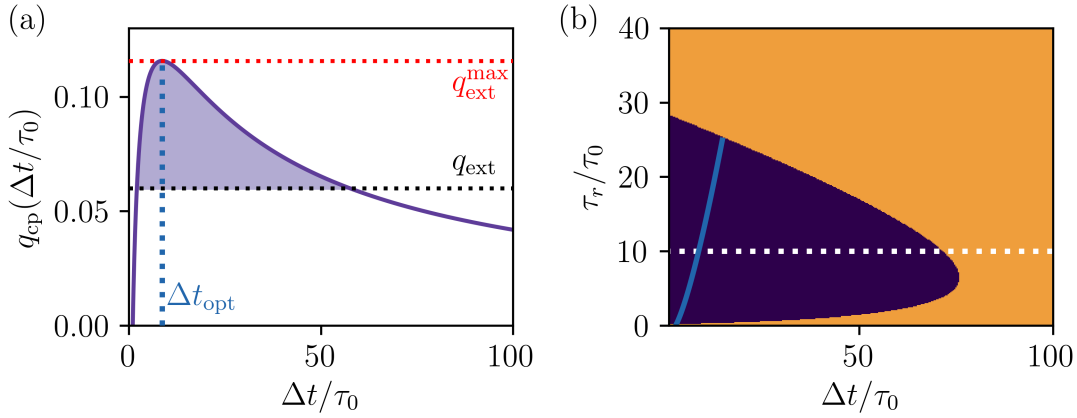

Figure 4.3: (a) The parameter $q_{\rm cp}$ is plotted as a function of $\Delta t/\tau_0$ (solid purple line) with the ration $\tau_r/\tau_0 = 10$. For an arbitrarily chosen values for the external heat leak $q_{\rm ext}$, marked by the black dashed line, cooling is possible in the purple shaded parameter regime. Above the maximum heat leak $q_{\rm ext}^{\rm max}$ (red dashed line) cooling is not possible. The blue dashed line indicates the optimal time $\Delta t_{\rm opt}$ for which cooling is most efficient. (b) The region for which cooling is possible is coloured purple for different values of the ratio of τ_r/τ_0. For the orange-shaded parameter region, cooling is not possible. The solid blue line indicates the location of the the optimal time Δt for given τ_r/τ_0. Panel (a) is the plot of $q_{\rm cp}$ for a cut along the white dashed line.

heat Q_r introduced into the setup during each pump cycle such that

$$Q_r < |4\alpha Q_z \rho_0| \ln\left(\frac{\xi \tau_T}{\hbar}\right). \tag{4.23}$$

Note that $Q_z\rho_0 \sim T$, so the heating Q_r by the re-initialisation imposes a constraint on the lowest temperature which can be reached. In panel (a) of Fig. 4.3 the efficiency of the cooling protocol $q_{\rm cp}$ is plotted as a function of $\Delta t/\tau_0$. The parameter range for which the condition in Eq. (4.19) is met and cooling is therefore possible is marked by the shaded area. The black dashed line is a specific choice of $q_{\rm ext}$, and below this cooling is no longer possible. Naturally, there is a maximum heat leak indicated by the red dashed line $q_{\rm ext}^{\rm max}$, for which the condition Eq. (4.19) is never met and cooling with the proposed pumping scheme is not possible. Maximising Eq. (4.20) with respect to the time Δt leads to an expression for the optimal time Δt between pulses

$$\Delta t_{\rm opt} = \frac{\tau_r}{W\left(\frac{\tau_r}{e\tau_0}\right)}, \tag{4.24}$$

where e is Euler's number and $W(z)$ is the Lambert W function, also know as product logarithm. It is defined as the inverse of the function

$$z(W) = We^W, \tag{4.25}$$

for complex numbers z, W. The argument $z = \tau_r/e\tau_0$ influences the optimal time Δt. The optimal time Δt for a specific choice of the argument is shown with the dashed blue line in Fig. 4.3(a). In panel (b) of Fig. 4.3 the parameter region where cooling is possible is marked purple for different values for the ratio τ_r/τ_0 as a function of $\Delta t/\tau_0$. For larger external heat leaks, the parameter region for which cooling is possible shrinks. The blue line indicates the location of the maxima which are determined by Eq. (4.24). If there is a large amount of heat dumped into the system in a pump cycle, then, according to Eq. (4.22), $z = \tau_r/e\tau_0 \ll 1$. In this limit

$$W(z) \approx \frac{z}{e}, \tag{4.26}$$

and therefore the optimal pumping time is of order of the characteristic time, $\Delta t \sim \tau_0$. In the opposite limit, $z = \tau_r/e\tau_0 \gg 1$ and the Lambert W function can be approximated with

$$W(z) \approx \ln(z) \tag{4.27}$$

which leads to $\Delta t \sim \tau_r$. Combining these results with the constraint in Eq. (4.23) for the maximum heat that can be absorbed by the system due to the pumping, the range of the optimal time Δt_{opt} is set by τ_r and τ_0.

Finally, the number of pump cycles N_P can be estimated with the heat Q_{el} flowing out of the electron system in Eq. (4.16). The conduction electron themselves form a large reservoir and we can assume that the individual induced spin flips do not alter the electronic state. Therefore, the electrons remain in an equilibrium state and we can assign thermodynamic quantities to the electron system. Its temperature T_{el} is given by

$$T_{\text{el}}(t) = T_{\text{el}}(0) + \frac{Q_{\text{el}}(t)}{C_{\text{el}}}, \tag{4.28}$$

where C_{el} is the specific heat for the electron system. Initially, before the cooling protocol starts, we can assign a temperature $T_I(0)$ to the nuclear spin system as well. However, as soon as the nuclear spin system undergoes repeated initialisations the definition of a temperature is no longer meaningful as the system is out of equilibrium at all times. Here, the initial temperature $T_I(0)$ is used as a lower bound for the final electronic temperature

such that

$$T_I(0) \approx T_{\mathrm{el}}(t), \tag{4.29}$$

after the duration t of the complete cooling protocol. Of course, this choice is rather optimistic as the electron temperature might influence the cooling efficiency q_{cp} as well as τ_0 and therefore has an impact on the lowest achievable electron temperature T_{el}. In the following we assume the temperature dependence of these parameters to be weak. Using Eq. (4.29) and replacing Q_{el} with Eq. (4.16) in Eq. (4.28) leads

$$N_P = \frac{C_{\mathrm{el}}\left[T_{\mathrm{el}}(0) - T_I(0)\right]}{\Delta Q(\Delta t) - Q_r - (\Delta t + \tau_r) J^Q_{\mathrm{ext}}} \tag{4.30}$$

as an estimate for the number of cycles. The largest quantity in the denominator has to be the transferred heat ΔQ between electron and nuclear spin system. It is, according to Eq. (4.13) proportional to α. Therefore, the cooling protocol needs to run through

$$N_P = \frac{1}{\alpha} \tag{4.31}$$

cycles under the condition that the full duration is smaller than the relaxation time T_1. With values of $\alpha \sim 10^{-6} - 10^{-10}$ this corresponds to a range of $N_P \sim 10^6 - 10^{10}$ but more concrete estimates for realistic systems will be provided below in Section 4.2.3.

4.2.2 Temperature dependence of ideal pulsing

Above it was assumed that the ideal time Δt is independent of the temperature T. In this subsection we discuss briefly the temperature dependence of the time Δt, assuming that Δt and τ_T are comparable. Instead of using the short-time, temperature independent decay to find in expression for ΔQ in Eq. (4.10) we use the full decay of the reduced density matrix from Eq. (3.145) in the limit for times $t \ll T_1$

$$\Delta Q(t) = |4\alpha Q_z \rho_0| \left(\ln\left(\xi\tau_T\right) + \ln\left(1 - e^{-t/\tau_T}\right)\right). \tag{4.32}$$

Using the definition for the transferred heat for the electron system leads to

$$Q_{\mathrm{el}}(t) = \frac{t}{\Delta t + \tau_P}\left[-|4\alpha\rho_0| Q_z \left(\ln\left(\xi\tau_T\right) + \ln\left(1 - e^{-\Delta t/\tau_T}\right)\right) + Q_r\right] + t J^Q_{\mathrm{ext}}. \tag{4.33}$$

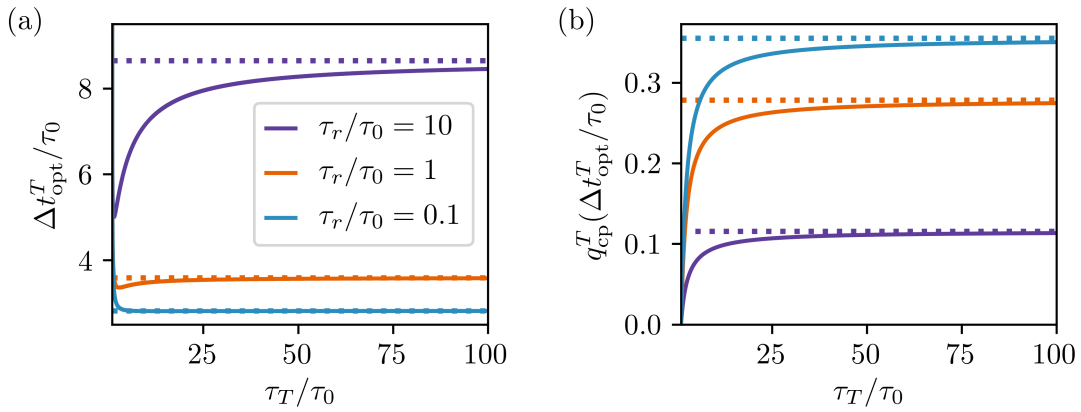

Figure 4.4: (a) The optimal time $\Delta t^T_{\mathrm{opt}}/\tau_0$ is shown as a function of the thermal time τ_T/τ_0 for different choices of τ_r/τ_0. Large τ_T correspond to low temperature T as $\tau_T \sim 1/T$, while a large ratio τ_r/τ_0 corresponds to less heat being dumped in the electronic system during the pumping, assuming a constant pulsing time τ_r. The dashed lines indicate Δt_{opt} for the temperature independent treatment in the previous section. The temperature dependence of Δt_{opt} is negligible for some parameters (orange and light blue line) and is small for small temperature in all cases. (b) Plot of the temperature dependent cooling efficiency q^T_{cp} across τ_T/τ_0 for the same choice of τ_r/τ_0 as in (a). The dashed line indicate the optimum in the temperature independent treatment. The latter is the maximum and is reached asymptotically in all cases.

With the requirement for cooling, i.e. $Q_{\mathrm{el}} < 0$, this leads again to a constraint

$$q^T_{\mathrm{ext}} < q^T_{\mathrm{cp}}. \tag{4.34}$$

Similar to Eq. (4.20) and Eq. (4.21), we introduce the dimensionless parameter q^T_{cp} which measures the cooling efficiency

$$q^T_{\mathrm{cp}} = \frac{1}{\Delta t + \tau_r}\left[\ln\left(\frac{\tau_T}{\tau_0}\right) + \ln\left(1 - e^{-\Delta t/\tau_T}\right)\right] \tag{4.35}$$

and the external heat leak is captured by

$$q^T_{\mathrm{ext}} = \frac{J^Q_{\mathrm{ext}}}{|4\alpha Q_z \rho_0|}. \tag{4.36}$$

The characteristic time τ_0 is defined as before in Eq. (4.22). A lower limit for Δt in the temperature dependent case can be found by assuming an ideal situation in which the external heat leak vanishes and $q^T_{\mathrm{cp}} > 0$. In this case, we can solve Eq. (4.35) for Δt. This

leads to the condition

$$\Delta t > \tau_T \ln\left(\frac{1}{1-\tau_0/\tau_T}\right). \tag{4.37}$$

Therefore, cooling is indeed only possible if $\tau_0 < \tau_T$, and again resulting in the requirement for the heat Q^r dumped in into the electrons due to the pulsing, as seen in Eq. (4.23). To find the impact of the temperature through τ_T on the cooling efficiency q_{cp}^T we evaluate the optimal time $\Delta t_{\mathrm{opt}}^T$, where q_{cp}^T reaches its maximum as a function of the parameter τ_T/τ_0 in Fig. 4.4(a). The ratios τ_r/τ_0 are chosen such that cases are covered where a large amount of heat is transferred through the pumping as well as the opposite. The dashed lines show the optimal time Δt_{opt} according to Eq. (4.24) of the temperature independent analysis for the corresponding choice of parameters. For a larger heat deposit during each pump cycle smaller Δt is required while there is no temperature dependence across the range of τ_T/τ_0, as shown by the light blue lines. In the opposite limit (purple) the optimal $\Delta t_{\mathrm{opt}}^T$ shows a temperature dependence, suggesting that a dynamically changed time Δt between pulses is beneficial when decreasing the pump frequency while approaching lower temperature and therefore higher τ_T/τ_0. In panel (b) of Fig. 4.4 the maximum efficiency q_{cp}^T is shown for a range of τ_T/τ_0. The dashed lines indicate the maximum q_{cp} according to Eq. (4.20). The growing value of the cooling efficiency for decreasing ratios of τ_r/τ_0 indicate, that while for smaller τ_r/τ_0 a larger amount of heat is deposited, the proposed scheme is more efficient in carrying out the heat with each cycle. The maximum efficiency set by the temperature independent case is reached asymptotically with larger deviations at small τ_T/τ_0. The actual efficiency of the cooling protocol therefore shows a temperature dependence for some parameters. However, as the protocol would operate at low temperatures, the temperature dependence of the cooling efficiency and its impact on the optimal time between pulses Δt_{opt} is small and in many cases negligible.

4.2.3 Estimate for a semiconductor

The cooling protocol can only be efficient if it is possible to re-initialise the nuclear or localised spin system repeatedly on a timescale that is smaller than the relaxation time T_1. Within each cycle a small amount of heat of order α is transferred. The small parameter $\alpha = (\nu_0 A)^2$ is set by the coupling constant A between nuclear and electronic spins and the density of states ν_0, which is approximately constant and proportional to the bandwidth ξ and therefore of the order of the Fermi energy E_F. The density of states ν_0 in low dimensional systems is set by the ratio of the electron spin density n_{el} and the nuclear or impurity spin density n_I, $\nu_0 \sim n_{\mathrm{el}}/n_I$ [154–157]. Thus, the parameter α

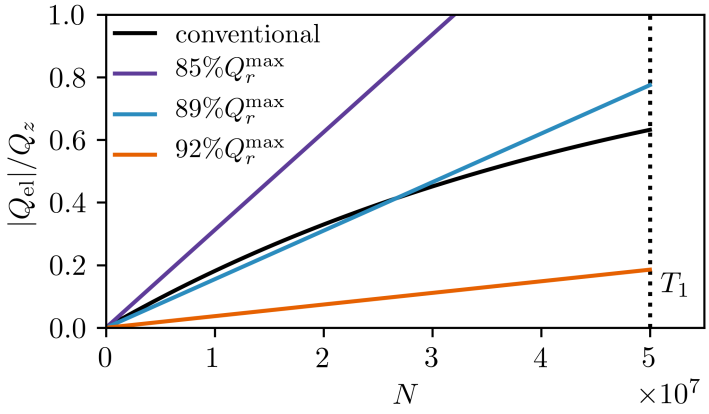

Figure 4.5: Plot of the $|Q_{\mathrm{el}}|$ according to Eq. (4.17) for different values of Q_r (colorful lines) where $Q_r^{\max}$ is set by Eq. (4.23). In comparison we show $|Q_{\mathrm{el}}|$ without pumping which simply follows an exponential set by T_1 time (black solid line). The T_1 is indicated by the dashed black line. The parameter settings are: $T = 0.1\,\mathrm{mK}$, $\alpha = 10^{-8}$, $\Delta t = 0.5\tau_T$ with $\tau_T = \hbar/2\pi k_B T$, $E_F = 10^{-3}\,\mathrm{eV}$, $T_1 = \hbar/4\alpha k_B T \approx 0.6\,\mathrm{s}$, and the duration of one pump cycle is $\Delta t + \tau_r = 2\Delta t$ with $N_p = 5 \cdot 10^7 \sim 1/\alpha$.

is highly dependent on the considered system. For nuclear spins in a bulk metal, the value is very small $\alpha \sim 10^{-10}$ [47]. The values reaches $\alpha \sim 10^{-4}$ for paramagnetic spins in correlated metals [158] and can even be larger than one in magnetic semiconductors [159, 160]. However, with our approach, values for $\alpha > 1$ are not valid as we rely on the smallness of α to determine the time evolution of the density matrix. Nonetheless, even for $\alpha > 1$ there will be coherent non-Markovian dynamics such that in principal a similar cooling effect through the protocol should persist.

As a specific example, we consider a semiconductor with nuclear spins, such as GaAs. The hyperfine interaction is $A = 90\,\mu\mathrm{eV}$ and the Fermi energy E_F is of the order of meV [134–136]. This leads to an estimate of $\alpha \sim (A/E_F)^2 = 10^{-8}$. The corresponding relaxation time T_1 is given by

$$T_1 = \frac{\hbar}{4\alpha\pi k_B T} \tag{4.38}$$

according to calculation of the relaxation rates in Section 3.2.4. At an electron temperature $T \sim 0.1\,\mathrm{mK}$, the relaxation time $T_1 \sim 1\,\mathrm{s}$ sets the maximal time for the cooling protocol. Within the T_1 time the pump cycle needs to be repeated $N_P \sim 1/\alpha$ such that one cycle maximally takes $\Delta t + \tau_r < \alpha T_1 \sim 10\,\mathrm{ns}$. Therefore, Δt and the re-initialisation time τ_r have to be of the same order, which is fast, but feasible for experimental techniques such as optical manipulation [150, 151], optical pumping [152] or partial measurements

[153]. Finally, the characteristic time τ_0 defined in Eq. (4.22) scales with $\hbar/\xi \sim \hbar/E_F$ and is of the order of picoseconds times an exponential. The exponent $Q_r/|4\alpha Q_z \rho_0|$, and importantly the heat Q_r released into the system during the re-initialisation are not too constrained such that there is some tunability to satisfy all requirements. To show that the conditions can be met for the GaAs parameters we plot the heat $|Q_{\mathrm{el}}|$ flowing out of the electron system according to Eq. (4.17) in Fig. 4.5. The maximum number of pump cycles is set by $N_P^{\max} \sim 1/\alpha = 10^8$ with pump cycles with each cycle taking $\Delta t + \tau_r = 2\Delta t$. Furthermore, we choose $\Delta t = 0.5\tau_T$ with $\tau_T \approx 12\,\mathrm{ns}$ for a temperature $T = 0.1\,\mathrm{mK}$. For this specific choice $T_1 \approx 0.6s$ which is marked by the black dashed line. The solid black line shows the heat $|Q_{\mathrm{el}}|$ if there is no pumping. In this case Q_{el} is defined by Eq. (4.10) and follows an exponential. The characteristic timescale of the exponential is given by T_1 time and stems from the long time decay of the density matrix $\rho_z(t)$. The coloured lines show $|Q_{\mathrm{el}}|$ for different choices of Q_r as a percentage of the maximal $Q_r^{\max}$ set by Eq. (4.23) where we chose $\xi = E_F = 1\,\mathrm{meV}$. For the largest chosen $Q_r = 0.92 Q_r^{\max}$ (orange line) the cooling protocol is not more efficient than the standard approach. Even for slightly smaller Q_r the protocol cools the electron system faster which can be improved further by reducing Q_r (light blue and purple line). The analysis shows that the conditions on Q_r are indeed not too restricting. We still need to be able to re-initialise the spin system on short time scales. The decay which needs to be reversed is small as it is $O(\alpha)$ such that the physical manipulation of the spin is not a limiting factor but rather is limited by the achievable repetition rate.

4.3 Summary and outlook

The proposed cooling protocol aims at an efficient transport of heat out of the electronic reservoir into a spin system. It is based on the fast, initial decay dynamics rooted in the coherent backaction effects and relies on fast repetition of the non-Markovian dynamics by pumping or pulsing the spin system repeatedly into their initial state. Such a pump scheme might be able to sidestep the bottleneck of adiabatic demagnetisation cooling at low temperature, in particular for semiconductor structures. Based on basic requirements for the relevant thermodynamic quantities we were able to provide an estimate for the parameter region in which the cooling protocol is efficient.

Possible future directions could include the extension of the thermodynamic treatment to underline the non-Markovian dynamics on a fundamental thermodynamic level. This could be done, e.g., through a description of how the entropy in the localised spin system builds up. The latter could then be connected with the build-up of entanglement and thus lead to the opportunity to provide an explicit microscopic connection between

entanglement and entropy production.

5

Multiple spins in a common environment

The dynamical behaviour for multiple impurity spins effectively coupled through the environment is interesting from a quantum information point of view. It has been shown that the entanglement dynamics are affected by dissipation and non-Markovian effects modify the behaviour further for directly coupled [39] or effectively coupled qubits [161]. In combination with exploiting non-Markovian dynamics mediated by the system-bath coupling it has been suggested that the coherent backaction can lead to noise cancellation [33, 34] and that memory effects play a role in error correction protocols [104].

We want to address the question if and how a localised spin and its dynamical behaviour is affected by the presence of an additional spin which shares the same electronic environment. We assume no direct interaction between the spins, only the interaction mediated by the conduction electrons. In the standard approach this corresponds to the RKKY interaction between nuclear spins and the itinerant electrons [35–37]. Here, we are seeking to extend this to a quantum coherent RKKY-type interaction which is time-dependent. We expect time delays to play a role simply because of the fact that it takes some time for an excitation in the bath to travel from one location of an impurity spin to the next.

To capture the dynamical response of a spin system with more than one localised spin one could in principle take the approach pursued in Chapter 3 and add additional impurity spins. However, the dimension of the basis grows as 2^{2N} with N being the number of impurity spin. For $N = 2$ the approach might still be feasible but treating more spins in a common bath is not tractable analytically. The self-consistent projection operator method introduced by Degenfeld-Schonburg and Hartmann [38] provides an elegant solution for the problem of quickly growing Hilbert space dimensions. The generalised master equation within this approach can be seen as an extension to the Nakajima-Zwanzig equation where the reference bath state is self-consistently determined. The bath correlation functions are updated with respect to the time-dependent bath reference state at every time step. Additional degrees of freedom within the system only enter through a sum

over all sites occupied with a localised spin.

The tradeoff is the challenge of solving a set of equations of motion describing the localised spins and the electronic bath dynamics. Formally, we can write down the equation of motion for the conduction electrons easily, but the proliferation of the infinite number of electronic degrees of freedom turns out to be a major challenge in this treatment. To make the problem tractable we turn our attention towards two essential aspects. First, we systematically reduce the number of coupled equations of motion from an infinite set to a set of 24 coupled equations. We carefully analyse the nature of the appearing interactions, correlations and fluctuations to reveal and interpret their physical significance. With this alone many nuances of the problem can be sufficiently understood without having to proceed to its full solution. Second, we identify and adapt a recently proposed numerical method [162] which is suited for the further analysis. The algorithm implements the rather inexpensive interpolation scheme for numerical integration developed in [163] and we thoroughly test it against the known analytical solution of the single spin derived in Chapter 3. In fact, this does not only lead to a corroboration of the applicability of the algorithm but also to a confirmation that the approximations made in the analytical solution capture all the relevant physics. The corrections picked up in the numerical integration can all be absorbed by a slight renormalisation of the parameters.

Although the last step, the final implementation of the coupled equations and their systematic investigation, had to be sacrificed within the scope of this thesis, we can administer the important identification of the relevant physics and the algorithmic foundation.

5.1 Interaction mediated by the bath

For a single localised moment in a metallic environment the local magnetic field is modulated by the surrounding electrons giving rise to the Knight shift as described in Section 3.1.4. The magnetic impurity induces modulations in the electron spin density [23] which in turn can be picked up by a second impurity some distance away. The fluctuations of the electron spin density effectively couple the two localised spins $\mathbf{I}_i$ and $\mathbf{I}_j$ at the sites x_i, x_j with $r_{ij} = |x_i - x_j|$. One can also understand the effective coupling as a double scattering process [16, 35]. The contact interaction between the impurity and electron spin $A\mathbf{I}_j \cdot \mathbf{S}_j$ scatters the electron from a state $|k\rangle \to |k'\rangle$ and the interaction with the second impurity reverses the process $|k'\rangle \to |k\rangle$. The long range interaction is

known as RKKY interaction [35–37] and is described by the Hamiltonian

$$H_{\mathrm{RKKY}} = \frac{1}{2}\sum_{i,j} A_{ij}\mathbf{I}_i \cdot \mathbf{I}_j, \tag{5.1}$$

for two impurity sites i and j. The most familiar form of the RKKY interaction is the three dimensional real space expression

$$A_{ij} = A^2 n \frac{1}{2\pi^2 r_{ij}^3}\left[\cos\left(2k_F r_{ij}\right) - \frac{\sin\left(2k_F r_{ij}\right)}{2k_F r_{ij}}\right]. \tag{5.2}$$

The local moments are separated by the distance r_{ij}. The coupling constant A corresponds to the contact interaction strength, k_F is the Fermi momentum and n the electron density of the Fermi liquid. Eq. (5.2) shows the general characteristics of an algebraic decay in addition to $2k_F$ Friedel type oscillations set by the backscattering vector across the Fermi surface. The exact power of the algebraic decay depends on the dimension d with $1/r_{ij}^d$. In lower dimension the decay is modified [164–166], but these general characteristics remain the same. Later on we will focus on a two dimensional electron gas as the environment for the localised spin. This circumvents the special case of one spatial dimension for which a Luttinger Liquid description is necessary while ensuring a more tractable analytical description. Furthermore, two dimensional systems are a widely used platform for designed nanosystems [167, 168].

5.2 Master equation within self-consistent projection operator approach

The starting point is the generalised master equation (2.109) which was proposed in [38]. It provides an equation of motion for the system of interest, i.e., the subsystem that contains the dynamics we are interested in while all other subsystem act as a bath for the system. We adjust Eq. (2.109) directly to a quantum system which consists of two localised spins coupled to the same electronic environment to access the dynamics. The example setup, made up of the three components, is sketched in Fig. 5.1. First, we identify the different subsystems and define the corresponding Hamiltonian. Each localised spin $\mathbf{I}_j$ is described by the Zeeman term

$$H_I^j = b_z^I I_{z,j}. \tag{5.3}$$

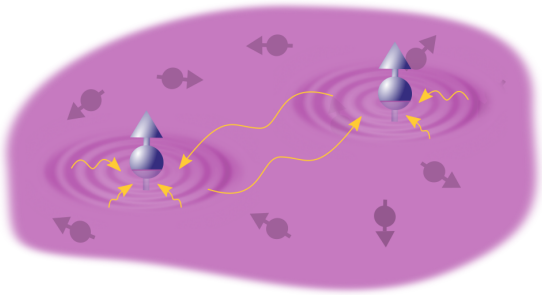

Figure 5.1: Sketch of the system: Two localised spins share the same environment and they are effectively coupled through the interaction with the bath. The bath itself is an itinerant electron gas and the interaction between localised spins and the electrons is a contact spin-spin interaction. The ripples and yellow wavy lines indicate coherent backaction effects. Our investigation focuses on the dynamics of one of the localised spins and how it is affected by the presence of the second one.

with $b_z^I = g_I \mu_I B_z$, where g_I is the appropriate g-factor for the localised spin and its magnetic moment μ_I in the uniform external field $\mathbf{B}$ along the z direction. The subscript $j = 1, 2$ refers to the position x_j of the localised spin. The electronic part is described by the Hamiltonian

$$H_{\mathrm{el}} = \sum_{k\sigma} \epsilon_k c_{k\sigma}^\dagger c_{k\sigma} + b_z^{\mathrm{el}} \sum_{l=1}^{N_{\mathrm{el}}} S_{z,l}. \tag{5.4}$$

Here, ϵ_k is the energy dispersion for the electronic system with $c_{k\sigma}^\dagger$ and $c_{k\sigma}$ being the electron creation and annihilation operators. The second term corresponds to the Zeeman term with $b_z^{\mathrm{el}} = g\mu_B B_z$ with the electron g-factor and the Bohr magneton μ_B. The sum runs over all real space positions l of N_{el} electrons forming the bath. The interaction term is given as before by a contact interaction between the localised spin $\mathbf{I}$ at x_j and the electrons spin $\mathbf{S}$

$$H_{\mathrm{int}}^j = A \sum_{l=1}^{N_{\mathrm{el}}} \delta(x_j - x_l) \mathbf{I}_j \cdot \mathbf{S}_l. \tag{5.5}$$

The full system Hamiltonian is given by the sum of Eqs. (5.3) to (5.5)

$$H = H_I^{(1)} + H_I^{(2)} + H_{\mathrm{el}} + H_{\mathrm{int}}^{(1)} + H_{\mathrm{int}}^{(2)}, \tag{5.6}$$

and correspondingly the system's Liouvillian $L = -i[H, \cdot]$ can be written as

$$L = L_I^{(1)} + L_I^{(2)} + L_{\mathrm{el}} + L_{\mathrm{int}}^{(1)} + L_{\mathrm{int}}^{(2)}. \tag{5.7}$$

We explicitly write all terms for each localised spin to emphasise that the entire considered system consists of three subsystems and that there is no direct coupling between the localised spins. The Zeeman term of localised spins can be eliminated by changing into a rotating frame of reference

$$H \to H - b_z^I J_z \tag{5.8}$$

where $J_z = \sum_j I_{z,j} + \sum_l S_{l,z}$ is the total angular momentum. The full system Hamiltonian is then given by

$$H = \sum_{k\sigma} \epsilon_k c_{k\sigma}^\dagger c_{k\sigma} + b_z \sum_{l=1}^{N_{\mathrm{el}}} S_{z,l} + A \sum_{j=1,2} \sum_{l=1}^{N_{\mathrm{el}}} \delta(x_j - x_l) \mathbf{I}_j \cdot \mathbf{S}_l \tag{5.9}$$

with $b_z = b_z^{\mathrm{el}} - b_z^I$.

We define the reduced density matrices corresponding to each subsystem by tracing over the degrees of freedom of the subsystems acting as the bath. With the full density matrix ρ of the entire quantum system, we then have for the localised spin

$$\rho_{I,j}(t) = \mathrm{Tr}_{\not{j}} \{\rho(t)\} \tag{5.10}$$

where $\not{j}$ implies the trace over the electronic degrees of freedem as well as the second impurity. Since there is no direct coupling between the localised spins, the corresponding reduced density matrices are copies of each other. Therefore, we keep the index j to refer to each of the spins located at x_j with $j = 1, 2$. Strictly speaking, the definition of the reduced density matrix for each localised spin has to also include the trace over the the other impurity spin as in Eq. (5.10). However, in the equation of motion for the localised spin derived below there is no direct dependence on the other impurity. The effective interaction between the two spins comes in purely through the interaction with the surrounding electrons. For Eq. (5.10) the trace $\not{j}$ therefore reduces to the only taking

the trace over the conduction electrons

$$\rho_{I,j}(t) = \mathrm{Tr}_{\mathrm{el}}\left\{\rho(t)\right\} \tag{5.11}$$

as tracing over the other spin within the equation of motion simplifies to the identity. The reduced density matrix for the conduction electrons is given by tracing over both localised spins

$$\rho_{\mathrm{el}}(t) = \mathrm{Tr}_{\cancel{el}}\{\rho(t)\} = \mathrm{Tr}_I\left\{\rho(t)\right\}. \tag{5.12}$$

The corresponding time-dependent projection operators for each subsystem according to Eq. (2.81) are defined as

$$P_t^{I,j} = \mathrm{Tr}_{\cancel{j}}\left\{\cdot\right\} \otimes \rho_{I,\cancel{j}}(t) \otimes \rho_{el}(t) = \mathrm{Tr}_{\mathrm{el}}\left\{\cdot\right\} \otimes \rho_{I,\cancel{j}} \otimes \rho_{el}(t), \tag{5.13}$$

$$P_t^{\mathrm{el}} = \mathrm{Tr}_{\cancel{el}}(t) \otimes \rho_{\cancel{el}}(t) = \mathrm{Tr}_I\left\{\cdot\right\} \otimes \rho_{I,j=1}(t) \otimes \rho_{I,j=2}(t). \tag{5.14}$$

Then, we state the expression for the superoperator $\mathcal{C}_t$ in Eq. (2.100) by inserting the projection operators Eqs. (5.13) and (5.14)

$$\mathcal{C}_t = \mathbb{1} - \sum_{S_n} P_t^{S_n} = \mathbb{1} - P_t^{I,j=1} - P_t^{I,j=2} - P_t^{\mathrm{el}}, \tag{5.15}$$

where S_n refers to the three subsystems, i.e., the two localised spins and the conduction electrons. Now we are in a position to tailor the general equation of motion in Eq. (2.109) to the current setup. Starting with the equation of motion for the localised spin at position x_j the only interaction is with the conduction electrons such that Eq. (2.109) reduces to

$$\begin{aligned}\dot{\rho}_{I,j}(t) = \mathrm{Tr}_{\mathrm{el}}\left\{L_{\mathrm{int}}^j \rho_{I,j}(t) \otimes \rho_{\mathrm{el}}(t)\right\} + \int_{t_0}^{t} dt' \,\mathrm{Tr}_{\mathrm{el}}\Bigg\{ L_{\mathrm{int}}^j e^{L_{\mathrm{el}}(t-t')}\Big[L_{\mathrm{int}}^j \rho_{\mathrm{el}}(t') \otimes \rho_{I,j}(t') \\ - \rho_{\mathrm{el}}(t') \otimes \mathrm{Tr}_{\mathrm{el}}\left\{L_{\mathrm{int}}^j \rho_{\mathrm{el}}(t') \otimes \rho_{I,j}(t')\right\} - \rho_{I,j}(t') \otimes \mathrm{Tr}_I\left\{L_{\mathrm{int}}^j \rho_{I,j}(t') \otimes \rho_{\mathrm{el}}(t')\right\}\Big]\Bigg\},\end{aligned} \tag{5.16}$$

where the trace over the other localised spin reduces to the identity. Note that in the rotating frame the unperturbed Hamiltonian corresponds to only the electronic part and the evolution under the Liouvillian is given by $L_0 = L_{\mathrm{el}}$. In comparison to the Nakajima-Zwanzig approach for the single spin case we find a term linear in the interaction which was not present before due to particle conservation. In the time-dependent projection approach also bath correlations of the form $\langle B \rangle$ are present and generally $\langle B \rangle \neq 0$.

The bath operators B correspond to the electron spin operators $S^{z,\pm}$. The terms under the time integral in Eq. (5.16) take into account the full history of all subsystems and capture the correlations building up between the different parts. Here, the first two terms with the trace over the electronic degrees of freedom will generate expectation values like $\sim \langle S^\alpha S^\beta \rangle(t)$ and $\sim \langle S^\alpha \rangle(t) \langle S^\beta \rangle(t)$. Apart from the explicit time dependence of the electron density matrix these correlators also appear in the Nakajima-Zwanzig approach. In contrast, the last term within the time integral does not appear. It generates terms $\sim \langle I^\alpha \rangle(t) \langle S^\beta \rangle(t)$ and can be interpreted as a renormalisation of the bath expectation value due to interaction with the system.

Reversing the situation and treating the localised spins as a bath to the electrons, we are able to write down an equation of motion for the conduction electrons. The only difference in comparison with the equation of motion for the localised spins of Eq. (5.16) is which subsystem's degrees of freedom are traced out and we have to add the term capturing the eigendynamics. Taking the trace over the localised spins leads to

$$\begin{aligned}
\dot{\rho}_{\mathrm{el}}(t) &= L_{\mathrm{el}} \rho_{\mathrm{el}}(t) \\
&+ \sum_{j=1,2} \mathrm{Tr}_I \left\{ L^j_{\mathrm{int}} \rho_{\mathrm{el}}(t) \otimes \rho_{I,j}(t) \right\} + \sum_{j=1,2} \int_{t_0}^{t} dt' \, \mathrm{Tr}_I \Bigg\{ L^j_{\mathrm{int}} e^{L_{\mathrm{el}}(t-t')} \Big[L^j_{\mathrm{int}} \rho_{I,j}(t') \otimes \rho_{\mathrm{el}}(t') \\
&- \rho_{I,j}(t') \otimes \mathrm{Tr}_I \left\{ L^j_{\mathrm{int}} \rho_{I,j}(t') \otimes \rho_{\mathrm{el}}(t') \right\} - \rho_{\mathrm{el}}(t') \otimes \mathrm{Tr}_{\mathrm{el}} \left\{ L^j_{\mathrm{int}} \rho_{\mathrm{el}}(t') \otimes \rho_{I,j}(t') \right\} \Big] \Bigg\}. \quad (5.17)
\end{aligned}$$

Since the conduction electrons are directly coupled to both localised spins we sum over $j = 1, 2$. At this point we can also see within the formalism how the effective coupling through the conduction electrons comes in. The discussion from Eq. (5.16) applies to Eq. (5.17) as well, we only need to insert the localised spin operators. Within the time integral the corresponding expectation values are therefore $\sim \langle I^\alpha_j I^\beta_j \rangle(t)$ and $\sim \langle I^\alpha_j \rangle(t) \langle I^\beta_j \rangle(t)$ for the first two terms while the structure for the last remains the same. The expectation values of the localised spins on different sites j do not mix which is again due to the lack of direct coupling between them.

Eqs. (5.16) and (5.17) form a set of coupled equations of motion that we need to solve in order to gain excess to the dynamics of the localised spins. To proceed we will choose a particular basis for the density matrices of the impurities which leads to a matrix representation of the different terms including L^j_{int}. At this point in Chapter 3 when treating the single spin case we used the Laplace transformation to solve the equation of motion. This is no longer possible as the integrand has a more complicated structure and apart form the system's density matrix also the reference bath state is time-dependent. Furthermore, the equation of motion for the conduction electrons in Eq. (5.17) cannot be

solved because there are infinitely many degrees of freedom. Limiting the consideration to a finite number of degrees of freedom would not do, as such an approach would not capture the universal physics which is dominated by Fermi statistics and the existence of a Fermi surface. Nonetheless, it could be interesting to treat finite chains with a finite number of modes. For long enough chains however a full numerical treatment would again require many degrees of freedom and quickly becomes impractical. In the end we are interested in the dynamics of the localised spins. In their equation of motion Eq. (5.16) only some correlation functions of the conduction electrons appear. Instead of needing to solve Eq. (5.17) we need to find the equation of motion for the required correlation functions. In the following sections we derive the equations of motion for the different subsystems explicitly.

5.2.1 Equation of motion for the localised spins

To find an expression for Eq. (5.16) we choose a particular basis spanned by the localised spin operators $\left\{I_j^{\uparrow}, I_j^{\downarrow}, I_j^{-}, I_j^{+}\right\}$ for the reduced density matrices of the localised spins such that

$$\rho_{I,j} = \rho_j^{\uparrow} I_j^{\uparrow} + \rho_j^{\downarrow} I_j^{\downarrow} + \rho_j^{-} I_j^{+} + \rho_j^{+} I_j^{-}, \tag{5.18}$$

analogous to Eq. (3.54) in the single spin case. We can then derive an equation of motion for each localised spin separately because their evolutions are formally decoupled, since the coupling occurs only through the electron density matrix. The interaction Hamiltonian can be written as

$$H_{\text{int}}^{j} = A\delta(x_j - x_l)\left(2I_j^{+}S_l^{-} + 2I_j^{-}S_l^{+} + I_j^{z}S_l^{z}\right). \tag{5.19}$$

Using the specific interaction Hamiltonian in the basis of the spin operators we can write the equation of motion Eq. (5.16) in a matrix representation

$$\dot{\vec{\rho}}_{I,j}(t) = \hat{\tilde{M}}(x_j, t)\vec{\rho}_{I,j}(t) \tag{5.20}$$

where

$$\vec{\rho}_{I,j}(t) = \left(\rho_j^{\uparrow}, \rho_j^{\downarrow}, \rho_j^{-}, \rho_j^{+}\right)^{T}. \tag{5.21}$$

and $\hat{\hat{M}}$ is the 4×4 matrix representation of the memory kernel coupling to spin j. The matrix $\hat{\hat{M}}$ includes the different terms of Eq. (5.16) which we write in the form

$$\begin{aligned}
&\hat{\hat{M}}(x_j,t)\vec{\rho}_{I,j}(t) \\
&= \hat{\hat{M}}_{\mathrm{lin}}(x_j,t)\vec{\rho}_{I,j}(t) \\
&+ \int_0^t dt' \left\{ \hat{\hat{M}}_{\mathrm{2nd},1}(x_j,t,t') + \hat{\hat{M}}_{\mathrm{2nd},2}(x_j,t,t') + \hat{\hat{M}}_{\mathrm{2nd},3}(x_j,t,t') \right\} \vec{\rho}_{I,j}(t'). \qquad (5.22)
\end{aligned}$$

The definitions for the different $\hat{\hat{M}}_i$ follow below. As the calculation is rather lengthy, we will only show some intermediate steps. Details for the full calculation including all arising commutators can be found in Appendix F.1.

5.2.1.1 Linear term M_{lin}

The first term in Eq. (5.16) of $O(A)$ is given by

$$\begin{aligned}
\mathrm{Tr}_{\mathrm{el}}\left\{ L^j_{\mathrm{int}} \rho_{I,j}(t) \otimes \rho_{\mathrm{el}}(t) \right\} &= -i2A\mathrm{Tr}_{\mathrm{el}}\left\{ S^+(x_j)\rho_{\mathrm{el}}(t) \right\} \left[I_j^-, \rho_j(t) \right] \\
&- i2A\mathrm{Tr}_{\mathrm{el}}\left\{ S^-(x_j)\rho_{\mathrm{el}}(t) \right\} \left[I_j^+, \rho_j(t) \right] \\
&- iA\mathrm{Tr}_{\mathrm{el}}\left\{ S^z(x_j)\rho_{\mathrm{el}}(t) \right\} \left[I_j^z, \rho_j(t) \right]. \qquad (5.23)
\end{aligned}$$

Inserting Eq. (5.18) and calculating the commutators leads to a matrix representation of the linear term acting on the density matrix $\vec{\rho}_{I,j}(t)$

$$\hat{\hat{M}}_{\mathrm{lin}}(x_j,t) = \begin{pmatrix} 0 & 0 & -R_+ & R_- \\ 0 & 0 & R_+ & -R_- \\ R_+ & -R_+ & -R_z & 0 \\ -R_- & R_- & 0 & R_z \end{pmatrix}, \qquad (5.24)$$

with the correlation functions

$$R_+(x_j,t) = -i2Ae^{ib_z^I t} \left\langle S_j^+ \right\rangle_{\mathrm{el},t}, \qquad (5.25)$$

$$R_-(x_j,t) = -i2Ae^{-ib_z^I t} \left\langle S_j^- \right\rangle_{\mathrm{el},t}, \qquad (5.26)$$

$$R_z(x_j,t) = -i2A \left\langle S_j^z \right\rangle_{\mathrm{el},t}, \qquad (5.27)$$

where we also included the phase factor due to the transformation into the rotating frame. Furthermore, we define the angular brackets as the expectation value of any operator O

$$\langle O_j \rangle_{\mathrm{el},t} = \mathrm{Tr}_{\mathrm{el}} \left\{ O_j \rho_{\mathrm{el}}(t) \right\} \tag{5.28}$$

over the electronic degrees of freedom. Correspondingly,

$$\langle O_j \rangle_{I,t} = \mathrm{Tr}_I \left\{ O_j \rho_{I,j}(t) \right\} \tag{5.29}$$

denotes the expectation with respect to the localised spin. The index t refers to the time argument of the density matrix. If the spin operator itself includes a time evolution we will write this explicitly, i.e., $\left\langle S_j^\alpha(t') \right\rangle_{\mathrm{el},t}$ while $\left\langle S_j^\alpha \right\rangle_{\mathrm{el},t} = \left\langle S_j^\alpha(t'=0) \right\rangle_{\mathrm{el},t}$.

5.2.1.2 $O(A^2)$: Two-point correlators $M_{\mathrm{2nd},1}$

The first term quadratic in the interaction corresponds to the second term in Eq. (5.16). Inserting the interaction Hamiltonian into Eq. (5.16) we need to find

$$\begin{aligned} &\int_{t_0}^{t} dt' \, \mathrm{Tr}_{\mathrm{el}} \left\{ L_{\mathrm{int}}^j e^{L_{\mathrm{el}}(t-t')} L_{\mathrm{int}}^j \rho_{\mathrm{el}}(t') \otimes \rho_{I,j}(t') \right\} \\ &= - \int_{t_0}^{t} dt' \, \mathrm{Tr}_{\mathrm{el}} \left\{ \left[H_{\mathrm{int}}^j, e^{L_{\mathrm{el}}(t-t')} \left[H_{\mathrm{int}}^j, \rho_{\mathrm{el}}(t') \otimes \rho_{I,j}(t') \right] \right] \right\}. \end{aligned} \tag{5.30}$$

This leads to the commutators between the localised spin operators and its density matrix of the form

$$\left[\rho_{I,j}(t') I_j^\alpha, I_j^\beta \right], \tag{5.31}$$

with $\alpha, \beta = \pm, z$. After calculating the commutators the integrand can be written in its matrix representation as

$$\hat{\tilde{M}}_{\mathrm{2nd},1}(x_j, t, t') = \begin{pmatrix} F_1 & -F_2 & -F_3 & -F_4 \\ -F_1 & F_2 & F_3 & F_4 \\ -F_{z+} + F_5 & F_{+z} + F_5 & F_- + F_z & 0 \\ -F_{-z} + F_6 & F_{z-} + F_6 & 0 & F_+ + F_z \end{pmatrix}, \tag{5.32}$$

with the correlation functions

$$F_1(x_j, t, t') = -4A^2 \left(e^{-ib_z^I(t'-t)} \left\langle S_j^-(t'-t) S_j^+ \right\rangle_{\mathrm{el},t'} + e^{ib_z^I(t'-t)} \left\langle S_j^- S_j^+(t'-t) \right\rangle_{\mathrm{el},t'} \right), \tag{5.33}$$

$$F_2(x_j,t,t') = -4A^2\left(e^{ib_z^I(t'-t)}\left\langle S_j^+(t'-t)S_j^-\right\rangle_{\mathrm{el},t'} + e^{-ib_z^I(t'-t)}\left\langle S_j^+S_j^-(t'-t)\right\rangle_{\mathrm{el},t'}\right), \tag{5.34}$$

$$F_+(x_j,t,t') = -4A^2e^{-ib_z^I(t'-t)}\left\langle\left\{S_j^-(t'-t),S_j^+\right\}\right\rangle_{\mathrm{el},t'}, \tag{5.35}$$

$$F_-(x_j,t,t') = -4A^2e^{ib_z^I(t'-t)}\left\langle\left\{S_j^+(t'-t),S_j^-\right\}\right\rangle_{\mathrm{el},t'}, \tag{5.36}$$

$$F_z(x_j,t,t') = -2A^2\left\langle\left\{S_j^z(t'-t),S_j^z\right\}\right\rangle_{\mathrm{el},t'}, \tag{5.37}$$

$$F_3(x_j,t,t') = -2A^2e^{ib_z^I(t'-t)}\left\langle\left\{S_j^+(t'-t),S_j^z\right\}\right\rangle_{\mathrm{el},t'}, \tag{5.38}$$

$$F_4(x_j,t,t') = -2A^2e^{-ib_z^I(t'-t)}\left\langle\left\{S_j^-(t'-t),S_j^z\right\}\right\rangle_{\mathrm{el},t'}, \tag{5.39}$$

$$F_5(x_j,t,t') = -2A^2e^{ib_z^I(t'-t)}\left\langle\left[S_j^+(t'-t),S_j^z\right]\right\rangle_{\mathrm{el},t'}, \tag{5.40}$$

$$F_6(x_j,t,t') = -2A^2e^{-ib_z^I(t'-t)}\left\langle\left[S_j^-(t'-t),S_j^z\right]\right\rangle_{\mathrm{el},t'}, \tag{5.41}$$

$$F_{z+}(x_j,t,t') = -4A^2\left\langle S_j^z(t'-t)S_j^+\right\rangle_{\mathrm{el},t'}, \tag{5.42}$$

$$F_{+z}(x_j,t,t') = -4A^2\left\langle S_j^+S_j^z(t'-t)\right\rangle_{\mathrm{el},t'}, \tag{5.43}$$

$$F_{z-}(x_j,t,t') = -4A^2\left\langle S_j^z(t'-t)S_j^-\right\rangle_{\mathrm{el},t'}, \tag{5.44}$$

$$F_{-z}(x_j,t,t') = -4A^2\left\langle S_j^-S_j^z(t'-t)\right\rangle_{\mathrm{el},t'}. \tag{5.45}$$

The matrix $\hat{\hat{M}}_{\mathrm{2nd},1}$ acts within the time integral on the localised spin density matrix $\vec{\rho}_{I,j}(t')$. The diagonal 2×2 blocks contain the same electron spin correlation functions as the memory kernel $\widetilde{\Sigma}(s)$ in Eq. (3.61) for a single spin in an electronic environment. Unlike Eq. (3.61) the correlators F_i lack time translation symmetry and as such no further simplifications can be done. Since in the time-dependent projector setup also single excitations such as $\left\langle S_j^{\pm}S^z\right\rangle \neq 0$ the longitudinal and transverse localised spin components are coupled.

5.2.1.3 $O(A^2)$: One-point correlators $M_{\mathrm{2nd},2}$

The one-point correlators arise from the third term in Eq. (5.16) which is given by

$$\begin{aligned}
&-\int_{t_0}^{t}dt'\,\mathrm{Tr}_{\mathrm{el}}\left\{L_{\mathrm{int}}^j e^{L_{\mathrm{el}}(t-t')}\rho_{\mathrm{el}}(t')\otimes\mathrm{Tr}_{\mathrm{el}}\left\{L_{\mathrm{int}}^j\rho_{\mathrm{el}}(t')\otimes\rho_{I,j}(t')\right\}\right\}\\
&=\int_{t_0}^{t}dt'\,\mathrm{Tr}_{\mathrm{el}}\left\{\left[H_{\mathrm{int}}^j,e^{L_{\mathrm{el}}(t-t')}\rho_{\mathrm{el}}(t')\otimes\mathrm{Tr}_{\mathrm{el}}\left\{\left[H_{\mathrm{int}}^j,\rho_{\mathrm{el}}(t')\otimes\rho_{I,j}(t')\right]\right\}\right]\right\}.
\end{aligned} \tag{5.46}$$

The inner trace is identical to the trace appearing in the linear term in Eq. (5.23) while the outer trace is given by the same bath correlation function but under the time evolution

$\exp[L_{\mathrm{el}}(t-t')]$. We find that the relevant commutators of the localised spins are the same as in Eq. (5.31). Collecting the results from all commutators we obtain the matrix representation of the integrand including the prefactor in Eq. (5.46)

$$\hat{\tilde{M}}_{\mathrm{2nd},2}(x_j,t,t') = \begin{pmatrix} G_1 & -G_1 & -G_2 & -G_3 \\ -G_1 & G_1 & G_2 & G_3 \\ -G_4 & G_4 & G_- + G_z & 0 \\ -G_5 & G_5 & 0 & G_+ + G_z \end{pmatrix}, \tag{5.47}$$

with the electronic response functions

$$G_+(x_j,t,t') = 4A^2 e^{-ib_z^I(t'-t)} \left\langle S_j^-(t'-t)\right\rangle_{\mathrm{el},t'} \left\langle S_j^+\right\rangle_{\mathrm{el},t'}, \tag{5.48}$$

$$G_-(x_j,t,t') = 4A^2 e^{ib_z^I(t'-t)} \left\langle S_j^+(t'-t)\right\rangle_{\mathrm{el},t'} \left\langle S_j^-\right\rangle_{\mathrm{el},t'}, \tag{5.49}$$

$$G_z(x_j,t,t') = 4A^2 \left\langle S_j^z(t'-t)\right\rangle_{\mathrm{el},t'} \left\langle S_j^z\right\rangle_{\mathrm{el},t'}, \tag{5.50}$$

$$G_1(x_j,t,t') = 4A^2 \left(G_+ + G_-\right), \tag{5.51}$$

$$G_2(x_j,t,t') = 2A^2 e^{ib_z^I(t'-t)} \left\langle S_j^+(t'-t)\right\rangle_{\mathrm{el},t'} \left\langle S_j^z\right\rangle_{\mathrm{el},t'}, \tag{5.52}$$

$$G_3(x_j,t,t') = 2A^2 e^{-ib_z^I(t'-t)} \left\langle S_j^-(t'-t)\right\rangle_{\mathrm{el},t'} \left\langle S_j^z\right\rangle_{\mathrm{el},t'}, \tag{5.53}$$

$$G_4(x_j,t,t') = 2A^2 \left\langle S_j^z(t'-t)\right\rangle_{\mathrm{el},t'} \left\langle S_j^+\right\rangle_{\mathrm{el},t'}, \tag{5.54}$$

$$G_5(x_j,t,t') = 2A^2 \left\langle S_j^z(t'-t)\right\rangle_{\mathrm{el},t'} \left\langle S_j^-\right\rangle_{\mathrm{el},t'}. \tag{5.55}$$

In comparison to the single spin setup we now find the correlators G_i. Before, all $G_i = 0$ since we excluded any magnetisation of the conduction electrons and the bath was in its equilibrium state.

5.2.1.4 $O(A^2)$: Renormalisation term $M_{\mathrm{2nd},3}$

The last remaining term in Eq. (5.16) is given by

$$\begin{aligned} &-\int_{t_0}^{t} dt' \,\mathrm{Tr}_{\mathrm{el}}\left\{L_{\mathrm{int}}^j e^{L_{\mathrm{el}}(t-t')}\rho_{I,j}(t')\otimes \mathrm{Tr}_I\left\{L_{\mathrm{int}}^j \rho_{I,j}(t')\otimes\rho_{\mathrm{el}}(t')\right\}\right\} \\ &= -\int_{t_0}^{t} dt' \,\mathrm{Tr}_{\mathrm{el}}\left\{\left[H_{\mathrm{int}}^j, e^{L_{\mathrm{el}}(t-t')}\rho_{I,j}(t')\otimes \mathrm{Tr}_{I,j}\left\{\left[H_{\mathrm{int}}^j,\rho_I(t')\otimes\rho_{\mathrm{el}}(t')\right]\right\}\right]\right\}. \end{aligned} \tag{5.56}$$

The inner trace will lead to an expectation value of the localised spin which in turn renormalises the electronic response function. The relevant spin commutators $\left[\rho_{I,j}(t'), I_j^\alpha\right]$ with $\alpha = \pm, z$ are identical to the localised spin commutators of the linear term in Eq. (5.23).

Making use of Eq. (5.18) we find the matrix representation of Eq. (5.56)

$$\hat{\hat{M}}_{\mathrm{2nd},3}(x_j,t,t') = \begin{pmatrix} 0 & 0 & H_1 & -H_2 \\ 0 & 0 & -H_1 & H_2 \\ -H_1 & H_1 & H_3 & 0 \\ H_2 & -H_2 & 0 & -H_3 \end{pmatrix}, \tag{5.57}$$

with the electron correlation functions

$$\begin{aligned} H_1(x_j,t,t') &= 4A^2\rho_j^+(t')e^{ib_z^I(t'-t)}\left\langle\left[S_j^+(t'-t),S_j^-\right]\right\rangle_{\mathrm{el},t'} \\ &\quad + 2A^2\rho_j^z(t')e^{ib_z^I(t'-t)}\left\langle\left[S_j^+(t'-t),S_j^z\right]\right\rangle_{\mathrm{el},t'}, \end{aligned} \tag{5.58}$$

$$\begin{aligned} H_2(x_j,t,t') &= 4A^2\rho_j^-(t')e^{-ib_z^I(t'-t)}\left\langle\left[S_j^-(t'-t),S_j^+\right]\right\rangle_{\mathrm{el},t'} \\ &\quad + 2A^2\rho_j^z(t')e^{-ib_z^I(t'-t)}\left\langle\left[S_j^-(t'-t),S_j^z\right]\right\rangle_{\mathrm{el},t'}, \end{aligned} \tag{5.59}$$

$$H_3(x_j,t,t') = 2A^2\rho_j^-(t')\left\langle\left[S_j^z(t'-t),S_j^+\right]\right\rangle_{\mathrm{el},t'} + 2A^2\rho_j^+(t')\left\langle\left[S_j^z(t'-t),S_j^-\right]\right\rangle_{\mathrm{el},t'}. \tag{5.60}$$

These correlations are weighted by the different localised spin components $\rho_j^\alpha(t)$ in the chosen basis. The components correspond to the expectation values defined by

$$\left\langle I_j^\alpha\right\rangle_{I,t} = \mathrm{Tr}_I\left\{I_j^\alpha\rho_{I,j}(t)\right\} = I\rho_j^\alpha(t), \tag{5.61}$$

which is a direct consequence of Eq. (5.18).

5.2.2 Equation of motion for the conduction electrons

The equation of motion for the electrons for the considered setup is obtained by inserting the interaction Hamiltonian of Eq. (5.19) into Eq. (5.17). As previously for the case of the localised spin, we will calculate the different terms in the first step separately. The structure will be similar to the different terms for the impurity Eqs. (5.23), (5.30), (5.46) and (5.56) by swapping the spin operators and taking the trace with respect to the localised spins. In contrast to the equation of motion for the localised spins we are not able to simplify the appearing commutators because we cannot choose a specific basis for the electron spin operators and we will be left with the general structure. In the second step, we approximate the electron density matrix to find a closed equation of motion for the relevant electron spin correlation functions.

5.2.2.1 Eigendynamics and $O(A)$ term

The first term of the right-hand side in Eq. (5.17) captures the eigendynamics of the conduction electrons under the electronic part H_{el} of the Hamiltonian Eq. (5.9) with

$$H_{\mathrm{el}} = \sum_{k\sigma} \epsilon_k c^\dagger_{k\sigma} c_{k\sigma} + b_z \sum_{l=1}^{N_{\mathrm{el}}} S_{z,l}. \tag{5.62}$$

At this point we make no assumptions on the specific form of the density matrix for the electrons and therefore cannot specify the action of L_{el} on $\rho_{\mathrm{el}}(t)$ any further. The $O(A)$ term corresponds to the second term of Eq. (5.17). Swapping the electrons spin operators and localised spin operators of Eq. (5.23) and adjusting the trace leads to

$$\begin{aligned}
&\sum_{j=1,2} \mathrm{Tr}_I \left\{ L^j_{\mathrm{int}} \rho_{el}(t) \otimes \rho_{\mathrm{I,j}}(t) \right\} \\
&= -i2A \sum_{j=1,2} \left\{ \rho^+_j(t) \left[S^-_j, \rho_{\mathrm{el}}(t) \right] + \rho^-_j(t) \left[S^+_j, \rho_{\mathrm{el}}(t) \right] + \left(\rho^\uparrow_j(t) - \rho^\downarrow_j(t) \right) \left[S^z_j, \rho_{\mathrm{el}}(t) \right] \right\}.
\end{aligned} \tag{5.63}$$

We also made use of Eq. (5.61) to replace the expectation value of the localised spin by the corresponding component of their density matrix.

5.2.2.2 $O(A^2)$: Two-point correlators

Following the procedure outlined above, the first term of $O(A^2)$ corresponds to the third term in Eq. (5.17) and can be written as

$$\begin{aligned}
&\sum_{j=1,2} \int_0^t dt' \, \mathrm{Tr}_I \left\{ L^j_{\mathrm{int}} e^{(t-t')L_{\mathrm{el}}} L^j_{\mathrm{int}} \rho_{\mathrm{el}}(t') \otimes \rho_j(t') \right\} \\
&= -A^2 \sum_{j=1,2} \int_0^t dt' \Big\{ 2\rho^+_j(t') \left(\left[S^z_j, e^{(t-t')L_{\mathrm{el}}} S^-_j \rho_{\mathrm{el}}(t') \right] - \left[e^{(t-t')L_{\mathrm{el}}} \rho_{\mathrm{el}}(t') S^-_j, S^z_j \right] \right) \\
&+ 2\rho^+_j(t') \left(\left[e^{(t-t')L_{\mathrm{el}}} \rho_{\mathrm{el}}(t') S^z_j, S^-_j \right] - \left[S^-_j, e^{(t-t')L_{\mathrm{el}}} S^z_j \rho_{\mathrm{el}}(t') \right] \right) \\
&+ 2\rho^-_j(t') \left(\left[e^{(t-t')L_{\mathrm{el}}} \rho_{\mathrm{el}}(t') S^+_j, S^z_j \right] - \left[S^z_j, e^{(t-t')L_{\mathrm{el}}} S^+_j \rho_{\mathrm{el}}(t') \right] \right) \\
&+ 2\rho^-_j(t') \left(\left[S^+_j, e^{(t-t')L_{\mathrm{el}}} S^z_j \rho_{\mathrm{el}}(t') \right] - \left[e^{(t-t')L_{\mathrm{el}}} \rho_{\mathrm{el}}(t') S^z_j, S^+_j \right] \right) \\
&+ 4 \left(\rho^\uparrow_j(t') - \rho^\downarrow_j(t') \right) \left(\left[S^-_j, e^{(t-t')L_{\mathrm{el}}} S^+_j \rho_{\mathrm{el}}(t') \right] + \left[e^{(t-t')L_{\mathrm{el}}} \rho_{\mathrm{el}}(t') S^-_j, S^+_j \right] \right) \\
&+ \left(\rho^\uparrow_j(t') + \rho^\downarrow_j(t') \right) \left(\left[S^z_j, e^{(t-t')L_{\mathrm{el}}} S^z_j \rho_{\mathrm{el}}(t') \right] + \left[e^{(t-t')L_{\mathrm{el}}} \rho_{\mathrm{el}}(t') S^z_j, S^z_j \right] \right) \Big\}.
\end{aligned} \tag{5.64}$$

Again, we used Eq. (5.61) to rewrite the expectation values $\left\langle I_j^\alpha I_j^\beta \right\rangle_{I,t'}$ in terms of the component of the localised spin density matrix.

5.2.2.3 $O(A^2)$: One-point correlators

The fourth term of Eq. (5.17) includes an additional trace over the localised spins and we find the same electron spin commutators as in Eq. (5.64) but with modified prefactors

$$
\begin{aligned}
&- \int_0^t dt' \, \mathrm{Tr}_I \left\{ L_{\mathrm{int}}^j e^{(t-t')L_{\mathrm{el}}} \rho_j(t') \otimes \mathrm{Tr}_I \left(L_{\mathrm{int}}^j \rho_{\mathrm{el}}(t') \otimes \rho_j(t') \right) \right\} \\
&= A^2 \sum_{j=1,2} \int_0^t dt' \Big\{ 2\rho_j^+(t') \left(\rho_j^\uparrow(t') - \rho_j^\downarrow(t') \right) \Big(\left[S_j^-, e^{(t-t')L_{\mathrm{el}}} S_j^z \rho_{\mathrm{el}}(t') \right] \\
&+ \left[e^{(t-t')L_{\mathrm{el}}} \rho_{\mathrm{el}}(t') S_j^z, S_j^- \right] + \left[S_j^z, e^{(t-t')L_{\mathrm{el}}} S_j^- \rho_{\mathrm{el}}(t') \right] + \left[e^{(t-t')L_{\mathrm{el}}} \rho_{\mathrm{el}}(t') S_j^-, S_j^z \right] \Big) \\
&+ 2\rho_j^-(t') \left(\rho_j^\uparrow(t') - \rho_j^\downarrow(t') \right) \Big(\left[S_j^+, e^{(t-t')L_{\mathrm{el}}} S_j^z \rho_{\mathrm{el}}(t') \right] + \left[e^{(t-t')L_{\mathrm{el}}} \rho_{\mathrm{el}}(t') S_j^z, S_j^+ \right] \\
&+ \left[S_j^z, e^{(t-t')L_{\mathrm{el}}} S_j^+ \rho_{\mathrm{el}}(t') \right] + \left[e^{(t-t')L_{\mathrm{el}}} \rho_{\mathrm{el}}(t') S_j^+, S_j^z \right] \Big) \\
&+ 4\rho_j^+(t') \rho_j^-(t') \Big(\left[S_j^-, e^{(t-t')L_{\mathrm{el}}} S_j^+ \rho_{\mathrm{el}}(t') \right] + \left[e^{(t-t')L_{\mathrm{el}}} \rho_{\mathrm{el}}(t') S_j^+, S_j^- \right] \\
&+ \left[S_j^+, e^{(t-t')L_{\mathrm{el}}} S_j^- \rho_{\mathrm{el}}(t') \right] + \left[e^{(t-t')L_{\mathrm{el}}} \rho_{\mathrm{el}}(t') S_j^-, S_j^+ \right] \Big) \\
&+ \left(\rho_j^\uparrow(t') - \rho_j^\downarrow(t') \right)^2 \left(\left[S_j^z, e^{(t-t')L_{\mathrm{el}}} S_j^z \rho_{\mathrm{el}}(t') \right] + \left[e^{(t-t')L_{\mathrm{el}}} \rho_{\mathrm{el}}(t') S_j^z, S_j^z \right] \right). \qquad (5.65)
\end{aligned}
$$

We find pairs of localised spin components due to the additional trace within the time integral.

5.2.2.4 $O(A^2)$: Renormalisation term

The last term of Eq. (5.17) with the renormalisation of the expectation values of the localised spin by the electronic contribution leads to

$$
\begin{aligned}
&- \sum_{j=1,2} \int_0^t dt' \, \mathrm{Tr}_I \left\{ L_{\mathrm{int}}^j e^{(t-t')L_{\mathrm{el}}} \rho_{\mathrm{el}}(t') \otimes \mathrm{Tr}_{\mathrm{el}} \left(L_{\mathrm{int}}^j \rho_{\mathrm{el}}(t') \otimes \rho_j(t') \right) \right\} \\
&= A^2 \sum_{j=1,2} \int_0^t dt' \Big(4 \left(\rho_j^\uparrow(t') - \rho_j^\downarrow(t') \right) \left\langle S_j^+ \right\rangle_{\mathrm{el},t'} \left[e^{(t-t')L_{\mathrm{el}}} \rho_{\mathrm{el}}(t'), S_j^- \right] \\
&- 4 \left(\rho_j^\uparrow(t') - \rho_j^\downarrow(t') \right) \left\langle S_j^- \right\rangle_{\mathrm{el},t'} \left[e^{(t-t')L_{\mathrm{el}}} \rho_{\mathrm{el}}(t'), S_j^+ \right] \\
&+ 2\rho_j^+(t') \left\langle S_j^- \right\rangle_{\mathrm{el},t'} \left[e^{(t-t')L_{\mathrm{el}}} \rho_{\mathrm{el}}(t'), S_j^z \right] - 2\rho_j^+(t') \left\langle S_j^z \right\rangle_{\mathrm{el},t'} \left[e^{(t-t')L_{\mathrm{el}}} \rho_{\mathrm{el}}(t'), S_j^- \right] \\
&+ 2\rho_j^-(t') \left\langle S_j^z \right\rangle_{\mathrm{el},t'} \left[e^{(t-t')L_{\mathrm{el}}} \rho_{\mathrm{el}}(t'), S_j^+ \right] - 2\rho_j^-(t') \left\langle S_j^+ \right\rangle_{\mathrm{el},t'} \left[e^{(t-t')L_{\mathrm{el}}} \rho_{\mathrm{el}}(t'), S_j^z \right] \Big). \qquad (5.66)
\end{aligned}
$$

We use Eqs. (5.63) to (5.66) to formulate an equation of motion for the electron spin expectation values.

5.2.3 Equation of motion for the electron correlation functions

The full dynamics of the conduction electrons are in theory fully captured and described by the eigendynamics $L_{\mathrm{el}}\rho_{\mathrm{el}}(t)$ and Eqs. (5.63) to (5.66). In the physical setup considered here, the electrons form a surrounding bath for the localised spins with many degrees of freedom and solving for the full dynamics is not possible. In Section 5.2.1 we found the relevant electron correlations functions that enter the equation of motion of the localised spins. In particular, an expression for the one- and two-point response functions $\langle S^{\alpha}\rangle_{\mathrm{el},t}$ and $\left\langle S_j^{\alpha} S_j^{\beta}\right\rangle_{\mathrm{el},t}$ are needed. To this end, we express the electron spin operators in terms of the real-space creation and annihilation operators for the electrons, $\Psi_{\sigma}^{\dagger}(x_l)$ and $\Psi_{\sigma'}(x_l)$,

$$\mathbf{S}_l = \sum_{\sigma\sigma'} \Psi_{\sigma}^{\dagger}(x_l)\boldsymbol{\tau}_{\sigma\sigma'}\Psi_{\sigma'}(x_l), \tag{5.67}$$

at position x_l with the vector $\boldsymbol{\tau}$ of Pauli matrices. In momentum space we then have

$$S_l^{\alpha} = \frac{(2\pi)^2}{N^2}\sum_{kk'}\sum_{\sigma\sigma'} e^{i(k-k')x_l} c_{k\sigma}^{\dagger}\tau_{\sigma\sigma'}^{\alpha} c_{k'\sigma'}, \tag{5.68}$$

with the fermionic creation and annihilation operators $c^{\dagger}, c$ and N available momentum states for the spin components $\alpha = z, \pm$ where

$$S_l^{\pm} = \frac{1}{2}\left(S_l^x \pm i S_l^y\right). \tag{5.69}$$

Using Eq. (5.68) we rewrite the required spin expectation values in terms of the fermionic operators which leads to

$$\left\langle S_j^{\bar{\sigma}}\right\rangle_{\mathrm{el},t} = \frac{(2\pi)^2}{N^2}\sum_{pp'} e^{i(p-p')x_j}\left\langle c_{p\sigma}^{\dagger} c_{p'\sigma'}\right\rangle_{\mathrm{el},t}, \tag{5.70}$$

$$\left\langle S_j^{\bar{\sigma}} S_j^{\bar{\gamma}}\right\rangle_{\mathrm{el},t} = \frac{(2\pi)^4}{N^4}\sum_{pp'}\sum_{rr'} e^{i(p-p')x_j} e^{i(r-r')x_j}\left\langle c_{p\sigma}^{\dagger} c_{p'\sigma'} c_{r\gamma}^{\dagger} c_{r'\gamma'}\right\rangle_{\mathrm{el},t}. \tag{5.71}$$

The spin indices $\bar{\sigma}, \bar{\gamma} = z, \pm$ on the left-hand side determine the spin indices σ, σ' and γ, γ' for the fermionic operators. We will use the bar above the spin index to generally

indicate at tuple of indices. Specifically we have

$$\begin{aligned}\bar{\sigma} = + \quad &\rightarrow \quad \sigma = \uparrow,\ \sigma' = \downarrow, \\ \bar{\sigma} = - \quad &\rightarrow \quad \sigma = \downarrow,\ \sigma' = \uparrow \\ \bar{\sigma} = z \quad &\rightarrow \quad \sigma = \sigma'. \end{aligned} \tag{5.72}$$

For the z component, the difference $c^\dagger_{p\uparrow}c_{p'\uparrow} - c^\dagger_{p\downarrow}c_{p'\downarrow}$ is implied. Applying the electron operators $S^{\bar{\sigma}}_j$ or $S^{\bar{\sigma}}_j S^{\bar{\gamma}}_j$ to the individual terms Eqs. (5.63) to (5.66) of Eq. (5.17) and taking the trace with respect to the electrons would lead directly to an equation of motion for Eqs. (5.70) and (5.71). Unfortunately, this is not possible as the right-hand side of Eq. (5.17) involves the time evolution of the correlation function and without any further assumption on ρ_{el} we are not able to find an equation for these specific correlators directly. Instead, we only apply the operator $c^\dagger_{p\sigma}c_{p'\sigma'}$ for all combinations of $\sigma, \sigma' = \uparrow, \downarrow$ to Eq. (5.17). For the one-point correlator in Eq. (5.70) we need to solve

$$\frac{d}{dt}\left\langle c^\dagger_{p\sigma}c_{p'\sigma'}\right\rangle_{\mathrm{el},t} = \mathrm{Tr}_{\mathrm{el}}\left\{c^\dagger_{p\sigma}c_{p'\sigma'}\left[h_{\mathrm{rhs}}(t,t',\rho_I,\rho_{\mathrm{el}})\right]\right\}, \tag{5.73}$$

where h_{rhs} is defined as the right-hand side of Eq. (5.17). For the electron spin-spin correlators corresponding to Eq. (5.71) the equation of motion is given by

$$\frac{d}{dt}\left\langle c^\dagger_{p\sigma}c_{p'\sigma'}c^\dagger_{r\gamma}c_{r'\gamma'}\right\rangle_{\mathrm{el},t} = \mathrm{Tr}_{\mathrm{el}}\left\{c^\dagger_{p\sigma}c_{p'\sigma'}c^\dagger_{r\gamma}c_{r'\gamma'}\left[h_{\mathrm{rhs}}(t,t',\rho_I,\rho_{\mathrm{el}})\right]\right\}. \tag{5.74}$$

In a first approach we tried to solve Eqs. (5.73) and (5.74) directly. However, this led to a large number of coupled equations of motion for each momentum state p, p', r, r'. Although the approach might still be feasible for a small enough many body system with a small number of momentum states, we will not be able to address the continuum limit.

To be able to address a large environment we take a step back to analyse the physics we want to capture. The underlying interest of looking at this problem focuses on the effective coupling between the localised spins mediated by the conduction electrons and its influence on the dynamics of one localised spin while also taking into account coherent backaction effects. We are interested in the short lived, single electron spin excitations by one of the localised spin which can then travel freely trough the electronic environment and induce a spin flip at the other localised spin. Therefore, all the physics we are interested in is happening at the Fermi level with an energy around the Fermi energy E_F of the electronic environment. Instead of attempting to keep track of all possible momentum states as in Eqs. (5.73) and (5.74) and all possible excitations, we approximate

the density matrix of the electrons as

$$\rho_{\mathrm{el}}(t) \approx \left[\mathbb{1} + \sum_{l}\sum_{\alpha\alpha'}\left(\Lambda^{\alpha}_{\alpha'}(x_l,t)\Psi^{\dagger}_{\alpha}(x_l)\Psi_{\alpha'}(x_l) + \tilde{\Lambda}^{\alpha}_{\alpha'}(x_l,t)\Psi_{\alpha'}(x_l)\Psi^{\dagger}_{\alpha}(x_l)\right)\right]\rho^{\mathrm{eq}}_{\mathrm{el}}. \quad (5.75)$$

The index $l = 1, 2$ refers to position where the excitation due to the contact interaction with the localised spins was created. The approximation in Eq. (5.75) allows for a single particle or hole excitation. Within this approach the electron spin fluctuations are captured for a particle excitation by the function $\Lambda^{\alpha}_{\alpha'}(x_l,t)$ and by $\tilde{\Lambda}^{\alpha}_{\alpha'}(x_l,t)$ for a hole excitation. They can be understood as a time and spin dependent amplitudes which assign a changing weight to the Fermi distribution function depending on the current state of environment. All dynamics is captured by these functions and what remains later on for the correlation functions is thus evaluated in the equilibrium distribution. In momentum space the approximation of the electron density matrix is given by

$$\rho_{\mathrm{el}}(t) \approx \left[\mathbb{1} + \sum_{kk',l}\sum_{\alpha\alpha'} e^{i(k-k')x_l}\left(\Lambda^{\alpha}_{\alpha'}(x_l,t)c^{\dagger}_{k\alpha}c_{k'\alpha'} + \tilde{\Lambda}^{\alpha}_{\alpha'}(x_l,t)c_{k'\alpha'}c^{\dagger}_{k\alpha}\right)\right]\rho^{\mathrm{eq}}_{\mathrm{el}}. \quad (5.76)$$

Since the time dependence of the electron density is picked up by the functions $\Lambda^{\alpha}_{\alpha'}(x_l,t)$, $\tilde{\Lambda}^{\alpha}_{\alpha'}(x_l,t)$ we are now able to immediately find an equation of motion for the full correlator in Eq. (5.70)

$$\frac{(2\pi)^2}{N^2}\sum_{pp'} e^{i(p-p')x_j}\frac{d}{dt}\left\langle c^{\dagger}_{p\sigma}c_{p'\sigma'}\right\rangle_{\mathrm{el,t}} = Y_{\bar{\sigma}}\left(t, \rho_{I,j}(t), \rho_{\mathrm{el}}(t)\right). \quad (5.77)$$

The function $Y_{\bar{\sigma}}$ includes all contributions for the right-hand side of the equation of motion, the eigendynamics term and Eqs. (5.63) to (5.66), after applying the operator

$$S^{\bar{\sigma}}_{j} = \sum_{pp'} e^{i(p-p')x_j}c^{\dagger}_{p\sigma}c_{p'\sigma'}, \quad (5.78)$$

and taking the trace only affects the electronic degrees of freedom. In particular we have

$$\begin{aligned} Y_{\bar{\sigma}}(t,\rho_{I,j},\rho_{\mathrm{el}}) = Y_{\mathrm{ED}}(t) + \sum_{j,\bar{\beta}}\rho^{\bar{\beta}}_{j}(t)Y_{\mathrm{lin}}(x_j,t,\bar{\beta}) + \sum_{j,\bar{\beta}\bar{\gamma}}\int_0^t dt'\Big\{\rho^{\bar{\beta}\bar{\gamma}}_{j}(t')Y_{\mathrm{2nd},1}(x_j,t,t',\bar{\beta},\bar{\gamma}) \\ + \rho^{\bar{\beta}\bar{\gamma}}_{j}(t')Y_{\mathrm{2nd},2}(x_j,t,t',\bar{\beta},\bar{\gamma}) + \rho^{\bar{\beta}\bar{\gamma}}_{j}(t')\left\langle S^{\bar{\beta}\bar{\gamma}}_{j}\right\rangle_{\mathrm{el},t'}Y_{\mathrm{2nd},3}(x_j,t,t',\bar{\beta},\bar{\gamma})\Big\}. \end{aligned} \quad (5.79)$$

We use $\rho^{\bar{\beta}}_{j}, \rho^{\bar{\beta}\bar{\gamma}}_{j}$ as a shorthand for the contributions from the localised spin at position

x_j from Eqs. (5.63) to (5.66). The superscripts $\bar{\beta}$ indicate that the correct component is determined by the electron spin configuration $\bar{\beta}$.

Substituting Eq. (5.76) into Eq. (5.77) will lead to a differential equation for the functions $\Lambda^{\alpha}_{\alpha'}(x_l,t)$ and $\tilde{\Lambda}^{\alpha}_{\alpha'}(x_l,t)$. Instead of coupled differential equations for all possible momenta, we reduced the number of equations to $N_j \times 4 \times 2$ with $N_j = 2$ the number of localised spins and four different combinations of the spins $\alpha, \alpha' = \uparrow, \downarrow$. For each combination we find two sets of decoupled equations, one for the particle excitations Λ and one for the hole excitations $\tilde{\Lambda}$. The different contributions Y_i from Eq. (5.79) generate different commutators for which we still require an expression. In particular, the eigendynamics term is given by

$$Y_{\mathrm{ED}}(t) = -i\mathrm{Tr}_{\mathrm{el}}\left\{\sum_{pp'} e^{i(p-p')x_j} c^{\dagger}_{p\sigma} c_{p'\sigma'} \left[H'_{\mathrm{el}}, \rho_{\mathrm{el}}(t)\right]\right\}. \tag{5.80}$$

The term linear in the interaction in Eq. (5.63) contains the commutator $\left[S^{\bar{\beta}}_j, \rho_{\mathrm{el}}(t)\right]$ and the corresponding electronic contribution is captured by

$$Y_{\mathrm{lin}}(t,\bar{\beta}) = \mathrm{Tr}_{\mathrm{el}}\left\{\sum_{pp'} e^{i(p-p')x_j} c^{\dagger}_{p\sigma} c_{p'\sigma'} \left[\sum_{nn'} e^{i(n-n')x_j} c^{\dagger}_{n\beta} c_{n'\beta'}, \rho_{\mathrm{el}}(t)\right]\right\}. \tag{5.81}$$

In both second order terms in Eqs. (5.64) and (5.65) the commutators

$$\left[S^{\bar{\beta}}, e^{(t-t')L_{\mathrm{el}}} S^{\bar{\gamma}} \rho_{\mathrm{el}}(t')\right] \quad \text{and} \quad \left[e^{(t-t')L_{\mathrm{el}}} \rho_{\mathrm{el}}(t') S^{\bar{\gamma}}, S^{\bar{\beta}}\right],$$

appear. Applying Eq. (5.78) and including the trace of the electronic degrees of freedom leads to

$$\mathrm{Tr}_{\mathrm{el}}\left\{S^{\bar{\sigma}}\left[S^{\bar{\beta}}, e^{(t-t')L_{\mathrm{el}}} S^{\bar{\gamma}} \rho_{\mathrm{el}}(t')\right]\right\} = \mathrm{Tr}_{\mathrm{el}}\left\{\left[S^{\bar{\sigma}}(t'-t), S^{\bar{\beta}}(t'-t)\right] S^{\bar{\gamma}} \rho_{\mathrm{el}}(t')\right\}, \tag{5.82}$$

$$\mathrm{Tr}_{\mathrm{el}}\left\{S^{\bar{\sigma}}\left[e^{(t-t')L_{\mathrm{el}}} \rho_{\mathrm{el}}(t') S^{\bar{\gamma}}, S^{\bar{\beta}}\right]\right\} = \mathrm{Tr}_{\mathrm{el}}\left\{S^{\bar{\gamma}}\left[S^{\bar{\beta}}(t'-t), S^{\bar{\sigma}}(t'-t)\right] \rho_{\mathrm{el}}(t')\right\} \tag{5.83}$$

where we used the cyclic property of the trace to shift the time evolution. In terms of the fermionic expectation values the contribution for the $O(A^2)$ term is defined by

$$\begin{aligned} &Y_{\mathrm{2nd},1}(t,t',\bar{\beta},\bar{\gamma}) \\ &= e^{ib^I_z(t'-t)\sigma(1-\delta_{\sigma\sigma'})} e^{ib^I_z(t'-t)\beta(1-\delta_{\beta\beta'})} \mathrm{Tr}_{\mathrm{el}}\Bigg\{\sum_{rr'} e^{i(r-r')x_j} c^{\dagger}_{r\gamma} c_{r'\gamma'} \rho_{\mathrm{el}}(t') \end{aligned}$$

$$\times \left[\sum_{pp'} e^{i(p-p')x_j} c^\dagger_{p\sigma}(t'-t) c_{p'\sigma'}(t'-t), \sum_{nn'} e^{i(n-n')x_j} c^\dagger_{n\beta}(t'-t) c_{n'\beta'}(t'-t)\right]\Bigg\}, \tag{5.84}$$

$$Y_{\mathrm{2nd},2}(t,t',\bar{\beta},\bar{\gamma})$$
$$= e^{ib_z^I(t'-t)\sigma(1-\delta_{\sigma\sigma'})} e^{ib_z^I(t'-t)\beta(1-\delta_{\beta\beta'})} \mathrm{Tr}_{\mathrm{el}}\Bigg\{\rho_{\mathrm{el}}(t') \sum_{rr'} e^{i(r-r')x_j} c^\dagger_{r\gamma} c_{r'\gamma'}$$
$$\times \left[\sum_{nn'} e^{i(n-n')x_j} c^\dagger_{n\beta}(t'-t) c_{n'\beta'}(t'-t), \sum_{pp'} e^{i(p-p')x_j} c^\dagger_{p\sigma}(t'-t) c_{p'\sigma'}(t'-t)\right]\Bigg\}. \tag{5.85}$$

The phase factor due to the magnetic field depends on the spin configuration of the original electron spin operator $S^{\bar{\sigma}}$. The factor $\sigma(1-\delta_{\sigma\sigma'})$ in the exponential determines the phase contribution, specifically

$$S^{\bar{\sigma}} = S^z : \sigma = \sigma' \quad \rightarrow \quad \sigma(1-\delta_{\sigma\sigma'}) = 0, \tag{5.86}$$
$$S^{\bar{\sigma}} = S^+ : \sigma = \uparrow, \sigma' = \downarrow \quad \rightarrow \quad \sigma(1-\delta_{\sigma\sigma'}) = +1, \tag{5.87}$$
$$S^{\bar{\sigma}} = S^- : \sigma = \downarrow, \sigma' = \uparrow \quad \rightarrow \quad \sigma(1-\delta_{\sigma\sigma'}) = -1. \tag{5.88}$$

Finally we require the expression for the last $O(A^2)$ term in Eq. (5.66) where the commutators take the form $\left[\exp[(t-t')L_{\mathrm{el}}]\rho_{\mathrm{el}}(t'), S^{\bar{\beta}}\right]$. Again applying Eq. (5.78) and taking the trace with respect to the electrons we have

$$\mathrm{Tr}_{\mathrm{el}}\left\{S^{\bar{\sigma}}\left[e^{(t-t')L_{\mathrm{el}}}\rho_{\mathrm{el}}(t'), S^{\bar{\beta}}\right]\right\} = \mathrm{Tr}_{\mathrm{el}}\left\{\left[S^{\bar{\beta}}(t'-t), S^{\bar{\sigma}}(t'-t)\right]\rho_{\mathrm{el}}(t')\right\}. \tag{5.89}$$

and we acquire the expression

$$Y_{\mathrm{2nd},3}(t,t',\bar{\beta},\bar{\gamma}) = e^{ib_z^I(t'-t)\sigma(1-\delta_{\sigma\sigma'})} e^{ib_z^I(t'-t)\beta(1-\delta_{\beta\beta'})}$$
$$\mathrm{Tr}_{\mathrm{el}}\left\{\left[\sum_{nn'} e^{i(n-n')x_j} c^\dagger_{n\beta}(t'-t) c_{n'\beta'}(t'-t), \sum_{pp'} e^{i(p-p')x_j} c^\dagger_{p\sigma}(t'-t) c_{p'\sigma'}(t'-t)\right]\rho_{\mathrm{el}}(t')\right\}. \tag{5.90}$$

In the following subsections when deriving the expressions for all Y_i explicitly we use the superscript 'p' or 'h' to indicate if the term describes the particle or hole contribution. Furthermore we follow the convention that the indices $\sigma, \sigma', \beta, \beta', \gamma, \gamma'$ are reserved to label the fixed components which are determined by the spin components of the relevant commutators from Eqs. (5.63) to (5.66) and according to the definitions above in Eqs. (5.80), (5.81), (5.84), (5.85) and (5.90). The sum of all those terms including their prefactors from the electron equation of motion define the right-hand side of the differ-

ential equation determining $\Lambda^{\alpha}_{\alpha'}(x_l,t), \tilde{\Lambda}^{\alpha}_{\alpha'}(x_l,t)$. To find a closed equation of motion for each $\Lambda^{\alpha}_{\alpha'}(x_l,t), \tilde{\Lambda}^{\alpha}_{\alpha'}(x_l,t)$ we will use the fact that the time evolution under the action of L_{el} is diagonal in the fermionic creation and annihilation operators and reduces to the phase factor $\exp(\pm i\epsilon_k t)$.

To deal with the expectation values of fermionic creation and annihilation operators we use a systematic cumulant expansion [169]. Up to lowest order this corresponds to the Wick theorem [128] and we will refer to the cumulant expansion as Wick decomposition. We are addressing short lived fluctuations therefore we expect the lowest order to be sufficiently accurate. Wick's theorem itself is not valid in our case as the electron density matrix is not quadratic when taking into account the full history [128, 170]. Using the Wick decomposition of the expectation values also bypasses the need to find an expression for Eq. (5.71) as every expectation value in the equation of motion for the localised spin can be decomposed into expectation values of a single pairs of creation and annihilation operators $\langle c^{\dagger}c\rangle$. For two pairs of fermionic creation and annihilation operators the Wick decomposition allows us to write

$$\left\langle c^{\dagger}_{p\sigma}c_{p'\sigma'}c^{\dagger}_{r\gamma}c_{r'\gamma'}\right\rangle_{\mathrm{el,eq}} = \left\langle c^{\dagger}_{p\sigma}c_{p'\sigma'}\right\rangle_{\mathrm{el,eq}}\left\langle c^{\dagger}_{r\gamma}c_{r'\gamma'}\right\rangle_{\mathrm{el,eq}} + \left\langle c^{\dagger}_{p\sigma}c_{r'\gamma'}\right\rangle_{\mathrm{el,eq}}\left\langle c_{p'\sigma'}c^{\dagger}_{r\gamma}\right\rangle_{\mathrm{el,eq}}, \tag{5.91}$$

and for three pairs we arrive at

$$\begin{aligned}
&\left\langle c^{\dagger}_{p\sigma}c_{p'\sigma'}c^{\dagger}_{r\gamma}c_{r'\gamma'}c^{\dagger}_{k\alpha}c_{k'\alpha'}\right\rangle_{\mathrm{el,eq}} \\
&= \left\langle c^{\dagger}_{p\sigma}c_{p'\sigma'}\right\rangle_{\mathrm{el,eq}}\left\langle c^{\dagger}_{r\gamma}c_{r'\gamma'}\right\rangle_{\mathrm{el,eq}}\left\langle c^{\dagger}_{k\alpha}c_{k'\alpha'}\right\rangle_{\mathrm{el,eq}} + \left\langle c^{\dagger}_{p\sigma}c_{p'\sigma'}\right\rangle_{\mathrm{el,eq}}\left\langle c^{\dagger}_{r\gamma}c_{k'\alpha'}\right\rangle_{\mathrm{el,eq}}\left\langle c_{r'\gamma'}c^{\dagger}_{k\alpha}\right\rangle_{\mathrm{el,eq}} \\
&+ \left\langle c^{\dagger}_{p\sigma}c_{r'\gamma'}\right\rangle_{\mathrm{el,eq}}\left\langle c_{p'\sigma'}c^{\dagger}_{r\gamma}\right\rangle_{\mathrm{el,eq}}\left\langle c^{\dagger}_{k\alpha}c_{k'\alpha'}\right\rangle_{\mathrm{el,eq}} - \left\langle c^{\dagger}_{p\sigma}c_{r'\gamma'}\right\rangle_{\mathrm{el,eq}}\left\langle c_{p'\sigma'}c^{\dagger}_{k\alpha}\right\rangle_{\mathrm{el,eq}}\left\langle c^{\dagger}_{r\gamma}c_{k'\alpha'}\right\rangle_{\mathrm{el,eq}} \\
&+ \left\langle c^{\dagger}_{p\sigma}c_{k'\alpha'}\right\rangle_{\mathrm{el,eq}}\left\langle c_{p'\sigma'}c^{\dagger}_{r\gamma}\right\rangle_{\mathrm{el,eq}}\left\langle c_{r'\gamma'}c^{\dagger}_{k\alpha}\right\rangle_{\mathrm{el,eq}} + \left\langle c^{\dagger}_{p\sigma}c_{k'\alpha'}\right\rangle_{\mathrm{el,eq}}\left\langle c_{p'\sigma'}c^{\dagger}_{k\alpha}\right\rangle_{\mathrm{el,eq}}\left\langle c^{\dagger}_{r\gamma}c_{r'\gamma'}\right\rangle_{\mathrm{el,eq}}.
\end{aligned} \tag{5.92}$$

The complicated dynamical behaviour of $\rho_{\mathrm{el}}(t)$ is picked up by the functions $\Lambda(x_j,t)$, $\tilde{\Lambda}(x_j,t)$. Therefore each expectation value of the number operator is taken with respect to the equilibrium state which is given by

$$\left\langle c^{\dagger}_{p\sigma}c_{p'\sigma'}\right\rangle_{\mathrm{el,eq}} = \delta_{pp'}\delta_{\sigma\sigma'}f(\epsilon_p), \tag{5.93}$$

with the Fermi-Dirac distribution $f(\epsilon_p) = (1+\exp[\epsilon_p/k_BT])^{-1}$. When inserting Eq. (5.76) into the left-hand side of Eq. (5.77), using the Wick decomposition Eq. (5.91) and the

relation in Eq. (5.93) we obtain for the particles

$$\sum_{pp'} e^{i(p-p')x_j} \frac{d}{dt} \left\langle c^\dagger_{p\sigma} c_{p'\sigma'} \right\rangle_{\mathrm{el},t} = \frac{1}{N^2} \sum_{pk} \sum_{\alpha,l=1,2} f(\epsilon_p) f(\epsilon_k) \frac{d}{dt} \Lambda^\alpha_\alpha(x_l,t) + \frac{1}{N^2} \sum_{pk} \sum_{l=1,2} e^{ip(x_j-x_l)} e^{-ik(x_j-x_l)} f(\epsilon_p) \left(1-f(\epsilon_k)\right) \frac{d}{dt} \Lambda^{\sigma'}_\sigma(x_l,t), \tag{5.94}$$

and for the holes

$$\sum_{pp'} e^{i(p-p')x_j} \frac{d}{dt} \left\langle c^\dagger_{p\sigma} c_{p'\sigma'} \right\rangle_{\mathrm{el},t} = \frac{1}{N^2} \sum_{pk} \sum_{\alpha,l=1,2} f(\epsilon_p) f(\epsilon_k) \frac{d}{dt} \tilde{\Lambda}^\alpha_\alpha(x_l,t) - \frac{1}{N^2} \sum_{pk} \sum_{l=1,2} e^{ip(x_j-x_l)} e^{-ik(x_j-x_l)} f(\epsilon_p) \left(1-f(\epsilon_k)\right) \frac{d}{dt} \tilde{\Lambda}^{\sigma'}_\sigma(x_l,t). \tag{5.95}$$

The position label j corresponds the location of the localised spin and is fixed just like the spin indices σ, σ'. In the following we derive the expressions for Eqs. (5.80), (5.81), (5.84), (5.85) and (5.90) and further details can be found in Appendix F.2.

5.2.3.1 Eigendynamics and linear term

To derive the contribution of $L_{\mathrm{el}}\rho_{\mathrm{el}}(t)$ to the equation of motion for $\Lambda^\alpha_{\alpha'}$ and $\tilde{\Lambda}^\alpha_{\alpha'}$ we rewrite the electron Hamiltonian of Eq. (5.62) fully in terms of fermionic creation and annihilation operators

$$H'_{\mathrm{el}} = \sum_{k\sigma} \left(\epsilon_k + \sigma b_z\right) c^\dagger_{k\sigma} c_{k\sigma}. \tag{5.96}$$

The spin index σ as prefactor of the magnetic field contribution b_z should be interpreted as the sign $+1$ if $\sigma = \uparrow$ and -1 if $\sigma = \downarrow$. Inserting Eq. (5.76) into Eq. (5.80) leads here to the commutator between two pairs of creation and annihilation operators which will regularly appear throughout the derivation. Generally it can be replaced by

$$\left[c^\dagger_{p\sigma} c_{p'\sigma'}, c^\dagger_{n\beta} c_{n'\beta'}\right] = \delta_{np'} \delta_{\beta\sigma'} c^\dagger_{p\sigma} c_{n'\beta'} - \delta_{n'p} \delta_{\beta'\sigma} c^\dagger_{n\beta} c_{p'\sigma'}. \tag{5.97}$$

Using the relation Eq. (5.97) after substituting the approximation for $\rho_{\mathrm{el}}(t)$ in Eq. (5.80) leads to

$$\begin{aligned} &Y^{\mathrm{p}}_{\mathrm{ED}}(t) \\ &= i \sum_{pn} \sum_{l=1,2} e^{ip(x_j-x_l)} e^{-in(x_j-x_l)} f(\epsilon_p)\left(1-f(\epsilon_n)\right) \Lambda^{\sigma'}_{\sigma}(x_l,t)\left[\epsilon_p-\epsilon_n+b_z\left(\sigma-\sigma'\right)\right], \end{aligned} \tag{5.98}$$

for the part capturing the particle excitation. For the hole contribution we obtain the same terms with the opposite sign due to the particle-hole symmetry

$$\begin{aligned} &Y^{\mathrm{h}}_{\mathrm{ED}}(t) \\ &= i \sum_{pn} \sum_{l=1,2} e^{ip(x_j-x_l)} e^{-in(x_j-x_l)} f(\epsilon_p)\left(1-f(\epsilon_n)\right) \tilde{\Lambda}^{\sigma'}_{\sigma}(x_l,t)\left[\epsilon_n-\epsilon_p+b_z\left(\sigma'-\sigma\right)\right]. \end{aligned} \tag{5.99}$$

To get to these results we additionally used the fact that $[H_{\mathrm{el}}, \rho^{\mathrm{eq}}_{\mathrm{el}}] = 0$. The linear term of Eq. (5.81) when inserting Eq. (5.76) and again using Eq. (5.97) yields

$$Y^{\mathrm{p}}_{\mathrm{lin}}(t,\bar{\beta}) = \sum_{pn} \sum_{l=1,2} e^{ip(x_j-x_l)} e^{-in(x_j-x_l)} f(\epsilon_p)\left(1-f(\epsilon_n)\right)\left[\delta_{\sigma'\beta}\Lambda^{\beta'}_{\sigma}(x_l,t) - \delta_{\sigma\beta'}\Lambda^{\sigma'}_{\beta}(x_l,t)\right]. \tag{5.100}$$

Similarly, the corresponding hole contribution is given by

$$Y^{\mathrm{h}}_{\mathrm{lin}}(t,\bar{\beta}) = -Y^{\mathrm{p}}_{\mathrm{lin}}(t,\bar{\beta}), \tag{5.101}$$

where Λ is replaced by $\tilde{\Lambda}$.

5.2.3.2 $O(A^2)$: Two- and one-point correlators

The first two $O(A^2)$ terms generate the same commutators. Substituting Eq. (5.76) into Eq. (5.84) for the particle contribution leads to

$$\begin{aligned} Y^{\mathrm{p}}_{\mathrm{2nd},1}(t,t',\bar{\beta},\bar{\gamma}) = {} & e^{ib^I_z(t'-t)\sigma(1-\delta_{\sigma\sigma'})} e^{ib^I_z(t'-t)\beta(1-\delta_{\beta\beta'})} \\ & \sum_{\substack{pp'\\nn'}} \sum_{\substack{rr'\\kk'}} \sum_{\substack{\alpha\alpha'\\l=1,2}} e^{i(p-p')x_j} e^{i(r-r')x_j} e^{i(n-n')x_j} e^{i(k-k')x_l} \Lambda^{\alpha}_{\alpha'}(x_l,t') \\ & \times \Bigg(\delta_{p'n}\delta_{\sigma'\beta} e^{i(\epsilon_p-\epsilon_{n'})(t'-t)} \left\langle c^{\dagger}_{p\sigma} c_{n'\beta'} c^{\dagger}_{r\gamma} c_{r'\gamma'} c^{\dagger}_{k\alpha} c_{k'\alpha'} \right\rangle_{\mathrm{el,eq}} \end{aligned}$$

$$- \delta_{pn'}\delta_{\sigma\beta'} e^{i(\epsilon_n-\epsilon_{p'})(t'-t)} \left\langle c^\dagger_{n\beta} c_{p'\sigma'} c^\dagger_{r\gamma} c_{r'\gamma'} c^\dagger_{k\alpha} c_{k'\alpha'} \right\rangle_{\text{el,eq}} \Bigg) \tag{5.102}$$

Decomposing the expectation values according to Eq. (5.92) and using the relation Eq. (5.93) leads to

$$\begin{aligned}
&Y^{\text{p}}_{2\text{nd},1}(t,t',\bar\beta,\bar\gamma) \\
&= e^{ib_z^I(t'-t)\sigma(1-\delta_{\sigma\sigma'})} e^{ib_z^I(t'-t)\beta(1-\delta_{\beta\beta'})} \\
&\Bigg[\sum_{prk} \sum_{\alpha,l=1,2} e^{i(\epsilon_p-\epsilon_r)(t'-t)} f(\epsilon_p) f(\epsilon_k) \left(1-f(\epsilon_r)\right) \Lambda^\alpha_\alpha(x_l,t') \left(\delta_{\sigma'\beta}\delta_{\sigma\gamma'}\delta_{\beta'\gamma} - \delta_{\beta'\sigma}\delta_{\beta\gamma'}\delta_{\sigma'\gamma}\right) \\
&+ \sum_{prk} \sum_{l=1,2} e^{i(\epsilon_p-\epsilon_k)(t'-t)} e^{ir(x_j-x_l)} e^{-ik(x_j-x_l)} f(\epsilon_p) f(\epsilon_r) \left(1-f(\epsilon_k)\right) \\
&\times \left(\delta_{\sigma'\beta}\delta_{\sigma\gamma'}\Lambda^{\beta'}_\gamma(x_l,t') - \delta_{\beta'\sigma}\delta_{\beta\gamma'}\Lambda^{\sigma'}_\gamma(x_l,t')\right) \\
&+ \sum_{prk} \sum_{l=1,2} e^{i(\epsilon_p-\epsilon_r)(t'-t)} e^{ip(x_j-x_l)} e^{-ik(x_j-x_l)} f(\epsilon_p) \left(1-f(\epsilon_r)\right) \left(1-f(\epsilon_k)\right) \\
&\times \left(\delta_{\sigma'\beta}\delta_{\beta'\gamma}\Lambda^{\gamma'}_\sigma(x_l,t') - \delta_{\beta'\sigma}\delta_{\sigma'\gamma}\Lambda^{\gamma'}_\beta(x_l,t')\right) \\
&+ \sum_{prk} \sum_{l=1,2} e^{i(\epsilon_p-\epsilon_k)(t'-t)} e^{ip(x_j-x_l)} e^{-ik(x_j-x_l)} f(\epsilon_p) f(\epsilon_r) \left(1-f(\epsilon_k)\right) \\
&\times \left(\delta_{\sigma'\beta}\delta_{\gamma\gamma'}\Lambda^{\beta'}_\sigma(x_l,t') - \delta_{\beta'\sigma}\delta_{\gamma'\gamma}\Lambda^{\sigma'}_\beta(x_l,t')\right) \Bigg].
\end{aligned} \tag{5.103}$$

For the hole contribution we can again make use of the particle-hole symmetry and

$$Y^{\text{h}}_{2\text{nd},1}(t,t',\bar\beta,\bar\gamma) = -Y^{\text{p}}_{2\text{nd},1}(t,t',\bar\beta,\bar\gamma) \tag{5.104}$$

where $\Lambda \to \tilde\Lambda$. Similarly, the second commutator and its corresponding trace in Eq. (5.85) reads

$$\begin{aligned}
Y^{\text{p}}_{2\text{nd},2}(t,t',\bar\beta,\bar\gamma) &= e^{ib_z^I(t'-t)\sigma(1-\delta_{\sigma\sigma'})} e^{ib_z^I(t'-t)\beta(1-\delta_{\beta\beta'})} \\
&\sum_{\substack{pp'\\nn'}} \sum_{\substack{rr'\\kk'}} \sum_{\substack{\alpha\alpha'\\l=1,2}} e^{i(p-p')x_j} e^{i(r-r')x_j} e^{i(n-n')x_j} e^{i(k-k')x_l} \Lambda^\alpha_{\alpha'}(x_l,t') \\
&\times \Bigg(\delta_{pn'}\delta_{\sigma\beta'} e^{i(\epsilon_n-\epsilon_{p'})(t'-t)} \left\langle c^\dagger_{r\gamma} c_{r'\gamma'} c^\dagger_{n\beta} c_{p'\sigma'} c^\dagger_{k\alpha} c_{k'\alpha'} \right\rangle_{\text{el,eq}} \\
&- \delta_{p'n}\delta_{\sigma'\beta} e^{i(\epsilon_p-\epsilon_{n'})(t'-t)} \left\langle c^\dagger_{r\gamma} c_{r'\gamma'} c^\dagger_{p\sigma} c_{n'\beta'} c^\dagger_{k\alpha} c_{k'\alpha'} \right\rangle_{\text{el,eq}} \Bigg)
\end{aligned} \tag{5.105}$$

after inserting the approximation Eq. (5.75). Using Wick's theorem according to Eq. (5.92) and rewriting the expectation values in terms of the Fermi distribution as in Eq. (5.93) we obtain

$$
\begin{aligned}
&Y^{\mathrm{p}}_{\mathrm{2nd},2}(t,t',\bar{\beta},\bar{\gamma}) \\
&= e^{ib_z^I(t'-t)\sigma(1-\delta_{\sigma\sigma'})} e^{ib_z^I(t'-t)\beta(1-\delta_{\beta\beta'})} \\
&\Bigg[\sum_{prk} \sum_{\alpha,l=1,2} e^{i(\epsilon_p-\epsilon_r)(t'-t)} f(\epsilon_r) f(\epsilon_k) \left(1-f(\epsilon_p)\right) \Lambda^{\alpha}_{\alpha}(x_l,t') \left(\delta_{\sigma\beta'}\delta_{\gamma\sigma'}\delta_{\beta\gamma'} - \delta_{\beta\sigma'}\delta_{\beta'\gamma}\delta_{\sigma\gamma'}\right) \\
&+ \sum_{prk} \sum_{l=1,2} e^{i(\epsilon_p-\epsilon_k)(t'-t)} e^{ip(x_j-x_l)} e^{-ik(x_j-x_l)} f(\epsilon_p) f(\epsilon_r) \left(1-f(\epsilon_k)\right) \\
&\times \left(\delta_{\sigma\beta'}\delta_{\gamma\gamma'}\Lambda^{\sigma'}_{\beta}(x_l,t') - \delta_{\beta\sigma'}\delta_{\gamma\gamma'}\Lambda^{\beta'}_{\sigma}(x_l,t')\right) \\
&+ \sum_{prk} \sum_{l=1,2} e^{i(\epsilon_p-\epsilon_r)(t'-t)} e^{ip(x_j-x_l)} e^{-ik(x_j-x_l)} f(\epsilon_p) f(\epsilon_r) \left(1-f(\epsilon_k)\right) \\
&\times \left(\delta_{\sigma\beta'}\delta_{\gamma\sigma'}\Lambda^{\gamma'}_{\beta}(x_l,t') - \delta_{\beta\sigma'}\delta_{\gamma\beta'}\Lambda^{\gamma'}_{\sigma}(x_l,t')\right) \\
&+ \sum_{prk} \sum_{l=1,2} e^{i(\epsilon_p-\epsilon_k)(t'-t)} e^{ir(x_j-x_l)} e^{-ik(x_j-x_l)} f(\epsilon_r) \left(1-f(\epsilon_p)\right) \left(1-f(\epsilon_k)\right) \\
&\times \left(\delta_{\sigma\beta'}\delta_{\beta\gamma'}\Lambda^{\sigma'}_{\gamma}(x_l,t') - \delta_{\beta\sigma'}\delta_{\sigma\gamma'}\Lambda^{\beta'}_{\gamma}(x_l,t')\right) \Bigg].
\end{aligned}
\tag{5.106}
$$

Upon replacing Λ by the $\tilde{\Lambda}$ and taking the opposite signs leads to hole contribution with

$$
Y^{\mathrm{h}}_{\mathrm{2nd},2}(t,t',\bar{\beta},\bar{\gamma}) = -Y^{\mathrm{p}}_{\mathrm{2nd},2}(t,t',\bar{\beta},\bar{\gamma}). \tag{5.107}
$$

5.2.3.3 $O(A^2)$: Renormalisation term

The final contribution to the equation of motion for the functions $\Lambda, \tilde{\Lambda}$ comes from Eq. (5.90). Substituting Eq. (5.75) for $\rho_{\mathrm{el}}(t')$ into the expression Eq. (5.90) the contribution can be written as

$$
\begin{aligned}
Y^{\mathrm{p}}_{\mathrm{2nd},3}(t,t',\bar{\beta},\bar{\gamma}) = {} & e^{ib_z^I(t'-t)\sigma(1-\delta_{\sigma\sigma'})} e^{ib_z^I(t'-t)\beta(1-\delta_{\beta\beta'})} \\
& \sum_{\substack{pp' \\ nn'}} \sum_{kk'} \sum_{\substack{\alpha\alpha' \\ l=1,2}} e^{i(p-p')x_j} e^{i(n-n')x_j} e^{i(k-k')x_l} \Lambda^{\alpha}_{\alpha'}(x_l,t') \\
& \times \Bigg(\delta_{pn'}\delta_{\sigma\beta'} e^{i(\epsilon_n-\epsilon_{p'})(t'-t)} \left\langle c^{\dagger}_{n\beta} c_{p'\sigma'} c^{\dagger}_{k\alpha} c_{k'\alpha'} \right\rangle_{\mathrm{el,eq}} \\
& - \delta_{p'n}\delta_{\sigma'\beta} e^{i(\epsilon_p-\epsilon_{n'})(t'-t)} \left\langle c^{\dagger}_{p\sigma} c_{n'\beta'} c^{\dagger}_{k\alpha} c_{k'\alpha'} \right\rangle_{\mathrm{el,eq}} \Bigg).
\end{aligned}
\tag{5.108}
$$

Utilising Eq. (5.91) and Eq. (5.93) we arrive at

$$\begin{aligned} Y^{\mathrm{p}}_{2\mathrm{nd},3}(t,t',\bar{\beta},\bar{\gamma}) = e^{ib_z^I(t'-t)\sigma(1-\delta_{\sigma\sigma'})}e^{ib_z^I(t'-t)\beta(1-\delta_{\beta\beta'})} \\ \sum_{pk} e^{i(\epsilon_p-\epsilon_k)(t-t')}e^{ip(x_j-x_l)}e^{-ik(x_j-x_l)}f(\epsilon_p)\left(1-f(\epsilon_k)\right) \\ \times\left(\delta_{\sigma\beta'}\Lambda^{\sigma'}_{\beta}(x_l,t')-\delta_{\beta\sigma'}\Lambda^{\beta'}_{\sigma}(x_l,t')\right), \end{aligned} \tag{5.109}$$

and accordingly for the hole contribution

$$Y^{\mathrm{h}}_{2\mathrm{nd},3}(t,t',\bar{\beta},\bar{\gamma}) = -Y^{p}_{2\mathrm{nd},3}(t,t',\bar{\beta},\bar{\gamma}). \tag{5.110}$$

With this last contribution we found all expressions Y_i entering the equation of motion of the electron correlation functions in Eq. (5.77).

5.2.4 Intermediate conclusion

Collecting all Y_i from Eqs. (5.98), (5.100), (5.103), (5.106) and (5.109) and their corresponding prefactors from the electron equation of motion Eqs. (5.63) to (5.66) leads to a closed set of equations of motion for the functions $\Lambda, \tilde{\Lambda}$ which capture the time-dependent electron spin fluctuations. From the analytical result up to this point we are able to make some observations. We can interpret the functions $\Lambda, \tilde{\Lambda}$ as a spin and time-dependent weight for the Fermi distribution functions. They therefore incorporate the small shift of the Fermi energy due to an excitation in the electronic bath. Furthermore, we find particle-hole fluctuations identical to the single spin case discussed in Chapter 3 as we see from the combinations of $f(\epsilon)\left(1-f(\epsilon)\right)$ in the different terms Y. In which way the temporal and spatial correlations enter can best be seen from the momentum integrals of the continuum limit appearing in the equation of motion of the electronic correlations in each Y_i which we discuss below. We find purely temporal contributions encoding the backaction of the electrons back onto the same localised spin which excited the environment to begin with. These are the same as in the single spin case. Furthermore, there are spatial contributions which we can attribute to the effective coupling of the localised spins through the bath and therefore identify it as an RKKY-like interaction. Lastly, there are combinations of both temporal and spatial correlations which mix the different localised spin sites leading to a dynamical RKKY interaction. The temporal correlations only enter in the $O(A^2)$ terms and stem from the action of the memory kernel. Similar to our results from the single spin case we expect that these contribution give rise to non-Markovian dynamics in the full solution of the problem. We analyse the momentum contributions to the spatial and temporal correlations below.

5.2.4.1 Continuum limit of momentum integrals

We specify the appearing momentum integrals in the different Y_i and more details on the calculation of the different integrals can be found in Appendix F.3. To evaluate the momentum and energy integrals we consider a two dimensional Fermi gas for the conduction electrons. The effective interaction mediated by the electrons decays as $1/r^d$ in d spatial dimensions, see Section 5.1, therefore in two dimensions the spatial correlations are more prominent than in three, and two dimensional electronic systems are an accessible experimental platform. We specifically mark all vector quantities where $|\mathbf{k}| = k$ is implied. Additionally, we assume a linear dispersion for the electrons

$$\epsilon_{\mathbf{k}} \sim \epsilon_k = v_F \left(k - k_F\right) \tag{5.111}$$

with k_F and v_F the Fermi momentum and the Fermi velocity respectively. Since all the important universal physics occurs in the vicinity of the Fermi surface, the linearisation corresponds to the wide band limit which is fulfilled for usual solid state systems. In the second order term of Eq. (5.103) for the contribution Λ_α^α diagonal in the spin components we find

$$I_t := \sum_{\mathbf{k}\mathbf{k}'} e^{i(\epsilon_{\mathbf{k}} - \epsilon_{\mathbf{k}'})(t'-t)} f(\epsilon_{\mathbf{k}}) \left(1 - f(\epsilon_{\mathbf{k}'})\right) \tag{5.112}$$

and its complex conjugate in Eq. (5.106). Together those terms are the same as we found in the Nakajima-Zwanzig master equation for the single spin case for the spin-spin correlation function in Eq. (3.79). We solve Eq. (5.112) by integrating over the density of states $\nu(\epsilon) = \nu_0 \exp\left(-|\epsilon|/\xi_0\right)$ and introducing the high energy cutoff ξ_0 as in Section 3.2.3, which incorporates all non-universal band structure effects. The unit cell volume V defines $\nu_0 = V/(2\pi)^2$. This leads to

$$\begin{aligned} I_t &= \int d\epsilon \nu(\epsilon) f(\epsilon) \int d\epsilon' \nu(\epsilon') \left(1 - f(\epsilon')\right) \\ &= \frac{\left(\pi k_B T\right)^2}{\sin^2\left(\pi k_B T \left(i(t'-t) + \xi_0^{-1}\right)\right)}. \end{aligned} \tag{5.113}$$

Eq. (5.113) together with its complex conjugate correspond to the electron spin-spin correlations function found in the standard Nakajima-Zwanzig approach. In the single spin setup their short time behaviour lead to memory effects and finally non-Markovian dynamics. In the current setup of two spins in a common environment they are further modulated by the time-dependent amplitude Λ and $\tilde{\Lambda}$.

The spatial modulations encoding the effective RKKY-type coupling enter through the term

$$I_x := \sum_{\mathbf{k},l=1,2} e^{i\mathbf{k}\cdot(\mathbf{x}_j-\mathbf{x}_l)} f(\epsilon_k) \tag{5.114}$$

which appears throughout the equation of motion for $\Lambda, \tilde{\Lambda}$ in all Y_i. It reduces to a similar sum as Eq. (5.112) if $\mathbf{x}_j = \mathbf{x}_l$ and we denote $\mathbf{x} = \mathbf{x}_j - \mathbf{x}_l$ for $j \neq l$. In the continuum limit Eq. (5.114) reads

$$\begin{aligned} I_x &= \int \frac{d^2k}{(2\pi)^2} \frac{e^{i\mathbf{k}\cdot\mathbf{x}}}{1+e^{\epsilon(\mathbf{k}-\mu)}/k_BT} \\ &= \frac{\nu_0}{2\pi} \int_{-\infty}^{\infty} d\epsilon \int_0^{2\pi} d\phi\, e^{i(k_F+\epsilon/v_F)x\cos\phi} \frac{1}{1+e^{\epsilon/k_BT}} \end{aligned} \tag{5.115}$$

where we write the momentum integral as an integral over the energy ϵ using Eq. (5.111). The integral can be evaluated making use of the residue theorem in the complex plane, see Appendix F.3, which leads to

$$\begin{aligned} I_x = -2\pi k_B T \nu_0 \mathrm{Re}\Bigg[i \sum_{n\geq 0} \Big\{ & J_0\left(k_F x + i\frac{\pi k_B T}{v_F}(2n+1)x\right) \\ & + iH_0\left(k_F x + i\frac{\pi k_B T}{v_F}(2n+1)x\right) \Big\}\Bigg], \end{aligned} \tag{5.116}$$

with the Bessel function $J_\lambda(z)$ [131]

$$J_\lambda(z) = \left(\frac{z}{2}\right)^\lambda \sum_{n=0}^{\infty} (-1)^n \frac{\left(\frac{z^2}{4}\right)^n}{n!\Gamma(\lambda+n+1)}, \tag{5.117}$$

and the Struve function $H_\lambda(z)$ [131]

$$H_\lambda(z) = \left(\frac{z}{2}\right)^{\lambda+1} \sum_{n=0}^{\infty} (-1)^n \frac{\left(\frac{z^2}{2}\right)^{2n}}{\Gamma\left(n+\frac{3}{2}\right)\Gamma\left(\lambda+n+\frac{3}{2}\right)}, \tag{5.118}$$

where $\Gamma(z)$ is Euler's Gamma function. The spatial modulations in the RKKY interaction generally come from the correlation of conduction electrons at different positions, i.e., $\langle \mathbf{S}_i \mathbf{S}_j \rangle$. In our case these correlations do not exist. The spatial mixing is more subtle and enters through the time-dependent bath reference state. Nonetheless, we find an RKKY-like coupling with a $1/\sqrt{x}$ behaviour instead of $1/x^2$. Apart from the varied algebraic

decay, the expression Eq. (5.116) is similar to the expressions for the RKKY interaction in lower spatial dimension found in the literature where Bessel functions or closely related functions often occur [164, 165, 171].

Inserting the asymptotic form of the Bessel and Struve functions $J_0(z)$ and $H_0(z)$

$$J_0(z) \sim \sqrt{\frac{2}{\pi z}} \sin\left(z + \frac{\pi}{4}\right), \tag{5.119}$$

$$H_0(z) \sim -\sqrt{\frac{2}{\pi z}} \cos\left(z + \frac{\pi}{4}\right), \tag{5.120}$$

into Eq. (5.116) leads to

$$I_x \approx -2\pi k_B T \nu_0 \mathrm{Re}\left[i\sqrt{\frac{2}{\pi}} \sum_{n\geq 0} \left\{ \frac{\sin\left(\tilde{z}_n + \frac{\pi}{4}\right) - i\cos\left(\tilde{z}_n + \frac{\pi}{4}\right)}{\sqrt{\tilde{z}_n}} \right\} \right] \tag{5.121}$$

with $\tilde{z}_n = k_F x + i\pi x k_B T(2n+1)/v_F$. Rearranging this last expression Eq. (5.116) can be written as

$$I_x \approx -2\nu_0 \sqrt{\frac{k_B T v_F}{x}} e^{-x/x_T} \mathrm{Re}\left[e^{ik_F x} \Phi\left(e^{-2x/x_T}, \frac{1}{2}, \frac{1}{2} - i\frac{v_F k_F}{\pi k_B T} \right) \right]. \tag{5.122}$$

where $\Phi(z, s, a)$ is Lerch's transcendent [131, 172]

$$\Phi(z, s, a) = \sum_{n=0}^{\infty} \frac{z^n}{(a+n)^s}. \tag{5.123}$$

Furthermore, we introduced the thermal length scale $x_T = v_F/\pi k_B T$. The last argument of Φ in Eq. (5.122) is large since $a = 1/2 - iv_F k_F/\pi k_B T$ with $v_F k_F = 2E_F$. In this limit an asymptotic expansion for $\Phi(z, s, a)$ is given by [173]

$$\Phi(z, s, a) \approx \frac{1}{1-z}\frac{1}{a^s}, \tag{5.124}$$

up to the lowest order in a^s. Using the asymptotic expansion in Eq. (5.122) and determining the real part immediately leads to

$$\begin{aligned} I_x &\approx 2\nu_0 \sqrt{\frac{k_B T v_F}{2x\sqrt{1 + 4k_F^2 x_T^2}}} e^{-x/x_T} \left(1 - \frac{1}{\tanh(x/x_T)}\right) \cos\left(k_F x\right) \\ &\approx 2\nu_0 k_B T e^{-x/x_T} \left(1 - \frac{1}{\tanh(x/x_T)}\right) \frac{\cos\left(k_F x\right)}{\sqrt{k_F x}}. \end{aligned} \tag{5.125}$$

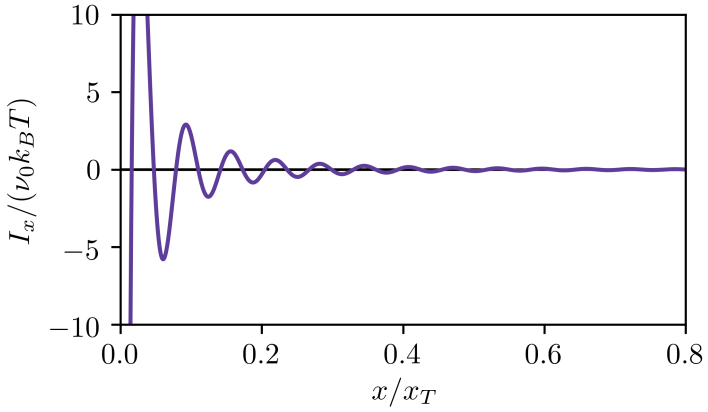

Figure 5.2: Plot of the asymptotic behaviour of spatial correlations captured by the integral I_x according to the expression Eq. (5.125) with $k_F x_T = 100$.

In the last line we approximated $\sqrt{1+4k_F^2 x_T^2} \approx 2k_F x_T$ in the denominator of the square root. The asymptotic behaviour Eq. (5.125) is plotted in Fig. 5.2 for $k_F x_T = 100$. Like the RKKY interaction it is oscillatory function and the spatial correlations are exponentially suppressed and tend to zero for $x/x_T \sim 1$.

Finally we find terms with mixed temporal and spatial modulations

$$I_{t,x} := \sum_{\mathbf{k},l=1,2} e^{i\epsilon_k t} e^{i\mathbf{k}\cdot(\mathbf{x}_j - \mathbf{x}_l)} f(\epsilon_k), \tag{5.126}$$

which reads in the continuum limit

$$\begin{aligned} I_{t,x} &= \int \frac{d^2k}{(2\pi)^2} e^{-i\epsilon_{\mathbf{k}} t} \frac{e^{i\mathbf{k}\cdot\mathbf{x}}}{1+e^{(\epsilon_{\mathbf{k}}-\mu)/k_B T}} \\ &= \frac{\nu_0}{2\pi} \int_{-\infty}^{\infty} d\epsilon \int_0^{2\pi} d\phi e^{i\epsilon\left(t - i\xi_0^{-1}\right)} \frac{e^{i(k_F + \epsilon/v_F)x\cos\phi}}{1+e^{\epsilon/k_B T}} \end{aligned} \tag{5.127}$$

The high energy cutoff $\xi_0 = E_F$ introduces the shortest time scale of the system we are able to resolve with $t > \xi_0^{-1}$. For the spatial part we need to compare the length x to the Fermi length $\lambda_F = 1/k_F$ as $E_F = k_F v_F/2$. If $x \ll \lambda_F$ the term in the integral involving x is irrelevant as we assume $t > \xi_0^{-1}$ to begin with. In this limit the exchange between the localised spins is too fast to resolve. If on the other hand $x \gg \lambda_F$ or even $x \sim \lambda_F$ we need to distinguish between long and short times t. In the short time limit $t \to 0$ the spatial contribution is given by Eq. (5.125). In the limit where $t + \cos\phi x/v_F > 0$ we can

directly evaluate the angular integral of Eq. (5.127) which leads to

$$I_{t,x} = \nu_0 \int d\epsilon e^{i\epsilon(t-i\xi_0)} \frac{J_0\left(k_F x + \frac{\epsilon}{v_F} x\right)}{1 + e^{\epsilon/k_B T}}, \tag{5.128}$$

with the Bessel function $J_0(z)$. The energy integral can again be solved by using the residue theorem and we obtain

$$I_{t,x} = -2\pi k_B T \nu_0 \sum_{n\geq 0} e^{-\pi k_B T(2n+1)(t-i\xi_0^{-1})} J_0\left(k_F x + i\frac{\pi k_B T}{v_F}(2n+1)x\right). \tag{5.129}$$

Again we introduce the asymptotic form of the Bessel function $J_0(z)$ of Eq. (5.119) and similar to above we find a combination of Lerch's transcendents

$$\begin{aligned} I_{t,x} = &-\nu_0 \sqrt{\frac{k_B T v_F}{x}} e^{-i\pi k_B T \xi_0^{-1} - t/2\tau_T} \\ &\times \left[e^{ik_F x - x/x_F} \Phi\left(e^{-t/\tau_T + i2\pi k_B T \xi_0^{-1} - 2x/x_F}, \frac{1}{2}, \frac{1}{2} - i\frac{v_F k_F}{2\pi k_B T}\right) \right. \\ &\left. + ie^{-ik_F x + x/x_F} \Phi\left(e^{-t/\tau_T + i2\pi k_B T \xi_0^{-1} + 2x/x_F)}, \frac{1}{2}, \frac{1}{2} - i\frac{v_F k_F}{2\pi k_B T}\right) \right], \end{aligned} \tag{5.130}$$

with the thermal time $\tau_T = 1/2\pi k_B T$ and the thermal length $x_T = v_F/\pi k_B T$. The temporal part of $I_{t,x}$ is suppressed exponentially but enters the more complicated description through the argument of Lerch's transcendent. The spatial contribution is more involved but it is nonetheless of a similar form as I_x in Eq. (5.125), leading again to the long range RKKY-type behaviour.

For the range of finite times where $t + \cos\phi x/v_F < 0$ we are not able to find a closed expression. But with the description of the purely spatial correlations in Eq. (5.125) and the mixed contributions of Eq. (5.130) we have controlled access to the limiting cases for very short times $t \to 0$ and longer times where $t + \cos\phi x/v_F > 0$. In the intermediate range the nature of the correlations does not change and therefore we can cover this range by interpolating between the two limiting results Eq. (5.125) and Eq. (5.130).

5.3 Numerical progress

Although we have reduced the degrees of freedom relevant for the system of two localised spins coupled to conduction electrons we are not able to solve the set of coupled equation of motions of their respective reduced density matrices analytically. The final equation

we need to solve is a Volterra integro-differential equation of the form

$$\frac{d}{dt}y(t) = g(t, y(t)) + \int_{t_0}^{t} dt' K(t, t', y(t')). \tag{5.131}$$

Just as a Volterra integral equation the integro-differential version Eq. (5.131) has a unique solution [162]. In our specific case y is the vector

$$y(t) = \left(\rho_{I,j=1}(t), \rho_{I,j=2}(t), \mathbf{\Lambda}(t, x_1), \tilde{\mathbf{\Lambda}}(t, x_1), \mathbf{\Lambda}(t, x_2), \tilde{\mathbf{\Lambda}}(t, x_2)\right)^T. \tag{5.132}$$

Here, each $\mathbf{\Lambda}, \tilde{\mathbf{\Lambda}}$ represents the tuple of all $\Lambda^{\alpha}_{\alpha'}, \tilde{\Lambda}^{\alpha}_{\alpha'}$ for every possible spin combination $\alpha, \alpha' = \uparrow\downarrow$, specifically

$$\mathbf{\Lambda}(t, x_l) = \left(\Lambda^{\uparrow}_{\uparrow}(t, x_l), \Lambda^{\uparrow}_{\downarrow}(t, x_l), \Lambda^{\downarrow}_{\uparrow}(t, x_l), \Lambda^{\downarrow}_{\downarrow}(t, x_l)\right). \tag{5.133}$$

The exact form of the function g and the kernel K in the integrand of Eq. (5.131) are determined by the exact form of the equation of motion for each subsystem. For the localised spin density matrix $\rho_{I,j}$ the function g corresponds to the $O(A)$ term as in Eq. (5.24). The kernel K is built from the matrices $M_{2\mathrm{nd},i}$ of electron spin correlation functions in Eq. (5.32). For the functions $\Lambda^{\alpha}_{\alpha'}, \tilde{\Lambda}^{\alpha}_{\alpha'}$ we collect the contributions from the different Y_i in Eqs. (5.98), (5.100), (5.103), (5.106) and (5.109). All together a system of 24 coupled integro-differential equations of motion needs to be solved. Although still quite a large number of equations this is a substantial improvement over the infinite dimensional set of equations that would need to be solved if the full bath density matrix were to be kept.

5.3.1 Patade-Bhalekar algorithm

To solve the integro-differential Eq. (5.131) we make use of an algorithm proposed by Patade and Bhalekar [162] and we sketch the derivation based on their paper in the following. The first step entails the integration of Eq. (5.131) and therefore turning the integro-differential equation into an ordinary Volterra equation

$$y(t_n + h) = y(t_n) + \int_{t_n}^{t_n+h} dt\, g(t, y(t)) + \int_{t_n}^{t_n+h} dt \int_{t_0}^{t} dt'\, K(t, t', y(t')). \tag{5.134}$$

The time t is discretised with h being the step size between two times t_n and t_{n+1}. The value of y at the next time step is determined iteratively and we denote $y(t_n) = y_n$. Using

the trapezoidal rule twice to evaluate the integrals in Eq. (5.134) leads to

$$\begin{aligned} y_{n+1} = y_n &+ \frac{h}{2} g(t_n, y_n) + \frac{h^2}{4} \left(K\left(t_n, t_0, y_0\right) + K\left(t_n, t_n, y_n\right) + K\left(t_{n+1}, t_0, y_0\right) \right) \\ &+ \frac{h^2}{2} \left(\sum_{i=1}^{n-1} K\left(t_n, t_i, y_i\right) + \sum_{i=1}^{j} K\left(t_{n+1}, t_i, y_i\right) \right) + \frac{h}{2} g\left(t_{n+1}, y_{n+1}\right) \\ &+ \frac{h^2}{4} K\left(x_{n+1}, x_{n+1}, y_{n+1}\right) + O\left(h^3\right). \end{aligned} \tag{5.135}$$

Up to second order in the step size h this can be rewritten as [162, 163]

$$y_{n+1} = M_1 + \frac{h}{2} g(x_{t+1}, M_1) + \frac{h^2}{4} K\left(t_{n+1}, t_{n+1}, M_2\right) \tag{5.136}$$

with

$$\begin{aligned} M_1 = y_n &+ \frac{h}{2} g(t_n, y_n) + \frac{h^2}{4} \left(K\left(t_n, t_0, y_0\right) + K\left(t_n, t_n, y_n\right) + K\left(t_{n+1}, t_0, y_0\right) \right) \\ &+ \frac{h^2}{2} \left(\sum_{i=1}^{n-1} K\left(t_n, t_i, y_i\right) + \sum_{i=1}^{j} K\left(t_{n+1}, t_i, y_i\right) \right), \end{aligned} \tag{5.137}$$

$$M_2 = M_1 + \frac{h}{2} g(t_{n+1}, M_1) + \frac{h^2}{4} K\left(t_{n+1}, t_{n+1}, M_1\right). \tag{5.138}$$

Eq. (5.136) provides an algorithm to iteratively solve the integro-differential Eq. (5.131) with an error of $O(h^3)$. The iterative scheme is very fast compared to other approaches, to the expense that the error is $O(h^3)$. However, this is completely sufficient for our needs. Indeed the approximations underlying the integro-differential equations are more significant than the errors accumulated here. As long as we choose $h < 1/\xi_0^{-1}$ the integration provides accurate results for the short-time dynamics which are most interesting.

5.3.2 ODE algorithm

To be able to perform a numerical cross check we use a second approach to solve Eq. (5.131). This algorithm relies on reducing the integro-differential equation subsequently to an ordinary differential equation [174, 175], therefore we will refer to this algorithm as ODE approach in the following. The procedure's starting point is an initial guess which is calculated from only the first term of Eq. (5.131)

$$\frac{d}{dt} y^{(0)}(t) = g(t, y(t)). \tag{5.139}$$

The solution $y^{(0)}$ is inserted into the right-hand side of Eq. (5.131), resulting in a new ordinary differential equation for a new guess $y^{(1)}$

$$\frac{d}{dt}y^{(1)}(t) = g\left(t, y^{(0)}(t)\right) + \int_{t_0}^{t} dt' K\left(t, t', y^{(0)}(t').\right). \tag{5.140}$$

The solution $y^{(1)}$ provides a better approximation to the general solution y and the step can be iterated using the new solution $y^{(1)}$ instead of $y^{(0)}$ on the right-hand side. The global error

$$\Delta y = \sqrt{\sum_n |y^{(i)}(t_n) - y^{(j)}(t_n)|} \tag{5.141}$$

between the two approximated solutions $y^{(i)}$ and $y^{(j)}$ for all n time steps defines a tolerance to decide if the algorithm is repeated. Although easy to implement the disadvantage of the algorithm is that the kernel K has to take the form

$$K\left(t, t', y(t')\right) = k_1(t, t')k_2(y(t')). \tag{5.142}$$

Depending on the structure of Eq. (5.131) this might not be possible. In fact we are able to use the ODE procedure as a cross check for the single spin system in an equilibrium bath, but the algorithm is not suited to find the full numerical solution for a time-dependent bath reference state.

5.3.3 Benchmarking of the single spin case

To test the algorithm in Eq. (5.136) we study the single spin case in an equilibrium environment in the zero-field limit and compare to the analytical results from Chapter 3. The corresponding equation of motions reads

$$\frac{d}{dt}\rho_I(t) = -\int_0^t dt' \Sigma(t - t')\rho_I(t), \tag{5.143}$$

as derived in Chapter 3. The memory kernel $\Sigma(t - t')$ and the reduced density matrix ρ_I define the kernel function K in Eq. (5.131). In the zero-field limit, the longitudinal and transverse components $\rho_z(t)$ and $\rho_\pm$ coincide, therefore we limit the current discussion to the z component $\rho_z(t) = \rho_\uparrow(t) - \rho_\downarrow(t)$. In the basis of the localised spin operator the

matrix representation of Eq. (5.143) is given by

$$\frac{d}{dt}\begin{pmatrix}\rho_\uparrow(t)\\ \rho_\downarrow(t)\end{pmatrix} = \int_0^t dt' \hat{\hat{\Sigma}}_z(t-t')\begin{pmatrix}\rho_\uparrow(t)\\ \rho_\downarrow(t)\end{pmatrix}, \tag{5.144}$$

with

$$\hat{\hat{\Sigma}}_z(t) = \begin{pmatrix}F_1(t) & -F_2(t)\\ -F_1(t) & F_2(t)\end{pmatrix}. \tag{5.145}$$

The Laplace transformations of the electron spin-spin correlation functions $F_{1,2}$ were derived in Eqs. (3.62) and (3.63) and the analytical expressions are given by Eqs. (3.97) and (3.98). Consequently we obtain for the time domain

$$\begin{aligned} F_1(t) = F_2(t) &= -2\alpha \mathrm{Re}\left[\langle S_-(t)S_+(0)\rangle\right] \\ &= -4\alpha\left(\pi k_B T\right)^2 \frac{1-\cos\left(2\pi k_B T/\xi_0\right)\cosh\left(2\pi k_B T t\right)}{\left(\cos\left(2\pi k_B T/\xi_0\right)-\cosh\left(2\pi k_B T t\right)\right)^2}, \end{aligned} \tag{5.146}$$

by simply not performing the Laplace transformation in Eqs. (3.97) and (3.98) and setting $b_I^z = 0$. In Chapter 3 the parameter $\alpha = A^2/E_F^2$ was the small expansion parameter and is set by the interaction A and the Fermi energy E_F. To obtain the analytical expressions Eqs. (3.97) and (3.98) we furthermore introduced the high energy cutoff ξ_0 which set the band width of the energy band to regulate the density of states. In the following we compare the numerical solution of Eq. (5.144) with the analytical result for the longitudinal component $\rho_z(t)$ in Eq. (3.145). In the top panel of Fig. 5.3 the numerical results for the Patade-Bhalekar algorithm (PB-algorithm, solid purple line) and the ODE procedure (green dotted line) are shown in comparison to the analytical solution (orange dashed line). For the ODE algorithm we choose the global error defined in Eq. (5.141) with $\Delta\rho_\alpha = 10^{-6}$ as a numerical cutoff, and the other parameters are set to $\alpha = 0.005$ and $\xi_0 = 200 k_B T$. For the entire time range the numerically captured decay matches qualitatively the analytic solution. The inset of Fig. 5.3(a) shows the short time decay including the non-Markovian time regime, $t < \tau_T \sim 1/T$. Both numerical solutions show an initially fast decay before it tends to an exponential at larger times matching the behaviour of the analytical result for the decay.

However, the characteristic exponential decay constants, which correspond to the relaxation time T_1, are different. This is a rather surprising result as the analytic result matches the standard long time Markovian behaviour and the Korringa relation. In the following we will investigate this discrepancy in full detail. We will see that is largely influenced by the band structure cutoff ξ_0. Hence, the discrepancy corresponds to a renor-

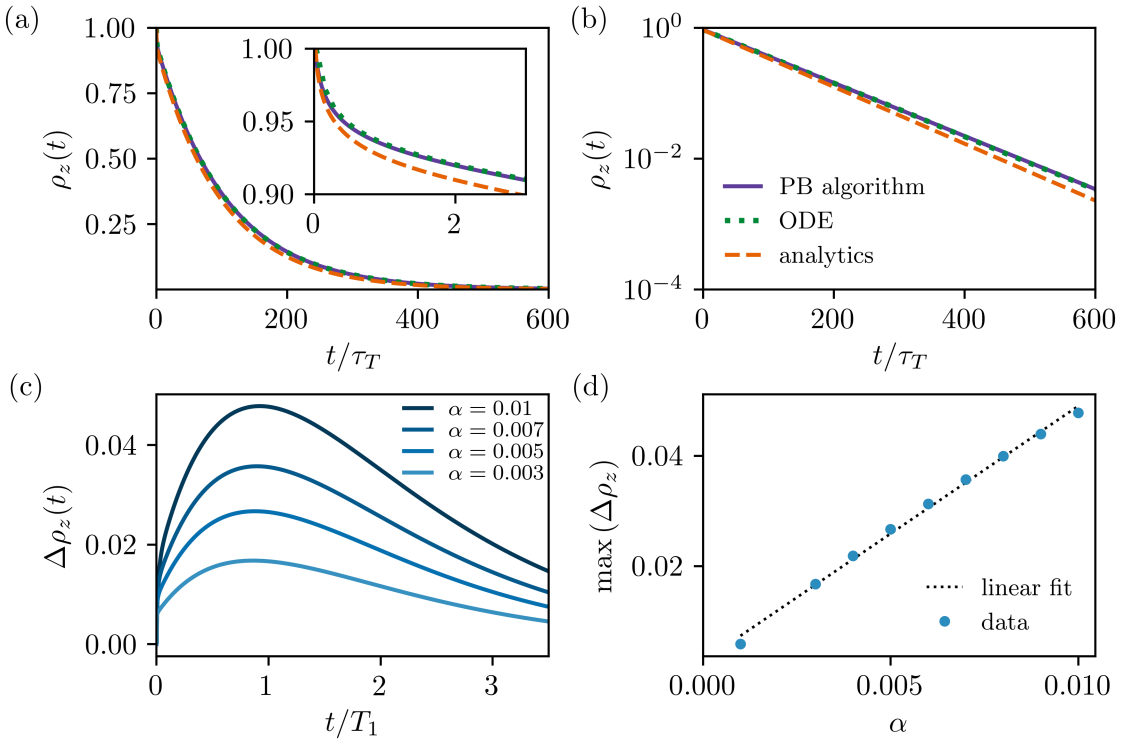

Figure 5.3: Top panel: The full the decay of $\rho_z(t)$ for $\alpha = 0.005$ and $\xi_0 = 200 k_B T$ is shown. The result obtained with the Patade-Bhalekar algorithm is plotted in purple, the solution for the ODE procedure corresponds to the dotted green line and the analytical one is shown in orange. The inset of panel (a) shows the short time behaviour and panel (b) shows the decay on a logarithmic scale to emphasise the offset between the numerical results and analytical solution. Panel (c) shows the difference between numerical and analytical result for different α as a function of time scaled to the corresponding relaxation time $T_1 = \hbar/4\alpha\pi k_B T$. In (d) the maximum values from (c) are plotted against the coupling α. The black dotted line represents the linear fit $g(\alpha) = (4.6 \pm 0.1)\alpha + (0.0027 \pm 0.0007)$.

malisation arising from higher energies which are neglected in the analytic expansion but which are fully captured by the numerical integration. Practically such a renormalisation falls within the uncertainty of the density of state factor ν_0 in the definition of $\alpha = A^2\nu_0^2$ so that the analytical and numerical results are consistent. We provide a recipe to incorporate the renormalisation in a modification of α. The numerics reveal a further correction arising from the expansion in α of the poles in Laplace space, in which we have neglected corrections in $O(\alpha^2)$. These are naturally included in the numerics and the analysis to follow shows again that they can essentially be captured by a renormalisation of α. Thus, we obtain two important results. Firstly, the analytical results of Chapter 3 are indeed

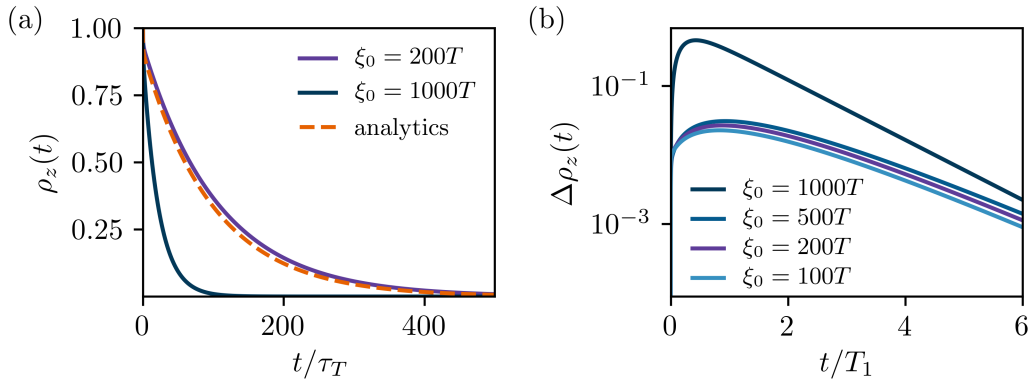

Figure 5.4: (a) The full decay for $\rho_z(t)$ obtained numerically is plotted for different values of the cutoff ξ_0 in units of the temperature T (solid lines) for the coupling $\alpha = 0.005$. The analytic solution (dashed orange line) does not visibly change for various choices of ξ. (b) The difference between the numerical and analytical solution is shown for a selection of ξ_0 values.

confirmed and the corrections do not cause any qualitative differences. Secondly, we find that the numerical integration scheme of the Patade-Bhalekar methods provides fast and qualitatively reliable results. To start the detailed analysis, let us consider the long time behaviour which is shown in Fig. 5.3(b) on a logarithmic scale. Both numerically obtained solutions coincide and the decay is slower compared to the analytical solution. In the bottom panel of Fig. 5.3 we show the dependence on the parameter α. Panel (c) shows the difference between the numerical solution obtained with the Patade-Bhalekar algorithm and the analytical solution. The difference between the numerical and analytical solution is linear in the coupling parameter α as shown in Fig. 5.3(d). The linear fit parameters for the gradient $m = 4.6 \pm 0.1$ and for the intercept $b = 0.0027 \pm 0.0007$.

Keeping the coupling strength α constant, the numerical solution for the decay shows a dependence on the high energy cutoff ξ_0, especially for large values $\xi_0 \sim 1000 k_B T$. In Fig. 5.4 the decay of $\rho_z(t)$ obtained numerically using the Patade-Bhalekar algorithm is shown for different values of the cutoff ξ_0 in comparison to the analytic solution. In panel (a) we only show two choices of ξ_0 as the decay curves for $\xi_0 < 500 k_B T$ are not distinguishable. To show the increasing difference between the numerical and analytical solution, their difference is plotted on a logarithmic scale in Fig. 5.4(b). In the derivation of the analytical solution we expanded the intermediate result in the inverse cutoff and we only kept the terms $O\left(\xi_0^{-1}\right)$. In the numerical solution in principle all orders of ξ_0 are present which could lead to the large cutoff dependence.

To differentiate the effect of the cutoff ξ_0 from the deviation from the analytical results analysed in Fig. 5.3 we study the single spin decay for a tight-binding model in one spatial

dimension. Its energy dispersion depending on the momentum k reads

$$\epsilon_k = -2w\cos(ka) - \mu, \tag{5.147}$$

with the chemical potential μ, the hopping amplitude w and the lattice constant a which we set to $a = 1$. The spin-spin correlators $F_{1,2}^{\mathrm{TB}}$ for the tight-binding model are given by

$$F_1^{\mathrm{TB}}(t) = -4\alpha\frac{(2\pi)^2}{L^2}\sum_{kk',\sigma} e^{i(\epsilon_k-\epsilon_{k'})t} f(\epsilon_k)\left(1 - f(\epsilon_{k'})\right), \tag{5.148}$$

similar to Eq. (3.79) without performing the Laplace transformation and $F_1^{\mathrm{TB}}(t) = F_2^{\mathrm{TB}}(t)$. Here, $f(\epsilon_k) = [1 + \exp(\epsilon_k/k_BT)]^{-1}$ is the Fermi-Dirac distribution and L is the system size which is set to $L = 300$ throughout. Calculating the electron response functions directly from Eq. (5.148) using the energy dispersion in Eq. (5.147) removes the need of the cutoff ξ_0. To ensure that we are observing the same physics the temperature T needs to be low enough such that only excitations close to the Fermi level are possible and we do not pick up contributions from the band edges which are located at $k = 0, \pm\pi/a$. Therefore, we require $T/w \ll 1$ and we set the chemical potential $\mu = 0$. In this limit the band structure of the tight-binding model is linear around the Fermi surface at $k = \pm\pi/2a$ and the physical behaviour is the same as in the description using a cutoff. In Fig. 5.5 the decay of $\rho_z(t)$ is plotted using the tight-binding dispersion for the numerical solution within the Patade-Bhalekar approach. The parameters are set to $\alpha = 0.005$ and $T = 0.05w$ in units of the hopping amplitude. Panel (a) shows the time evolution of $\rho_z(t)$. The analytical results corresponds to the dashed orange line. The decay within the tight-binding model is displayed in light blue and we plot the result for the cutoff dependent model for comparison for $\xi_0 = 200k_BT$. This particular value was chosen because for $\xi_0 < 500k_BT$ the decay is not altered much by the actual choice of ξ_0. The numerical tight-binding decay recovers the slower exponential decay from the ξ_0 model. The short time behaviour shown in Fig. 5.5(b) again captures the fast initial decay on the non-Markovian time scale before becoming exponential and therefore matches the analytic solution qualitatively. The oscillations in the decay are a remnant of the tight-binding with its periodic band structure.

In conclusion we find that the numerical solution of Eq. (5.145) qualitatively agrees with the analytic solution. The algorithm proposed by Patade and Bhalekar [162] is able to capture the decay in non-Markovian regime $t < \tau_T$ where the evolution is non-exponential. For larger times we recover an exponential decay for a Markovian evolution. The exponential decay of the numerical solution, in both the tight-binding and ξ_0 model,

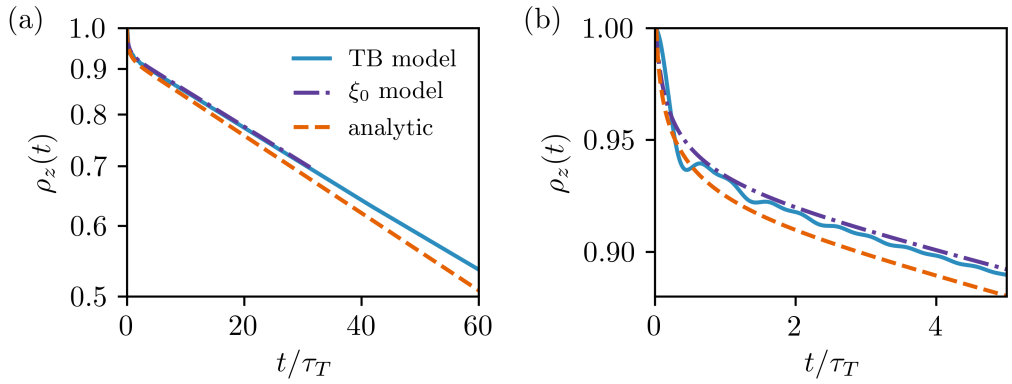

Figure 5.5: (a) Decay of $\rho_z(t)$ on a logarithmic scale, the numerical solution for the tight-binding model is shown in light blue. For comparison the numerical solution for the model including the high energy cutoff ξ_0 is shown (dashed purple line). The analytical solution corresponds to the dashed orange line. Both numerical solutions decay slower than the predicated by the analytical solution. (b) shows the same curves as (a) in the short time regime $t \sim \tau_T$. The non-Markovian regimes corresponds to $t < \tau_T$. The evolution of $\rho_z(t)$ within this interval is non-exponential. After the fast initial decay it becomes exponential. The parameters in the plot are set to $\alpha = 0.005$, $T = 0.05w$ and $\xi_0 = 200 k_B T$.

is slower than predicted analytically. But otherwise it shows the identical Markovian behaviour and can be matched with the analytical solution by a renormalisation of α. In Fig. 5.6 we fit the long time numerical solution to an exponential decay to determine the relaxation time T_1^{fit}. From this we obtain the renormalised coupling

$$\alpha^* = \frac{\hbar}{4\pi k_B T T_1^{\text{fit}}}. \tag{5.149}$$

From the exponential fits to the decay of tight-binding and ξ_0 model in Fig. 5.5 we find

$$\begin{aligned} \alpha^*_{\text{TB}} &= 4.48361 \cdot 10^{-3} \pm 2 \cdot 10^{-8}, \\ \alpha^*_{\xi_0} &= 4.6930 \cdot 10^{-3} \pm 10^{-7}. \end{aligned} \tag{5.150}$$

as compared to $\alpha = 0.005$. In Fig. 5.6 the analytic solution with the renormalised coupling α^* according to Eq. (5.150) is plotted (orange dashed line) alongside the analytical solution (dotted black line) for the same $\alpha = 0.005$ as for the numerically calculated ρ_z (solid lines) for $T = 0.05$ and $\xi_0 = 200 k_B T$. In the top panel the results for the tight-binding model and in the bottom panel the results for the ξ_0 model are depicted. Fig. 5.6(a) and (c) show the long time behaviour on logarithmic scale. The short time decay is plotted in Fig. 5.6(b) and (d). Using the renormalised coupling α^* improves

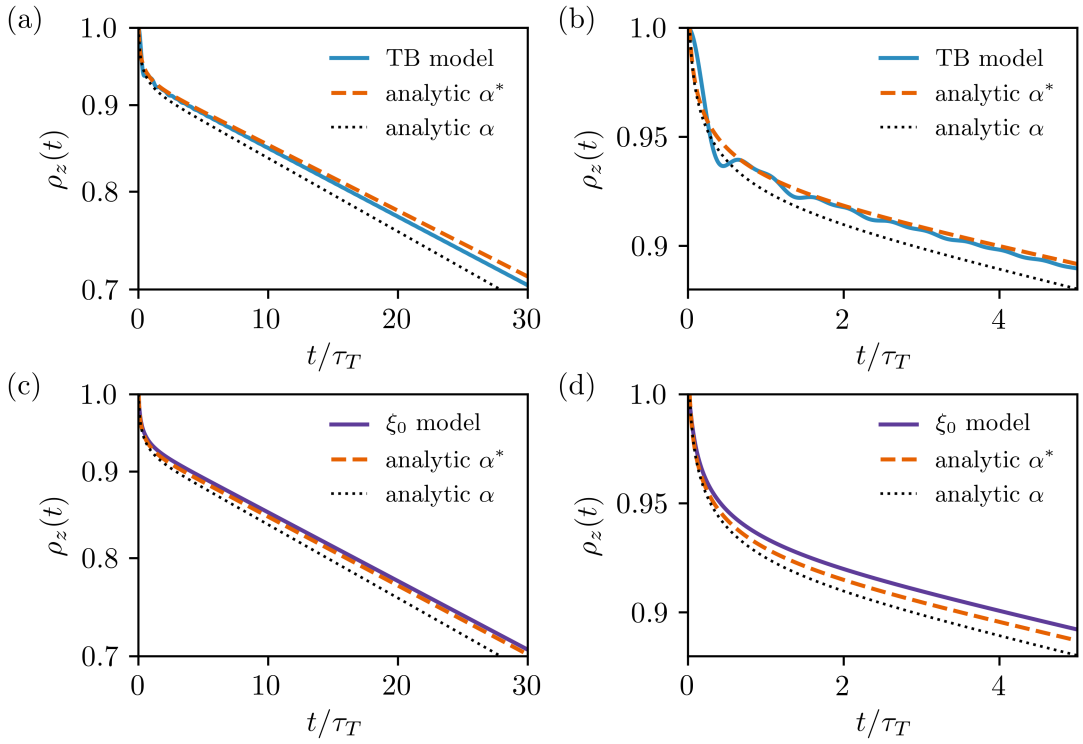

Figure 5.6: Top: The decay of $\rho_z(t)$ is plotted. The solid light blue lines corresponds to the numerically obtained decay for the tight binding model as in Fig. 5.5 with $\alpha = 0.005$ and $T = 0.05w$. The orange line corresponds to the decay with the renormalised coupling $\alpha^*_{\mathrm{TB}} = 4.48361 \cdot 10^{-3}$. For comparison the analytic solution for $\alpha = 0.005$ is shown by the dotted black line. (a) shows the long time decay focusing on the exponential behaviour. The short time decay is depicted in (b). Bottom: Similar to the top panel the solid purple lines shows the decay of ρ_z for the model including the cutoff $\xi_0 = 200 k_B T$ and $\alpha = 0.005$. The dashed lines correspond to the analytical solution. The renormalised coupling is $\alpha^*_{\xi_0} = 4.6930 \cdot 10^{-3}$ and shown in orange. (c) shows the long time evolution and (d) the short time regime. For both cases the analytical solution with the renormalised coupling α^* is in better agreement with the numerical solutions.

the quantitative agreement between the numerical and analytic solution for both studied models across the entire time range. This implies that the full numerical solution indeed renormalises the coupling strength. The choice of the cutoff ξ_0 adds to this effect which is suggested by the findings in Fig. 5.4.

To understand the discrepancy let us recall that in the derivation of the analytic solution we analysed the pole structure in Laplace space to determine the dynamics. To locate the poles we expanded in the small parameter α and kept the terms linear in α while higher orders were neglected. Due to this fact we find a discrepancy between the analytical and

numerical results with a direct α dependence, because higher orders of α are naturally included in the numeric. After a renormalisation of the coupling strength α the numerical results recovers the analytic one. Furthermore, the numerical analysis shows that the Patade-Bhalekar method used to solve the integro-differential equations as in Eq. (5.131) is suitable to obtain access to the qualitative features of the short and long dynamics.

5.4 Summary and outlook

We adapted the time-dependent projection operator approach proposed by Degenfeld-Schonburg and Hartmann [38] to derive an equation of motion for two localised spins with no direct coupling in the same electronic environment. Unlike the standard Nakajima-Zwanzig equation the approach allows for a time-dependent bath reference state which is self-consistently determined. The generalised master equation leads to coupled equations of motion for each individual part of the considered quantum system, here two localised spins and the conduction electrons. In order to capture the dynamics of the electrons we approximated the electrons density matrix such that single particle or hole excitations are allowed. This lead finally to an equation of motion for the expectation values of the electron spin operators. The additional time dependence is captured by two amplitudes $\Lambda^{\alpha}_{\alpha'}, \tilde{\Lambda}^{\alpha}_{\alpha'}$ for each spin configuration. Through the derivation we gained analytical insight in the nature of the temporal and spatial correlations influencing the dynamics of the localised spins. The shared environment mediates an effective RKKY-like interaction between the impurity spins. In addition to the spatial modulations we find temporal ones driven by the coherent backaction between the spins and the conduction electrons which leads to a dynamical quantum coherent extension to the RKKY interaction.

In a final step and to fully solve the problem we need to determine the time-dependent amplitudes numerically. We proposed to find the numerical solution with the Patade-Bhalekar approach. The algorithm was tested in the set up for a single spin in an electronic bath within the standard Nakajima-Zwanzig formulation which we compared to the analytical results from Chapter 3. Currently, to address two spins we need to solve 24 coupled equations of motions. The number of equations scales according to $12N$ for N spins which could be further reduced by taking into account the rapidly decaying spacial correlations. The advantage of the time-dependent projection operator approach is the straightforward procedure to add more degrees of freedom into the quantum system. With no direct coupling between the localised spins, only the electron equation of motion is affected by adding spins to the bath. In the actual calculation this includes an extra term as the localised spin contribution enter through a sum.

With our work we have established the foundation to address the dynamics of an

effectively coupled pair of localised spins. Already we identified the important temporal and spatial correlations which will lead to the coherent backaction and the resulting non-Markovian dynamics in this system. The full description of the, in principal, complicated many-body problem can be reduced to a controlled set of equations which in turn can be used as a tool for further investigations such as the implication for the entanglement dynamics [39, 40, 161] or a direct coupling between localised spins [176].

6 Conclusion and future work

In this work we investigated the effect of a coherent environment backaction on the system's dynamics. This is motivated by experimental advances to probe quantum correlations in a variety of systems across different disciplines, ranging from condensed matter to quantum information and quantum thermodynamics. The quantum systems in focus of our study consist of a single or a pair of localised spins coupled to an electronic environment. Our key findings concern the short time dynamics of localised spin systems beyond a purely Markovian description and how to utilise the non-Markovian spin dynamics to manipulate the surroundings.

To access the dynamical behaviour of a single spin we derived the explicit form of a generalised master equation based on the Nakajima-Zwanzig approach in Chapter 3 which goes beyond the standard description for the decay of magnetic moment. The localised spin is coupled via a contact spin-spin interaction to an itinerant electron gas. Although the Fermi gas is non-interacting, it nevertheless resembles a correlated system because its quantum and thermal fluctuations only depend on a small number of parameters, namely the temperature T and the Fermi energy E_F.

The exact quantum dynamics are accessible analytically via a careful analysis of the spin's equation of motion in Laplace space. In particular, the full time dynamics are encoded in the specific pole structure. Analysing the nature and positions of the poles in Laplace space allowed us to identify and separate the poles responsible for the Markovian and the non-Markovian behaviour. Since the non-Markovian behaviour is non-exponential an infinity of non-Markovian poles has to be considered and their contributions in the time domain have to be summed up. We showed that this summation can be done explicitly if we rely on an expansion in the small parameter α, which produces a result valid within the Born approximation considered for the generalised master equation. We were able to show analytically that on short time scales the non-Markovian dynamics driven by the coherent backaction from the bath is dominant. For longer times, beyond the thermal time $\tau_T \sim 1/T$, the Markovian behaviour takes over and is characterised by the conventional relaxation time T_1 and the decoherence time T_2. The non-Markovian decay at short times is logarithmic. This is a manifestation of the bosonic zero-energy particle-

hole fluctuations of the electron bath at the Fermi level that also underlie the Fermi edge singularity and Kondo physics. Before the decay crosses over into the exponential Markovian decay, this logarithm causes a rapid drop corresponding to an initial slip. If the initial conditions are altered according to the slippage the full evolution can be described as Markovian for times longer than the system's memory time.

The general framework of analysing the pole structure is by no means limited to the considered Fermi gas. To probe strongly correlated systems the itinerant electron gas could be exchanged, for instance, by a quantum critical field theory. Presumably the simplest access to such a theory would be in the form of a Luttinger liquid. In such a system all correlations are already algebraic with a slower decay than a Fermi gas. This naturally modifies the location of the poles in Laplace space, adding structure beyond the pure Matsubara-type spacing of the non-Markovian poles. A detailed analysis of the consequences could then be used as a novel channel to gain information on the correlated nature of this itinerant bath.

In the spirit of utilising memory effects, we proposed a cooling protocol in Chapter 4. The application exploits the fast initial decay of the non-Markovian dynamics to cool the electronic environment. The initial decay is driven by pure quantum effects and is largely temperature independent and therefore the analysis of the cooling protocol pushes into the realm of quantum thermodynamics. The amplitude of the short time dynamics is set by the small parameter $\alpha = A^2/E_F^2$ and as a result the protocol relies on the rapid repetition of the initial dynamics. The underlying idea is to drive an ensemble of localised spins through a pump cycle. With each repetition a small amount of heat is transferred from the conduction electrons into the spin system and consequently cooling the environment. Taking advantage of the initially fast decay sidesteps the natural bottleneck of cooling via demagnetisation. The latter method is slow at low temperatures due to the long relaxation times $T_1 \sim 1/T$. The efficiency of our protocol highly depends on the value of α, which is very small in a typical metal. Although it therefore might not be able to compete with the standard demagnetisation cooling for a bulk metal we provided an estimate for a semiconductor structure which are generally difficult to cool down. Considering GaAs the cooling protocol proved robust. Even for a rather large heat deposit due to the pumping of the localised spin system, cooling by pumping remains possible for a wide parameter regime. Our example shows that the cooling protocol might be especially suited to cool semiconducting structures.

In a realistic setup a single spin is not isolated and can be influenced by other localised spins even with no direct coupling between the impurity spins. In this case the environment does not only act as a dissipation channel but can mediate an effective interaction between the localised spins. Our main goal in Chapter 5 was to understand the effects

of the mediated interaction between two localised spins, coupled to the same electronic environment, on their dynamical behaviour. To study the system's dynamics we derived a generalised master equation using a self-consistent projection operator method. In the derivation we identified the relevant degrees of freedom and arrived at an equation of motion which is in fact given by a set of coupled integro-differential equations. From these equations we were able to deduce the nuances of the dynamical response. As in Chapter 3 the dynamics is partly driven by the temporal particle-hole fluctuations of the electronic environment. In addition we find a spatial contribution due to the presence of the second spin. Combining both the spatial and the temporal correlations leads to RKKY-type interaction between the localised spins, which is mediated by the conduction electrons. Although the full solution of this problem is so far missing, we gained a deep physical understanding about the interplay of the fluctuations in time and space. In order to obtain the full solution we propose an algorithm which implements an inexpensive numerical integration scheme. Testing the algorithm against the known analytical solution from Chapter 3 proved not only its efficiency but additionally confirms our analytical solution of the single spin case.

The generalised master equation, including a time-dependent bath reference state, provides an excellent tool to address larger quantum systems with more than two spins. Within the formalism additional system degrees of freedom enter through an extra term in a sum rather than an increase in the number of equations. In this sense the two spin system is a stepping stone to address the dynamics of larger many-body systems. Connecting back to treating strongly correlated systems one could again choose a Luttinger liquid as an environment to probe the dynamical response in strongly correlated systems. One would then be able to handle one or several many-body systems embedded in a non-trivial environment with important backaction effects.

Appendices

A Time-dependent projection: Proof of identity

In the following we prove the identity

$$\dot{P}Q = 0. \tag{A1}$$

For simplicity the sub- and superscripts for the time-dependent projection operators are suppressed. From the identity

$$P + Q = \mathbb{1} \tag{A2}$$

it follows immediately that

$$\dot{P} = \frac{\partial}{\partial t}(\mathbb{1} - Q) = -\dot{Q}. \tag{A3}$$

Accordingly,

$$\dot{Q}P = -\dot{P}P \quad \text{and} \quad \dot{P}Q = -\dot{Q}Q. \tag{A4}$$

From the identity $PQ = 0$

$$\frac{d}{dt}(PQ) = 0 \iff \dot{P}Q = -\dot{Q}P \tag{A5}$$

Combining Eq. (A4) and Eq. (A5) leads to a contradiction

$$\dot{P}Q = -\dot{Q}Q = -\dot{Q}P \iff Q = P, \tag{A6}$$

and it has to hold that

$$\dot{P}Q = \dot{Q}P = 0. \tag{A7}$$

B Laplace transform of the Nakajima Zwanzig equation

Eq. (3.44) in the main text is of the form

$$\dot{f}(t) = \int_0^t dt'\, K(t-t')f(t). \tag{B1}$$

The Laplace transformation of this equation is given by

$$s\tilde{f}(s) - f(t=0) = \int_0^\infty dt \int_0^t dt'\, e^{-ts} K(t-t')f(t), \tag{B2}$$

with the Laplace variable $s \in \mathbb{C}$ with $\tilde{f}(s)$ the Laplace transformation of $f(t)$. Using the convolution theorem for integral over t' we arrive at

$$\tilde{f}(s) - f(t=0) \;= \tilde{K}(s)\tilde{f}(s) \tag{B3}$$

$$\iff \qquad \tilde{f}(s) = \left(s - \tilde{K}(s)\right)^{-1} f(t=0). \tag{B4}$$

For the reduced density matrix $\rho_I(t)$ and the memory kernel $\Sigma(t-t')$ we therefore have

$$\tilde{\rho}_I(s) = \left(s\mathbb{1} = \widetilde{\Sigma}(s)\right)^{-1} \rho_I(t=0), \tag{B5}$$

which corresponds to Eq. (3.50) The Laplace transform of the memory kernel is given by

$$\begin{aligned}\widetilde{\Sigma}(s) &= \mathrm{Tr}_{\mathrm{el}}\left\{\int_0^\infty e^{-ts} L_{\mathrm{int}} e^{L_0(t-t')} L_{\mathrm{int}} \rho_{\mathrm{el}}\right\} \\ &= \mathrm{Tr}_{\mathrm{el}}\left\{L_{\mathrm{int}}\left(s\mathbb{1} + L_0\right)^{-1} L_{\mathrm{int}}\rho_{\mathrm{el}}\right\}\end{aligned} \tag{B6}$$

which is the expression stated in Eq. (3.51).

C Matrix representation of the superoperators

C.1 Matrix representation L_{INT}

The matrix representation of $\hat{\hat{L}}_{\mathrm{int}}$ of Eq. (3.60) is found by computing the commutator $[H_{\mathrm{int}}, O]$ with the interaction Hamiltonian H_{int}

$$H_{\mathrm{int}} = h_\uparrow I_\uparrow + h_\downarrow I_\downarrow + h_+ I_- + h_- I_+, \tag{C1}$$

and the operator O is the localised spin basis $\{I_\uparrow, I_\downarrow, I_-, I_+\}$

$$O = o_\uparrow I_\uparrow + o_\downarrow I_\downarrow + o_+ I_- + o_- I_+. \tag{C2}$$

Note that bath operators a denoted by the lower case, upper case operators correspond to the system operators. The matrix entries are then labelled by the combinations $o_\alpha I_\beta$ with $\alpha, \beta = \uparrow, \downarrow, -, +$. The system operator I_β determines the column $(I_\uparrow, I_\downarrow, I_-, I_+)$ and the row $(o_\uparrow, o_\downarrow . o_+, o_-)$ is determined by the bath operator o_α. The system spin operators I_β obey the following commutation relations

$$[I_\uparrow, I_-] = [I_z, I_-] = -I_- \tag{C3}$$
$$[I_\downarrow, I_-] = -[I_z, I_-] = I_- \tag{C4}$$
$$[I_\uparrow, I_+] = [I_z, I_+] = I_+ \tag{C5}$$
$$[I_\downarrow, I_+] = -[I_z, I_+] = -I_+. \tag{C6}$$

Further we have the relations

$$\begin{aligned}\left(I_{\uparrow/\downarrow}\right)^2 &= \left[\frac{1}{2}\left(\mathbb{1} \pm I_z\right)\right]^2 = \frac{1}{4}\left(\mathbb{1} \pm 2I_z + (I_z)^2\right) \\ &= \frac{1}{4}\left(2\mathbb{1} \pm 2I_z\right) = \frac{1}{2}\left(I_\uparrow + I_\downarrow \pm I_\uparrow \mp I_\downarrow\right) \\ &= I_{\uparrow/\downarrow},\end{aligned} \tag{C7}$$

and

$$\begin{aligned}I_+ I_- &= \frac{1}{4}\left(I_x + iI_y\right)\left(I_x - iI_y\right) \\ &= \frac{1}{4}\left[(I_x)^2 + (I_y)^2 + iI_y I_x - iI_x I_y\right] \\ &= \frac{1}{4}\left(2\mathbb{1} + 2I_z\right) \\ &= \frac{1}{4}\left[2\left(I_\uparrow + I_\downarrow\right) + 2\left(I_\uparrow - I_\downarrow\right)\right] \\ &= I_\uparrow,\end{aligned} \tag{C8}$$
$$I_- I_+ = I_\downarrow. \tag{C9}$$

With these relations all terms $[H_{\text{int}}, O]$ can be calculated. In the following we evaluate each commutator using the relations above where we treat the different terms of the operator O separately.

1. $[H_{\text{int}}, o_\uparrow I_\uparrow]$:

We start with the first term of H_{int}

$$\begin{aligned}[h_\uparrow I_\uparrow, o_\uparrow I_\uparrow] &= h_\uparrow o_\uparrow I_\uparrow I_\uparrow - o_\uparrow h_\uparrow I_\uparrow I_\uparrow \\ &= [h_\uparrow, o_\uparrow] \left(I_\uparrow\right)^2 \\ &= [h_\uparrow, o_\uparrow] \, I_\uparrow. \end{aligned} \tag{C10}$$

This is already the full $o_\uparrow I_\uparrow$ contribution as all other commutators from the different H_{int} terms vanish. Therefore the first entry in L_{int} corresponding to the $o_\uparrow I_\uparrow$ component is given by $[h_\uparrow, o_\uparrow] = L^-_{h_z} o_\uparrow$ with $h_\uparrow = h_z$. The second term of H_{int}

$$[h_\downarrow I_\downarrow, o_\uparrow I_\uparrow] = 0, \tag{C11}$$

as $[I_\uparrow, I_\downarrow] = 0$ and also $I_\uparrow I_\downarrow = I_\downarrow I_\uparrow = 0$. The third term is given by

$$\begin{aligned}[h_+ I_-, o_\uparrow I_\uparrow] &= h_+ o_\uparrow I_- I_\uparrow - o_\uparrow h_+ I_\uparrow I_- \\ &= h_+ o_\uparrow \left(I_- + I_\uparrow I_-\right) - o_\uparrow h_+ I_\uparrow I_- \\ &= h_+ o_\uparrow I_- \\ &= h^L_+ o_\uparrow I_-, \end{aligned} \tag{C12}$$

because $I_\uparrow I_- = 0$. The last term of H_{int} produces

$$\begin{aligned}[h_- I_+, o_\uparrow I_\uparrow] &= h_- o_\uparrow I_+ I_\uparrow - o_\uparrow h_- I_\uparrow I_+ \\ &= h_- o_\uparrow I_\uparrow I_+ - o_\uparrow h_- \left(I_+ + I_\uparrow I_+\right) \\ &= -o_\uparrow h_- I_+ \\ &= -h^R_- o_\uparrow I_+. \end{aligned} \tag{C13}$$

All these commutators determine the first column of $\hat{\hat{L}}_{\text{int}}$

$$\Longrightarrow \left(L^-_{h_z}, 0, h^L_+, -h^R_-\right) \tag{C14}$$

2. $H[_{\text{int}}, o_\downarrow I_\downarrow]$:
The first term

$$[h_\uparrow I_\uparrow, o_\downarrow I_\downarrow] = 0 \tag{C15}$$

because $[I_\uparrow, I_\downarrow] = 0$ and also $I_\uparrow I_\downarrow = I_\downarrow I_\uparrow = 0$. The second term of H_{int} is given by

$$\begin{aligned}
[h_\downarrow I_\downarrow, o_\downarrow I_\downarrow] &= h_\downarrow o_\downarrow I_\downarrow I_\downarrow - o_\downarrow h_\downarrow I_\downarrow I_\downarrow \\
&= [h_\downarrow, o_\downarrow] (I_\downarrow)^2 \\
&= [h_\downarrow, o_\downarrow] I_\downarrow \\
&= - [h_z, o_\downarrow] I_\downarrow,
\end{aligned} \tag{C16}$$

where we used $h_z = -h_\downarrow$ as stated in the main text and $[h_\uparrow, o_\uparrow] = -L^-_{h_z} o_\downarrow$. The third term is given by

$$\begin{aligned}
[h_+ I_-, o_\downarrow I_\downarrow] &= h_+ o_\downarrow I_- I_\downarrow - o_\downarrow h_+ I_\downarrow I_- \\
&= h_+ o_\downarrow I_\downarrow I_- - o_\downarrow h_+ (I_- + I_\downarrow I_-) \\
&= -o_\downarrow h_+ I_- \\
&= -h^R_+ o_\downarrow I_-.
\end{aligned} \tag{C17}$$

The remaining term is

$$\begin{aligned}
[h_- I_+, o_\downarrow I_\downarrow] &= h_- o_\downarrow I_+ I_\downarrow - o_\downarrow h_- I_\downarrow I_+ \\
&= h_- o_\downarrow (I_+ + I_\downarrow I_+) - o_\downarrow h_- I_\downarrow I_+ \\
&= h_- o_\downarrow I_+ \\
&= h^L_- o_\downarrow I_+,
\end{aligned} \tag{C18}$$

All these commutators determine the second column of $\hat{\hat{L}}_{\text{int}}$

$$\Longrightarrow \left(0, -L^-_{h_z}, -h^R_+, h^L_-\right) \tag{C19}$$

3. $[H_{\text{int}}, o_+ I_-]$:
The first term is given by

$$\begin{aligned}
[h_\uparrow I_\uparrow, o_+ I_-] &= h_\uparrow o_+ I_\uparrow I_- - o_+ h_\uparrow I_- I_\uparrow \\
&= h_\uparrow o_+ I_\uparrow I_- - o_+ h_\uparrow (I_- + I_- I_\uparrow) \\
&= -o_+ h_\uparrow I_- \\
&= -o_+ h_z I_-
\end{aligned} \tag{C20}$$

and the second

$$\begin{aligned}[h_\downarrow I_\downarrow, o_+ I_-] &= h_\downarrow o_+ I_\downarrow I_- - o_+ h_\downarrow I_- I_\downarrow \\ &= h_\downarrow o_+ \left(I_- - I_- I_\downarrow\right) - o_+ h_\downarrow I_- I_\downarrow \\ &= h_\downarrow o_+ I_- \\ &= -h_z o_+ I_-. \end{aligned} \tag{C21}$$

Combining these two terms leads to the anticommuator $-\{h_z, o_+\} = -L^+_{h_z}$. The third term of H_{int}

$$[h_+ I_-, o_+ I_-] = 0, \tag{C22}$$

as we are dealing with a two level system and $I_- I_- = 0$. The last term results in

$$\begin{aligned}[h_- I_+, o_+ I_-] &= h_- o_+ I_+ I_- - o_+ h_- I_- I_+ \\ &= h_- o_+ I_\uparrow - o_+ h_- I_\downarrow \\ &= h^L_- o_+ I_\uparrow - h^R_- o_+ I_\downarrow \end{aligned} \tag{C23}$$

All these commutators determine the third column of $\hat{\hat{L}}_{\text{int}}$

$$\Longrightarrow \left(h^L_-, -h^R_-, -L^+_{h_z}, 0\right). \tag{C24}$$

4. $[H_{\text{int}}, o_- I_+]$:
The first term is given by

$$\begin{aligned}[h_\uparrow I_\uparrow, o_- I_+] &= h_\uparrow o_- I_\uparrow I_+ - o_- h_\uparrow I_+ I_\uparrow \\ &= h_\uparrow o_- \left(I_+ - I_\uparrow I_+\right) - o_- h_\uparrow I_+ I_\uparrow \\ &= h_\uparrow o_+ I_+ \\ &= h_z o_+ I_+ \end{aligned} \tag{C25}$$

and the second

$$\begin{aligned}[h_\downarrow I_\downarrow, o_- I_+] &= h_\downarrow o_- I_\downarrow I_+ - o_- h_\downarrow I_+ I_\downarrow \\ &= h_\downarrow o_- I_\downarrow I_+ - o_+ h_\downarrow \left(I_+ - I_\downarrow I_+\right) \\ &= -o_- h_\downarrow I \\ &= o_- h_z I_+. \end{aligned} \tag{C26}$$

Combining these two terms leads again to the anticommuator $\{h_z, o_-\} = L^+_{h_z}$. The third term leads to the contribution

$$\begin{aligned}[h_+ I_-, o_- I_+] &= h_+ o_- I_- I_+ - o_- h_+ I_+ I_- \\ &= h_+ o_- I_\downarrow - o_- h_+ I_\uparrow \\ &= h^L_+ o_- I_\downarrow - h^R_+ o_- I_\uparrow. \end{aligned} \tag{C27}$$

And the last term is zero as $I_+ I_+ = 0$. Collecting all term for this component leads to fourth column of $\hat{\hat{L}}_{\text{int}}$

$$\implies \left(-h^R_+, h^L_+, 0, L^+_{h_z}\right). \tag{C28}$$

Combing all components Eqs. (C14), (C19), (C24) and (C28) we arrive at the matrix representation for the interaction Hamiltonian L_{int}

$$\hat{\hat{L}}_{\text{int}} = \begin{pmatrix} L^-_{h_z} & 0 & h^L_- & -h^R_+ \\ 0 & -L^-_{h_z} & -h^R_- & h^L_+ \\ h^L_+ & -h^R_+ & -L^+_{h_z} & 0 \\ -h^R_- & h^L_- & 0 & L^+_{h_z} \end{pmatrix}, \tag{C29}$$

which corresponds to Eq. (3.60) in the main text.

C.2 Matrix representation $\widetilde{\Sigma}(s)$

To express the memory kernel of Eq. (3.51) in the basis of the localised spin operators $\{I_\uparrow, I_\downarrow, I_-, I_+\}$ we first define [64]

$$\left(s\mathbb{1} + \hat{\hat{L}}_0\right)^{-1} = \tilde{g}^0_{\text{el}}(s)\mathbb{1}, \tag{C30}$$

where the matrix representation of $\hat{\hat{L}}_0$ is given by Eq. (3.58). Together with the matrix representation of the interaction Liouvillian $\hat{\hat{L}}_{\text{int}}$ Eq. (3.60) a straight forward matrix multiplication leads to the matrix representation of the memory kernel in Laplace space Eq. (3.51)

$$\hat{\hat{\Sigma}}(s) = \begin{pmatrix} M & 0 \\ 0 & M' \end{pmatrix} \tag{C31}$$

with

$$M = \begin{pmatrix} \left\langle L^-_{h_z} \tilde{g}^0_{\mathrm{el}} L^-_{h_z} + h^L_- \tilde{g}^0_{\mathrm{el}} h^L_+ + h^R_+ \tilde{g}^0_{\mathrm{el}} h^R_- \right\rangle & \left\langle -h^L_- \tilde{g}^0_{\mathrm{el}} h^R_+ - h^R_+ \tilde{g}^0_{\mathrm{el}} h^L_- \right\rangle \\ \left\langle -h^R_- \tilde{g}^0_{\mathrm{el}} h^L_+ - h^L_+ \tilde{g}^0_{\mathrm{el}} h^R_- \right\rangle & \left\langle L^-_{h_z} \tilde{g}^0_{\mathrm{el}} L^-_{h_z} + h^R_- \tilde{g}^0_{\mathrm{el}} h^R_+ + h^L_+ \tilde{g}^0_{\mathrm{el}} h^L_- \right\rangle \end{pmatrix} \tag{C32}$$

$$M' = \begin{pmatrix} \left\langle h^L_+ \tilde{g}^0_{\mathrm{el}} h^L_- + h^R_+ \tilde{g}^0_{\mathrm{el}} h^R_- + L^+_{h_z} \tilde{g}^0_{\mathrm{el}} L^+_{h_z} \right\rangle & 0 \\ 0 & \left\langle h^R_- \tilde{g}^0_{\mathrm{el}} h^R_+ + h^L_- \tilde{g}^0_{\mathrm{el}} h^L_+ + L^+_{h_z} \tilde{g}^0_{\mathrm{el}} L^+_{h_z} \right\rangle \end{pmatrix} \tag{C33}$$

where $\langle \cdot \rangle = \mathrm{Tr}_{\mathrm{el}} \{ \cdot \rho^{\mathrm{eq}}_{\mathrm{el}} \}$. We present the steps for the first element in detail. It is given by

$$\hat{\tilde{\Sigma}}(s)_{11} = \mathrm{Tr}_{\mathrm{el}} \left\{ h^L_- \tilde{g}^0_{\mathrm{el}} h^L_+ \rho^{\mathrm{eq}}_{\mathrm{el}} + h^R_+ \tilde{g}^0_{\mathrm{el}} h^R_- \rho^{\mathrm{eq}}_{\mathrm{el}} + L^-_{h_z} \tilde{g}^0_{\mathrm{el}} L^-_{h_z} \rho^{\mathrm{eq}}_{\mathrm{el}} \right\}. \tag{C34}$$

For the frist term we obtain

$$\begin{aligned} \mathrm{Tr}_{\mathrm{el}} \left\{ h^L_- \tilde{g}^0_{\mathrm{el}} h^L_+ \rho^{\mathrm{eq}}_{\mathrm{el}} \right\} &= \mathrm{Tr}_{\mathrm{el}} \left\{ h^L_- [s + L_0]^{-1} h^L_+ \rho^{\mathrm{eq}}_{\mathrm{el}} \right\} \\ &= \mathrm{Tr}_{\mathrm{el}} \left\{ \int dt\, e^{-ts} \left(h^L_- e^{-iH_0 t} h^L_+ \rho^{\mathrm{eq}}_{\mathrm{el}} e^{iH_0 t} \right) \right\} \\ &= A^2 \mathrm{Tr}_{\mathrm{el}} \left\{ \int dt\, e^{-ts} \left(S_- e^{-iH_0 t} S_+ e^{iH_0 t} \rho^{\mathrm{eq}}_{\mathrm{el}} \right) \right\} \\ &= A^2 \int dt\, e^{-ts} \left\langle S_-(t) S_+ \right\rangle. \end{aligned} \tag{C35}$$

In the first step we explicitly write the Laplace transform as the time integral and use

$$e^{L_0 t}(\cdot) = e^{-iH_0 t}(\cdot) e^{iH_0 t}. \tag{C36}$$

With $[H_0, \rho^{\mathrm{eq}}_{\mathrm{el}}] = 0$ and writing the time evolution of the electron spin operator as explicit time dependence we arrive at the last line. Similarly the second term is given by

$$\begin{aligned} \mathrm{Tr}_{\mathrm{el}} \left\{ h^R_+ \tilde{g}^0_{\mathrm{el}} h^R_- \rho^{\mathrm{eq}}_{\mathrm{el}} \right\} &= \mathrm{Tr}_{\mathrm{el}} \left\{ h^R_+ [s + iL_0]^{-1} h^R_- \rho^{\mathrm{eq}}_{\mathrm{el}} \right\} \\ &= \mathrm{Tr}_{\mathrm{el}} \left\{ \int dt\, e^{-ts} \left(h^R_+ e^{-iH_0 t} \left(h^R_- \rho^{\mathrm{eq}}_{\mathrm{el}} \right) e^{iH_0 t} \right) \right\} \\ &= A^2 \mathrm{Tr}_{\mathrm{el}} \left\{ \int dt\, e^{-ts} \left(e^{-H_0 t} \rho^{\mathrm{eq}}_{\mathrm{el}} S_- e^{iH_0 t} S_+ \right) \right\} \\ &= A^2 \int dt\, e^{-ts} \left\langle S_- S_+(t) \right\rangle. \end{aligned} \tag{C37}$$

The last term of Eq. (C34) evaluates to

$$\mathrm{Tr}_{\mathrm{el}} \left\{ L^-_{h_z} \tilde{g}^0_{\mathrm{el}} L^-_{h_z} \rho^{\mathrm{eq}}_{\mathrm{el}} \right\} = \mathrm{Tr}_{\mathrm{el}} \left\{ \int d\, t e^{-ts} \left(L^-_{h_z} e^{L_0 t} L^-_{h_z} \rho^{\mathrm{eq}}_{\mathrm{el}} \right) \right\}$$

$$
\begin{aligned}
=&\mathrm{Tr}_{\mathrm{el}}\left\{\int d\,t e^{-ts}\left(\left[h_z, e^{-iH_0 t}\left[h_z,\rho_{\mathrm{el}}^{\mathrm{eq}}\right]e^{iH_0 t}\right]\right)\right\}\\
=&\mathrm{Tr}_{\mathrm{el}}\left\{\int dt\, e^{-ts}\left(\left[h_z,\left[h_z(-t),\rho_{\mathrm{el}}^{\mathrm{eq}}\right]\right]\right)\right\}\\
=&A^2\int dt\, e^{-ts}\Big(\mathrm{Tr}_{\mathrm{el}}\left\{S_z S_z(-t)\rho_{\mathrm{el}}^{\mathrm{eq}}\right\}-\mathrm{Tr}_{\mathrm{el}}\left\{S_z(-t)S_z\rho_{\mathrm{el}}^{\mathrm{eq}}\right\}\\
&-\mathrm{Tr}_{\mathrm{el}}\left\{S_z S_z(-t)\rho_{\mathrm{el}}^{\mathrm{eq}}\right\}+\mathrm{Tr}_{\mathrm{el}}\left\{S_z(-t)S_z\rho_{\mathrm{el}}^{\mathrm{eq}}\right\}\Big)\\
=&0.
\end{aligned}
\tag{C38}
$$

Eq. (C35) and is the complex conjugate of Eq. (C37) and combining both expressions we obtain

$$
\widetilde{\Sigma}_{11}(s)=F_1(s)=2A^2\int dt\, e^{-ts}\mathrm{Re}\left[e^{ib_z^I t}\left\langle S_-(t)S_+(0)\right\rangle\right] \tag{C39}
$$

which corresponds to the spin-spin correlation function of Eq. (3.62) when we include the phase factor due the rotating frame of reference. All other spin-spin correlators Eqs. (3.63) to (3.66) are obtained following the same pattern by first explicitly writing the Laplace transformation, making use of Eq. (C36) and finally utilising $[H_0,\rho_{\mathrm{el}}^{\mathrm{eq}}]=0$.

D Complex contour integration of response function

D.1 Laplace transformation – Energy integral

Starting from Eq. (3.85), we show the steps leading to Eq. (3.86) in detail. We require an expression for the energy integral in Eq. (3.85)

$$
\int_{-\infty}^{\infty} d\epsilon\ \frac{1}{1+e^{\beta\epsilon}}\ e^{i\epsilon(t-i\xi_0^{-1})} \tag{D1}
$$

with β the inverse temperature. Note that we need to integrate over all occupied states $\epsilon\in[-\infty,E_F]$ and we choose $E_F=0$. Then $-|\epsilon|\xi_0^{-1}\to\epsilon\xi_0^{-1}$. To capture all occupied states for finite temperatures we can integrate $\epsilon\in[-\infty,\infty]$ as the integral is well behaved for the upper limit due to the fast decaying Fermi function. The high energy cutoff ξ_0 ensures the convergence of the integral for the lower limit. We can solve the integral in using the residue theorem

$$
\oint_C dz g(z)=2\pi i\sum_{z_n}\mathrm{Res}_{z_n}g(z_n), \tag{D2}
$$

with z_n the poles of the function g(z). In our case the poles are given by the zeros of the Fermi function which sit are given by the Matsubara frequencies $z_n = i\omega_n = i(2n+1)\pi/\beta$. Closing the contour in the upper half plan leads to

$$\int_{-\infty}^{\infty} d\epsilon e^{i\epsilon(t-i\xi_0^{-1})} f(\epsilon) = 2\pi i \sum_n \mathrm{Res}_{z_n} e^{iz_n(t-i\xi_0^{-1})}. \tag{D3}$$

The residue for each poles z_n is given by

$$\mathrm{Res}_{z\to z_n} \frac{1}{1+\mathrm{e}^{\beta z}} = \lim_{z\to i\omega_n} \frac{z-i\omega_n}{1+e^{\beta z}} = \lim_{\delta\to 0} \frac{\delta}{1+\mathrm{e}^{i\omega_n\beta}\mathrm{e}^{\beta\delta}} = -\frac{1}{\beta} \tag{D4}$$

If we close the complex contour of Eq. (D2) in a half circle in the upper half of the complex plane we find

$$\begin{aligned}\int_{-\infty}^{\infty} d\epsilon e^{i\epsilon(t-i\xi_0^{-1})} f(\epsilon) &= -i\frac{2\pi}{\beta} \sum_n e^{-\frac{\pi}{\beta}(2n+1)(t-i\xi_0^{-1})} \\ &= -\frac{2\pi i}{\beta} e^{-\frac{\pi}{\beta}(t-i\xi_0^{-1})} \sum_{n=0}^{\infty} \left[e^{-\frac{2\pi}{\beta}(t-i\xi_0^{-1})}\right]^n. \end{aligned} \tag{D5}$$

In the last step we find a geometric series and a closed expression for the converging integral

$$\int_{-\infty}^{\infty} d\epsilon e^{i\epsilon(t-i\xi_0^{-1})} f(\epsilon) = -\frac{2\pi i}{\beta}\ e^{-\frac{\pi}{\beta}(t-i\xi_0^{-1})} \frac{1}{1-e^{-\frac{2\pi}{\beta}(t-i\xi_0^{-1})}}. \tag{D6}$$

Factoring out the exponential $\exp\left[-(t-i\xi_0^{-1})\pi/\beta\right]$ in the denominator which cancels the corresponding factor in the nominator we can rewrite Eq. (D6) as

$$\int_{-\infty}^{\infty} d\epsilon e^{i\epsilon(t-i\xi_0^{-1})} f(\epsilon) = \frac{\pi}{\beta} \frac{1}{i\sinh\left(\frac{\pi}{\beta}\left(t-i\xi_0^{-1}\right)\right)}. \tag{D7}$$

Using the identity $i\sinh(-ix) = \sin(x)$ we arrive at

$$\int_{-\infty}^{\infty} d\epsilon e^{i\epsilon(t-i\xi_0^{-1})} f(\epsilon) = -\frac{\pi}{\beta} \frac{1}{\sin\left(\frac{\pi}{\beta}\left(it+\xi_0^{-1}\right)\right)} \tag{D8}$$

The square of the expression Eq. (D8) corresponds to the integrand of the Laplace transform in Eq. (3.86).

D.2 Laplace transformation – Time integral

Starting with the expression in Eq. (3.86) we want to evaluate

$$F(s) = -\int_0^\infty dt\, e^{-ts} \frac{(\pi k_B T)^2}{\sin^2\left(\pi k_B T\left(it + \xi_0^{-1}\right)\right)}. \tag{D9}$$

We first make the substitution

$$x = \pi k_B T(it + \xi_0^{-1}) \tag{D10}$$

$$\implies x(0) = \pi k_B T \xi_0^{-1} \quad \text{and} \quad x(t \to \infty) \to i\infty, \tag{D11}$$

which leads to

$$F(s) = -\left(-i\pi k_B T\right) e^{-is\xi_0^{-1}} \int_{\pi k_B T \xi_0^{-1}}^{i\infty} \frac{e^{i\frac{sx}{\pi k_B T}}}{\sin^2 x}. \tag{D12}$$

With a second substitution

$$z = -ix \tag{D13}$$

$$\implies z(\pi k_B T \xi_0^{-1}) = -i\pi k_B T \xi_0^{-1} \quad \text{and} \quad z(x \to i\infty) \to \infty, \tag{D14}$$

we obtain

$$F(s) = i\pi k_B T\, e^{-is\xi_0^{-1}} \int_{-i\pi k_B t \xi_0^{-1}}^{\infty} dz\, \frac{e^{-z\frac{s}{\pi k_B T}}}{\sinh^2(z)}, \tag{D15}$$

where we also made use of $\sin(iz) = i\sinh(z)$. Expressing sinh in terms of exponentials leads to

$$F(s) = i\pi k_B T\, \mathrm{e}^{-is\xi_0^{-1}} \int_{-i\pi k_B t \xi_0^{-1}}^{\infty} dz\, \frac{4\mathrm{e}^{-z\frac{s}{\pi k_B T}}}{\left(\mathrm{e}^z\left(1 - \mathrm{e}^{-2z}\right)\right)^2}. \tag{D16}$$

A third substitution

$$y = \exp\left[-2z\right] \tag{D17}$$

$$\implies y(-i\pi k_B T \xi_0^{-1}) = \exp\left[i2\pi k_B T \xi_0^{-1}\right] \quad \text{and} \quad y(z \to \infty) = 0 \tag{D18}$$

then leads to

$$F(s) = (2\pi k_B T)\,\mathrm{e}^{-is\xi_0^{-1}} \int_0^{\exp\left[i2\pi k_B T\xi_0^{-1}\right]} dy \frac{y^{\frac{s}{2\pi k_B T}}}{(1-y)^2} \tag{D19}$$

and after a partial integration

$$\int_0^u dy\, \frac{y^m}{(1-y)^2} = \left[y^m \frac{1}{1-y}\right]_0^u - \int_0^u dy\, \frac{m y^{m-1}}{1-y}, \tag{D20}$$

we arrive at

$$\begin{aligned} &F(s) \\ &= 2\pi k_B T \mathrm{e}^{-is\xi_0^{-1}} \left\{ \left[-y^{\frac{s}{2\pi k_B T}} \frac{1}{1-y} \right]_0^{\exp\left[i2\pi k_B T\xi_0^{-1}\right]} + \int_0^{\exp\left[i2\pi k_B T\xi_0^{-1}\right]} dy\, \frac{s}{2\pi k_B T} \frac{y^{\frac{s}{2\pi k_B T}}}{1-y} \right\}. \end{aligned} \tag{D21}$$

The remaining integral is listed in [177] [Sec. 3.194.5]

$$\int_0^x dx\, \frac{x^{\mu-1}}{1+\beta x} = \frac{u^\mu}{\mu} {}_2F_1(1, \mu; \mu+1; -\beta u), \tag{D22}$$

where ${}_2F_1$ is the hypergeometric function. Using Eq. (D22) for Eq. (D21) with $\mu = s/2\pi k_B T, \beta = -1$ we obtain

$$\begin{aligned} &F(s) \\ &= 2\pi k_B T \mathrm{e}^{-is\xi_0^{-1}} \left\{ -\frac{\mathrm{e}^{is\xi_0^{-1}}}{1-\mathrm{e}^{i2\pi k_B T\xi_0^{-1}}} + \mathrm{e}^{is\xi_0^{-1}} {}_2F_1\left(1, \frac{s}{2\pi k_B T}; 1+\frac{s}{2\pi k_B T}; \mathrm{e}^{i2\pi k_B T\xi_0^{-1}}\right) \right\}. \end{aligned} \tag{D23}$$

The hypergeometric function can be expression as the series [131]

$$\begin{aligned} &{}_2F_1(a, b; a+b; z) \\ &= \frac{\Gamma(a+b)}{\Gamma(a)\Gamma(b)} \sum_{n=0}^{\infty} \frac{(a)_n (b)_n}{(n!)^2} \left[2\psi(n+1) - \psi(a+n) - \psi(b+n) - \ln(1-z)\right] (1-z)^n, \end{aligned} \tag{D24}$$

where Γ is Euler's Gammafunction, ψ is the digamma function and $(a)_n$) are the Pochhammer symbols for integer n. Using the series to express ${}_2F_1$ in Eq. (D23) leads to

$$F(s) = 2\pi k_B T \Bigg\{ -\frac{1}{1-\mathrm{e}^{i2\pi k_B T \xi_0^{-1}}} + \frac{\Gamma\left(1+\frac{s}{2\pi k_B T}\right)}{\Gamma(1)\Gamma\left(\frac{s}{2\pi k_B T}\right)} \cdot \\ \cdot \sum_{n=0}^{\infty} \frac{(1)_n \left(\frac{s}{2\pi k_B T}\right)_n}{(n!)^2} \left[\psi(n+1) - \psi\left(\frac{s}{2\pi k_B T}+n\right) - \ln\left(1-\mathrm{e}^{i2\pi k_B T \xi_0^{-1}}\right)\right] \\ \left(1-\mathrm{e}^{i2\pi k_B T \xi_0^{-1}}\right)^n \Bigg\}.$$

At this point we expand in the inverse cutoff ξ_0^{-1} and we replace

$$\frac{1}{\mathrm{e}^{i2\pi k_B T \xi_0^{-1}}} \approx \frac{1}{i2\pi k_B T \xi_0^{-1}} - \frac{1}{2}. \tag{D25}$$

Keeping only the terms up to $O(\xi_0^{-1})$ we finally arrive at

$$F(s) = i\xi_0 - \pi k_B T + s\left[\ln\left(\frac{2\pi k_B T}{i\xi'}\right) + \psi\left(\frac{s}{2\pi k_B T}+1\right)\right], \tag{D26}$$

where we made use of the identity $\Gamma(b+1)/\Gamma(b) = b$ and

$$\psi(z+1) = \frac{1}{z} + \psi(z) \tag{D27}$$

$$\implies \psi\left(\frac{s}{2\pi k_B T}\right) = \psi\left(\frac{s}{2\pi k_B T}+1\right) - \frac{2\pi k_B T}{s}. \tag{D28}$$

This last expression corresponds to Eq. (3.87) in the main text.

E Poles and residues

E.1 Markovian poles and residues

Apart from the simple pole at $s = 0$ for the we find further poles by solving

$$s - F_1(s) - F_2(s) = 0, \tag{E1}$$

and

$$s - F_+(s) - F_z(s) = 0, \tag{E2}$$

as stated in the main text, see Eqs. (3.104) and (3.105). Starting with Eq. (E1) we insert the definitions for the correlation functions Eqs. (3.97) and (3.98) which leads to

$$\begin{aligned} & s\left\{1-2\alpha\left[2\ln\left(\frac{2\pi k_BT}{\xi'}\right)+\psi\left(1+\frac{s+ib}{2\pi k_BT}\right)+\psi\left(1+\frac{s-ib}{2\pi k_BT}\right)\right]\right\} \\ & = -4\pi k_BT+\alpha 2ib\left[\psi\left(1+\frac{s+ib}{2\pi k_BT}\right)-\psi\left(1+\frac{s-ib}{2\pi k_BT}\right)\right], \qquad \text{(E3)} \\ \implies \tilde{s} &= \frac{-4\pi k_BT+\alpha 2ib\left[\psi\left(1+\frac{s+ib}{2\pi k_BT}\right)-\psi\left(1+\frac{s-ib}{2\pi k_BT}\right)\right]}{1-4\alpha\left\{\ln\left(\frac{2\pi k_BT}{\xi'}\right)+\mathrm{Re}\left[\psi\left(1+\frac{s+ib}{2\pi k_BT}\right)\right]\right\}}, \qquad \text{(E4)} \end{aligned}$$

with $b = b_z^I$. The last line is the full solution for Eq. (E1), including higher order in α. Within the Born-approximation we can neglect those. The Markovian pole $s_0^{\mathrm{M}} \approx 0$. To this end we evaluate Eq. (E4) in the limit $s \to 0$ and keep only terms of $O(\alpha)$. This leads to

$$s_{0,z}^{\mathrm{M}} = -4\alpha\pi k_BT + 2\alpha ib\left[\psi\left(1+\frac{ib}{2\pi k_BT}\right)-\psi\left(1-\frac{ib}{2\pi k_BT}\right)\right]. \qquad \text{(E5)}$$

Using the identity $2\mathrm{Im}\psi(1+ix) = -1/x + \pi/\tanh(\pi x)$ [131], Sec. 5.4.18, we can replace

$$ib\left[\psi\left(1+\frac{ib}{2\pi k_BT}\right)-\psi\left(1-\frac{ib}{2\pi k_BT}\right)\right] = -2\pi k_BT + \frac{b}{\tanh\left(\frac{b}{2\pi k_BT}\right)}, \qquad \text{(E6)}$$

which leads to

$$s_{0,z}^{\mathrm{M}} = -2\alpha\frac{b_z^I}{\tanh\left(\frac{b_z^I}{2\pi k_BT}\right)}, \qquad \text{(E7)}$$

for the longitudinal component $\rho_z(t)$ as stated in Eq. (3.106).

To solve Eq. (E2) we insert Eqs. (3.99) to (3.101) which leads to

$$\begin{aligned} & s\left\{1-4\alpha\ln\left(\frac{2\pi k_BT}{\xi'}\right)-2\alpha\psi\left(1+\frac{s}{2\pi k_bT}\right)-2\alpha\psi\left(1+\frac{s\mp ib}{2\pi k_BT}\right)\right\} \\ & = -4\alpha\pi k_BT \mp 2\alpha ib\ln\left(\frac{2\pi k_BT}{\xi'}\right)\mp 2\alpha ib\psi\left(1+\frac{s\mp i}{2\pi k_BT}\right) \qquad \text{(E8)} \\ \implies \tilde{s} &= \frac{-4\alpha\pi k_BT \mp 2\alpha ib\left[\ln\left(\frac{2\pi k_BT}{\xi}\right)+\psi\left(1+\frac{s\mp ib}{2\pi k_BT}\right)\right]}{1-4\alpha\ln\left(\frac{2\pi k_BT}{\xi'}\right)-2\alpha\psi\left(1+\frac{s}{2\pi k_BT}\right)-2\alpha\psi\left(1+\frac{s\mp ib}{2\pi k_BT}\right)}. \qquad \text{(E9)} \end{aligned}$$

Keeping only $O(\alpha)$ term the Markovian pole for the transverse components is then given

by

$$s_{\pm}^{\mathrm{M}} = -4\alpha\pi k_B T \mp i2\alpha b_z^I \left[2\ln\left(\frac{2\pi k_B T}{\xi'}\right) + \psi\left(1 \mp \frac{ib_z^I}{2\pi k_B T}\right)\right], \tag{E10}$$

as in Eq. (3.107).

The residue to the pole s_z^{M} is given by

$$\begin{aligned}
\mathrm{Res}_{s\to s_z^{\mathrm{M}}} &= \lim_{s\to s_z^{\mathrm{M}}} \left(s - s_z^{\mathrm{M}}\right) \frac{e^{ts}\rho_z(t=0)}{s - F_1(s) - F_2(s)} \\
&= \lim_{s\to s_{0,z}^{\mathrm{M}}} e^{ts}\rho_z(t=0)\left(s - s_z^{\mathrm{M}}\right) \\
&\times \left[s - s_{0,z}^{\mathrm{M}} - s4\alpha\left\{\ln\left(\frac{2\pi k_B T}{\xi'}\right) + \mathrm{Re}\left[\psi\left(1 + \frac{s+ib}{2\pi k_B T}\right)\right]\right\}\right]^{-1} \\
&= \lim_{s\to s_z^{\mathrm{M}}} e^{ts}\rho_z(t=0)\left(s - s_z^{\mathrm{M}}\right)\left[1 - 4\alpha\left\{\ln\left(\frac{2\pi k_B T}{\xi'}\right) + \mathrm{Re}\left[\psi\left(1 + \frac{s+ib}{2\pi k_B T}\right)\right]\right\}\right]^{-1} \\
&\times \left[s - \frac{s_z^{\mathrm{M}}}{1 - 4\alpha\left\{\ln\left(\frac{2\pi k_B T}{\xi'}\right) + \mathrm{Re}\left[\psi\left(1 + \frac{s+ib}{2\pi k_B T}\right)\right]\right\}}\right]^{-1}.
\end{aligned} \tag{E11}$$

In the last line, the factor $\left(s - s_z^{\mathrm{M}}\right)$ cancels with $s - s_z^{\mathrm{M}}/[\dots]$ because

$$\frac{s_z^{\mathrm{M}}}{1 - 4\alpha\left\{\ln\left(\frac{2\pi k_B T}{\xi'}\right) + \mathrm{Re}\left[\psi\left(1 + \frac{s+ib}{2\pi k_B T}\right)\right]\right\}} = s_z^{\mathrm{M}} + O(\alpha). \tag{E12}$$

and we obtain for the residue

$$\mathrm{Res}\left(s_z^{\mathrm{M}}\right) = \frac{e^{s_z^{\mathrm{M}} t}\rho_z(t=0)}{1 - 4\alpha\left\{\ln\left(\frac{2\pi k_B T}{\xi'}\right) + \mathrm{Re}\left[\psi\left(1 + \frac{s+ib}{2\pi k_B T}\right)\right]\right\}}, \tag{E13}$$

which corresponds to Eq. (3.108). Similarly, the residue for the transverse pole can be determined. Following the exact same steps as in Eqs. (E11) and (E12) leads to Eq. (3.109). In fact, the residues can be read off the denominator in Eq. (E9) at $s = 0$.

E.2 Non-Markovian residues

The residues for the non-Markovian poles are dominated by derivative of the digamma function $\psi(z)$ at the pole s_n. Using the series expansion ψ we again only keep the relevant

term at the corresponding pole an calculate

$$\begin{aligned}\mathrm{Res}(s_n) &\sim \left[\frac{d}{ds}\left(s - F_1(s) - F_2(s)\right)\right]^{-1}\Big|_{s=s_n} \\ &\sim \left[\frac{d}{ds}\left(-F_1(s) - F_2(s)\right)\right]^{-1}\Big|_{s=s_n}\end{aligned} \tag{E14}$$

where we can neglect the contribution from s as the derivative of the digamma function is much larger. In the zero-field limit we obtain

$$\begin{aligned}\mathrm{Res}(s_n) &\sim \left[\frac{d}{ds}\left(-4\alpha\frac{\frac{s^2}{2\pi k_B T}}{n\left(\frac{s}{2\pi k_B T}+n\right)}\right)\right]^{-1}\Big|_{s=s_n} \\ &\sim \left[-\frac{8\alpha}{2\pi k_B T}\frac{s}{n\left(\frac{s}{2\pi k_B T}+n\right)} + \frac{4\alpha}{(2\pi k_B T)^2}\frac{s^2}{n\left(\frac{s}{2\pi k_b T}+n\right)^2}\right]^{-1}\Big|_{s=s_n}\end{aligned} \tag{E15}$$

In the main text we derived the location of the pole s_n

$$s_n = -2\pi k_B T n - 8\alpha\pi k_B T. \tag{E16}$$

Inserting s_n into Eq. (E15) leads to

$$\begin{aligned}\mathrm{Res}(s_n) &\sim \left[-8\alpha\frac{-2\pi k_B T n + p}{np} + 4\alpha\frac{(-2\pi k_B T n + p)^2}{np^2}\right]^{-1} \\ &\sim \left[2\pi k_B T\frac{8\alpha}{p} - \frac{8\alpha}{n} + (2\pi k_B T)^2 n\frac{4\alpha}{p^2} - 4\pi k_B T\frac{4\alpha}{p} + \frac{4\alpha}{n}\right]^{-1}\end{aligned} \tag{E17}$$

The dominant contribution will come from the third as it is are $O(1/\alpha)$ which leads to

$$\mathrm{Res}(s_n) \sim \frac{4\alpha}{n}. \tag{E18}$$

The full residue, in the zero-field limit, for each non-Markovian poles is then given by

$$\mathrm{Res}(s_n) = \frac{4\alpha}{n}e^{s_n t}\rho_z(t=0) \tag{E19}$$

which corresponds to Eq. (3.129).

For finite field we follow the same steps and again the residue is dominated by Eq. (E14) where we this time use the finite field expressions for the spin-spin correlation functions

Eqs. (3.97) and (3.98) for F_1,F_2. This leads to

$$\mathrm{Res}\left(s^z_{n,r}\right) \sim \left[\frac{d}{ds}\left(-2\alpha\frac{\frac{(s+ib^I_z)^2}{2\pi k_BT}}{n\left(\frac{s+ib^I_z}{2\pi k_BT}+n\right)} - 2\alpha\frac{\frac{(s-ib^I_z)^2}{2\pi k_BT}}{n\left(\frac{s-ib^I_z}{2\pi k_BT}+n\right)}\right)\right]^{-1}\Bigg|_{s=s^z_{n,r}} \tag{E20}$$

and the location of the pole is given by

$$s^z_{n,r} = -2\pi k_BTn + p^z_r, \tag{E21}$$

with

$$p^z_r = -4\alpha\pi k_BT + r\sqrt{(4\alpha\pi k_BT)^2 - \left(b^I_z\right)^2} \tag{E22}$$

as stated we derived in the main text, see Eq. (3.137). Following the same steps as in Eq. (E17) and neglecting all terms that are not $O(1/\alpha)$ we arrive at

$$\begin{aligned}\mathrm{Res}\left(s^z_{n,r}\right) &\sim \left[(2\pi k_BT)^2\frac{2\alpha n}{\left(p+ib^I_z\right)^2} + (2\pi k_BT)^2\frac{2\alpha n}{\left(p-ib^I_z\right)^2}\right]^{-1}\\ &\sim \left[2\alpha\left(2\pi k_BT\right)^2 n\left(\frac{1}{\left(p^z_r+ib^I_z\right)^2}+\frac{1}{\left(p^z_r-ib^I_z\right)^2}\right)\right]^{-1}.\end{aligned} \tag{E23}$$

Inserting p^z_r leads to the full residue

$$\mathrm{Res}\left(s^z_{n,r}\right) = \frac{2\alpha}{n}e^{s^z_{n,r}t}\left[1 - r\frac{4\alpha\pi k_BT}{\sqrt{(4\alpha\pi k_BT)^2-\left(b^I_z\right)^2}}\right]\left(\rho_z(t=0)-\rho^{\mathrm{eq}}_z\right). \tag{E24}$$

This is the expression stated in Eq. (3.138). For $b^I_z \to 0$ we recover Eq. (E18).

For the transverse component the arguments of the digamma functions are shifted

$$s + ib^I_z \to s \tag{E25}$$

$$s - ib^I_z \to s \mp ib^I_z, \tag{E26}$$

where $\mp$ refers to the sign in the definition of $F_\pm$ (Eqs. (3.99) and (3.100)). If we take

$$b^I_z \to b^I_z/2 \tag{E27}$$

$$s \to s \mp ib^I_z/2 \tag{E28}$$

the arguments of the digamma function in transverse case are given by $\psi(s \mp ib^I_z/2)$ and $\psi(s \pm ib^I_z/2)$. Then the same calculation as for z component applies for the residue with

the result

$$\mathrm{Res}\left(s^{\pm}_{n,r}\right) = \frac{2\alpha}{n} e^{s^{\pm}_{n,r} t} \left[1 - r \frac{4\alpha\pi k_B T}{\sqrt{(4\alpha\pi k_B T)^2 - (b^I_z)^2}}\right] \rho_{\pm}(t=0), \tag{E29}$$

and the pole

$$s^{\pm}_{n,r} = -2\pi k_B T n \mp \frac{i}{2} b^I_z + p^{\pm}_r, \tag{E30}$$

with

$$p^{\pm}_r = p^z_r|_{b^I_z \to b^I_z/2} = -4\alpha\pi k_B T + r\sqrt{(4\alpha\pi k_B T)^2 - (b^I_z/2)^2}. \tag{E31}$$

F Time-dependent projection

F.1 Equation of motion for $\rho_{I,j}$

In the following we calculate all commutators which lead to the matrix expression $\hat{\hat{M}}$ in Section 5.2.1 The density matrix defined in Eq. (5.18) is given by

$$\rho_{I,j} = \rho^{\uparrow}_j I^{\uparrow}_j + \rho^{\downarrow}_j I^{\downarrow}_j + \rho^{-}_j I^{+}_j + \rho^{+}_j I^{-}_j. \tag{F1}$$

The spin operators I^{α}_j obey the same relations states in Appendix C.1, in particular Eqs. (C3) to (C7) and (C9).

The following commutators are useful as well

$$\begin{aligned}
\left[\rho_j(t'), I^{-}_j\right] &= \left[I^{\uparrow}_j, I^{-}_j\right] \rho^{\uparrow}_j(t') + \left[I^{\downarrow}_j, I^{-}_j\right] \rho^{\downarrow}_j(t') + \left[I^{-}_j, I^{-}_j\right] \rho^{-}_j(t') + \left[I^{+}, j, I^{-}_j\right] \rho^{+}_j(t') && \text{(F2)}\\
&= -I^{-}_j \rho^{\uparrow}_j(t') + I^{-}_j \rho^{\downarrow}_j(t') + I^{\uparrow}_j \rho^{+}_j(t') - I^{\downarrow}_j \rho^{+}_j(t'), && \text{(F3)}\\
\left[\rho_j(t'), I^{+}_j\right] &= \left[I^{\uparrow}_j, I^{+}_j\right] \rho^{\uparrow}_j(t') + \left[I^{\downarrow}_j, I^{+}_j\right] \rho^{\downarrow}_j(t') + \left[I^{-}_j, I^{+}_j\right] \rho^{-}_j(t') + \left[I^{+}, j, I^{+}_j\right] \rho^{+}_j(t') && \text{(F4)}\\
&= I^{+}_j \rho^{\uparrow}_j(t') - I^{\downarrow}_j \rho^{\downarrow}_j(t') - I^{\uparrow}_j \rho^{-}_j(t') + I^{\downarrow}_j \rho^{-}_j(t'), && \text{(F5)}\\
\left[\rho_j(t'), I^{z}_j\right] &= \left[\rho_j(t'), I^{\uparrow}_j\right] - \left[\rho_j(t'), I^{\downarrow}_j\right] \\
&= 2I^{-}_j \rho^{-}_j(t') - 2I^{+}_j \rho^{+}_j(t') && \text{(F6)}
\end{aligned}$$

F.1.1 Linear term

The linear term is given by

$$\mathrm{Tr}_{\mathrm{el}}\left\{L^{j}_{\mathrm{int}} \rho_{I,j}(t) \otimes \rho_{\mathrm{el}}(t)\right\} = -i2A\mathrm{Tr}_{\mathrm{el}}\left\{S^{+}(x_j)\rho_{\mathrm{el}}(t)\right\}\left[I^{-}_j, \rho_j(t)\right]$$

$$
\begin{aligned}
&- i2A\mathrm{Tr}_{\mathrm{el}}\left\{S^{-}(x_j)\rho_{\mathrm{el}}(t)\right\}\left[I_j^{+},\rho_j(t)\right]\\
&- iA\mathrm{Tr}_{\mathrm{el}}\left\{S^{z}(x_j)\rho_{\mathrm{el}}(t)\right\}\left[I_j^{z},\rho_j(t)\right],
\end{aligned}
\tag{F7}
$$

which corresponds to Eq. (5.23). Using the commutator relations in Appendix C.1 and Eqs. (F3), (F5) and (F6) we find

$$\left[I_j^{-},\rho_j(t)\right] = I_j^{-}\rho_j^{\uparrow}(t) - I_j^{-}\rho_j^{\downarrow}(t) - I_j^{\uparrow}\rho_j^{+}(t) + I_j^{\downarrow}\rho_j^{+}(t), \tag{F8}$$

$$\left[I_j^{+},\rho_j(t)\right] = -I_j^{+}\rho_j^{\uparrow}(t) + I_j^{+}\rho_j^{\downarrow}(t) + I_j^{\uparrow}\rho_j^{-}(t) - I_j^{\downarrow}\rho_j^{-}(t), \tag{F9}$$

$$\left[I_j^{z},\rho_j(t)\right] = -2I_j^{-}\rho_j^{+}(t) + 2I^{+}j\rho_j^{-}(t). \tag{F10}$$

Identifying the elements where I^{α} label the columns similar to Appendix C.1, we arrive at the matrix $\hat{\hat{M}}_{\mathrm{int}}$ of Eq. (5.24).

F.1.2 $O(A^2)$: Two-point correlators

The full expression for the term defined in Eq. (5.30) found by applying the specific interaction Liouvillian L_{int}^{j}. This leads to

$$
\begin{aligned}
M_{\mathrm{2nd,1}} \sim & 4\mathrm{Tr}_{\mathrm{el}}\left\{S^{\mp}(x_j,t'-t)S^{\pm}(x_j)\rho_{\mathrm{el}}(t')\right\}\left[I_j^{\pm},I_j^{\mp}\rho_j(t')\right]\\
&+ 4\mathrm{Tr}_{\mathrm{el}}\left\{S^{\pm}(x_j)S^{\mp}(x_j,t'-t)\rho_{\mathrm{el}}(t')\right\}\left[\rho_j(t')I_j^{\mp},I_j^{\pm}\right]\\
&+ 2\mathrm{Tr}_{\mathrm{el}}\left\{S^{z}(x_j,t'-t)S^{\pm}(x_j)\rho_{\mathrm{el}}(t')\right\}\left[I_j^{z},I_j^{\mp}\rho_j(t')\right]\\
&+ 2\mathrm{Tr}_{\mathrm{el}}\left\{S^{\pm}(x_j)S^{z}(x_j,t'-t)\rho_{\mathrm{el}}(t')\right\}\left[\rho_j(t')I_j^{\mp},I_j^{z}\right]\\
&+ 2\mathrm{Tr}_{\mathrm{el}}\left\{S^{+}(x_j,t'-t)S^{z}(x_j)\rho_{\mathrm{el}}(t')\right\}\left[I_j^{-},I_j^{z}\rho_j(t')\right]\\
&+ 2\mathrm{Tr}_{\mathrm{el}}\left\{S^{z}(x_j)S^{+}(x_j,t'-t)\rho_{\mathrm{el}}(t')\right\}\left[\rho_j(t')I_j^{z},I_j^{-}\right]\\
&+ 2\mathrm{Tr}_{\mathrm{el}}\left\{S^{-}(x_j,t'-t)S^{z}(x_j)\rho_{\mathrm{el}}(t')\right\}\left[I_j^{+},I_j^{z}\rho_j(t')\right]\\
&+ 2\mathrm{Tr}_{\mathrm{el}}\left\{S^{z}(x_j)S^{-}(x_j,t'-t)\rho_{\mathrm{el}}(t')\right\}\left[\rho_j(t')I_j^{z},I_j^{+}\right]\\
&+ \mathrm{Tr}_{\mathrm{el}}\left\{S^{z}(x_j,t'-t)S^{z}(x_j)\rho_{\mathrm{el}}(t')\right\}\left[I_j^{z},I_j^{z}\rho_j(t')\right]\\
&+ \mathrm{Tr}_{\mathrm{el}}\left\{S^{z}(x_j)S^{z}(x_j,t'-t)\rho_{\mathrm{el}}(t')\right\}\left[\rho_j(t')I_j^{z},I_j^{z}\right].
\end{aligned}
\tag{F11}
$$

Note that we need to have both combinations for the superscripts $\pm$. Then, the commutators of the density matrix with the impurity spin operators are (dropping the spacial index j, and often also suppressing the time dependence of ρ_j^{α}), first for the upper sign

in Eq. (F11)

$$\begin{aligned}
\left[I^+, I^-\rho_j(t')\right] &= \left[I^+, I^-\right]\rho_j(t') + I^-\left[I^+, \rho_j(t')\right] \\
&= I^\uparrow\rho_j^\uparrow - I^\downarrow\rho_j^\uparrow + I^+\rho_j^+ && \text{(F12)} \\
\left[\rho_j(t')I^-, I^+\right] &= \rho_j(t')\left[I^-, I^+\right] + \left[\rho_j(t'), I^+\right]I^- \\
&= -I^\uparrow\rho_j^\downarrow + I^\downarrow\rho_j^\downarrow + I^+\rho_j^+ && \text{(F13)} \\
\left[I^z, I^-\rho_j(t')\right] &= \left[I^z, I^-\right]\rho_j(t') + I^-\left[I^z, \rho_j(t')\right] \\
&= -2I^-\rho_j^\uparrow && \text{(F14)} \\
\left[\rho_j(t')I^-, I^z\right] &= \rho_j(t')\left[I^-, I^z\right] + \left[\rho_j(t'), I^z\right]I^- \\
&= 2I^-\rho_j^\downarrow. && \text{(F15)}
\end{aligned}$$

For the bottom sign in Eq. (F11) the commutators are

$$\begin{aligned}
\left[I^-, I^+\rho_j(t')\right] &= \left[I^-, I^+\right]\rho_j(t') + I^+\left[I^-, \rho_j(t')\right] \\
&= I^\downarrow\rho_j^\downarrow - I^\uparrow\rho_j^\downarrow + I^-\rho_j^- && \text{(F16)} \\
\left[\rho_j(t')I^+, I^-\right] &= \rho_j(t')\left[I^+, I^-\right] + \left[\rho_j(t'), I^-\right]I^+ \\
&= I^\uparrow\rho_j^\uparrow - I^\downarrow\rho_j^\uparrow + I^-\rho_j^- && \text{(F17)} \\
\left[I^z, I^+\rho_j(t')\right] &= \left[I^z, I^+\right]\rho_j(t') + I^+\left[I^z, \rho_j(t')\right] \\
&= 2I^+\rho_j^\downarrow && \text{(F18)} \\
\left[\rho_j(t')I^+, I^z\right] &= \rho_j(t')\left[I^+, I^z\right] + \left[\rho_j(t'), I^z\right]I^+ \\
&= -2I^+\rho_j^\uparrow. && \text{(F19)}
\end{aligned}$$

And the last few commutators of Eq. (F11) are given by

$$\begin{aligned}
\left[I^-, I^z\rho_j(t')\right] &= \left[I^-, I^z\right]\rho_j(t') + I^z\left[I^-, \rho_j(t')\right] \\
&= I^-\rho_j^\uparrow(t') + I^-\rho_j^\downarrow(t') - I^\uparrow\rho_j^+(t') + I^\downarrow\rho_j^+(t') && \text{(F20)} \\
\left[I^+, I^z\rho_j(t')\right] &= \left[I^+, I^z\right]\rho_j(t') + I^z\left[I^+, \rho_j(t')\right] \\
&= -I^+\rho_j^\uparrow(t') - I^+\rho_j^\downarrow(t') - I^\uparrow\rho_j^-(t') + I^\downarrow\rho_j^-(t') && \text{(F21)} \\
\left[\rho_j(t')I^z, I^-\right] &= \rho_j(t')\left[I^z, I^-\right] + \left[\rho_j(t'), I^-\right]I^z \\
&= -I^-\rho_j^\uparrow(t') - I^-\rho_j^\downarrow(t') - I^\uparrow\rho_j^+(t') + I^\downarrow\rho_j^+(t') && \text{(F22)} \\
\left[\rho_j(t')I^z, I^+\right] &= \rho_j(t')\left[I^z, I^+\right] + \left[\rho_j(t'), I^+\right]I^z \\
&= I^+\rho_j^\uparrow(t') + I^+\rho_j^\downarrow(t') - I^\uparrow\rho_j^-(t') + I^\downarrow\rho_j^-(t') && \text{(F23)}
\end{aligned}$$

$$\begin{aligned}\left[I^z, I^z\rho_j(t')\right] &= \left[I^z, I^z\right]\rho_j(t') + I^z\left[I^z, \rho_j(t')\right] \\ &= 2I^-\rho_j^- + 2I^+\rho_j^+ \qquad \text{(F24)} \\ \left[\rho_j(t')I^z, I^z\right] &= \rho_j(t')\left[I^z, I^z\right] + \left[\rho_j(t'), I^z\right] I^z \\ &= 2I^-\rho_j^- + 2I^+\rho_j^+ \qquad \text{(F25)}\end{aligned}$$

Rearranging all elements according to their components (I^α determines the columns, ρ^β the rows), leads to the matrix $\hat{\hat{M}}_{\text{2nd,1}}$ Eq. (5.32) in the main text.

F.1.3 $O(A^2)$: One-point correlators

The full expression for the term defined in Eq. (5.46) is given by

$$\begin{aligned}&M_{\text{2nd,2}} \\ &\sim 4\text{Tr}_{\text{el}}\left\{S^-(x_j, t'-t)\rho_{\text{el}}(t')\right\}\text{Tr}_{\text{el}}\left\{S^+(x_j)\rho_{\text{el}}(t')\right\}\left(\left[I_j^+, I_j^-\rho_j(t')\right] + \left[\rho_j(t')I_j^-, I_j^+\right]\right) \\ &+ 2\text{Tr}_{\text{el}}\left\{S^z(x_j, t'-t)\rho_{\text{el}}(t')\right\}\text{Tr}_{\text{el}}\left\{S^+(x_j)\rho_{\text{el}}(t')\right\}\left(\left[I_j^z, I_j^-\rho_j(t')\right] + \left[\rho_j(t')I_j^-, I_j^z\right]\right) \\ &+ 4\text{Tr}_{\text{el}}\left\{S^+(x_j, t'-t)\rho_{\text{el}}(t')\right\}\text{Tr}_{\text{el}}\left\{S^-(x_j)\rho_{\text{el}}(t')\right\}\left(\left[I_j^-, I_j^+\rho_j(t')\right] + \left[\rho_j(t')I_j^+, I_j^-\right]\right) \\ &+ 2\text{Tr}_{\text{el}}\left\{S^z(x_j, t'-t)\rho_{\text{el}}(t')\right\}\text{Tr}_{\text{el}}\left\{S^-(x_j)\rho_{\text{el}}(t')\right\}\left(\left[I_j^z, I_j^+\rho_j(t')\right] + \left[\rho_j(t')I_j^+, I_j^z\right]\right) \\ &+ 2\text{Tr}_{\text{el}}\left\{S^+(x_j, t'-t)\rho_{\text{el}}(t')\right\}\text{Tr}_{\text{el}}\left\{S^z(x_j)\rho_{\text{el}}(t')\right\}\left(\left[I_j^-, I_j^z\rho_j(t')\right] + \left[\rho_j(t')I_j^z, I_j^-\right]\right) \\ &+ 2\text{Tr}_{\text{el}}\left\{S^-(x_j, t'-t)\rho_{\text{el}}(t')\right\}\text{Tr}_{\text{el}}\left\{S^z(x_j)\rho_{\text{el}}(t')\right\}\left(\left[I_j^+, I_j^z\rho_j(t')\right] + \left[\rho_j(t')I_j^z, I_j^+\right]\right) \\ &+ \text{Tr}_{\text{el}}\left\{S^z(x_j, t'-t)\rho_{\text{el}}(t')\right\}\text{Tr}_{\text{el}}\left\{S^z(x_j)\rho_{\text{el}}(t')\right\}\left(\left[I_j^z, I_j^z\rho_j(t')\right] + \left[\rho_j(t')I_j^z, I_j^z\right]\right) \qquad \text{(F26)}\end{aligned}$$

The relevant commutators are the same as for the two point correlators. The matrix entries are only slightly modified prefactors due to the additional trace. In the same way as before we can identify all entries and arrange the matrix $\hat{\hat{M}}_{\text{2nd,2}}$ which is stated in Eq. (5.47)

F.1.4 $O(A^2)$: Renormalisation term

The full expression for the term defined in Eq. (5.56) is given by

$$\begin{aligned}M_{\text{2nd,3}} \sim\ & 4\text{Tr}_{\text{el}}\left\{\left[S^\pm(x_j, t-t'), S^\mp(x_j)\right]\rho_{\text{el}}(t')\right\}\text{Tr}_j\left\{I^\pm\rho_j(t')\right\}\left[\rho_j(t'), I_j^\mp\right] \\ &+ 2\text{Tr}_{\text{el}}\left\{\left[S^\pm(x_j, t-t'), S^z(x_j)\right]\rho_{\text{el}}(t')\right\}\text{Tr}_j\left\{I_j^z\rho_j(t')\right\}\left[\rho_j(t'), I_j^\mp\right] \\ &+ 2\text{Tr}_{\text{el}}\left\{\left[S^z(x_j, t-t'), S^+(x_j)\right]\rho_{\text{el}}(t')\right\}\text{Tr}_j\left\{I_j^-\rho_j(t')\right\}\left[\rho_j(t'), I_j^z\right] \\ &+ 2\text{Tr}_{\text{el}}\left\{\left[S^z(x_j, t-t'), S^-(x_j)\right]\rho_{\text{el}}(t')\right\}\text{Tr}_j\left\{I_j^+\rho_j(t')\right\}\left[\rho_j(t'), I_j^z\right]\end{aligned}$$

$$+\,\mathrm{Tr}_{\mathrm{el}}\left\{\left[S^z(x_j,t-t'),S^z(x_j)\right]\rho_{\mathrm{el}}(t')\right\}\mathrm{Tr}_j\left\{I_j^z\rho_j(t')\right\}\left[\rho_j(t'),I_j^z\right]. \tag{F27}$$

The commutators are given by Eqs. (F3), (F5) and (F6) and arranging all components a matrix leads to $\hat{\hat{M}}_{\mathrm{2nd},3}$ of Eq. (5.57).

F.2 Equation of motion for ρ_{EL}

F.2.1 Eigendynamics and linear term

Starting from Eq. (5.80) we present more details to reach the final result of Y_{ED} in Eq. (5.98). Inserting Eq. (5.76) into Eq. (5.80) lead to

$$\begin{aligned}
Y_{\mathrm{ED}} \sim\ & \mathrm{Tr}_{\mathrm{el}}\left\{\sum_{pp'}e^{i(p-p')x_j}c_{p\sigma}^\dagger c_{p'\sigma'}\left[H_{\mathrm{el}},\rho_{\mathrm{el}}^{\mathrm{eq}}\right]\right\}\\
&+\mathrm{Tr}_{\mathrm{el}}\left\{\sum_{pp'}e^{i(p-p')x_j}c_{p\sigma}^\dagger c_{p'\sigma'}\left[H_{\mathrm{el}},\sum_{\alpha\alpha',l}\sum_{kk'}\Lambda_{\alpha'}^{\alpha}e^{i(k-k')x_l}c_{k\alpha}^\dagger c_{k'\alpha'}\rho_{\mathrm{el}}^{\mathrm{eq}}\right]\right\}\\
&+\mathrm{Tr}_{\mathrm{el}}\left\{\sum_{pp'}e^{i(p-p')x_j}c_{p\sigma}^\dagger c_{p'\sigma'}\left[H_{\mathrm{el}},\sum_{\alpha\alpha',l}\sum_{kk'}\tilde{\Lambda}_{\alpha'}^{\alpha}e^{i(k-k')x_l}c_{k'\alpha'}c_{k\alpha}^\dagger\rho_{\mathrm{el}}^{\mathrm{eq}}\right]\right\}.
\end{aligned} \tag{F28}$$

The first term is zero as $[H_{\mathrm{el}},\rho_{\mathrm{el}}^{\mathrm{eq}}]=0$. We will consider the the second term including the particle contribution in more detail. Inserting H_{el} defined in Eq. (5.96) leads to

$$Y_{\mathrm{ED}}^{\mathrm{P}} \sim \mathrm{Tr}_{\mathrm{el}}\left\{\sum_{pp'}\sum_{n\beta}\sum_{\alpha\alpha',l}\sum_{kk'}e^{i(p-p')x_j}e^{i(k-k')x_l}\Lambda_{\alpha'}^{\alpha}c_{p\sigma}^\dagger c_{p'\sigma'}\left[c_{n\beta}^\dagger c_{n\beta},c_{k\alpha}^\dagger c_{k'\alpha'}\rho_{\mathrm{el}}^{\mathrm{eq}}\right]\right\}. \tag{F29}$$

The fermionic operators can be rearranged as follows

$$c_{p\sigma}^\dagger c_{p'\sigma'}\left[c_{n\beta}^\dagger c_{n\beta},c_{k\alpha}^\dagger c_{k'\alpha'}\rho_{\mathrm{el}}^{\mathrm{eq}}\right]=\left[c_{p\sigma}^\dagger c_{p'\sigma'},c_{n\beta}^\dagger c_{n\beta}\right]c_{k\alpha}^\dagger c_{k'\alpha'}\rho_{\mathrm{el}}^{\mathrm{eq}}. \tag{F30}$$

The commutator can be replaced with Eq. (5.97). Then, decoupling the operators under the trace according to Eq. (5.91) leads to Eq. (5.98) after making use of Eq. (5.93).

The linear term Eq. (5.81) after inserting Eq. (5.76) leads to

$$\begin{aligned}
Y_{\mathrm{lin}} \sim\ & \mathrm{Tr}_{\mathrm{el}}\left\{\sum_{pp'}e^{i(p-p')x_j}c_{p\sigma}^\dagger c_{p'\sigma'}\left[\sum_{nn'}e^{i(n-n')x_j}c_{n\beta}^\dagger c_{n'\beta'},\rho_{\mathrm{el}}^{\mathrm{eq}}\right]\right\}\\
&+\mathrm{Tr}_{\mathrm{el}}\left\{\sum_{pp'}e^{i(p-p')x_j}c_{p\sigma}^\dagger c_{p'\sigma'}\left[\sum_{nn'}e^{i(n-n')x_j}c_{n\beta}^\dagger c_{n'\beta'},\sum_{\alpha\alpha',l}\sum_{kk'}e^{i(k-k')x_l}\Lambda_{\alpha'}^{\alpha}c_{k\alpha}^\dagger c_{k'\alpha'}\rho_{\mathrm{el}}^{\mathrm{eq}}\right]\right\}
\end{aligned}$$

$$+ \mathrm{Tr}_{\mathrm{el}} \left\{ \sum_{pp'} e^{i(p-p')x_j} c^\dagger_{p\sigma} c_{p'\sigma'} \left[\sum_{nn'} e^{i(n-n')x_j} c^\dagger_{n\beta} c_{n'\beta'}, \sum_{\alpha\alpha',l} \sum_{kk'} e^{i(k-k')x_l} \tilde{\Lambda}^{\alpha}_{\alpha'} c_{k'\alpha'} c^\dagger_{k\alpha} \rho^{\mathrm{eq}}_{\mathrm{el}} \right] \right\} \tag{F31}$$

Again, the first term is zero. Using Eq. (F30) and Eq. (5.91) leads to Y_{lin} Eq. (5.100) in the main text.

F.2.2 $O(A^2)$ terms

The contribution for the the two- and one-point correlation functions consists of the contributions from the two traces Eqs. (5.82) and (5.83). We denote

$$X_1 = \mathrm{Tr}_{\mathrm{el}} \left\{ \left[S^{\bar{\sigma}}(t'-t), S^{\bar{\beta}}(t'-t) \right] S^{\bar{\gamma}} \rho_{\mathrm{el}}(t') \right\} \tag{F32}$$

which corresponds to Eq. (5.82).

For Eq. (F32) we have

$$\begin{aligned}
X_1 = \mathrm{Tr}_{\mathrm{el}} \Bigg\{ & \sum_{pp'} \sum_{nn'} \sum_{rr'} e^{i(\epsilon_p - \epsilon_{p'})(t'-t)} e^{i(\epsilon_n - \epsilon_{n'})(t'-t)} e^{i(p-p')x_j} e^{i(n-n')x_j} e^{i(r-r')x_j} \\
& \times \left[c^\dagger_{p\sigma} c_{p'\sigma'}, c^\dagger_{n\beta} c_{n\beta} \right] c^\dagger_{r\gamma} c_{r'\gamma'} \rho^{\mathrm{el}}_{\mathrm{el}} \Bigg\} \\
& + \mathrm{Tr}_{\mathrm{el}} \Bigg\{ \sum_{pp'} \sum_{nn'} \sum_{rr'} e^{i(\epsilon_p - \epsilon_{p'})(t'-t)} e^{i(\epsilon_n - \epsilon_{n'})(t'-t)} e^{i(p-p')x_j} e^{i(n-n')x_j} e^{i(r-r')x_j} \\
& \times \left[c^\dagger_{p\sigma} c_{p'\sigma'}, c^\dagger_{n\beta} c_{n\beta} \right] c^\dagger_{r\gamma} c_{r'\gamma'} \sum_{\alpha\alpha',l} \sum_{kk'} e^{i(k-k')x_l} \Lambda^{\alpha}_{\alpha'} c^\dagger_{k\alpha} c_{k'\alpha'} \rho^{\mathrm{el}}_{\mathrm{el}} \Bigg\} \\
& + \mathrm{Tr}_{\mathrm{el}} \Bigg\{ \sum_{pp'} \sum_{nn'} \sum_{rr'} e^{i(\epsilon_p - \epsilon_{p'})(t'-t)} e^{i(\epsilon_n - \epsilon_{n'})(t'-t)} e^{i(p-p')x_j} e^{i(n-n')x_j} e^{i(r-r')x_j} \\
& \times \left[c^\dagger_{p\sigma} c_{p'\sigma'}, c^\dagger_{n\beta} c_{n\beta} \right] c^\dagger_{r\gamma} c_{r'\gamma'} \sum_{\alpha\alpha',l} \sum_{kk'} e^{i(k-k')x_l} \tilde{\Lambda}^{\alpha}_{\alpha'} c_{k'\alpha'} c^\dagger_{k\alpha} \rho^{\mathrm{el}}_{\mathrm{el}} \Bigg\}
\end{aligned} \tag{F33}$$

where we used $\exp(\pm i\epsilon_p t)$ for the creation and annihilation operators $c^\dagger, c$. Replacing the commutator with Eq. (5.97) and using the decompositions Eqs. (5.91) and (5.92) leads to $Y_{\mathrm{2nd},1}$ in Eq. (5.103) and the corresponding hole contribution.

The expression for the second trace Eq. (5.83) as well as the trace for the renormalisation term Eq. (5.89) are obtained by following the same steps.

F.3 Momentum integrals in the continuum limit

F.3.1 Temporal contribution I_t

The integral Eq. (5.112) in the main text corresponds to the square of the integral in Eq. (D1) which is solved in Appendix D.1. Squaring the result Eq. (D8) immediately leads to Eq. (5.113).

F.3.2 Spatial contribution I_x

We find a closed expression for the integral Eq. (5.115) using the residue theorem. For the integral to converge we need to treat two different cases, $x\cos\phi > 0$ and $x\cos\phi < 0$, and close the contour in the appropriate half of the complex plane. We therefore split the integral I_x of Eq. (5.115) into two contributions

$$I_x = I_x^+ + I_x^-, \tag{F34}$$

with

$$I_x^+ = \frac{\nu_0}{2\pi}\int_{-\pi/2}^{\pi/2} d\phi \int_{-\infty}^{\infty} d\epsilon \frac{e^{i(k_F+\epsilon/v_F)x\cos\phi}}{1+e^{\beta\epsilon}}, \tag{F35}$$

for the case $x\cos\phi > 0$ and

$$I_x^- = \frac{\nu_0}{2\pi}\int_{\pi/2}^{3\pi/2} d\phi \int_{-\infty}^{\infty} d\epsilon \frac{e^{i(k_F+\epsilon/v_F)x\cos\phi}}{1+e^{\beta\epsilon}}, \tag{F36}$$

for $x\cos\phi < 0$ and β is the inverse temperature. In fact, $I_x^- = (I_x^+)^*$ because in the interval $\phi \in [\pi/2, 3\pi/2]$ we have $\cos\phi = -|\cos\phi|$. To solve for I_x^+ in Eq. (F35) we start by evaluating the energy integral. The poles of the integrand lie at the Matsubara frequencies $z_n = i\omega_n = i\pi(2n+1)/\beta$ with the residues $\mathrm{Re}_{z_n} - -1/\beta$ which was shown in Eq. (D4). If we close the integration contour in the upper half of the complex plane the contribution from the half circle vanishes and we are left with expression for the integral I_x^+ along the real axis

$$I_x^+ = -i\frac{\nu_0}{\beta}\int_{\pi/2}^{-\pi/2} d\phi \sum_{n\geq 0} e^{i\left(k_F + i\frac{\pi}{\beta v_F}(2n+1)\right)x\cos\phi}. \tag{F37}$$

The angular integral can be expressed in terms of the Bessel function $J_0(z)$ and the Struve function $H_0(z)$ and we obtain

$$I_x^+ = -i\frac{\nu_0}{\beta}\sum_{n\geq}\left\{\pi\left[J_0\left(k_F x + i\frac{\pi}{\beta}(2n+1)\,x\right) + iH_0\left(k_F x + i\frac{\pi}{\beta}(2n+1)\,x\right)\right]\right\}. \quad \text{(F38)}$$

Then the spatial correlations are captured by I_x

$$\begin{aligned} I_x &= I_x^+ + \left(I_x^+\right)^* = 2\mathrm{Re}I_x^+ \\ &= 2\mathrm{Re}\left[-i\frac{\nu_0\pi}{\beta}\sum_{n\geq 0}\left\{J_0\left(k_F x + i\frac{\pi}{\beta}(2n+1)\,x\right) + iH_0\left(k_F x + i\frac{\pi}{\beta}(2n+1)\,x\right)\right\}\right], \end{aligned} \quad \text{(F39)}$$

which is the expression in Eq. (5.116) stated in the main text. Inserting the asymptotic form of $J_0(z)$ and $H_0(z)$

$$J_0(z) \sim \sqrt{\frac{2}{\pi z}}\sin\left(z+\frac{\pi}{4}\right), \quad \text{(F40)}$$

$$H_0(z) \sim -\sqrt{\frac{2}{\pi z}}\cos\left(z+\frac{\pi}{4}\right), \quad \text{(F41)}$$

into Eq. (F39) leads to

$$I_x \approx -2\frac{\nu_0\pi}{\beta}\mathrm{Re}\left[i\sqrt{\frac{2}{\pi}}\sum_{n\geq 0}\left\{\frac{\sin\left(\tilde{z}_n+\frac{\pi}{4}\right) - i\cos\left(\tilde{z}_n+\frac{\pi}{4}\right)}{\sqrt{\tilde{z}_n}}\right\}\right], \quad \text{(F42)}$$

with $\tilde{z}_n = k_F x + i\pi x(2n+1)/\beta v_F$. Rearranging this expression we obtain

$$\begin{aligned} I_x &\approx -2\frac{\nu_0\pi}{\beta}\sqrt{\frac{2}{\pi}}\mathrm{Re}\left[\sum_{n\geq}\frac{\exp\left(i\frac{\pi}{4} + k_F x - i\frac{\pi x}{\beta v_F}(2n+1)\right)}{\sqrt{k_F x + i\frac{\pi x}{\beta v_F}(2n+1)}}\right] \\ &\approx -2\frac{\nu_0\pi}{\beta}\sqrt{\frac{2}{\pi}}\mathrm{Re}\left[e^{ik_F x + i\pi/4}e^{-\pi x/\beta v_F}\sum_{n\geq 0}\frac{\left(e^{2\pi x/\beta v_F}\right)^n}{\sqrt{i2\frac{\pi x}{\beta v_F}\left(n+\frac{1}{2}-i\frac{\beta v_F k_F}{\pi}\right)}}\right]. \end{aligned} \quad \text{(F43)}$$

In the last line we can identify the sum as a Lerch transcendent [131, 172]

$$\Phi(z,s,a) = \sum_{n=0}^{\infty}\frac{z^n}{(a+n)^s}, \quad \text{(F44)}$$

and we arrive at

$$I_x \approx -2\nu_0\sqrt{\frac{v_F}{\beta x}}e^{-x/x_T}\mathrm{Re}\left[e^{ik_F x}\Phi\left(e^{-2x/x_T},\frac{1}{2},\frac{1}{2}-i\frac{v_F k_F \beta}{\pi}\right)\right] \tag{F45}$$

with the thermal length $x_T = \beta v_F/\pi$. This results corresponds to Eq. (5.122).

F.3.3 Mixed contribution $I_{x,t}$

In contrast to the purely spatial contribution Eq. (5.115) we can directly evaluate the angular integral of Eq. (5.127) under the assumption that $v_F t + x\cos\phi > 0$ which leads to

$$I_{t,x} = \nu_0 \int d\epsilon e^{i\epsilon(t-i\xi_0)}\frac{J_0\left(k_F x + \frac{\epsilon}{v_F}x\right)}{1+e^{\epsilon\beta}}. \tag{F46}$$

Just as in the calculation above for I_x^+ we close the contour in upper half of the complex plane to perform the energy integral. Again, the poles are determined by the Matsubara frequencies and we obtain directly

$$I_{t,x} = -2\frac{\pi\nu_0}{\beta}\sum_{n\geq 0} e^{-\pi(2n+1)(t-i\xi_0^{-1})\beta}J_0\left(k_F x + i\frac{\pi}{\beta v_F}(2n+1)x\right), \tag{F47}$$

which corresponds to the expression in Eq. (5.129). Inserting the asymptotic form for the Bessel function Eq. (F40) we obtain

$$\begin{aligned} I_{t,x} &\approx -i2\pi\frac{\nu_0}{\beta}\sqrt{\frac{2}{\pi}}e^{-\pi(t-i\xi_0^{-1})/\beta}\sum_{n\geq 0} e^{-2\pi n(t-i\xi_0^{-1})/\beta}\frac{\sin\left(k_F x + i\frac{\pi}{\beta v_F}(2n+1)+\frac{\pi}{4}\right)}{\sqrt{k_F x + i\frac{\pi}{\beta v_F}(2n+1)\,x}} \\ &\approx -\pi\frac{\nu_0}{\beta}\sqrt{\frac{2}{\pi}}e^{-\pi(t-i\xi_0^{-1})/\beta}\sum_{n\geq 0}\frac{e^{-2\pi n(t-i\xi_0^{-1})/\beta}}{\sqrt{k_F x + i\frac{\pi}{\beta v_F}(2n+1)\,x}} \\ &\times\left[\exp\left(ik_F x - \frac{\pi}{\beta v_F}(2n+1)+i\frac{\pi}{4}\right) - \exp\left(-ik_F x + \frac{\pi}{\beta v_F}(2n+1)-i\frac{\pi}{4}\right)\right], \end{aligned} \tag{F48}$$

where we used the identity $\sin(z) = (\exp(iz)-\exp(-iz))/2i$. The two terms within the sum can be written as

$$\begin{aligned} &\frac{e^{-2\pi n(t-i\xi_0^{-1})/\beta}}{\sqrt{k_F x + i\frac{\pi}{\beta v_F}(2n+1)\,x}}\exp\left(ik_F x - \frac{\pi}{\beta v_F}(2n+1)+i\frac{\pi}{4}\right) \\ &= \frac{e^{ik_F x - \pi x/\beta v_F}e^{i\pi/4}}{\sqrt{i2\pi x/\beta v_F}}\Phi(e^{-2\pi(t+i\xi_0^{-1}+x/v_F)/\beta},\frac{1}{2},\frac{1}{2}-i\frac{\beta v_F k_F}{2\pi}), \end{aligned} \tag{F49}$$

and

$$
\begin{aligned}
&-\frac{e^{-2\pi n(t-i\xi_0^{-1})/\beta}}{\sqrt{k_F x + i\frac{\pi}{\beta v_F}(2n+1)\,x}}\exp\left(-ik_F x+\frac{\pi}{\beta v_F}(2n+1)-i\frac{\pi}{4}\right)\\
&=-\frac{e^{-ik_F x+\pi x/\beta v_F}e^{-i\pi/4}}{\sqrt{i2\pi x/\beta v_F}}\Phi(e^{-2\pi(t+i\xi_0^{-1}-x/v_F)/\beta},\frac{1}{2},\frac{1}{2}-i\frac{\beta v_F k_F}{2\pi}).
\end{aligned}
\tag{F50}
$$

Replacing the sum in Eq. (F48) with the expressions Eqs. (F49) and (F50) leads to

$$
\begin{aligned}
I_{t,x} &= -\nu_0\sqrt{\frac{v_F}{\beta x}}e^{-i\pi k_B T\xi_0^{-1}-t/2\tau_T}\\
&\quad\times\left[e^{ik_F x-x/x_F}\Phi\left(e^{-t/\tau_T+i2\pi k_B T\xi_0^{-1}-2x/x_F},\frac{1}{2},\frac{1}{2}-i\frac{v_F k_F}{2\pi k_B T}\right)\right.\\
&\quad\left.+ie^{-ik_F x+x/x_F}\Phi\left(e^{-t/\tau_T+i2\pi k_B T\xi_0^{-1}+2x/x_F)},\frac{1}{2},\frac{1}{2}-i\frac{v_F k_F}{2\pi k_B T}\right)\right],
\end{aligned}
\tag{F51}
$$

where we introduced the thermal length x_T and the thermal time $\tau_T = 1/2\pi k_B T$. This last expression is the final result in Eq. (5.130).

For the case $v_F t + x\cos\phi < 0$ a closed expression for Eq. (5.127) is less obvious. For the spatial contribution we were able to split the angular integral in the contribution I_x^+ and I_x^-, depending on the value for $\cos\phi$. Here, this is no longer possible since we also have contribution from the time t. Depending on the actual value for t we would need to shift the limits of the angular integral according to regimes where $v_F t + x\cos\phi > 0$ or $v_F t + x\cos\phi < 0$. Since this changes smoothly with t we cannot determine the correct interval for the angle ϕ to decide in which complex half plane we need to close the contour in order for the integral to reduce to the real axis.

Bibliography

[1] I. Bloch, J. Dalibard and W. Zwerger,
"Many-body physics with ultracold gases", *Rev. Mod. Phys.* 80 (2008) 885–964,
DOI: 10.1103/RevModPhys.80.885.

[2] I. Bloch, J. Dalibard and S. Nascimbéne,
"Quantum simulations with ultracold quantum gases",
Nature Physics 8 (2012) 267–276, DOI: 10.1038/nphys2259.

[3] T. Langen, R. Geiger and J. Schmiedmayer,
"Ultracold Atoms Out of Equilibrium",
Annual Review of Condensed Matter Physics 6.1 (2015) 201–217,
DOI: 10.1146/annurev-conmatphys-031214-014548.

[4] C. Gross and I. Bloch,
"Quantum simulations with ultracold atoms in optical lattices",
Science 357.6355 (2017) 995–1001, DOI: 10.1126/science.aal3837.

[5] H. J. Mamin, M Poggio, C. L. Degen and D Rugar,
"Nuclear magnetic resonance imaging with 90-nm resolution",
Nature Nanotechnology 2.5 (2007), DOI: 10.1038/nnano.2007.105.

[6] C. L. Degen, M Poggio, H. J. Mamin, C. T. Rettner and D Rugar,
"Nanoscale magnetic resonance imaging", *PNAS* 106.5 (2009),
DOI: 10.1073/pnas.0812068106.

[7] H. J. Mamin, M. Kim, M. H. Sherwood, C. T. Rettner, K. Ohno,
D. D. Awschalom and D. Rugar,
"Nanoscale Nuclear Magnetic Resonance with a Nitrogen-Vacancy Spin Senor",
Science 339 (2013) 557–560, DOI: 10.1126/science.1231540.

[8] A. O. Sushkov, I Lovchinsky, N Chisholm, R. L. Walsworth, H Park and
M. D. Lukin, "Magnetic Resonance Detection of Individual Proton Spins Using
Quantum Reporters", *Phys. Rev. Letters* 113.197601 (2014),
DOI: 10.1103/PhysRevLett.113.197601.

[9] D. Loss and D. P. DiVincenzo, "Quantum computation with quantum dots", *Phys. Rev. A* 57 (1998) 120–126, DOI: 10.1103/PhysRevA.57.120.

[10] L. M. K. Vandersypen and M. A. Eriksson, "Quantum computing with semiconductor spins", *Physics Today* 72 (2019) 8, 38, DOI: 10.1063/PT.3.4270.

[11] G. Wendin, "Quantum information processing with superconducting circuits: a review", *Reports on Progress in Physics* 80.10 (2017) 106001, DOI: 10.1088/1361-6633/aa7e1a.

[12] M. Kjaergaard, M. E. Schwartz, J. Braumüller, P. Krantz, J. I.-J. Wang, S. Gustavsson and W. D. Oliver, "Superconducting Qubits: Current State of Play", *Annual Review of Condensed Matter Physics* 11.1 (2020) 369–395, DOI: 10.1146/annurev-conmatphys-031119-050605.

[13] M Saffman, "Quantum computing with atomic qubits and Rydberg interactions: progress and challenges", *Journal of Physics B: Atomic, Molecular and Optical Physics* 49.20 (2016) 202001, DOI: 10.1088/0953-4075/49/20/202001.

[14] R. Horodecki, P. Horodecki, M. Horodecki and K. Horodecki, "Quantum entanglement", *Rev. Mod. Phys.* 81 (2009) 865–942, DOI: 10.1103/RevModPhys.81.865.

[15] E. Chitambar and G. Gour, "Quantum resource theories", *Rev. Mod. Phys.* 91 (2019) 025001, DOI: 10.1103/RevModPhys.91.025001.

[16] C. P. Slichter, *Principles of Magnetic Resonance*, Springer-Verlag Berlin Heidelberg, 1990.

[17] A. Abragam, *Principles of Nuclear Magnetism*, Oxford University Press, 1961.

[18] F. Bloch, "Nuclear Induction", *Phys. Rev.* 70 (1946) 460–474, DOI: 10.1103/PhysRev.70.460.

[19] J. Korringa, "Nuclear magnetic relaxation and resonance line shift in metals", *Physica* 16.7 (1950) 601, DOI: https://doi.org/10.1016/0031-8914(50)90105-4.

[20] T. Moriya, "The Effect of Electron-Electron Interaction on the Nuclear Spin Relaxation in Metals", *J. Phys. Soc. Jpn.* 18.4 (1963) 516, DOI: 10.1143/JPSJ.18.516.

[21] D. Kölbl, D. M. Zumbühl, A. Fuhrer, G. Salis and S. F. Alvarado, "Breakdown of the Korringa Law of Nuclear Spin Relaxation in Metallic GaAs", *Phys. Rev. Lett.* 109 (2012) 086601, DOI: 10.1103/PhysRevLett.109.086601.

[22] H. Maebashi, T. Hirosawa, M. Ogata and H. Fukuyama, "Nuclear magnetic relaxation and Knight shift due to orbital interaction in Dirac electron systems", *Journal of Physics and Chemistry of Solids* 128 (2019), Spin-Orbit Coupled Materials 138 –143, DOI: https://doi.org/10.1016/j.jpcs.2017.12.034.

[23] P. Coleman, *Introduction to Many-Body Physics*, Cambridge University Press, 2015.

[24] L. M. K. Vandersypen and I. L. Chuang, "NMR techniques for quantum control and computation", *Rev. Mod. Phys.* 76 (2005) 1037–1069, DOI: 10.1103/RevModPhys.76.1037.

[25] A. J. Daley, "Quantum trajectories and open many-body quantum systems", *Advances in Physics* 63.2 (2014) 77–149, DOI: 10.1080/00018732.2014.933502.

[26] A. Mitra, "Quantum Quench Dynamics", *Annual Review of Condensed Matter Physics* 9.1 (2018) 245–259, DOI: 10.1146/annurev-conmatphys-031016-025451.

[27] A. M. Alhambra, J. Riddell and L. P. García-Pintos, "Time Evolution of Correlation Functions in Quantum Many-Body Systems", *Phys. Rev. Lett.* 124 (2020) 110605, DOI: 10.1103/PhysRevLett.124.110605.

[28] J. R. Petta, A. C. Johnson, J. M. Taylor, E. A. Laird, A Yacoby, M. D. Lukin, C. M. Marcus, M. P. Hanson and A. C. Gossard, "Coherent Manipulation of Coupled Electron Spins in Semiconductor Quantum Dots", *Science* 309 (2005).

[29] G. M. Palma, K.-a. Suominen and A. Ekert, "Quantum computers and dissipation", *Proceedings of the Royal Society of London. Series A: Mathematical, Physical and Engineering Sciences* 452.1946 (1996) 567–584, DOI: 10.1098/rspa.1996.0029, eprint: https://royalsocietypublishing.org/doi/pdf/10.1098/rspa.1996.0029.

[30] J. Ma, B. Yadin, D. Girolami, V. Vedral and M. Gu, "Converting Coherence to Quantum Correlations", *Phys. Rev. Lett.* 116 (2016) 160407, DOI: 10.1103/PhysRevLett.116.160407.

[31] A. Rivas, S. F. Huelga and M. B. Plenio,
"Entanglement and Non-Markovianity of Quantum Evolutions",
Phys. Rev. Lett. 105 (2010) 050403, DOI: 10.1103/PhysRevLett.105.050403.

[32] "Non-Markovianity and reservoir memory of quantum channels: a quantum information theory perspective", *Scientific Reports* 4 (2014) 5720,
DOI: 10.1038/srep05720.

[33] M. Hell, M. R. Wegewijs and D. P. DiVincenzo,
"Coherent backaction of quantum dot detectors: Qubit isospin precession",
Phys. Rev. B 89 (2014) 195405, DOI: 10.1103/PhysRevB.89.195405.

[34] M. Hell, M. R. Wegewijs and D. P. DiVincenzo, "Qubit quantum-dot sensors: Noise cancellation by coherent backaction, initial slips, and elliptical precession",
Phys. Rev. B 93 (2016) 045418, DOI: 10.1103/PhysRevB.93.045418.

[35] M. A. Ruderman and C. Kittel, "Indirect Exchange Coupling of Nuclear Magnetic Moments by Conduction Electrons", *Phys. Rev.* 96 (1954) 99–102,
DOI: 10.1103/PhysRev.96.99.

[36] T. Kasuya,
"A Theory of Metallic Ferro- and Antiferromagnetism on Zener's Model",
Progress of Theoretical Physics 16.1 (1956) 45–57, DOI: 10.1143/PTP.16.45.

[37] K. Yosida, "Magnetic Properties of Cu-Mn Alloys",
Phys. Rev. 106 (1957) 893–898, DOI: 10.1103/PhysRev.106.893.

[38] P. Degenfeld-Schonburg and M. J. Hartmann,
"Self-consistent projection operator theory for quantum many-body systems",
Phys. Rev. B 89 (2014) 245108, DOI: 10.1103/PhysRevB.89.245108.

[39] M. Q. Lone, "Entanglement dynamics of two interacting qubits under the influence of local dissipation", *Pramana* 87 (2016) 16,
DOI: 10.1007/s12043-016-1228-4.

[40] J. Zou, S. K. Kim and Y. Tserkovnyak,
"Tuning entanglement by squeezing magnons in anisotropic magnets",
Phys. Rev. B 101 (2020) 014416, DOI: 10.1103/PhysRevB.101.014416.

[41] P. Debye, "Einige Bemerkungen zur Magnetisierung bei tiefer Temperatur",
Annalen der Physik 386.25 (1926) 1154–1160, DOI: 10.1002/andp.19263862517,
eprint:
https://onlinelibrary.wiley.com/doi/pdf/10.1002/andp.19263862517.

[42] W. F. Giauque,
"Paramagnetism and the third law of thermodynamics. Interpretation of the low-temperature magnetic susceptibility of gadolinium sulfate",
J. Am. Chem. Soc. 49 (1927) 1870–1877, DOI: 10.1021/ja01407a004.

[43] A. C. Clark, K. K. Schwarzwälder, T. Bandi, D. Maradan and D. M. Zumbühl,
"Method for cooling nanostructures to microkelvin temperatures",
Rev. Sci. Instr. 81.10 (2010) 103904, DOI: 10.1063/1.3489892.

[44] S. Abe and K. Matsumoto,
"Nuclear demagnetization for ultra-low temperatures", *Cryogenics* 62 (2014) 213,
DOI: https://doi.org/10.1016/j.cryogenics.2014.04.004.

[45] M. Palma, D. Maradan, L. Casparis, T.-M. Liu, F. N. M. Froning and D. M. Zumbühl,
"Magnetic cooling for microkelvin nanoelectronics on a cryofree platform",
Rev. Sci. Instr. 88.4 (2017) 043902, DOI: 10.1063/1.4979929.

[46] M. Palma, C. P. Scheller, D. Maradan, A. V. Feshchenko, M. Meschke and D. M. Zumbühl,
"On-and-off chip cooling of a Coulomb blockade thermometer down to 2.8 mK",
Appl. Phys. Lett. 111.25 (2017) 253105, DOI: 10.1063/1.5002565.

[47] F. Pobell, *Matter and Methods at Low Temperatures*, 3rd,
Springer-Verlag Berlin Heidelberg, 2007.

[48] R. S. Lous, I. Fritsche, M. Jag, B. Huang and R. Grimm, "Thermometry of a deeply degenerate Fermi gas with a Bose-Einstein condensate",
Phys. Rev. A 95 (2017) 053627, DOI: 10.1103/PhysRevA.95.053627.

[49] C. Galland, A. Högele, H. E. Türeci and A. Imamoglu, "Non-Markovian Decoherence of Localized Nanotube Excitons by Acoustic Phonons",
Phys. Rev. Lett. 101 (2008) 067402, DOI: 10.1103/PhysRevLett.101.067402.

[50] X. Chen, A. Ruschhaupt, S. Schmidt, A. del Campo, D. Guéry-Odelin and J. G. Muga, "Fast Optimal Frictionless Atom Cooling in Harmonic Traps: Shortcut to Adiabaticity", *Phys. Rev. Lett.* 104 (2010) 063002,
DOI: 10.1103/PhysRevLett.104.063002.

[51] R. Härtle, C. Schinabeck, M. Kulkarni, D. Gelbwaser-Klimovsky, M. Thoss and U. Peskin, "Cooling by heating in nonequilibrium nanosystems",
Phys. Rev. B 98 (2018) 081404, DOI: 10.1103/PhysRevB.98.081404.

[52] K. Funo, N. Lambert, B. Karimi, J. Pekola, Y. Masuyama and F. Nori, "Speeding up a quantum refrigerator via counterdiabatic driving", *Phys. Rev. B* 100 (2019) 035407, DOI: 10.1103/PhysRevB.100.035407.

[53] R. Uzdin, A. Levy and R. Kosloff, "Equivalence of Quantum Heat Machines, and Quantum-Thermodynamic Signatures", *Phys. Rev. X* 5 (2015) 031044, DOI: 10.1103/PhysRevX.5.031044.

[54] J. Roßnagel, S. T. Dawkins, K. N. Tolazzi, O. Abah, E. Lutz, F. Schmidt-Kaler and K. Singer, "A single-atom heat engine", *Science* 352.6283 (2016) 325–329, DOI: 10.1126/science.aad6320.

[55] M Wiedmann, J. T. Stockburger and J Ankerhold, "Non-Markovian dynamics of a quantum heat engine: out-of-equilibrium operation and thermal coupling control", *New Journal of Physics* 22.3 (2020) 033007, DOI: 10.1088/1367-2630/ab725a.

[56] H. Breuer and F. Petruccione, *The Theory of Open Quantum Systems*, Oxford University Press, Oxford, 2007.

[57] A. Rivas and S. F. Huelga, *Open quantum systems*, Springer, Berlin, Heidelberg, 2012.

[58] I. Rotter and J. P. Bird, "A review of progress in the physics of open quantum systems: theory and experiment", *Reports on Progress in Physics* 78.11 (2015) 114001, DOI: 10.1088/0034-4885/78/11/114001.

[59] H.-P. Breuer, E.-M. Laine, J. Piilo and B. Vacchini, "Colloquium: Non-Markovian dynamics in open quantum systems", *Rev. Mod. Phys.* 88 (2016) 021002, DOI: 10.1103/RevModPhys.88.021002.

[60] I. de Vega and D. Alonso, "Dynamics of non-Markovian open quantum systems", *Rev. Mod. Phys.* 89 (2017) 015001, DOI: 10.1103/RevModPhys.89.015001.

[61] G. Lindblad, "On the generators of quantum dynamical semigroups", *Communications in Mathematical Physics* 48.2 (1976) 119 –130, DOI: 10.1007/BF01608499.

[62] V. Gorini, A. Kossakowski and E. C. G. Sudarshan, "Completely positive dynamical semigroups of N-level systems", *Journal of Mathematical Physics* 17.5 (1976) 821–825, DOI: 10.1063/1.522979, eprint: https://aip.scitation.org/doi/pdf/10.1063/1.522979.

[63] A. Redfield, "The Theory of Relaxation Processes",
Advances in Magnetic Resonance, ed. by J. S. Waugh, vol. 1,
Advances in Magnetic and Optical Resonance, Academic Press, 1965 1 –32,
DOI: https://doi.org/10.1016/B978-1-4832-3114-3.50007-6.

[64] W. Coish and D. Loss, "Hyperfine Interaction in a Quantum Dot:
Non-Markovian Electron Spin Dynamics", *Phys. Rev. B* 70 (2004) 195340.

[65] E. Fick and G. Sauermann, *The Quantum Statistics of Dynamic Processes*,
Springer-Verlag, Berlin Heidelberg, 1990.

[66] R. Feynman and F. Vernon, "The theory of a general quantum system
interacting with a linear dissipative system",
Annals of Physics 24 (1963) 118 –173,
DOI: https://doi.org/10.1016/0003-4916(63)90068-X.

[67] S. Nakajima, "On Quantum Theory of Transport Phenomena: Steady Diffusion",
Progr. Theor. Phys. 20.6 (1958) 948, DOI: 10.1143/PTP.20.948.

[68] R. Zwanzig, "Ensemble Method in the Theory of Irreversibility",
J. Chem. Phys. 33.5 (1960) 1338, DOI: 10.1063/1.1731409.

[69] H. Mori, "Transport, Collective Motion, and Brownian Motion",
Progress of Theoretical Physics 33.3 (1965) 423–455, DOI: 10.1143/PTP.33.423.

[70] G. S. Agarwal, *Quantum Optics*, Cambridge University Press, 2013.

[71] S. Maniscalco and F. Petruccione, "Non-Markovian dynamics of a qubit",
Phys. Rev. A 73 (2006) 012111, DOI: 10.1103/PhysRevA.73.012111.

[72] A. Caldeira and A. Leggett,
"Path integral approach to quantum Brownian motion",
Physica A: Statistical Mechanics and its Applications 121.3 (1983) 587 –616,
DOI: https://doi.org/10.1016/0378-4371(83)90013-4.

[73] B. L. Hu, J. P. Paz and Y. Zhang,
"Quantum Brownian motion in a general environment: Exact master equation
with nonlocal dissipation and colored noise", *Phys. Rev. D* 45 (1992) 2843–2861,
DOI: 10.1103/PhysRevD.45.2843.

[74] R. S. Whitney,
"Staying positive: Going beyond Lindblad with perturbative master equations",
J. Phys. A 41.17 (2008) 175304.

[75] A. Smirne and B. Vacchini, "Nakajima-Zwanzig versus time-convolutionless master equation for the non-Markovian dynamics of a two-level system", *Phys. Rev. A* 82 (2010) 022110, DOI: 10.1103/PhysRevA.82.022110.

[76] C. Timm, "Time-convolutionless master equation for quantum dots: Perturbative expansion to arbitrary order", *Phys. Rev. B* 83 (2011) 115416, DOI: 10.1103/PhysRevB.83.115416.

[77] A. J. Leggett, S. Chakravarty, A. T. Dorsey, M. P. A. Fisher, A. Garg and W. Zwerger, "Dynamics of the dissipative two-state system", *Rev. Mod. Phys.* 59 (1987) 1–85, DOI: 10.1103/RevModPhys.59.1.

[78] T. Brandes, "Coherent and collective quantum optical effects in mesoscopic systems", *Physics Reports* 408.5 (2005) 315 –474, DOI: https://doi.org/10.1016/j.physrep.2004.12.002.

[79] D. P. DiVincenzo and D. Loss, "Rigorous Born approximation and beyond for the spin-boson model", *Phys. Rev. B* 71 (2005) 035318, DOI: 10.1103/PhysRevB.71.035318.

[80] H. Wang and M. Thoss, "From coherent motion to localization: dynamics of the spin-boson model at zero temperature", *New Journal of Physics* 10.11 (2008) 115005, DOI: 10.1088/1367-2630/10/11/115005.

[81] E. Barnes and S. Das Sarma, "Master equation approach to the central spin decoherence problem: Uniform coupling model and role of projection operators", *Phys. Rev. B* 84 (2011) 155315, DOI: 10.1103/PhysRevB.84.155315.

[82] N. Fröhling, F. B. Anders and M. Glazov, "Nuclear spin noise in the central spin model", *Phys. Rev. B* 97 (2018) 195311, DOI: 10.1103/PhysRevB.97.195311.

[83] Y. Ashida, T. Shi, R. Schmidt, H. R. Sadeghpour, J. I. Cirac and E. Demler, "Quantum Rydberg Central Spin Model", *Phys. Rev. Lett.* 123 (2019) 183001, DOI: 10.1103/PhysRevLett.123.183001.

[84] V. V. Sargsyan, G. G. Adamian, N. V. Antonenko and D. Lacroix, "Non-Markovian dynamics with fermions", *Phys. Rev. A* 90 (2014) 022123, DOI: 10.1103/PhysRevA.90.022123.

[85] E. A. Polyakov and A. N. Rubtsov,
"Non-Markovian Quantum State Diffusion in a Fermionic Bath" (2019),
arXiv: 1909.05760 [cond-mat.str-el].

[86] A. Nüßeler, I. Dhand, S. F. Huelga and M. B. Plenio,
"Efficient simulation of open quantum systems coupled to a fermionic bath",
Phys. Rev. B 101 (2020) 155134, DOI: 10.1103/PhysRevB.101.155134.

[87] S. Matern, D. Loss, J. Klinovaja and B. Braunecker,
"Coherent backaction between spins and an electronic bath: Non-Markovian dynamics and low-temperature quantum thermodynamic electron cooling",
Phys. Rev. B 100 (2019) 134308, DOI: 10.1103/PhysRevB.100.134308.

[88] R. Blatt and C. F. Roos, "Quantum simulations with trapped ions",
Nature Physics 8 (2012) 277–284, DOI: 10.1038/nphys2252.

[89] C. D. Bruzewicz, J. Chiaverini, R. McConnell and J. M. Sage,
"Trapped-ion quantum computing: Progress and challenges",
Applied Physics Reviews 6.2 (2019) 021314, DOI: 10.1063/1.5088164,
eprint: https://doi.org/10.1063/1.5088164.

[90] M. Born, "Quantenmechanik der Stoßvorgänge",
Zeitschrift für Physik 38 () 803–827, DOI: 10.1007/BF01397184.

[91] A. G. Redfield, "On the Theory of Relaxation Processes",
IBM Journal of Research and Development 1.1 (1957) 19–31,
DOI: 10.1147/rd.11.0019.

[92] A. Pereverzev and E. R. Bittner,
"Time-convolutionless master equation for mesoscopic electron-phonon systems",
The Journal of Chemical Physics 125.10 (2006) 104906,
DOI: 10.1063/1.2348869, eprint: https://doi.org/10.1063/1.2348869.

[93] S. Lorenzo, F. Ciccarello, G. M. Palma and B. Vacchini,
"Quantum Non-Markovian Piecewise Dynamics from Collision Models",
Open Systems & Information Dynamics 24.04 (2017) 1740011,
DOI: 10.1142/S123016121740011X.

[94] A. W. Chin, A. Rivas, S. F. Huelga and M. B. Plenio,
"Exact mapping between system-reservoir quantum models and semi-infinite discrete chains using orthogonal polynomials",
Journal of Mathematical Physics 51.9 (2010) 092109, DOI: 10.1063/1.3490188.

[95] N. Makri and D. E. Makarov, "Tensor propagator for iterative quantum time evolution of reduced density matrices. I. Theory", *The Journal of Chemical Physics* 102.11 (1995) 4600–4610, DOI: 10.1063/1.469508, eprint: https://doi.org/10.1063/1.469508.

[96] N. Makri and D. E. Makarov, "Tensor propagator for iterative quantum time evolution of reduced density matrices. II. Numerical methodology", *The Journal of Chemical Physics* 102.11 (1995) 4611–4618, DOI: 10.1063/1.469509, eprint: https://doi.org/10.1063/1.469509.

[97] A. H. Werner, D. Jaschke, P. Silvi, M. Kliesch, T. Calarco, J. Eisert and S. Montangero, "Positive Tensor Network Approach for Simulating Open Quantum Many-Body Systems", *Phys. Rev. Lett.* 116 (2016) 237201, DOI: 10.1103/PhysRevLett.116.237201.

[98] A. Strathearn, P. Kirton, D. Kilda, J. Keeling and B. W. Lovett, "Efficient non-Markovian quantum dynamics using time-evolving matrix product operators", *Nature Communications* 9 (2018) 3322, DOI: 10.1038/s41467-018-05617-3.

[99] R. Rosenbach, J. Cerrillo, S. F. Huelga, J. Cao and M. B. Plenio, "Efficient simulation of non-Markovian system-environment interaction", *New Journal of Physics* 18.2 (2016) 023035, DOI: 10.1088/1367-2630/18/2/023035.

[100] D. Chruściński and A. Kossakowski, "From Markovian semigroup to non-Markovian quantum evolution", *EPL (Europhysics Letters)* 97.2 (2012) 20005, DOI: 10.1209/0295-5075/97/20005.

[101] M. M. Wolf, J. Eisert, T. S. Cubitt and J. I. Cirac, "Assessing Non-Markovian Quantum Dynamics", *Phys. Rev. Lett.* 101 (2008) 150402, DOI: 10.1103/PhysRevLett.101.150402.

[102] R. Hartmann and W. T. Strunz, "Accuracy assessment of perturbative master equations: Embracing nonpositivity", *Phys. Rev. A* 101 (2020) 012103, DOI: 10.1103/PhysRevA.101.012103.

[103] And S. Maniscalco, "Degree of Non-Markovianity of Quantum Evolution", *Phys. Rev. Lett.* 112 (2014) 120404, DOI: 10.1103/PhysRevLett.112.120404.

[104] Y. L. Len and H. K. Ng, "Open-system quantum error correction", *Phys. Rev. A* 98 (2018) 022307, DOI: 10.1103/PhysRevA.98.022307.

[105] M. Q. Lone and T. Byrnes, "Suppression of the ac-Stark-shift scattering rate due to non-Markovian behavior", *Phys. Rev. A* 92 (2015) 011401, DOI: 10.1103/PhysRevA.92.011401.

[106] S. Hamedani Raja, M. Borrelli, R. Schmidt, J. P. Pekola and S. Maniscalco, "Thermodynamic fingerprints of non-Markovianity in a system of coupled superconducting qubits", *Phys. Rev. A* 97 (2018) 032133, DOI: 10.1103/PhysRevA.97.032133.

[107] A. del Campo, J. Goold and M. Paternostro, "More bang for your buck: Super-adiabatic quantum engines", *Sci. Rep.* 4 (2014) 6208, DOI: 10.1038/srep06208.

[108] P. Abiuso and V. Giovannetti, "Non-Markov enhancement of maximum power for quantum thermal machines", *Phys. Rev. A* 99 (2019) 052106, DOI: 10.1103/PhysRevA.99.052106.

[109] M. Pezzutto, M. Paternostro and Y. Omar, "An out-of-equilibrium non-Markovian quantum heat engine", *Quantum Science and Technology* 4.2 (2019) 025002, DOI: 10.1088/2058-9565/aaf5b4.

[110] P. A. Camati, J. F. G. Santos and R. M. Serra, "Employing non-Markovian effects to improve the performance of a quantum Otto refrigerator", *Phys. Rev. A* 102 (2020) 012217, DOI: 10.1103/PhysRevA.102.012217.

[111] U. Geigenmüller, U. M. Titulaer and B. U. Felderhof, "Systematic elimination of fast variables in linear systems", *Physica A Statistical Mechanics and its Applications* 119 (1983) 41–52, DOI: 10.1016/0378-4371(83)90144-9.

[112] F. Haake and M. Lewenstein, "Adiabatic drag and initial slip in random processes", *Phys. Rev. A* 28 (1983) 3606–3612, DOI: 10.1103/PhysRevA.28.3606.

[113] F. Haake and R. Reibold, "Strong damping and low-temperature anomalies for the harmonic oscillator", *Phys. Rev. A* 32 (1985) 2462–2475, DOI: 10.1103/PhysRevA.32.2462.

[114] A. Suárez, R. Silbey and I. Oppenheim, "Memory effects in the relaxation of quantum open systems", *The Journal of Chemical Physics* 97.7 (1992) 5101–5107, DOI: 10.1063/1.463831.

[115] P. Gaspard and M. Nagaoka,
"Slippage of initial conditions for the Redfield master equation",
The Journal of Chemical Physics 111.13 (1999) 5668–5675,
DOI: 10.1063/1.479867, eprint: https://doi.org/10.1063/1.479867.

[116] T. Yu, L. Diósi, N. Gisin and W. T. Strunz,
"Post-Markov master equation for the dynamics of open quantum systems",
Phys. Lett. A 265.5 (2000) 331 –336,
DOI: https://doi.org/10.1016/S0375-9601(00)00014-1.

[117] S. Sachdev, *Quantum Phase Transitions*, Cambridge University Press, 2000.

[118] P. W. Anderson and G. Yuval, "Exact Results in the Kondo Problem: Equivalence to a Classical One-Dimensional Coulomb Gas",
Phys. Rev. Lett. 23 (1969) 89–92, DOI: 10.1103/PhysRevLett.23.89.

[119] P. W. Anderson, G. Yuval and D. R. Hamann, "Exact Results in the Kondo Problem. II. Scaling Theory, Qualitatively Correct Solution, and Some New Results on One-Dimensional Classical Statistical Models",
Phys. Rev. B 1 (1970) 4464–4473, DOI: 10.1103/PhysRevB.1.4464.

[120] G. D. Mahan, "Excitons in Metals", *Phys. Rev. Lett.* 18 (1967) 448–450,
DOI: 10.1103/PhysRevLett.18.448.

[121] G. D. Mahan, "Excitons in Metals: Infinite Hole Mass",
Phys. Rev. 163 (1967) 612–617, DOI: 10.1103/PhysRev.163.612.

[122] P. W. Anderson,
"Infrared Catastrophe in Fermi Gases with Local Scattering Potentials",
Phys. Rev. Lett. 18 (1967) 1049–1051, DOI: 10.1103/PhysRevLett.18.1049.

[123] P. Nozières and C. T. De Dominicis, "Singularities in the X-Ray Absorption and Emission of Metals. III. One-Body Theory Exact Solution",
Phys. Rev. 178 (1969) 1097–1107, DOI: 10.1103/PhysRev.178.1097.

[124] P. A. M. Dirac and N. H. D. Bohr,
"The quantum theory of the emission and absorption of radiation",
Proceedings of the Royal Society of London. Series A, Containing Papers of a Mathematical and Physical Character 114.767 (1927) 243–265,
DOI: 10.1098/rspa.1927.0039.

[125] E. Fermi, *Nuclear Physics*, University of Chicago Press, Chicago, 1950.

[126] R. K. Wangsness and F. Bloch, "The Dynamical Theory of Nuclear Induction",
Phys. Rev. 89 (1953) 728–739, DOI: 10.1103/PhysRev.89.728.

[127] W. D. Knight, "Nuclear Magnetic Resonance Shift in Metals", *Phys. Rev.* 76 (1949) 1259–1260, DOI: 10.1103/PhysRev.76.1259.2.

[128] G. C. Wick, "The Evaluation of the Collision Matrix", *Phys. Rev.* 80 (1950) 268–272, DOI: 10.1103/PhysRev.80.268.

[129] A. Carmi and Y. Oreg, "Enhanced shot noise in asymmetric interacting two-level systems", *Phys. Rev. B* 85 (2012) 045325, DOI: 10.1103/PhysRevB.85.045325.

[130] G Bevilacqua, "Some integrals related to the Fermi function" (2013), arXiv: 1303.6206 [math-ph].

[131] *NIST Digital Library of Mathematical Functions*, http://dlmf.nist.gov/, Release 1.0.22 of 2019-03-15, F. W. J. Olver, A. B. Olde Daalhuis, D. W. Lozier, B. I. Schneider, R. F. Boisvert, C. W. Clark, B. R. Miller and B. V. Saunders, eds.

[132] V. N. Golovach, A. Khaetskii and D. Loss, "Phonon-Induced Decay of the Electron Spin in Quantum Dots", *Phys. Rev. Lett.* 93 (2004) 016601, DOI: 10.1103/PhysRevLett.93.016601.

[133] M. Borhani, V. N. Golovach and D. Loss, "Spin decay in a quantum dot coupled to a quantum point contact", *Phys. Rev. B* 73 (2006) 155311, DOI: 10.1103/PhysRevB.73.155311.

[134] D. Paget, G. Lampel, B. Sapoval and V. I. Safarov, "Low field electron-nuclear spin coupling in gallium arsenide under optical pumping conditions", *Phys. Rev. B* 15 (1977) 5780–5796, DOI: 10.1103/PhysRevB.15.5780.

[135] J. Schliemann, A. Khaetskii and D. Loss, "Electron spin dynamics in quantum dots and related nanostructures due to hyperfine interaction with nuclei", *Journal of Physics: Condensed Matter* 15.50 (2003) R1809–R1833, DOI: 10.1088/0953-8984/15/50/r01.

[136] P.-F. Braun, B. Urbaszek, T. Amand, X. Marie, O. Krebs, B. Eble, A. Lemaitre and P. Voisin, "Bistability of the nuclear polarization created through optical pumping in $In_{1-x}Ga_xAs$ quantum dots", *Phys. Rev. B* 74 (2006) 245306, DOI: 10.1103/PhysRevB.74.245306.

[137] J. Fischer, B. Trauzettel and D. Loss, "Hyperfine interaction and electron-spin decoherence in graphene and carbon nanotube quantum dots", *Phys. Rev. B* 80 (2009) 155401, DOI: 10.1103/PhysRevB.80.155401.

[138] T. Giamarchi, *Quantum Physics in one dimension*,
Clarendon Press, Oxford, 2004.

[139] J. Goold, M. Huber, A. Riera, L. del Rio and P. Skrzypczyk,
"The role of quantum information in thermodynamics—a topical review",
Journal of Physics A: Mathematical and Theoretical 49.14 (2016) 143001,
DOI: 10.1088/1751-8113/49/14/143001.

[140] J. Sun, Y.-N. Sun, C. feng Li, G.-C. Guo, K. Luoma and J. Piilo,
"Non-Markovian discrete qubit dynamics",
Science Bulletin 61.13 (2016) 1031 –1036,
DOI: https://doi.org/10.1007/s11434-016-1089-8.

[141] R. S. Whitney,
"Most Efficient Quantum Thermoelectric at Finite Power Output",
Phys. Rev. Lett. 112 (2014) 130601, DOI: 10.1103/PhysRevLett.112.130601.

[142] G. Watanabe, B. P. Venkatesh, P. Talkner and A. del Campo,
"Quantum Performance of Thermal Machines over Many Cycles",
Phys. Rev. Lett. 118 (2017) 050601, DOI: 10.1103/PhysRevLett.118.050601.

[143] R. S. Whitney,
"Non-Markovian quantum thermodynamics: Laws and fluctuation theorems",
Phys. Rev. B 98 (2018) 085415, DOI: 10.1103/PhysRevB.98.085415.

[144] T. A. Knuuttila, J. T. Tuoriniemi, K. Lefmann, K. I. Juntunen, F. B. Rasmussen and K. K. Nummila,
"Polarized Nuclei in Normal and Superconducting Rhodium",
J. Low Temp. Phys. 123.1 (2001) 65, DOI: 10.1023/A:1017545531677.

[145] P. J. Hakonen, R. T. Vuorinen and J. E. Martikainen,
"Nuclear antiferromagnetism in rhodium metal at positive and negative nanokelvin temperatures", *Phys. Rev. Lett.* 70 (1993) 2818,
DOI: 10.1103/PhysRevLett.70.2818.

[146] W. Wendler, T. Herrmannsdörfer, S. Rehmann and F. Pobell, "Electronic and nuclear magnetism in $PtFe_x$ at milli-, and nanokelvin temperatures",
EPL 38.8 (1997) 619, DOI: 10.1209/epl/i1997-00293-9.

[147] C. P. Scheller, S. Heizmann, K. Bedner, D. Giss, M. Meschke, D. M. Zumbühl, J. D. Zimmerman and A. C. Gossard,
"Silver-epoxy microwave filters and thermalizers for millikelvin experiments",
Appl. Phys. Lett. 104.21 (2014) 211106, DOI: 10.1063/1.4880099.

[148] A. A. Zyuzin, T. Meng, V. Kornich and D. Loss,
"Nuclear spin relaxation in Rashba nanowires", *Phys. Rev. B* 90 (2014) 195125,
DOI: 10.1103/PhysRevB.90.195125.

[149] J. M. Kikkawa and D. D. Awschalom,
"Resonant Spin Amplification in n-Type GaAs",
Phys. Rev. Lett. 80 (1998) 4313–4316, DOI: 10.1103/PhysRevLett.80.4313.

[150] G. Salis, D. T. Fuchs, J. M. Kikkawa, D. D. Awschalom, Y. Ohno and H. Ohno,
"Optical Manipulation of Nuclear Spin by a Two-Dimensional Electron Gas",
Phys. Rev. Lett. 86 (2001) 2677–2680, DOI: 10.1103/PhysRevLett.86.2677.

[151] G. Salis, D. D. Awschalom, Y. Ohno and H. Ohno,
"Origin of enhanced dynamic nuclear polarization and all-optical nuclear magnetic resonance in GaAs quantum wells", *Phys. Rev. B* 64 (2001) 195304,
DOI: 10.1103/PhysRevB.64.195304.

[152] B. D. Gerardot, D. Brunner, P. A. Dalgarno, P. Öhberg, S. Seidl, M. Kroner, K. Karrai, N. G. Stoltz, P. M. Petroff and R. J. Warburton,
"Optical pumping of a single hole spin in a quantum dot",
Nature 451 (2008) 441–444, DOI: 10.1038/nature06472.

[153] M. S. Blok, C. Bonato, M. L. Markham, D. J. Twitchen, V. V. Dobrovitski and R. Hanson, "Manipulating a qubit through the backaction of sequential partial measurements and real-time feedback", *Nature Phys.* 10 (2014) 189–193,
DOI: 10.1038/nphys2881.

[154] P. Simon and D. Loss, "Nuclear Spin Ferromagnetic Phase Transition in an Interacting Two Dimensional Electron Gas", *Phys. Rev. Lett.* 98 (2007) 156401,
DOI: 10.1103/PhysRevLett.98.156401.

[155] P. Simon, B. Braunecker and D. Loss, "Magnetic ordering of nuclear spins in an interacting two-dimensional electron gas", *Phys. Rev. B* 77 (2008) 045108,
DOI: 10.1103/PhysRevB.77.045108.

[156] B. Braunecker, P. Simon and D. Loss,
"Nuclear Magnetism and Electronic Order in ^{13}C Nanotubes",
Phys. Rev. Lett. 102 (2009) 116403, DOI: 10.1103/PhysRevLett.102.116403.

[157] B. Braunecker, P. Simon and D. Loss, "Nuclear magnetism and electron order in interacting one-dimensional conductors", *Phys. Rev. B* 80 (2009) 165119,
DOI: 10.1103/PhysRevB.80.165119.

[158] P. Bonville, J. Hodges, P. Imbert, G. Jéhanno, D. Jaccard and J. Sierro, "Magnetic ordering and paramagnetic relaxation of Yb^{3+} in $YbNi_2Si_2$", *J. Magn. Magn. Mat.* 97.1 (1991) 178 –186, DOI: https://doi.org/10.1016/0304-8853(91)90178-D.

[159] J. Okabayashi, A. Kimura, O. Rader, T. Mizokawa, A. Fujimori, T. Hayashi and M. Tanaka, "Core-level photoemission study of $Ga_{1-x}Mn_xAs$", *Phys. Rev. B* 58 (1998) R4211–R4214, DOI: 10.1103/PhysRevB.58.R4211.

[160] T. Jungwirth, K. Y. Wang, K. W. Edmonds, M. Sawicki, M. Polini, J. Sinova, A. H. MacDonald, R. P. Campion, L. X. Zhao, N. R. S. Farley, T. K. Johal, G. van der Laan, C. T. Foxon and B. L. Gallagher, "Low-temperature magnetization of (Ga,Mn)As semiconductors", *Phys. Rev. B* 73 (2006) 165205, DOI: 10.1103/PhysRevB.73.165205.

[161] V. Purohit, B. Braunecker and B. W. Lovett, "Probing charge fluctuator correlations using quantum dot pairs", *Phys. Rev. B* 91 (2015) 245301, DOI: 10.1103/PhysRevB.91.245301.

[162] J. Patade and S. Bhalekar, "A Novel Numerical Method for Solving Volterra Integro-Differential Equations", *International Journal of Applied and Computational Mathematics* 6 (2019) 7, DOI: 10.1007/s40819-019-0762-4.

[163] V. Daftardar-Gejji and H. Jafari, "An iterative method for solving nonlinear functional equations", *Journal of Mathematical Analysis and Applications* 316.2 (2006) 753 –763, DOI: https://doi.org/10.1016/j.jmaa.2005.05.009.

[164] V. Dugaev, V. Litvinov and P. Petrov, "Magnetic impurity interactions in a quantum well on the base of IV-VI semiconductors", *Superlattices and Microstructures* 16.4 (1994) 413 –417, DOI: https://doi.org/10.1006/spmi.1994.1160.

[165] D. N. Aristov, "Indirect RKKY interaction in any dimensionality", *Phys. Rev. B* 55 (1997) 8064–8066, DOI: 10.1103/PhysRevB.55.8064.

[166] V. I. Litvinov and V. K. Dugaev, "RKKY interaction in one- and two-dimensional electron gases", *Phys. Rev. B* 58 (1998) 3584–3585, DOI: 10.1103/PhysRevB.58.3584.

[167] H. Takagi and H. Y. Hwang, "An Emergent Change of Phase for Electronics", *Science* 327.5973 (2010) 1601–1602, DOI: 10.1126/science.1182541, eprint: https://science.sciencemag.org/content/327/5973/1601.full.pdf.

[168] Z. D. Kvon, E. B. Olshanetsky, N. N. Mikhailov and D. A. Kozlov, "Two-dimensional electron systems in HgTe quantum wells", *Low Temperature Physics* 35.1 (2009) 6–14, DOI: 10.1063/1.3064862, eprint: https://doi.org/10.1063/1.3064862.

[169] R. Kubo, "Generalized Cumulant Expansion Method", *Journal of the Physical Society of Japan* 17.7 (1962) 1100–1120, DOI: 10.1143/JPSJ.17.1100.

[170] P Danielewicz, "Quantum theory of nonequilibrium processes, I", *Annals of Physics* 152.2 (1984) 239 –304, DOI: https://doi.org/10.1016/0003-4916(84)90092-7.

[171] B. Fischer and M. W. Klein, "Magnetic and nonmagnetic impurities in two-dimensional metals", *Phys. Rev. B* 11 (1975) 2025–2029, DOI: 10.1103/PhysRevB.11.2025.

[172] H. Bateman, *Higher Transcendental Functions, vol. I*, McGraw–Hill Book Company, New York, 1953.

[173] C. Ferreira and J. L. López, "Asymptotic expansions of the Hurwitz–Lerch zeta function", *Journal of Mathematical Analysis and Applications* 298.1 (2004) 210 –224, DOI: https://doi.org/10.1016/j.jmaa.2004.05.040.

[174] C. A. Gelmi and H. Jorquera, "IDSOLVER: A general purpose solver for nth-order integro-differential equations", *Computer Physics Communications* 185.1 (2014) 392 –397, DOI: https://doi.org/10.1016/j.cpc.2013.09.008.

[175] J. T. Karpel, "IDESolver: a general purpose integro-differential equation solver", *Journal of Open Source Software* 3.21 (2018) 542, DOI: 10.21105/joss.00542.

[176] D. Gribben, A. Strathearn, J. Iles-Smith, D. Kilda, A. Nazir, B. W. Lovett and P. Kirton, "Exact quantum dynamics in structured environments", *Phys. Rev. Research* 2 (2020) 013265, DOI: 10.1103/PhysRevResearch.2.013265.

[177] I. Gradsteyn and I. Ryzhik, *Table of Integrals, Series, and Products*, Academic Press, Inc., Boston., 1994.